

Su-Pos227

RECTIFICATION OF CFTR CHLORIDE CHANNEL MEDIATED BY EXTRACELLULAR DIVALENT CATIONS. (B. Zerhusen, J. Zhao, T. Tao, J. Xie, M.L. Drumm*, P.B. Davis and J. Ma) Dept. of Physiology & Biophysics, and Pediatrics*, Case Western Reserve Univ., Cleveland, OH.

Patch clamp studies identify the cystic fibrosis transmembrane conductance regulator (CFTR) as a linear conductance Cl channel. We report here distinct rectification of the CFTR channel reconstituted in lipid bilayer membranes. Under symmetrical ionic condition of 200 mM KCl (with 1 mM MgCl₂ in *cis*-intracellular and 0 MgCl₂ in *trans*-extracellular solutions), inward currents (*cis*→*trans* Cl movement) through a single CFTR channel were always larger than the outward currents (*i* = -0.68 ± 0.03 pA, V = -80 mV; *i* = 0.56 ± 0.04 pA, V = +80 mV). The linear I-V relationship of the CFTR channel could be restored through addition of divalent cations to the *trans* solution. In the presence of 5 mM [Mg]_o or [Ca]_o, the I-V curve became linear with a slope conductance of 8.6 ± 0.6 pS. The dose responses for [Mg]_o and [Ca]_o had half dissociation constants of 152 ± 81 μM and 290 ± 129 μM, respectively. Rectification of the CFTR channel seemed to be due to negative surface charges on the channel protein, since in pure neutral phospholipid bilayers (PE), clear rectification of the channel could also be observed when the extracellular solution did not contain divalent cations. The CFTR protein contains clusters of negatively charged amino acids on several extracellular loops joining the transmembrane segments, which could constitute the putative binding sites for Ca and Mg. Supported by NIH, CFF, and AHA.

Su-Pos229

MUTATION OF THE NARROW REGION OF THE CFTR CHANNEL PORE. (Paul Linsdell, Johanna M. Rommens, Yue-Xian Hou, Xiu-Bao Chang, Lap-Chee Tsui, John R. Riordan and John W. Hanrahan) Dept. Physiology, McGill University, Montréal, PQ; Research Institute, Hospital for Sick Children, Toronto, ON; and Mayo Clinic, Scottsdale, AZ.

CFTR is a phosphorylation-regulated and nucleotide-dependent Cl channel. Several lines of evidence suggest that the sixth membrane-spanning region of CFTR (TM6) is a major constituent of the channel pore. Mutation of a threonine residue at position 338 in TM6 is associated with an unusual, mild cystic fibrosis phenotype. Since threonine side-chains have been implicated in the formation of ion channel permeation pathways, we have examined the role of this and an adjacent threonine residue in CFTR channel function using the Chinese hamster ovary cell expression system. Mutation of both these residues to alanines (the TT338,339AA mutant) led to an approximately 25% increase in single channel conductance with symmetrical 150mM Cl solutions. Saturating conductance seen at higher Cl concentrations was similarly increased. In addition, TT338,339AA channels had increased permeability to several large extracellular anions, consistent with an increase in the size of the narrowest part of the pore. We suggest that one or both of these threonine residues normally line a constriction in the permeation pathway of CFTR, and that interaction between permeating Cl ions and this narrow region slows flux through the pore. Supported by MRC, CCF and NIH(NIDDK).

Su-Pos228

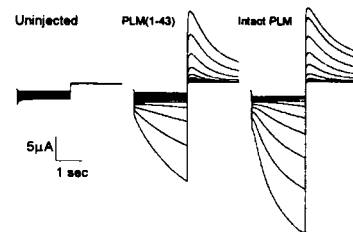
MODULATION OF CFTR CHANNEL BY MEMBRANE SURFACE CHARGES. (Tao Tao, Junxia Xie, Mitch L. Drumm*, Jiying Zhao, Pamela B. Davis and Jianjie Ma) Dept. of Physiol. & Biophys., and Pediatrics*, Case Western Reserve University, Cleveland, OH. (Spon. by D. Dearborn)

The effect of surface charges on the function of CFTR channels was studied in the bilayer reconstitution system. The bilayer membranes were formed with a lipid mixture of phosphatidylethanolamine (PE), phosphatidylserine (PS) and cholesterol (CL). We found that both Cl conductance and open probability of the CFTR channel were sensitive to negative charges on the bilayer membrane. The inward, as well as the outward, currents through a single CFTR channel increased significantly (~30%), when the lipid composition of the bilayers was changed from PE:PS:CL=6:6:1 to 12:0:1. Open probability of the channel followed inversely with negative charges on the bilayer (*P*_o=0.45, 0.33, and 0.05 in PE:PS=12:0, 6:6, and 1:11). The conductance-activity relationship of the CFTR channel saturated at a maximum conductance of 16.7 ± 0.7 pS with half Cl concentrations of 148 ± 20 mM in PE:PS:CL = 6:6:1. The steep dependence of CFTR channel on Cl concentration and surface charge could account for the different conductance values (7-12 pS) reported in literature. Our data indicate that the conduction pore of the CFTR channel lies well within the region of the lipid membrane. Thus, hydrophilic portions of the CFTR molecule (nucleotide-binding folds and regulatory domain) would constitute mostly mobile structures, which could regulate the Cl conductance pathway through direct electrostatic or allosteric mechanisms.

Su-Pos230

EXPRESSION OF PHOSPHOLEMMAN 1-43 INDUCES CHLORIDE CURRENTS IN XENOPUS OOCYTES (J. Paul Mounsey, Zhenhui Chen, J. Edward John, J. Randall Moorman, Larry R. Jones) University of Birmingham, UK; University of Virginia, Charlottesville, VA; Indiana University, Indianapolis, IN.

Phospholemmann (PLM) induces Cl currents when expressed in *Xenopus* oocytes and forms anion channels when reconstituted in phospholipid bilayers. It has a single transmembrane domain with intracellular and extracellular domains: at 72 aa in length, it is the smallest membrane protein known to form ion channels. To investigate whether the cytoplasmic domain is a necessary part of the ion pore, we expressed mRNA encoding only the transmembrane domain and extracellular peptide of PLM (PLM 1-43) in *Xenopus* oocytes. The Figure shows hyperpolarization-activated oocyte currents recorded during two-microelectrode voltage clamp. The currents induced by expression of PLM 1-43 (center) and intact PLM (right) have similar kinetics, threshold, voltage dependence of activation, and reversal potential-dependence on external [Cl]. The similarity of the currents suggests that the PLM molecule does not require the cytoplasmic tail for function. The finding of a membrane current induced by PLM 1-43 establishes a new estimate of the minimum size required for an ion channel subunit.



MODULATION OF CHANNELS

Su-Pos231

Acetylcholine inhibits voltage-dependent Ca²⁺ channels in mouse pancreatic B-cells. Gilon P.^{1,2,3}, Yakel J.², Gromada J.¹, Zhu Y.², Henquin JC³ and Rorsman P.¹

¹Islet Cell Physiology, Novo Nordisk A/S, Denmark. ²Laboratory of Cellular and Molecular Pharmacology, NIH, North Carolina. ³Laboratoire d'Endocrinologie et de Métabolisme, UCL, Belgium.

Acetylcholine (ACh) stimulates insulin secretion by activating muscarinic receptors in B-cells. However, it has recently been reported that ACh exerts both stimulatory and inhibitory effects on the concentration of cytoplasmic Ca²⁺ ([Ca²⁺]_i). In the present study, we have tested the hypothesis that ACh lowers [Ca²⁺]_i by inhibiting the voltage-dependent Ca²⁺ channels. Voltage-clamp Ca²⁺ currents were recorded in individual mouse pancreatic B-cells using the standard whole-cell configuration. ACh (2.5 - 250 μM) reversibly and dose-dependently inhibited the Ca²⁺ current elicited by depolarizations from -80 mV to 0 mV. The maximum inhibition, observed at concentrations > 25 μM, averaged 30%. The effect was blocked by atropine (10 μM). Indicative of an involvement of G-proteins, the inhibitory effect of ACh on the Ca²⁺ current was more pronounced and irreversible after inclusion of 10 μM GTPγS in the pipette solution (dialyzing the cell interior) and was prevented by 2 mM GDPβS in the pipette. However, overnight pretreatment of the cells with either pertussis or cholera toxin (500 ng/ml) both failed to prevent the effect of ACh on the Ca²⁺ current. The effect of ACh was not due to the activation of PKC as suggested by the observation that TPA (500 nM) failed to reproduce the inhibitory action. Likewise, it is unlikely to result from Ca²⁺-induced inhibition of the Ca²⁺ current as: 1) the effect remained observable when Ba²⁺ was used as the charge carrier; and 2) all intracellular solutions contained 10 mM EGTA to buffer [Ca²⁺]_i to very low concentrations. The effects of ACh on the Ca²⁺ current were not prevented by including 100 μM (2,4,5)IP₃ or 1 mg/ml heparin in the pipette solution suggesting that ACh-induced elevation of IP₃ does not account for the action on the Ca²⁺ current. In conclusion, ACh inhibits voltage-dependent Ca²⁺ current by a Ca²⁺-independent mechanism following activation of a pertussis toxin- and cholera toxin-insensitive G protein.

Su-Pos232

PURINERGIC MODULATION OF A VOLTAGE GATED POTASSIUM CHANNEL IN RAT BROWN ADIPOCYTES. (S.M. Wilson & P.A. Pappone) Univ. of California, Davis 95616.

We found that stimulation of P_{2y} purinergic receptors with 20 nM - 10 μM extracellular ATP induced a 50 - 100% decrease in voltage gated potassium (IKv) currents evoked from a -60 mV holding potential in rat brown adipocytes. This IKv current decrease developed over several minutes following ATP exposure in whole cell patch voltage clamped cells with a nucleotide-free internal pipette solution. The IKv membrane current decrease is due to hyperpolarizing shifts in the V_{1/2} of steady state inactivation which ranged from -14 to greater than -60 mV. The voltage dependence of activation was shifted negative also, but by a lesser amount, 0 to -27 mV in the same cells (n=13).

The response of the brown adipocytes to extracellular ATP was dependent upon the cytosolic integrity. In whole cell experiments with the nucleotide-free internal pipette solution the effects of external ATP exposure were irreversible. Adding mM ATP to the pipette solution required a 5 fold increase in the extracellular ATP dose to induce a measurable IKv current decrease. Furthermore, in perforated patch clamped cells IKv current only transiently decreased when ATP was applied, suggesting that a non-membrane bound component may be involved in modulating the purinergic response.

Su-Pos233

A STRONGLY INWARDLY RECTIFYING K CHANNEL MODULATED BY M1 ACETYLCHOLINE RECEPTOR (H. Chuang, Y.N. Jan, and L.Y. Jan) HHMI, Depts. of Physiology and Biochemistry, University of California, San Francisco, CA 94143-0724 (Spon. by P.A. Slesinger)

To study the modulation of an inwardly rectifying K channel IRK3(HIT), we coexpressed it with human m1AChR in *Xenopus* oocytes. When 2 μ M carbachol was applied to the oocyte, the K current carried by IRK3 is inhibited in 2 to 5 minutes; this inhibition is reversible after washing out carbachol in the bath. When the similar experiment was done on IRK1, another cloned channel in the same family, it is insensitive to m1 stimulation. In the absence of coexpression of m1 AChR, IRK3 current is not modulated by carbachol, suggesting the modulation is not due to activation of endogenous muscarinic receptors in the oocytes. Microinjection of PKC peptide inhibitor or EGTA cannot abolish this m1 receptor dependent modulation. Neither can the application of calcium ionophore mimic the m1 effect. However, in the cell attached patches, it is shown that this modulation is due to cytoplasmic diffusible messengers. To further define the molecular mechanism of this regulation, we are currently generating chimeras between IRK3 and IRK1 to test if they will be modulated by m1 receptor stimulation.

Su-Pos235

NUCLEOTIDE REGULATION OF Ca^{2+} -ACTIVATED K^+ CHANNELS.

(C. Wachter*, K. Turnheim*, H. Wiener*, T. Zeuthen* and D. Klaerke*) *Biomembrane Research Centre, University of Copenhagen, Denmark and *Dept. of Pharmacology, University of Vienna, Austria. (Spon. by S. Dissing)

High conductance Ca^{2+} -activated K^+ channels from the basolateral membrane of surface cells from rabbit distal colon epithelium may play an important role in the regulation of epithelial transport. Regulation of these channels by membrane potential, intracellular Ca^{2+} , Mg^{2+} , pH and phosphorylation has already been well characterized. In the present study the Ca^{2+} -activated K^+ channels are measured at a single channel level in planar lipid bilayers consisting of either phosphatidylethanolamine and phosphatidylserine (PE/PS) or phosphatidylethanolamine and phosphatidylcholine (PE/PC). At a free Ca^{2+} concentration of 30 μ M, the open probability (P_o) is stable for hours in PE/PS bilayers. Addition of high, but still physiological concentrations of ATP leads to an inhibition of the K^+ channel from the intracellular face; the $K_{0.5}$ for inhibition is 2.5 mM. The inhibition cannot be reversed by high concentrations of Ca^{2+} or ADP. At the extracellular face of the channel, there is no effect of ATP. In PE/PC bilayers P_o decreases from initially 0.8 to less than 0.1 within 5 - 25 min after channel fusion ("rundown"). Increasing free Ca^{2+} to 100 μ M reactivates the channels only transiently. Addition of the non-hydrolyzable GTP-analogue, GTP- γ -S (100 μ M), to the intracellular face of the channel restores P_o to approximately the initial value. This effect requires Mg^{2+} (1 mM). GDP- β -S, an inhibitor of G-protein mediated effects, also reactivates the channels, suggesting that G-proteins are not involved. GTP, ATP, ATP- γ -S and ADP can restore channel activity less efficiently. In conclusion, these findings suggest that Ca^{2+} -activated K^+ channels may be regulated directly by nucleotides; micromolar concentrations activate the channels at a site, which may be exposed only in PE/PC membranes, whereas millimolar concentrations inhibit the channels.

Su-Pos237

Up-regulation of the voltage-gated *Shaker B* ($\Delta 6-46$) and endogenous K^+ channels in COS cell line by fatty acids. ((S. Bendahhou, and W. S. Agnew*)) Depts. of Physiology and Neuroscience, Johns Hopkins University, School of Medicine, Baltimore, MD, 21205

We previously reported that the muscle Na channel ($\mu 1$) was down-regulated by cis-unsaturated fatty acids. This modulation was mediated neither by arachidonic acid (AA) metabolic pathways nor by activation of protein kinase C. Here, we describe the effect of AA and oleic acid (OA) on a *Shaker B* channel lacking fast inactivation (ShB $\Delta 6-46$), transiently expressed in a COS cell line, and similar effects on endogenous K channels in COS cells.

In contrast to Na channel behavior, bath application of 1-10 μ M AA or OA increased the *Shaker K* current by 4.6 ± 2.7 and 6.8 ± 3.9 fold respectively (mean \pm S.D.; n = 3). In untransfected control cells, the same concentrations of fatty acids induced similar current increase of the endogenous outward K currents (6.1 ± 2 (n=6) and 4.8 ± 2.3 (n=3) fold for AA and OA respectively) at 40 mV. Inhibition of either cyclooxygenase (with 10 μ M indomethacin) or epoxigenase (with 10 μ M eicosatetrayonic acid) metabolic pathways did not prevent the AA-induced K current increase. However, inhibition of lipoxygenase enzyme, with 20 μ M nordihydroguaiaretic acid, did prevent the AA modulatory effect. At this point, we cannot eliminate the possible direct interaction of K channels with fatty acids. Additional experiments may reveal the contribution of metabolic pathways and direct interaction of fatty acids with K channels; the differential modulation of Na and K channels suggests that voltage-gated ion channels could be specifically targeted by fatty acids.

Su-Pos234

A STRONGLY INWARDLY RECTIFYING K^+ CHANNEL THAT IS SENSITIVE TO ATP ((A. Collins, M. S. German*, Y. N. Jan, L. Y. Jan and B. Zhao)) HHMI, Depts. of Physiology and Biochemistry, and *Hormone Research Institute, University of California, San Francisco, CA 94143-0724.

We have cloned an inwardly rectifying K^+ channel, IRK3(HIT), from a hamster insulinoma cDNA library and shown that it is inhibited by cytoplasmic ATP. The channel is 90-97% identical to the IRK3 channels cloned from other species, and its mRNA is primarily found in the brain. When expressed in *Xenopus* oocytes, the channel displays strong inward rectification typical of inward rectifiers. In excised inside-out membrane patches the channel is inhibited reversibly by 50% by physiological concentrations of ATP ($K_i = 1.5$ mM), in the presence or absence of Mg^{2+} . The non-hydrolyzable ATP analogues AMP-PNP and AMP-PCP both inhibited the current. Application of 10-50 μ M ADP in the presence of ATP caused an increase in the current, indicating that the ATP effect is antagonized by ADP within the range of estimates of physiological [free ADP]. IRK3(HIT) may therefore be sensitive to the index of metabolic state, i.e. the intracellular [ATP]/[ADP] ratio. ADP alone had a moderate inhibitory effect at higher concentrations ($K_i = 0.4$ mM). In the presence of Mg^{2+} , a stimulatory effect of ATP (≥ 100 μ M MgATP) was observed in some patches, and was superimposed on the inhibitory effect.

Su-Pos236

DISRUPTION OF ACTIN FILAMENTS INCREASES THE ACTIVITY OF NA-CONDUCTING CHANNELS IN HUMAN MYELOID LEUKEMIA CELLS. ((Yu.A. Negulyaev, V.A. Maximov, E.A. Vedernikova)) Institute of Cytology, Russian Academy of Sciences, St.Petersburg, Russia. (Spons. by A.K. Ritchie).

With the use of patch clamp technique the role of cytoskeleton in the regulation of ion channels in leukemic K562 cells has been examined. Single channel measurements in different patch configurations indicated that disruption of actin filaments with cytochalasin D (CD) resulted in a considerable increase of the activity of non-voltage-gated Na-conducting channels of 15 pS unitary conductance (145 NaCl, 23°C) in the plasma membrane. Cell-attached and whole-cell recordings showed that the activation of Na channels was elicited within 1-3 minutes after the addition of 10-20 μ g/ml CD to the bath extracellular solution. In about 4 minutes open probability P reached maximum values; NP was 0.15 ± 0.03 (N is a number of channels). Pretreatment of K562 cells with CD during 1 hour also increased drastically the activity of 15 pS Na channels. The channels were cationic-selective, permeable to monovalent cations (presumably for Na and Li), but not to divalent cations (Ca, Ba). Mechanical stretch of the plasma membrane by application of the negative pressure resulted in activation of Na-permeable channels with similar characteristics. Colchicine did not influence channel activity in K562 cells. The data show that the F-actin network interacts with and possibly regulates Na-permeable channels in the plasma membrane which, under physiological conditions, may provide Na entry from the extracellular medium to cytosol in the blood cells.

Su-Pos238

EFFECTS OF CHANGING pH ON IONIC CURRENTS IN ISOLATED MYOMETRIAL CELLS. ((R.D. Smith, A.V. Shmigel, M.J. Taggart, S. Wray and D.A. Eisner*)) Department of Physiology, The University of Liverpool, PO Box 147, Liverpool, L69 3BX, U.K.

Previous work has shown that intracellular acidification decreases and alkalization increases magnitude and frequency of uterine contraction (Taggart & Wray, 1993). The cellular mechanism of this effect is not clear. The present study has used the whole cell patch clamp technique to investigate changes in intra- and extracellular pH on calcium and potassium currents from rat isolated myometrial cells.

Single myometrial cells were voltage clamped at -60mV. Changes in intracellular pH were achieved by isosmotic substitution of either sodium butyrate (20mM) or NH_4Cl (20mM) for NaCl, whilst changes in extracellular pH (6.9-7.9) were achieved by addition of strong acid or base. All experiments were performed at room temperature. Peak calcium currents (516 ± 50 pA, n=12) were obtained by depolarizing to +10 mV. Addition of 20mM sodium butyrate decreased the calcium current by $58 \pm 6\%$ (n=6) whereas 20mM NH_4Cl produced a $165 \pm 15\%$ (n=7) increase. Changes in extracellular pH produced similar effects but over a considerably slower time course. Changes in either intra- or extracellular pH had no effect on K-currents.

The results clearly show that changes in intra- or extracellular pH affect the membrane calcium current. This change in calcium current may account for the effects of pH on both frequency and magnitude of contraction.

References

Taggart, M.J. & Wray, S. (1993). Simultaneous measurement of intracellular pH and contraction in uterine smooth muscle. *Pflügers Arch.* 423, 527-529.

Su-Pos239

INTRINSIC XENOPUS OOCYTES INWARD RECTIFIERS ARE MODULATED BY CHANGES IN REDOX POTENTIAL. ((Amarillo, Y.[¶] Nakamura, T. Y.[§] Oliveros, W.[¶] Coetzee, W.[§] Rudy, B.[¶] and Moreno, H.[¶])) [¶]Centro Internacional de Física- Universidad Nacional Bogotá Colombia, [§] Pediatric Cardiology and [¶] Physiology New York Univ Med Ctr.

The *Xenopus laevis* oocyte is the most common transient heterologous expression system of transcripts encoding ion channels. Three characteristics make this expression system particularly convenient: 1) oocytes promiscuously express functional channels when micro injected with specific mRNAs or cDNAs. 2) the large size simplifies its manipulation and maintenance and 3) oocytes membrane possess ion channels, which so far have not represented a major problem for the electrophysiological studies of foreign channels. In this study stage V-VI collagenase treated oocytes have been used to examine the effects of redox agents on intrinsic currents using two electrode voltage clamping. A rapid and strong potentiation of an inward rectifier barium sensitive current (Ir) was observed upon bath application of two membrane permeable reducing agents dithiothreitol (DTT) or 2-mercapto ethanol (β MOH), for example 6 mM DTT produced a 5-6 fold increase in Ir, similar results were obtained with 10 mM β MOH. Such modulation was dose dependent, reversible by washing out and the rate of washout was enhanced in the presence of the oxidizing agent H_2O_2 at 3 mM. The membrane-impermeable reducing agent glutathione (GSH) at concentration of up to 10 mM and 5 minute incubation periods did not produce a significant change in the Ir current. H_2O_2 at 1 mM inhibited Ir by 25-35 %. No significant change was observed in the outward currents with any of these reagents. Although the kinetics of the currents were found to be variable these findings have been reproduced in 5 different batches of oocytes in two different countries, however in one batch Ir was almost 0 and the modulation was absent. The presented results suggest that care should be taken when studying the effects of redox modulation in expressed ion channels in oocytes. The biophysical mechanism of redox modulation of Ir current in single channel analysis is being carried out.

Su-Pos241

EFFECTS OF CHRONIC HYPOXIA ON DEVELOPMENTAL CHANGES IN ACTION POTENTIAL AND IONIC CURRENTS OF CULTURED NEONATAL RAT VENTRICULAR MYOCYTES. ((K. Kamiya, W. Guo and J. Toyama)) Nagoya University, Nagoya, Japan. (Spon. by K. Yasui)

We studied effects of continuous exposure to hypoxia on developmental changes in action potential (APD) and repolarizing potassium channels in cultured neonatal rat cardiac myocytes. Ventricular myocytes from day-old rat were cultured in normoxic condition (21% O_2). To test the effect of hypoxia, O_2 tension was lowered to 7.5% in some cells at day 6 during culture. Action potentials, Ito and IK were measured at day 5 and 15 both in these two groups. In 15-day cells of normoxic condition, APDs were shortened by 44% (n=10-11) compared with 5-day cells. Ito density was increased by 194% (n=11-12) and IK density was gradually increased by 113% (n=10-12) at 15 day. In the hypoxic condition, APD did not change significantly (16%, n=6). Ito was slightly increased (53%, n=8) under hypoxic conditions due to the loss of the fast inactivating component of Ito. IK was not increased in hypoxic condition. These results suggest that 1) cultured neonatal rat ventricular myocytes still possess the ability to undergo the cell differentiation, 2) the shortening of action potential during culture was prevented by hypoxic condition, 3) sensitivity to hypoxia of developmental change is different dependent on each ion channel.

Su-Pos243

DIFFERENTIAL EFFECTS OF CELL SWELLING ON CARDIAC ION CHANNELS. ((Y.-Y. Zhou, J.-A. Yao, M. E. Sanchez*, and G.-N. Tseng)) Dept of Pharmacol., Columbia Univ., New York, NY 10032, * Univ. of Valle, Cali, Colombia.

We studied the effects of cell swelling on K and Ca channels in canine ventricular myocytes using the whole-cell configuration of patch clamp method. Cell swelling was induced by reducing the tonicity of the bath solution from 290 to 160 mOsm. The cell width was measured using a video monitor along with currents during the course of experiments. Cells swelled when exposed to the hypotonic solution, but the rate and degree of swelling varied. The slow delayed rectifier current (I_{Kr}) was increased during swelling, with the degree of increase higher when the control current was small or when the rate of swelling was fast. This increase could not be prevented by H-8 (100 μ M via the pipette), by colchicine (100 μ M) or by taxol (50 μ M). Swelling caused a consistent acceleration of inactivation of the L-type Ca channel (I_{CaL}) during depolarization. However, the peak amplitude of I_{CaL} during swelling showed variable changes: it was reduced or not altered, sometimes with the reduction preceded by a transient increase. Swelling caused an increase in the inward rectifier current (I_{K1}) in the voltage range negative to E_K . There was little or no change in I_{K1} in the outward direction. Swelling caused a small reduction in the peak amplitude of the transient outward current (I_{to} , at +60 mV reduced to 80-90% of control). On returning to the isotonic solution, the cell width rapidly recovered, along with a reversal of the changes in I_{Kr} , I_{K1} and I_{to} . However, the reduction of I_{CaL} was not reversible. We conclude that cell swelling has complicated effects on K and Ca channels in canine ventricular myocytes. The increase in I_{Kr} and the acceleration of I_{CaL} inactivation should contribute to action potential shortening under these conditions.

Su-Pos240

FATTY ACID ETHYL ESTER-INDUCED ALTERATIONS IN THE ACTIVATION KINETICS OF KVL1.1 ((R.A. Gubitosi-Klug and R.W. Gross)) Departments of Medicine, Chemistry, Molecular Biology and Pharmacology, Washington University School of Medicine, St. Louis, MO 63110

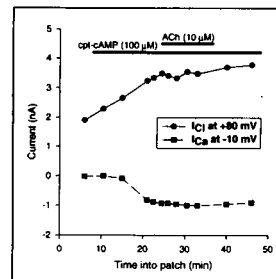
(Spon. by D.F. Stickle)

Recent studies have documented the enzymatic synthesis of ethanol to fatty acid ethyl esters by the brain. Herein we demonstrate that fatty acid ethyl esters, non-oxidative metabolites of ethanol, induce substantial alterations in the kinetics of activation of the human brain delayed rectifier potassium channel, Kvl1.1 (HuK1). When applied externally to Sf9 cells expressing recombinant Kvl1.1, ethyl arachidonate caused a dose-dependent increase in the rate of activation of the macroscopic current over the range of -20mV to +20mV (0 mV activation rate constant decreased from 27.3 ± 1.7 ms to 13.0 ± 1.8 ms with 20 μ M ethyl arachidonate) and a 10 mV hyperpolarizing shift in the voltage of activation without evidence of channel inactivation. These effects were not due solely to the nature of the aliphatic group since ethyl esters comprised of 16:0, 18:1 and 22:6 fatty acyl chains produced identical effects. Furthermore, extended ester linkages (e.g., propyl and butyl) mimicked the effects whereas shortened ester linkages (e.g., methyl) did not induce any kinetic alterations. Finally, although application of ethanol alone or oleic acid alone did not result in the observed alterations in activation kinetics, the concomitant application of ethanol and oleic acid reproduced the effects of ethyl esters which is likely due to the intracellular production of fatty acid ethyl esters by Sf9 cells. Collectively, these results suggest that fatty acid ethyl esters modulate the function of ion channels and thus may play a role in the pathophysiologic sequelae of ethanol abuse in excitable tissues.

Su-Pos242

LACK OF CHOLINERGIC ANTAGONISM OF cAMP-INDUCED CHLORIDE CURRENT IN CAT CARDIOCYTES. ((T.E. Schackow and R.E. Ten Eick)) Department of MPBC, Northwestern University, Chicago, IL 60611.

In guinea-pig (GP) ventricular myocytes (VM), it is known that acetylcholine (ACh) can antagonize β -adrenergic inhibition of inwardly-rectifying K^+ current (I_{K1}) through direct activation of protein phosphatases (PPs), independently of its effect on adenylate cyclase (Koumi *et al.*, *J Physiol* 486:647, 1995). To determine if ACh has a similar antagonistic effect on cAMP-induced chloride current (I_{Cl}) in cat VM, a conventional whole-cell patch-clamp technique was used to record I_{Cl} in adult feline left VM isolated from collagenase-perfused hearts. Using I_{Cl} -specific solutions at 35° C, both I_{Cl} and L-type calcium current (I_{CaL}) could be induced by extracellular exposure to 8-(4-chlorophenylthio)-cAMP (cpt-cAMP, 100 μ M). Addition of ACh (10 μ M) to the extracellular solution while continuing cpt-cAMP failed to antagonize the stimulatory effect of cpt-cAMP on either I_{Cl} or I_{CaL} , and subsequent washout of ACh failed to elicit a rebound increase in either current (see figure). Because this finding differs from the effect of ACh on cAMP-inhibited I_{K1} in GP (see above), it suggests that there is a dissimilarity between cat and GP in the coupling of cholinergic receptors to PPs.



Su-Pos244

Ca^{2+} -DEPENDENT INWARD RECTIFICATION OF CARDIAC CELLS IS CONTROLLED BY THE CYTOSKELETON. ((M. Mazzanti, A. Ferroni, A. Assandri, and D. DiFrancesco)) Dipartimento di Fisiologia e Biochimica Generali, Laboratorio di Elettrofisiologia, via Celoria 26, I-20133, Milano, ITALY.

The cardiac inward-rectifier K-channel (IR) is modulated by several intracellular components. Current rectification, for example, disappears when divalent ions and polyamines are removed from the cytoplasm (Matsuda *et al.*, 1987, *Nature* 325, 156; Mazzanti and DiFrancesco, 1989, *Pflügers Arch.* 413, 322; Lopatin *et al.*, 1994, *Nature* 372, 366). It is still controversial if outward current blockade is achieved in a unique way or by means of separate mechanisms. Mg^{2+} operates a voltage-dependent block and so do polyamines. In a previous study we described the modulation of the IR outward current by submicromolar concentration of intracellular Ca^{2+} , which is able to restore rectification after abolishment in divalent-cation-free solutions. Abolishment of Ca^{2+} -dependent rectification develops slowly with time, as if an intracellular mechanism important in this process were lost. We hypothesize a role of cytoskeleton in the Ca^{2+} -induced rectification. In this study we investigate the rectification mechanism in single IR channel from ventricular guinea-pig cardiac cells using inside-out patches. Addition of Cytochalasin D to the internal side of the membrane speeds up loss of rectification and prevents Ca^{2+} , but not Mg^{2+} , action. We suggest that cytoskeleton mediates the ability of Ca^{2+} ions to modulate outward current in IR channels.

Su-Pos245

EFFECTS OF FK506 ANALOGS ON RYANODINE RECEPTORS ((Gohar Jamil, Robert Hagar, Edward J. Kaftan and Barbara E. Ehrlich)) Department of Physiology, University of Connecticut Health Center, Farmington, CT 06030-1305

The ryanodine receptor (RyR), the major intracellular calcium release channel in striated muscle, is tightly associated with FK-binding protein (FKBP), a 12 kDa polypeptide possessing cis-trans peptidyl-prolyl isomerase (PPI) activity. FKBP forms a complex with the immunosuppressant drug FK506 and this complex inhibits calcineurin, a calcium dependent protein phosphatase. The molecular mechanism by which FKBP modulates the calcium release channel is unknown. Analogs of FK506, which do not react with calcineurin and which have varying K_i's for inhibition of PPI activity, were added to RyR incorporated into planar lipid bilayers. As found for FK506 and rapamycin, addition of the test compounds increased the channel open probability and induced subconductance states. These results show that calcineurin does not play a significant role in FKBP dependent modulation of the calcium release channel and that these compounds will be useful probes of FKBP-RyR interactions.

Supported by NIH grant HL33026 and the Patrick and Catherine Weldon Donaghue Medical Research Foundation. Compounds used in this study were generously provided by David Amistead, Vertex Pharmaceuticals, Inc.

Su-Pos246

MODIFICATION OF RYANODINE RECEPTOR CHANNEL KINETICS BY AB-RYANODINE, A PHOTOACTIVATABLE DERIVATIVE OF RYANODINE. ((T. Connelly¹, A. J. Lokuta¹, D. R. Witcher², K. P. Campbell² and H. H. Valdivia¹)) ¹University of Wisconsin-Madison and ²University of Iowa, Iowa City.

10-O-[3-(4-AzidoBenzamido)propionyl]ryanodine (AB-ryanodine), a photoactivatable derivative of ryanodine, profoundly modifies both gating and conduction of single ryanodine receptor (RyR) reconstituted in lipid bilayers. Three discrete, time- and concentration-dependent effects were evident. 1. At nanomolar concentrations, AB-ryanodine increases open probability *without modifying channel conductance*. This effect occurs with a relatively fast onset and is fully reversible. However, application of a train of high-power UV laser flashes to AB-ryanodine-modified channels renders the effect irreversible, presumably by covalent binding to the RyR. Thus, AB-ryanodine is a powerful tool to identify high-affinity ryanodine binding domains. 2. At low micromolar concentrations, AB-ryanodine induces the appearance of a subconductance state that represents ~50% of the full conductance level. This effect, like that of native ryanodine, is irreversible within the timeframe of bilayer experiments. However, a remarkable difference is that AB-ryanodine-treated channels do not "lock" into a single conducting mode, but fluctuate freely and stochastically between modified and unmodified conduction states. 3. At concentrations $\geq 300 \mu\text{M}$, AB-ryanodine irreversibly locks the channel in a non-conducting state. The results indicate that binding of AB-ryanodine to the high affinity site is a relatively rapid and reversible phenomenon and that the sequential occupation of sites with lower affinity leads to an irreversible conformational rearrangement of the channel protein that reduces ion translocation. (AB-ryanodine was synthesized and provided by Terry Lewis, ZENECA Agrochemicals, Jealott's Hill Research Station, Bracknell, Berkshire RG12 6EY, Great Britain). Supported by AHA, NIH and HHMI.

CHANNELS - LIGAND GATING

Su-Pos247

VOLTAGE DEPENDENT SWITCHING BETWEEN SUB AND MAIN CONDUCTANCE LEVELS IN RECOMBINANT MUTANT NMDA RECEPTOR CHANNELS. ((Louis S. Premkumar and Anthony Auerbach)) Dept. Biophysics, SUNY at Buffalo, Buffalo, NY 14214. (Spon. by A. Auerbach)

Single channel currents were recorded from recombinant mouse NMDA receptor channels having mutations in both ζ_1 and ζ_2 subunits of the M2 segment (expressed in *Xenopus* oocytes). Asparagine (N) in wild type was replaced by glutamine (Q) in both subunits at positions 598 and 589, respectively. When activated by NMDA (25 to 50 μM) in the absence of extracellular calcium or magnesium (ultrapure salts, 1.5 mM EGTA) the channel main conductance was 92 pS, the subconductance was 62 pS. These conductance levels occurred with about equal probability. The kinetic and conductance properties were estimated using hidden Markov model algorithms. The main to sub and sub to main transition rate constants were 416 ± 30 and $326 \pm 22 \text{ s}^{-1}$ at -80 mV ($n = 14$ patches, mean \pm s.e.m.). When the membrane potential was depolarized both switching rate constants decreased (224 and 217 s^{-1} , at -40 mV) and when the membrane was hyperpolarized both switching rate constants increased (650 and 484 s^{-1} , at -120 mV). Both rate constants increased e-fold with the hyperpolarization of $\sim 125 \text{ mV}$ ($z\delta=0.2$). These results suggest the membrane potential influences the height of an energy barrier that separates the main and subconductance structures. Scale: H-60 ms V-10 pA (supported by NSF 9102232).



Su-Pos249

THE EFFECT OF AMINO ACID SUBSTITUTIONS IN RECOMBINANT NMDA CHANNELS ON THE BLOCK BY INTERNAL AND EXTERNAL MAGNESIUM ((Jürgen Kupper, Jacques Neyton and Philippe Ascher)) Laboratoire de Neurobiologie, Ecole Normale Supérieure, 75005 Paris, France.

Magnesium ions can block NMDA channels by entering the pore from either the extracellular or the cytoplasmic surface of the membrane in a voltage dependent manner. To determine the location of the blocking site(s) within the permeation pathway we have studied wild type and mutant NMDA channels expressed in *Xenopus* oocytes. We have made several amino acid substitutions downstream of the Q/R/N site in the TMII region. Mutant NR1 subunits were coexpressed with wild type NR2A subunits and vice versa. The effect of these mutations on the block by external Mg^{2+} ions was determined by measuring the reduction of macroscopic currents in response to increasing concentrations of Mg^{2+} using two-electrode voltage clamp. To determine the effect of the mutations on the block by internal Mg^{2+} , we measured the single-channel conductance in outside-out patches in the presence and absence of 4 mM internal magnesium. We found that individually mutating the first four amino acid residues downstream to the Q/R/N site affects both the block by external and the block by internal Mg^{2+} . Mutations of residues six and seven positions downstream of the Q/R/N site do not influence the external Mg^{2+} block. However, they dramatically influence the block by internal Mg^{2+} . Together, these data confirm the hypothesis, that TMII forms a loop that reemerges towards the cytoplasmic site of the membrane. In addition, they demonstrate clearly that the blocks produced by internal and external Mg^{2+} can be separated, leaving little doubt that there are two separate binding sites for magnesium ions within the permeation pathways of NMDA channels. Supported in part by a HFSP fellowship to JK.

Su-Pos248

DIFFERENT GATING CHARGE MOVEMENTS IN DOUBLY-, SINGLY-, AND UNLIGANDED ACETYLCHOLINE RECEPTORS ((A. Auerbach, W. Sigurdson, J. Chen, G. Akk)) Dept. of Biophysical Sciences, SUNY, Buffalo, NY 14214.

The voltage dependence of binding and gating in wild-type and mutant recombinant mouse nicotinic acetylcholine receptors expressed in HEK cells were examined at the single-channel level (cell attached patches). The association, dissociation, and channel opening rates were not voltage-sensitive, but the closing rate constant of doubly-liganded receptors decreased e-fold with $\sim 66 \text{ mV}$ hyperpolarization in both wild type (adult and embryonic) and mutant receptors (αG153S , αD200N , αL251C , ϵT264P , βT265P , δS268P , αY93F). The voltage dependence of closing in singly-liganded receptors was examined in receptors with a binding site (αG153S) or a pore (αL251C and ϵT264P) mutation. The closing rate constant of these singly-liganded receptors decreased e-fold with $\sim 124 \text{ mV}$ hyperpolarization. The voltage dependence of closing in unliganded receptors was examined in the receptors αL251C , ϵT264P (at 22 and 10°C). The closing rate constant of unliganded receptors was not voltage dependent. The results suggest that the charge movement during channel closure is $z\delta=0.4$ in doubly-liganded receptors, 0.2 in singly-liganded receptors, and 0.0 in unliganded receptors, where z is the amount of charge and δ is the distance that the charge moves in the electric field. It is unlikely that ACh^+ moves in the field during gating, thus the voltage-dependence gating charges probably arises from the movement of charge in receptor protein. The results suggest that in addition to closed-vacant and open-occupied conformations, the receptor can assume intermediate structures that differ with regard to charge distribution. (supported by NIH NS-23513 and MDA).

Su-Pos250

FTIR SPECTROSCOPY AND $^1\text{H}/^2\text{H}$ EXCHANGE SUGGEST AN EXCHANGE RESISTANT CORE OF α -HELICAL PEPTIDE HYDROGENS IN THE NICOTINIC ACETYLCHOLINE RECEPTOR ((N. Methot and J.E Baenziger)) Dept. Biochemistry, University of Ottawa, Ottawa, Canada, K1H 8M5

FTIR spectra of the nAChR recorded after 3 days in $^2\text{H}_2\text{O}$ at 4°C exhibit a residual amide II band intensity indicative of roughly 25% exchange resistant peptide hydrogens in the nAChR. To investigate the secondary structure of the exchange resistant peptide hydrogens, the downshifts in frequency of individual α -helix and β -sheet amide I component bands upon peptide $^1\text{H}/^2\text{H}$ exchange have been monitored using resolution enhanced and difference spectroscopy. The downshifts in frequency of bands due to the exchange of β -sheet are relatively intense over the first 12 hours after exposure to $^2\text{H}_2\text{O}$ whereas only weak bands are observed for the exchange of α -helical peptide hydrogens. After 3 days in $^2\text{H}_2\text{O}$, substantial amide I band intensity remains at 1655 cm^{-1} suggesting a large population of unexchanged α -helical peptide hydrogens. Conversely, the intensity near 1655 cm^{-1} decreases under conditions that lead to the exchange of the 25% exchange resistant peptide hydrogens. The results suggest that the majority of the 25% exchange resistant peptide hydrogens in the nAChR are α -helical in nature and argue for predominantly α -helical transmembrane domains.

Su-Pos251

ORIGIN OF ANTAGONIST- AND AGONIST-INDUCED CHANGES IN THE CIRCULAR DICHROISM OF THE nAChR PEPTIDE FRAGMENTS. ((Qing-luo Shi, *Daina Avizonis, *V. J. Basus and Edward Hawrot)) Dept. of Molecular Pharmacology and Biotechnology, Brown University, Providence, RI 02912 and *Dept. of Pharmaceutical Chemistry, Univ. Calif., San Francisco, San Francisco, CA 94143

The invariant Cys-192 and Cys-193 in the α -subunit of the nicotinic acetylcholine receptor (nAChR) have been implicated by numerous studies as being involved in the binding domain for nicotinic agonists and antagonists. These two cysteines participate in an unusual and rare vicinal disulfide bond that forms an eight-membered ring whose detailed structure in the protein has yet to be elucidated. Our previous studies have shown that nAChR peptide fragments containing α 192/193 disulfide bond, e.g. α 181-198 (18mer) or α 185-196 (12mer), can bind to α -bungarotoxin as well as agonists, acetylcholine or carbamylcholine, and exhibit binding-induced circular dichroism (CD) in both the sidechain and backbone regions. Our present efforts compare a 5mer, TCCPD (α 191-195), containing the disulfide bond, with a tetramer, WVYY (α 187-190), rich in aromatics, in order to understand the binding mechanism and the binding-induced CD change observed in the longer nAChR peptides. We find that the ligand-binding activity of nAChR peptides may require the interaction of the vicinal disulfide with adjacent aromatics or other residues, as neither TCCPD nor WVYY alone can exhibit the same ligand-binding induced CD changes as observed with the longer nAChR peptides. Both TCCPD and WVYY appear essentially structureless by CD in contrast to the longer 12mer and 18mer nAChR peptides. The absence of ligand-induced CD changes with TCCPD or WVYY is consistent with the notion that the binding-induced CD changes observed for the 12mer and 18mer may reflect real conformational changes rather than a microenvironmental perturbation of the sidechain chromophores. (Supported by NIH-GM32629)

Su-Pos253

EXAMINATION OF AGONIST INTERACTIONS WITH UNNATURAL NICOTINIC ACETYLCHOLINE RECEPTOR MUTANTS. ((M.W. Nowak¹, P.C. Kearney¹, W. Zhong², S. K. Silverman¹, C.G. Labarca¹, M.E. Saks¹, J.R. Sampson¹, J. Abelson¹, N. Davidson¹, D.A. Dougherty² and H.A. Lester¹)). ¹Div. of Biology, ²Div. of Chemistry, Caltech, Pasadena, CA 91125. (Spon. by C. Doupnik)

We have previously demonstrated the ability to introduce unnatural amino acids into ion channels employing the stop codon suppression method in *Xenopus* oocytes. Oocytes are coinjected with tRNA containing a UAG codon at the position of interest and a suppressor tRNA with the corresponding anticodon, CUA, and chemically acylated with the unnatural amino acid. We examined the interaction of acetylcholine (ACh) with conserved tyrosine residues in the α subunit at positions 93, 190 and 198 of the mouse nicotinic acetylcholine receptor (nAChR) by introducing derivatives of tyrosine and phenylalanine (Nowak et al., Science 268, 439, 1995).

We have extended the stop codon suppression method to examine the interaction of agonists with nAChR. To further understand the interaction of agonists with nAChR we compared the dose-response relationships for ACh to that for the simple quaternary ammonium tetramethylammonium (TMA). Since the millimolar TMA concentrations required for activation of the unnatural mutant nAChRs also block the channel we introduced leucine to serine mutations at the 9' position within the pore region of the α , β and γ subunits. These mutations shift the TMA activation of nAChR toward lower agonist concentrations (Labarca et al., Nature 376, 514, 1995) where channel block does not occur. TMA activation of the mutant nAChRs showed a similar pattern to that observed for ACh. These findings provide new insights on the interaction of the quaternary ammonium moiety of ACh with nAChR. Support: AHA, NIH, TRDRP.

Su-Pos255

MUTATIONS AT 10' IN THE CHANNEL PORE ALTER THE INTERACTION OF ISOFLURANE WITH NICOTINIC ACh RECEPTOR CHANNELS IN AN UNEXPECTED WAY. ((M. Barann, A.M. Vidal and J.P. Dilger)) Depts. of Anesthesiology, Physiology & Biophysics, SUNY, Stony Brook, NY 11794.

Our previous studies showed that the general anesthetic isoflurane (Iso) and other uncharged drugs inhibit the muscle-type acetylcholine receptor channel by directly binding to the channel protein. The data are consistent with Iso sterically blocking the flow of ions through the pore, but an allosteric mechanism cannot be excluded. To test the idea Iso binds within the pore, we studied wild-type (WT) and mutant channels transiently expressed in HEK293 cells. WT channels consist of mouse $\alpha_2\beta\gamma\delta$ subunits. Mutant channels have polar-to-nonpolar substitutions at the 10' level of the M2 region that lines the pore: α S10'A, β T10'A. Because the nonpolar end of the quaternary amine QX-222 binds at 10' (Neuron 2: 87, '90), Iso may also bind there. Macroscopic currents were activated by rapid perfusion of outside-out patches with 100 μ M ACh. Control currents were compared with currents obtained during constant exposure of the patch to Iso. The mutants were 4-times as sensitive to inhibition by Iso; the IC_{50} s were 1.3 mM (WT) and 0.3 mM (mutant). Single channels were activated by perfusion with 0.2 μ M ACh. Surprisingly, the frequency and duration of gaps within Iso-induced bursts were the same for WT and mutant channels. Thus, the mutation does not change the kinetics of Iso binding. Macroscopic currents recorded during transient exposure of mutants to Iso confirm this. We conclude that Iso does not bind at 10'. The apparent high affinity of the mutant for Iso may be related to a mutation-induced 2-fold acceleration of desensitization. We hypothesize that Iso desensitizes closed mutant channels. Supported by GM42095.

Su-Pos252

PROBING THE STRUCTURE OF THE NICOTINIC ACETYLCHOLINE RECEPTOR (nAChR) WITH 4-BENZOYLBENZOYLCHOLINE (Bz₂choline), A NOVEL PHOTOAFFINITY COMPETITIVE ANTAGONIST. ((D. Wang, Y. Xie, and J.B. Cohen)) Department of Neurobiology, Harvard Medical School, Boston, Ma. 02115.

Bz₂choline, a photoreactive acetylcholine (ACh) analog, was synthesized and its interactions with *Torpedo* nAChR studied. For *Torpedo* nAChR expressed in *Xenopus* oocytes, Bz₂choline acts as an antagonist with an $K_i=1.2 \mu$ M. Based upon direct radioligand binding, [³H]Bz₂choline binds at equilibrium with equal affinity ($K_d=1.4 \mu$ M) to the two ACh sites per AChR, and it is bound with 3-fold higher affinity in the presence of the noncompetitive antagonist, proadifen. Upon UV irradiation, [³H]Bz₂choline is specifically incorporated into AChR γ - and δ -subunits with similar efficiency, but not at all into α - (or β -) subunits. After 30 min irradiation, the level of ³H incorporation is equal to 15% of γ - or δ -subunit. The selective photolabeling of non- α subunits contrasts with the patterns of incorporation seen previously for other antagonist affinity reagents where labeling of α -subunit was seen predominantly or exclusively and even for [³H]tubocurarine where labeling of γ - and δ -subunits was of similar efficiency as α -subunit. With its defined photochemistry, [³H]Bz₂choline will serve as a unique probe to identify amino acids of the ACh binding site interacting with the aromatic groups of choline ester antagonists.

Su-Pos254

MUTATIONS CAN ALTER THE IONIC SELECTIVITY OF THE ACETYLCHOLINE RECEPTOR TRANSMITTER BINDING SITE. ((G. Akk and A. Auerbach)) Dep. of Biophysical Sciences, SUNY, Buffalo, NY 14214.

Inorganic, monovalent cations are competitive inhibitors of ACh binding. In adult, wild type mouse ACh receptors, the EC_{50} of the dose response curve is 16, 28, and 46 μ M in 142 mM Na⁺, K⁺, and Cs⁺, respectively. Single-channel kinetic analysis (mouse AChR expressed in HEK cells; cell attached patches) reveals that the ACh association rate constant is slowed by the presence of the ions in a manner that is consistent with competitive inhibition. The K_s for Na⁺, K⁺, and Cs⁺ are 150, 92, and 38 mM, respectively. This observation raises the possibility that mutations that shift dose-response curves do so by altering the K_s for the competing cation. We have examined the ionic selectivity of several AChR that have mutations near the putative transmitter binding site. The mutants α D200N, α Y198F, α Y93W, α Y93S, ϵ D175N, and ϵ E184Q have right-shifted dose-response curves. In all except α D200N and ϵ E184Q the mutation decreases the ACh association rate constant. The K_s for K⁺ in the mutants are similar to those of the wild type except for α Y93S (~60 mM) and ϵ E184Q (322 mM). In ϵ E184Q both the affinity for ions, and selectivity between ions, of the binding site are reduced as the K_s for Na⁺, K⁺, and Cs⁺ are 381, 322, and 110 mM, respectively. In this mutant the ACh⁺ dissociation rate constant is ~5 times faster than the wild type, and we speculate that the lower affinity for inorganic ions is due to a similarly increased dissociation constant. These results suggest that residue ϵ E184 electrostatically stabilizes both ACh⁺ and inorganic ions in the ACh receptor transmitter binding pocket. (Supported by NIH NS-23513 and MDA).

Su-Pos256

A FAMILY OF DYES AS HIGH AFFINITY NONCOMPETITIVE ANTAGONISTS OF THE NICOTINIC ACETYLCHOLINE RECEPTOR. ((M. M. Lurtz and S. E. Pedersen)) Department of Molecular Physiology and Biophysics, Baylor College of Medicine, Houston, TX 77030.

The binding of aminotriaryl methane dyes to the nicotinic acetylcholine receptor (AChR) of *Torpedo californica* has been characterized. The affinity of these compounds for the noncompetitive antagonist binding site was measured by inhibition of [³H]phencyclidine binding. Observed affinities in physiological saline ranged from 60 nM to 7.5 μ M. The affinity depended upon the amine substitution and degree of methylation of the dyes and the conformational state of the receptor. Desensitization of the AChR by the agonist carbamylcholine increased the affinities 4 to 10 fold. Binding was insensitive to changes in ionic strength. Aminotriaryl methane dyes do not bind the agonist binding site as measured by inhibition of [³H]acetylcholine binding ($K_s \geq 100 \mu$ M). The high affinities and high extinction coefficients make the dyes crystal violet, ethyl violet, and new fuchsin excellent acceptors for diffusion enhanced fluorescence energy transfer using Tb³⁺ and Eu³⁺ as fluorescent donors. Bimolecular rate constants for energy transfer to these three dyes ranged from 45 to 600 $\times 10^6$ M⁻¹s⁻¹. (This work was supported by NIH grant NS28879.)

Su-Pos257

THRESHOLD CHOLESTEROL CONCENTRATIONS REQUIRED FOR RAPID AGONIST-INDUCED STATE TRANSITIONS IN THE NICOTINIC ACETYLCHOLINE RECEPTOR ((Saffron E. Rankin and Keith W. Miller)) Department of Anesthesia, Massachusetts General Hospital, and Department of Biological Chemistry and Molecular Pharmacology, Harvard Medical School, Boston, MA 02114

Nicotinic acetylcholine receptor-mediated ion flux recorded over 30 seconds indicated that channel opening only occurs when cholesterol is present in the surrounding membrane (Fong and McNamee, *Biochemistry* 25, 830 (1986)). We have used stopped-flow fluorescence to investigate whether cholesterol mediates rapid conformational changes. Ethidium bromide, a non-competitive inhibitor, binds to the nAChR with a large increase in fluorescence intensity within 10 milliseconds of mixing in the presence of high, but not low, concentrations of carbachol. This component was characterized over increasing carbachol concentrations and was found to have a K_d equal to that reported for carbachol-induced channel opening (1 mM) and an observed rate that was equivalent to that of fast desensitization. We concluded that ethidium fluorescence was reporting the development of the fast desensitized state. This component was sensitive to changes in bilayer composition and was not observed when the receptor was reconstituted into DOPC, DOPC-DOPA, and DOPC-cholesterol bilayers. Increasing the cholesterol content in DOPC-DOPA membranes from 0 to 5% had no effect on the amplitude of this component. From 5% cholesterol the amplitude increased rapidly reaching a maximum when the membrane contained 20% cholesterol. No further influence on the amplitude was observed as the cholesterol content was increased to 50%. Its observed rate constant, however, was independent of cholesterol concentration. This has led us to hypothesize that cholesterol facilitates channel opening and the onset of fast desensitization either by binding to specific sites at the lipid-protein interface on the nAChR, which must be occupied for a functionally viable receptor (Jones and McNamee, *Biochemistry*, 22, 2364 (1988)), or by flipping from the outer to the inner leaflet of the bilayer to release membrane bending stresses caused by the onset of fast desensitization.

(Supported by GM15904)

Su-Pos259

Diadenosine-polyphosphates: Inhibitory ligands of cardiac ATP-sensitive K^+ channels.

((A. Jovanovic and A. Terzio)) Division of Cardiovascular Diseases, Mayo Clinic, Rochester, MN, USA.

The intracellular mononucleotide-dependent gating of ATP-sensitive K^+ (KATP) channels is well established. To assess whether dinucleotide polyphosphates, a family of endogenous compounds structurally-related to ATP and associated with intracellular signaling during metabolic stress, could also modulate this ion conductance, currents were measured in the inside-out configuration and diadenosine tetra-, penta- and hexa-phosphates (Ap₄A, Ap₅A, Ap₆A) applied to the internal side of patches excised from guinea-pig ventricular cardiomyocytes. Ap₄A, Ap₅A and Ap₆A inhibited KATP channel activity, in a reversible and concentration-dependent manner (half-maximal concentrations ~17, 16, and 14 μ M, and Hill coefficients 1.2, 1.6, and 1.1, respectively). Hence, diadenosine polyphosphates are potent inhibitors of KATP channel activity. This represents a previously unrecognized property of dinucleotide polyphosphates, as well as the discovery of potentially novel endogenous ligands of myocardial KATP channels.

Su-Pos258

CO-EXPRESSION OF RAT GABA_A β 1 AND β 3 SUBUNITS WITH α 5 AND γ 2L IN L929 FIBROBLASTS PRODUCES A UNIQUE RECEPTOR CONTAINING BOTH β SUBUNITS. ((J.L. Donnelly* and R.L. Macdonald*)) Departments of Neurology* and Physiology*, University of Michigan, Ann Arbor, MI 48104-1687.

GABA_A receptor (GABA_R) isoforms in the CNS are composed of pentameric combinations of α 1-6, β 1-4, γ 1-4 and δ 1 and ρ subunit subtypes. Individual cell types appear to express high levels of mRNA encoding different subunits and even multiple subunit subtypes. The stoichiometry of GABA_R isoforms, however, is unclear, and the number and identity of subtypes that are coassembled remain unanswered questions. To determine whether multiple β subtypes can be coassembled in functional GABA_Rs, recombinant cDNAs encoding rat β 1, β 3, α 5 and γ 2L subunits were cotransfected into the L929 fibroblasts, and the properties of the expressed receptors were determined using whole-cell and single-channel recording techniques. Expression of α 5 β 1 γ 2L or α 5 β 3 γ 2L receptors produced currents with different GABA EC₅₀s (β 1, 48 μ M; β 3, 8 μ M). Cells transfected with α 5 β 1 β 3 γ 2L subunits had an intermediate EC₅₀ for GABA of 17 μ M. GABA concentration response curves for all three isoforms were well fit by a single-site model with a Hill slope near 2.0, suggesting homogeneous populations of receptors. Loreclezole enhances β 3- but not β 1-containing isoforms; however, α 5 β 1 β 3 γ 2L receptors were loreclezole-insensitive. Single channel recording demonstrated that 1 μ M loreclezole increased channel open probability in outside-out patches from cells transfected with α 5 β 3 γ 2L subtypes but not from those transfected with α 5 β 1 β 3 γ 2L subtypes. All three isoforms were equally sensitive to pentobarbital. α 5 β 1 β 3 γ 2L currents were sensitive to diazepam, indicating that the γ subunit was incorporated into the receptors. These results suggest that functional GABA_A receptors can be formed that contain two different β subunits. Both β subunits contribute to the GABA binding sites, producing a receptor with properties different from either β subunit alone.

CHANNELS, SELECTIVITY

Su-Pos260

PROTON AND CHLORIDE CURRENTS IN CHINESE HAMSTER OVARY CELLS ((V.V. Cherny, *L.M. Henderson, T.E. DeCoursey)) Department of Molecular Biophysics and Physiology, Rush Presbyterian St. Luke's Medical Center, Chicago, IL, *Department of Biochemistry, University of Bristol, United Kingdom

Proton and anion conductances were studied in Chinese hamster ovary (CHO) cells using whole-cell recording. The pipette solution contained tetramethylammonium methanesulfonate, highly buffered to pH 5.5. An outwardly rectifying anion conductance was observed in nearly all cells, with a relative permeability of $\text{MeSO}_3^- \leq 0.5$ that of Cl^- . The anion conductance was small immediately after establishing whole-cell configuration, increased rapidly to a maximum at ~5 min, and then decreased more slowly to a small value over tens of minutes. A small voltage-activated H^+ -selective conductance (g_{H}) was also observed in most cells, and was studied after the Cl^- conductance had subsided. The tail current reversal potential shifted 78 mV when pH_o was changed from 7.0 to 5.5, compared with 87 mV for E_{H} . The g_{H} was activated by depolarization and high pH_o , and exhibited gating kinetics comparable with H^+ currents in other mammalian cells. The average H^+ current at +40 mV at pH_o 7.0 was 1.6 pA/pF. The presence of endogenous anion and H^+ conductances should be taken into consideration when CHO cells are used for expression of ion channels.

Support: American Heart Association Grant-in-Aid, NIH grant HL52671.

Su-Pos261

CATION PERMEATION AND TEA BLOCK IN A DELAYED RECTIFIER K^+ CHANNEL IN DORSAL ROOT GANGLION NEURONS. ((S.J. Korn)) Physiol. and Neurobiol., Univ. Connecticut, Storrs, CT 06269

The delayed rectifier potassium channel in chick dorsal root ganglion neurons allows Na^+ to permeate in the absence of K^+ . Addition of K^+ blocks Na^+ conductance in a concentration-dependent manner. Furthermore, external TEA blocks currents carried by K^+ but not Na^+ (Callahan and Korn, *J. Gen. Physiol.*, 1994). These results suggested that selectivity was based on a competition for pore occupancy, and that the channel pore was conformationally flexible. To further understand the permeation characteristics of this channel, we've extended these studies to other ions. In the presence of Na^+ , Li^+ conductance was negligible. Replacement of intracellular Na^+ with the impermeant ion NMG⁺ permitted Li^+ to conduct. Li^+ conductance was inhibited in a concentration-dependent fashion by addition of Na^+ , with approximately half the Li^+ current inhibited by 10 mM Na^+ . In biionic experiments, K^+ almost completely prevented Cs^+ conductance and Cs^+ had little influence on K^+ conductance. However, replacement of K^+ by Na^+ resulted in a large Cs^+ conductance. External TEA blocked K^+ and Cs^+ currents but not Na^+ and Li^+ currents. These data further support the hypothesis that the channel pore is conformationally flexible, and can be shaped by the permeating ion. However, they argue against the hypothesis that the pore assumes a conformation that permits occupancy by just the largest permeant cation. Supported by NSF and the UCONN Research Foundation.

Su-Pos262

CATION BINDING TO GRAMICIDIN A IN WATER/METHANOL MIXTURES STUDIED BY EU³⁺ EXCITATION SPECTROSCOPY. ((Wojciech P. Grygiel and Michael E. Starzak)) Department of Chemistry, State University of New York at Binghamton, Binghamton, NY 13902-6018.

An aqueous complex of europium ion and gramicidin is characterized using environment-sensitive laser excitation spectroscopy of the Eu³⁺ ion. As the mole percent of water in a water/methanol mixture is increased, a single absorption line for the aqueous ion at 578.9 is augmented by two narrow lines at 579.1 nm while the lifetimes observed following selective excitation to each of these new lines signal the loss of two and three waters, respectively, from the inner hydration sphere on formation of the ion/gramicidin complexes. The local ligand field symmetry is deduced from the ⁷F₀ - ⁵D₂ transitions. The eight absorption lines remaining after elimination of known lines for the aqueous ions are resolved into a triplet and pentet for the two gramicidin binding sites. The triplet is generated by ions at a binding site having at least C_{2v} symmetry. This symmetry is consistent with binding to the interior or ends of a double helix or the ends of a single helix of the molecule. Three waters are displaced from the inner hydration sphere of the more symmetrical complex.

Su-Pos264

SELECTIVITY AND ACTIVATION OF THE INFLUENZA VIRUS M₂ ION CHANNEL ((L.H. Pinto*, K. Shimbo**, D. Brassard*, and R.A. Lamb**)) Dep'ts of *Neurobiology & Physiology and *Biochemistry, Molecular Biology & Cell Biology and #Howard Hughes Medical Institute, Northwestern University, Evanston, IL 60208

The influenza A virus-associated M₂ ion channel is thought to function by acidifying the virion interior and equilibrating the pH gradient across the trans Golgi network in the infected cell. A necessary test of these roles is to show directly that the M₂ ion channel conducts protons. We measured the intracellular pH (pH_{in}) of voltage-clamped oocytes, their current-voltage relationship, and their flux of ⁸⁶Rb. We also studied the effects of low pH_{in} on activation. We found that (a) oocytes incubated in low pH medium underwent a slow acidification that was blocked by the M₂ ion channel inhibitor, amantadine; (b) the current-voltage relationship shifted to more positive values and had greater conductance when the pH_{out} was lowered, and this relationship was modified when Na⁺ was replaced by NH₄⁺ or Li⁺; (c) the oocytes had a slow, amantadine-sensitive influx of Rb⁺, and (d) the effects on the current-voltage relationship of reduced pH_{in} were opposite to the increased conductance found with reduced extracellular pH. We interpret these results to mean that the M₂ ion channel is capable of conducting H⁺ as well as other ions and that the channel conductance is reduced by decreased pH_{in}. These findings are consistent with the proposed roles of the M₂ protein in the life cycle of influenza A virus.

Su-Pos266

ROLE OF THE H5 REGION IN ION SELECTIVITY AND PERMEATION IN AN INWARD RECTIFIER K⁺ CHANNEL. ((J. Yang, Y.N. Jan and L.Y. Jan)) HHMI, Dept. of Physiol. and Biochem., Univ. of California, San Francisco, CA 94143. (Spon. by E. Reuveny)

Inward rectifier K⁺ channels conduct inward current more efficiently than outward current and, like voltage-gated K⁺ channels, are highly selective for K⁺ ions. The two classes of channels differ markedly in their overall amino acid sequence but share a high homology in a short stretch (~18 amino acids) called the H5 region. It has been shown that this region is critical for ion selectivity and permeation in the voltage-gated K⁺ channels. In contrast, little is known about the functional importance of the H5 region in the inwardly rectifying K⁺ channels. One difficulty that has hampered the study of the H5 region in inward rectifiers is that many point mutations are "lethal" - they completely abolish current flow, thus making it difficult to characterize the functional consequences of the mutations. We have overcome this problem by constructing tandem tetramers that contain only one or two mutant subunit(s) together with three or two wild-type subunits (IRK1) and examining the functional properties of the channels expressed in *Xenopus* oocyte. Our results indicate that while the H5 region in inward rectifier K⁺ channels is crucial for ion conduction, it appears to have properties distinct from those in voltage-gated K⁺ channels.

Su-Pos263

STRUCTURAL DETERMINANTS FOR K⁺ AND Ca²⁺ SELECTIVITY IN THE VOLTAGE-GATED Na CHANNEL. ((I. Favre*, E. Moczydlowski* and L. Schild**)) *Institut de Pharmacologie et Toxicologie de l'Université, CH-1005 Lausanne, Switzerland; #Dept. of Pharmacology, Yale Univ. School of Medicine, New Haven, CT 06520-8066.

Residues Asp/Glu/Lys/Ala (D/E/K/A) in P-regions of Na channel domains I/II/III/IV corresponding to Glu/Glu/Glu/Glu (E/E/E/E) in voltage-gated Ca channels have been found to determine the selective permeability of monovalent vs. divalent inorganic cations (Heinemann et al., 1992). We have carried out systematic mutations of the charged residues D400, E755 and K1237 in the μ 1 isoform and determined their effect on P_K/P_{Na} and P_{Ca}/P_{Na} permeability ratios.

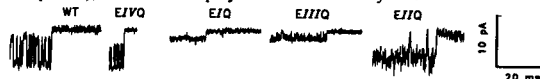
Mutants were expressed in *X. laevis* oocytes and permeability ratios determined from changes in reversal potentials after external ionic substitutions using two electrode voltage-clamp. Data obtained for single and combined mutations are shown in the Table. They indicate that the changes in P_K/P_{Na} or P_{Ca}/P_{Na} are greater for mutations in domain III>II>I. Furthermore Ca²⁺ permeation through the Na channel requires the absence of a positively charged residue at position K1237 and the presence of a negatively charged residue at any of the positions 400, 755 or 1237 in μ 1 channel isoform. Therefore K1237 plays a critical role for maintaining selective Na⁺ permeability in voltage-gated Na channels.

mutants	P _K /P _{Na}	P _{Ca} /P _{Na}
wt (DEKA)	0.03	0
D400A (AEKA) ¹	0.03	0
E755A (DAKA) ²	0.1	0
K1237A (DEAA) ³	1.1	7.6
K1237R (DERA)	0.9	0
K1237F (DEFA)	1.1	4.4
AAAA ¹⁽²⁺³⁾	1.0	0
DAAA ⁽²⁺³⁾	0.9	1.0
AEEA ⁽¹⁺³⁾	1.1	3.3
AAEA ^(1+2+K1237E)	1.0	6.2

Su-Pos265

HOW PROTON BLOCK OF L-TYPE Ca²⁺ CHANNELS IS AFFECTED BY MUTATIONS OF P-REGION GLUTAMATES ((X.-H. Chen, I. Bezprozvanny and R.W. Tsien)) Dept. of Mol. Cell. Physiol., Stanford, CA 94305.

To study structural determinants of Ca channels responsible for proton block (Prod'homme et al., 1987), we obtained single-channel recordings from L-type Ca channels ($\alpha_{1C}\beta_{2A}\alpha_2$) expressed in *Xenopus* oocytes. The cell-attached patch pipette solution contained 150 mM K⁺ in D₂O. Blockade by H⁺ ions (D⁺ in our experiments) was strongly affected by mutations of the four P-region glutamates that form the locus of high affinity Ca²⁺ interaction (Yang et al., 1993). Individual Glu→Gln replacements in each of four P-regions produced varied effects on proton block (Figure, -100 mV, pD=8.5 with HEPES). Wild type channels (WT) displayed two conductance states, 140 pS (deprotonated) and 40 pS (protonated). Similar conductances were seen with the E1/Q mutant but occupancy of the protonated state was reduced by acceleration of the H⁺ off-rate. The E/Q mutant displayed the ~40 pS state without apparent sublevels. The E1/Q mutant showed the ~40 pS conductance, but also transient block to an even lower level. The E1/Q mutant was the only one to exhibit three conductance states, somewhat reminiscent of CNG channels (Root & MacKinnon, 1994). The middle level (~70 pS) was strongly predominant. These three conductances may correspond to the deprotonated state and two distinct protonated states. We hypothesize that the protonation site in L-type channel is formed by multiple glutamate side chains acting in coordination (E/ and E1/ and perhaps E1/), whereas E1/Q plays a more secondary role.



Su-Pos267

RNA EDITING MAKES HOMOMERIC GLUR6 SUBUNIT CHANNELS PERMEABLE TO ANIONS WITHOUT ALTERING THE APPARENT SIZE OF THE PORE. ((N. Burnashev and B. Sakmann)) MPI für medizinische Forschung, Heidelberg, D-69120, Germany.

Ion flow through non-NMDAR channels depends critically on the amino acid present at the Q/R site, a position in the M2 domain presumably forming a part of the permeation pathway. Subunit specific RNA editing generates two isoforms, either an R (edited) or a Q (unedited). We investigated whether pore dimensions of these two isoforms were different. The Q- and R-forms of the kainate receptor GluR6 subunit were expressed in HEK 293 cells and bilinear reversal potentials for organic cations of different mean diameters were determined (with Cs⁺ as internal reference cation). The permeability-diameter relation suggests that the diameter of the narrow portion of the homomeric Q-form channels is approximately 7.5 Å. Surprisingly, homomeric R-form channels showed a measurable anion permeability (P_{Cl}/P_{Cs} of 0.7) which attenuated the reversal potential measurements for organic cations. The permeability-diameter plot corrected for the anion permeability indicates that the apparent pore size for the R-form channels is close to 7.3 Å, comparable to that of the Q-form and identical to the diameter of the heteromeric channels composed of Q- and R- form subunits (7.3 Å). The heteromeric channels were purely cation selective suggesting that a ring of the positively charged amino acids in the pore is necessary to impart the anion permeability.

Su-Pos268

DETERMINATION OF THE RELATIVE STABILITY OF DIFFERENT CONFORMERS OF GRAMICIDIN A ANALOGUES – A NOVEL FREE ENERGY PERTURBATION APPROACH. ((S. Shobana¹, B. Roux², G. Saberwal¹, O. S. Andersen¹, and R. E. Koeppe II³)) ¹Dept. Physiology & Biophysics, Cornell Univ. Med. Coll., New York, NY 10021, ²Dept. Chem., Univ. de Montreal, Montreal, Canada H3C 3J7, ³Dept. Chem. & Biochem., Univ. of Arkansas, Fayetteville, Arkansas 72701. (Spon. by L. G. Palmer)

We have carried out free energy perturbation (FEP) calculations to determine the effect of a single point mutation on the relative stability of channel formed Gramicidin A (gA) analogues. The mutations were performed on the analogue gLW (Formyl-L-Val-Gly-L-Ala-D-Leu-L-Ala-D-Val-L-Val-D-Val-L-Leu-D-Trp-L-Leu-D-Trp-L-Leu-D-Trp-L-Leu-ethanolamine). The relative free energies associated with the right- and left-handed, single-stranded $\beta^{6,3}$ -helical conformers of gLW were computed to estimate how an Ala⁵→Val⁵ point mutation affected the conformational preferences between the single-stranded $\beta^{6,3}$ -helical channels formed by gLW. A novel mutation procedure was adopted in the FEP calculations, and the relative free energies were verified by means of WHAM (weighted histogram analysis method). The computed energies are being compared with experimental results.

Su-Pos270

RESIDUE 5 OF GRAMICIDIN LW AS A CONFORMATIONAL "SWITCH"

((Le, N.H.*¹, Greathouse, D.V.*², Koeppe, R.E. II*, Saberwal, G.*³, Providence, L.L.*⁴, & Andersen, O.S.*)) ¹Univ. Arkansas, Fayetteville, AR, ²Cornell Univ. Med. Coll., N.Y., NY

A series of gramicidin A (gA) analogues in which the alternating (L-Trp-D-Leu)-L-Trp C-terminal sequence has been changed to (L-Leu-D-Trp)-L-Leu (gLW) have been shown to form multiple conformations in lipid bilayers (Saberwal, et al. 1995, Biophys. J. 68, A151). Single-channel conductance measurements reveal that while gLW and V⁹gLW form double-stranded (DS) channels, V⁵gLW and V⁵A⁸gLW do not. All of these gLW's (also) form both left- and right-handed single-stranded (SS) channels. Circular dichroism spectra of gLW and V⁹gLW in DMPC vesicles are similar to that of gA (mirror-image of gA), while those of V⁵gLW and V⁵A⁸gLW differ dramatically, exhibiting large positive ellipticities at 229 nm. Size-exclusion chromatography demonstrates that gLW, V⁹gLW, V⁵gLW and V⁵A⁸gLW are 30%, 40%, 74%, and 60% DS in DMPC, respectively. Together, these results suggest that residue 5 regulates a SS↔DS conformational switch in the gLW family, with V⁵ inducing a non-conducting DS conformation and A⁵ favoring a conducting DS conformation, presumably due to a wider pore.

Su-Pos272

CONFORMATIONAL STUDIES OF MIXTURES OF GRAMICIDIN A ANALOGUES THAT DIFFER IN LENGTH BY ±1 RESIDUE

((Lundquist, J. J., Greathouse, D. V., and Koeppe, R. E. II.)) Dept. of Chem. & Biochem., Univ. of Arkansas, Fayetteville, Arkansas 72701

Gramicidin (gA) analogues with a length difference of ±1 residue have been shown to form destabilized heterodimeric channels with gA due to a "gap" in the peptide backbone (Durkin, et al. 1993, J. Mol. Biol. 231, 1102-1121). In addition, *endo*-Gly⁰-gC/gA and *des*-Val¹-[Gly²]-gC/gA heterodimeric channels exhibit multi-state (flickering) behavior with voltage dependent transitions between two conductance levels that are not seen with the corresponding Ala analogues (Durkin, 1993). Size-exclusion chromatography (SE-HPLC) and circular dichroism spectroscopy (CD) were used to study mixtures of *endo*-Gly⁰-gA, *endo*-D-Ala⁰-gA, *des*-Val¹-[D-Ala²]-gA, and *des*-Val¹-[Gly²]-gA with gA in dimyristoylphosphatidylcholine vesicles. The CD spectra of *endo*-D-Ala⁰-gA and *endo*-Gly⁰-gA are similar to that of gA. *Endo*-Gly⁰-gA, however, displays increased negative ellipticity at 229 nm, suggesting the presence of a mixture of single-stranded (SS) and double-stranded (DS) conformers. In mixtures with gA, an increase in the amount of DS-dimer was observed by both CD and SE-HPLC with increasing mole fraction of *endo*-Gly⁰-gA. Similar trends were observed for *des*-Val¹-[D-Ala²]-gA and *des*-Val¹-[Gly²]-gA. The results parallel earlier findings with Tyr¹ gramicidins (Blount, et al. 1995, Biophys. J. 68, A152) in suggesting that a 'tension' between SS and DS conformations may relate to the bistable, voltage-dependent behavior of some heterodimeric gramicidin channels

Su-Pos269

GRAMICIDIN CHANNELS IN PHOSPHOLIPID BILAYERS HAVING UNSATURATED ACYL CHAINS. ((J. Girshman¹, O. S. Andersen¹, D. Greathouse², and R. E. Koeppe II³)) ¹Dept. Physiol. Biophys., Cornell Univ. Med. Coll., New York, NY 10021, ²Dept. Chem. Biochem., Univ. Arkansas, Fayetteville, AR 72701. (Spon. by O. S. Andersen)

In organic solvents, gramicidin A (gA) exists as a mixture of double-stranded (DS) dimers, but membrane-spanning gA channels are single-stranded (SS) $\beta^{6,3}$ -helical dimers. Recently Cox et al. (*Biochemistry* 31:1112, 1992) and Sychev et al. (*Eur. Biophys. J.* 22:279, 1993) showed that the conformational preference of gA varies with bilayer acyl chain unsaturation: $\pi\pi^{5,6}$ DS helices predominate over SS helices in membranes with unsaturated chains (C_{18:2}). Na⁺ promotes the formation of $\pi\pi^{5,6}$ DS helices, implying that Na⁺ binds to $\pi\pi^{5,6}$ DS-helices. This raises the possibility that $\pi\pi^{5,6}$ DS helices could function as ion conducting channels. We characterized the channels formed by gA in POPC/*n*-decane, DOPC/*n*-decane, and DLoPC/*n*-decane membranes. There was no evidence for (long-lived) channels that could be $\pi\pi^{5,6}$ DS helices in any of these membranes. We conclude that the SS $\beta^{6,3}$ -helical dimer is the only conducting species in these membranes. Surprisingly, the average channel duration and channel-forming potency of gA is increased in DLoPC membranes, as compared to POPC and DOPC membranes. Experiments with other gA analogues suggest that the changes in average duration result not only from a tryptophan stabilization in the more polar membrane interior in the DLoPC membranes, but also from changes in membrane mechanical properties.

Su-Pos271

INFLUENCE OF SPACER RESIDUES BETWEEN TRYPTOPHANS ON GRAMICIDIN CHANNEL PROPERTIES

((A.R. Jude¹, D.V. Greathouse², R.E. Koeppe³ II, L.L. Providence⁴, O.S. Andersen⁵)) ¹Dept. Chem. Biochem., Univ. Arkansas, Fayetteville, AR 72701, ²Dept. Physiol. Biophys., Cornell Univ. Medical College, N.Y., N.Y. 10021

Substitutions of the "spacer" Leu residues between the tryptophans of gramicidin A (gA) with Ala, Val, and Ile have shown that both bulk and branching are important determinants of channel properties (Jude, et al., (1995) Biophys. J. 68, A151). Ala^{10,12,14} gA exhibited the largest deviations from gA with dramatically reduced channel life-time and channel-forming potency. To further examine the effect of size at these positions, Phe^{10,12,14}gA and Ala¹⁰gA where synthesized and examined by circular dichroism spectroscopy (CD), size-exclusion chromatography (SE-HPLC), and single-channel measurements. The CD spectra of Phe^{10,12,14}gA and Ala¹⁰gA are similar to that of Ala^{10,12,14}gA exhibiting a single positive ellipticity at 220 nm and negative ellipticity below 208 nm. The Phe^{10,12,14}gA and Ala¹⁰gA display larger positive ellipticities at 220 nm than Ala^{10,12,14}gA, but relatively similar ellipticities to gA. SE-HPLC indicates that Phe^{10,12,14}gA and Ala¹⁰gA elute mainly as single-stranded subunits. The elution profile for Ala¹⁰gA is much narrower than for Ala^{10,12,14}gA, suggesting less conformational mixing.

Su-Pos273

SOLUTION STRUCTURE OF A PARALLEL LEFT-HANDED DOUBLE-HELICAL GRAMICIDIN A DETERMINED BY 2D ¹H NMR. ((Y. Chen*, A. Tucker* and B.A. Wallace*))

^{*}Dept. of Crystallography and ^{*}Biomedical NMR Centre, Dept. of Chemistry Birkbeck College, University of London, London, U.K..

The structure of a parallel left-handed double-helical gramicidin form was determined in CaCl₂/methanol solution using 600 MHz NMR. Measurements of TOCSY, DQF-COSY and NOESY spectra were converted into distant and dihedral angle constraints for the structure calculations. 610 NOEs and 28 coupling constants were used to generate structures. Chi I angles were calculated using ³J_{AB}, d_{AB}(i,i) and d_{AB}(i,i). Stereospecific assignments of leucine and valine methyl groups were achieved by analysis of ³J_{AB}, d_{AB}(i,i), d_{AB}(i,i) and d_B(i,i). The calculations of initial structures performed using the distance geometry/simulated annealing method in XPLOR. Refinement of the initial structures was done using simulated annealing/molecular dynamics methods. Back-calculations for every generated structure were also performed to check their consistency with the experimental data. Twenty final structures with no violation of the threshold conditions (0.05Å, 5°, 5°, 0.5Å and 5° for bonds, angles, improper, noe and cdhe respectively) were produced from the fifty structures calculated. The RMSD for the final structure is 0.1Å for backbone and 1.2 Å for all non-hydrogen heavy atoms. The motif of this parallel structure has 6.0 residues per turn. The length along the helical axis is 30.5 Å and the inner pore diameter varies between 2.3 Å and 3.4 Å. It is different from all other gramicidin structures determined to date.

(Supported by grants from the BBSRC (to baw) and the ULIRS (for NMR facilities))

Su-Pos274

SOLID STATE NMR OF GRAMICIDIN A TO STUDY CHANNEL SELECTIVITY AND GRAMICIDIN ANALOGS TO PROBE THE FUNCTIONAL ROLES OF TRYPTOPHAN. ((F. Tian¹, M. Cotten¹, D. Busath², and T.A. Cross¹)) ¹Department of Chemistry, Florida State University, Tallahassee, FL 32306-4005, ²Department of Biology, Brigham Young University, Provo, Utah 84602.

The affinity of gramicidin A transmembrane channel for the Group I cations ranged from 32 for Li⁺ to about 55 M⁻¹ for K⁺, Rb⁺, and Cs⁺. However, the selectivity between Li⁺ and Cs⁺ is 1:15. It has been suggested that factors other than equilibrium binding contribute to the selectivity of the channel. One possibility is that the binding of different cations to the channel modulates channel structure which may enhance or decrease the permeability of cations. Details of the structural modification induced by the different cations will be reported.

Tryptophan substitution is one of the chemical modifications that may dramatically affect channel activity and the conformation of gramicidin. Possible explanations describe two roles for tryptophan. The first one involves electrostatic effects of the indole ring dipole moment on channel function. The second role relates the amphipathic property and location of tryptophan to the folding and stability of gramicidin in lipid bilayers. These two roles may be investigated separately in gramicidin A analogs containing the appropriate amino acids. For instance, fluoro-substituted tryptophans provide a way to modulate the dipole moment orientation of the aromatic side chains while preserving closely the other properties of tryptophan. Conversely, substituting phenylalanine for tryptophan modifies the amphipathic character and hydrogen-bonding capacity of the peptide. In light of the solid state NMR characterization, conclusions about the roles of tryptophan will be presented.

Su-Pos276

FREE ENERGY PROFILES FOR ORGANIC CATIONS IN GRAMICIDIN A CHANNELS. ((Y. Hao and D.D. Busath)) Brown University, Providence, RI 02912.

Umbrella sampling molecular dynamics was used to compute the free energy profiles for four organic cations in right-handed single-helix gramicidin A dimers. The umbrella sampling was computed with Charmm using the following system: The dimeric channel structured in the Arseniev conformation with extended-atom representation of nonpolar hydrogens was oriented along the x-axis. A column was formed of 30 water molecules with the ion of interest in the center and was placed along the x-axis. Two 13 Å radius water balls with vacant ~3 Å diameter cores through the center (187 molecules total) were positioned at the ends of the channel with the cores along the x-axis so as to surround the water column. Pieces of the free energy profile were computed from 10 ps dynamics runs at each of 70-90 ion positions along the channel ranging from x=0 Å (channel center) to x=15 Å (outside the channel). The overlapping pieces were connected using the method of umbrella potential differences. Neglected long-range electrostatic energies from the bulk water and the bilayer were computed using Delphi and added to the profile. The approach was corroborated for the formamidinium-guanidinium pair using perturbation dynamics at four key spots on the pathway: x=0, 6, 12, and 15 Å. The barrier to ethylammonium entry was prohibitive at 21 kcal/mol, whereas for methylammonium it was 5.5 kcal/mol and the profile was quite flat through the channel, roughly consistent with conductance measurements. The profile for formamidinium was very similar to that of methylammonium. Guanidinium had a high entry barrier ($\Delta G=+8.6$ kcal/mol) and a narrow deep central well ($\Delta G=-2.6$ kcal/mol), qualitatively consistent with predictions from voltage-dependent potassium current block measurements. Its deep central well was verified with perturbation dynamics and was correlated with its high propensity to form hydrogen bonds with the channel at the dimer junction (not shared by the other three cations). Analysis of the ensemble average radial forces on the ions demonstrates that all four ions undergo compressive forces in the channel which are maximal at the center of the monomer and relieved at the dimer junction illustrating increased flexibility of the channel walls in the center of the channel.

Su-Pos278

SOLVENT ISOTOPE SUBSTITUTION EFFECTS ON THE KINETICS OF AMINO ACID RESIDUE IONIZATION IN THE α -TOXIN CHANNEL.

((J.J. Kasianowicz[†] and S.M. Bezrukov[‡])) [†] NIST, Biotechnology Div., Gaithersburg, MD 20899; [‡] DCRT, NIH, Bethesda, MD 20892

Staphylococcus aureus α -toxin forms a relatively large ion channel that exhibits pH dependent properties. Specifically, the single channel current increases markedly when the pH decreases. We reported earlier using noise analysis that this behavior is caused by the reversible ionization of several amino acid residues inside the channel (Kasianowicz & Bezrukov, 1995, *Biophys. J.* 70:94). We show that solvent substitution (D₂O for H₂O)-induces a change in the steady-state, equilibrium, and kinetic properties of this channel. In particular, D⁺/H⁺ substitution causes a decrease in the channel NaCl conductance of ~15%, a shift in the pK ($\Delta pK = +0.5$), a 3.8-fold decrease in the dissociation rate constant, and a reduction of the association rate constant by a factor of 1.2. We compare here our results to previous reports on the influence of solvent substitution on ion channel characteristics. We discuss the pK shifts that were observed by others for short oligopeptides and globular proteins. Finally, the mechanisms by which isotopic substitution elicits these effects are reviewed and analyzed. Supported by the NAS/NRC (JJK) and by the ONR (V.A. Parsegian).

Su-Pos275

SIMULATION OF A GRAMICIDIN CHANNEL IN A FLUID PHASE DMPC BILAYER ((S. W. Chiu, S. Subramaniam, and E. Jakobsson)) University of Illinois, National Center for Supercomputing Applications, Urbana, IL 61801

We have simulated a gramicidin channel in a fluid phase DMPC membrane. The simulated preparation includes the channel, 96 DMPC molecules, and 3200 water molecules. The simulation uses NVT boundary conditions, similar to constant pressure but with the virial component in the lateral direction set according to the surface tension rather than the pressure in the experimental chamber. At the present writing, approximately 1 simulated nsec after the channel insertion, the preparation is equilibrated by the standard of stabilization of potential energy, and data analysis has begun. Contrary to simulations of the gramicidin channel in vacuum, the simulated protein is completely stable in the membrane with no artificial restraints. The mobility of water in the channel is about 1/4 that of bulk water. The presence of the channel seems to stabilize the membrane against short range thickness fluctuations, as compared to comparable lipid bilayer simulations with no protein present. We hypothesize that this is because of the interactions between the tryptophan side chains and the phospholipid head groups. The space around the mouth of the channel is impinged on by phospholipid head groups, which must form part of the access path for ions entering the channel. Statistical and energetic information about the structure and dynamics of the system will be presented. Supported by the National Science Foundation and the National Center for Supercomputing Applications

Su-Pos277

BOUNDARY CONDITIONS FOR SINGLE-ION DIFFUSION. ((Pete McGill and Mark F. Schumaker)) Department of Pure and Applied Mathematics, Washington State University, Pullman, WA 99164-3113.

We have constructed a theory for diffusion through the pore of a single-ion channel by taking a limit of a random walk around a cycle of states. Similar to Levitt's theory of single-ion diffusion (1986, *Annu. Rev. Biophys. Biophys. Chem.* 15:29-57), one obtains boundary conditions for the Nernst-Planck equation which guarantee that the pore is occupied by at most one ion. Two of the terms in the boundary conditions are identical to those given by Levitt. However, the construction gives rise to a third term not found in Levitt's theory. With this term, the channel spends exponentially distributed intervals in the empty state. Ion sample paths have been simulated to help visualize trajectories near the channel entrances, with and without the new term. We use the Modified Levitt Theory to fit several potential profiles to the conductance data of Barrett-Russell et al. (1986, *Biophysical J.* 49:673-686). Potentials which give the best fit to the data have binding sites 9 or 10 Å from the channel center, in agreement with recent NMR measurements. In particular, we have analyzed the profile for Na⁺ in gramicidin calculated by Roux and Karplus (1993, *J. Am. Chem. Soc.* 115:3250-3262). The peak-to-peak amplitude of their result must be reduced to at most 35% of its original value to fit the data. But with this reduction, excellent fits are obtained.

Su-Pos279

LIPID BILAYER SURFACE CHARGE EFFECTS ON ALAMETHICIN CHANNEL CONDUCTANCE AND NOISE.

((S.M. Bezrukov¹, I. Vodyanoy^{1,2}, V.A. Parsegian¹)) ¹DCRT & NIDDK, NIH, Bethesda, MD 20892, USA; ²ONR, Europe, London, NW1 5TH, UK.

Proton titration of "charged" bilayers varies the density of surface charge that influences ion channel transport properties. To examine the effects of lipid charge on ion currents through mesoscopic channels, we are studying alamethicin channels in L- α -Phosphatidylserine (PS) bilayers. We measure average current and current noise at a particular conductance level as functions of pH. Different levels of the channel respond differently to the change in the surface charge density. Specifically, higher conductance levels are relatively less sensitive to the charge on the bilayer surface. Studying the screening of surface charge by changing ionic strength, we relate these differences to the channel structural features using an approach similar to that developed earlier (Bell & Miller, 1984, *Biophys. J.*, 45, 279; Green, et al., 1987, *J. Gen. Physiol.*, 89, 841). To address the kinetics of the process we search for current noise from reversible protonization of lipid headgroups near the channel. To describe the results we extend a recent model, previously used in the studies of protonization of amino acid residues in an ion channel water pore (Bezrukov & Kasianowicz, 1993, *Phys. Rev. Lett.*, 70, 2352; Kasianowicz & Bezrukov, 1995, *Biophys. J.*, 69, 94), to include lateral mobility of lipid molecules in the two-dimensional lipid shell surrounding the channel.

Su-Pos280

STRUCTURE AND DYNAMICS OF A VOLTAGE-GATED PEPTIDE: NMR STUDIES OF ALAMETHICIN AND ITS ANALOGS ((J. Jacob, J. F. Ellena, D. S. Cafiso)). Department of Chemistry and Biophysics Program, The University of Virginia, Charlottesville, VA 22901.

Alamethicin (ALM) produces a voltage dependent ion-conductance in lipid bilayer systems. It belongs to a family of peptides called Peptaibols which have an abundance of Aib (α -methylalanine) residues and a reduced C-terminus. A more hydrophobic analog based on the replacement of Leu for Aib (L1) was shown previously to elicit alamethicin-like activity (Molle et al., Biopolymers 28, 173, 1989). We have determined the structure of L1 in SDS micelles by simulated annealing of ^1H NMR data. L1 appears to be less helical than native ALM, which could be the basis for the higher voltage dependence of this analog. The dynamics of alamethicin is being investigated by measuring paramagnetic enhancements of nuclear relaxation produced by a nitroxide label attached to the peptide C-terminus. Distances obtained from these enhancements are much shorter than those expected for a linear structure and are expected to reflect the r^{-6} weighted average of electron-nuclear distances. This data provides strong evidence that alamethicin is flexible in solution, which could be a result of proline at position 14. In order to investigate the role of proline in the dynamics of this peptide, an analog of alamethicin where proline is replaced by alanine has been synthesized. Distance measurements that are obtained in this analog will be presented.

Su-Pos282

CHEMICALLY CROSS-LINKED ALAMETHICIN CHANNELS. ((L. Lien, K.A. Crowhurst, S. You and G.A. Woolley)) Department of Chemistry, University of Toronto, Toronto M5S 1A1, Canada

Native alamethicin channels exhibit a characteristic pattern of conductance transitions. We find that covalently linking the C-terminal ends of two alamethicin molecules leads to selective stabilization of alternate conductance levels, providing support for the barrel-stave model of the channel architecture. In addition, a preferred maximum conductance state of channels formed by dimers is observed. This state, which has a lifetime of nearly 0.3 s and current homogeneity comparable to gramicidin channels, is proposed to correspond to a channel consisting of 6 alamethicin molecules (3 dimers). The shape of the IV curve for these stabilized channels depends on ionic strength, a feature which gives insight into the molecular structure of the pore.

Su-Pos284

PORE FORMATION KINETICS OF MASTOPARAN ANALOGS IN UNILAMELLAR LIPID VESICLES.

((A. Arbuzova and G. Schwarz)) Biocenter of the University, Basel, Switzerland.

Mastoparins, amphipathic tetradecapeptides isolated from wasp venom, associate with membranes inducing apparent pore formation. The interaction of polystyrene Mastoparan (MPP) and Mastoparan-X (MPX) with the membrane of unilamellar POPC and DOPC vesicles has been investigated with fluorescence assays. The time course of the pore formation was monitored by the fluorescence signal $F(t)$ reflecting the release of the marker substance carboxyfluorescein, entrapped in the vesicles at a self-quenching concentration. The data were analyzed according to a recently proposed theory allowing a quantitative evaluation of the pore kinetics and the mode of dye release. A mode of graded release was found for both peptides and large unilamellar vesicles (LUVs). The average dye retention factor of a single pore in POPC LUVs turned out to be $p=0.70\pm0.05$ for MPP and $p=0.55\pm0.05$ for MPX. The measured fluorescence signal $F(t)$ has been converted into the average retention function $R(t)$, i.e. the fraction of marker retained inside the liposomes. Then the number of pore openings per liposome could be determined and fitted to a pertinent time function. The same mechanism of the pore formation is envisaged for both peptides as they have a very similar amphipathic structure and the relevant kinetic parameters show qualitatively the same dependence on the concentration of actually bound peptide.

Su-Pos281

TRANSMEMBRANE MIGRATION OF HYDROPHOBIC CHANNEL FORMING PEPTIDES IN LIPID VESICLES DETERMINED USING ^1H AND ^{31}P NUCLEAR MAGNETIC RESONANCE SPECTROSCOPY. ((Sajith Jayasinghe, Melissa Barranger-Mathys, Jeffery F. Ellena, Craig Franklin and David S. Cafiso)). Department of Chemistry and Biophysics Program, University of Virginia, Charlottesville, VA 22901.

Alamethicin is a 20 amino acid peptide that forms voltage dependent ion channels in lipid bilayers. ^1H and ^{31}P nuclear magnetic resonance spectroscopy techniques were used to determine the transmembrane migration rate of the C-terminus of native alamethicin and a more hydrophobic analog that incorporates leucine in place of α -methylalanine (MeA). In the absence of a membrane potential the migration rate (or flip-flop) of native alamethicin was found to be no greater than $1.4 \times 10^{-4} \text{ min}^{-1}$. The analog of alamethicin incorporating leucine in place of MeA was found to migrate at least a 1000 times faster than the native peptide. Continuous wave power saturation EPR spectroscopy has shown that the leucine analog sits 3-4 Å deeper in the membrane than does the native alamethicin. It is proposed that the loss of hydrogen bonding between water and the C-terminus prevents the migration of this peptide. The leucine analog does not experience as large a barrier because the energy price for breaking hydrogen bonds at the C-terminus has already been paid by the additional hydrophobic partition energy of this analog.

Su-Pos283

THE MECHANISM OF VOLTAGE-GATING OF A PEPTIDE ION CHANNEL INVESTIGATED USING MAGNETIC RESONANCE. ((C. L. North, J. R. Lewis, M. R. Barranger-Mathys and D. S. Cafiso)). Department of Chemistry and Biophysics Program, University of Virginia, Charlottesville, VA 22901.

Alamethicin is a linear peptide that forms voltage-gated ion channels in lipid bilayers. We have investigated the orientation and membrane insertion of alamethicin in order to provide insight into the mechanism of gating of this channel. Solid-state ^{15}N NMR spectra of oriented DMPC bilayer samples indicate that alamethicin is linearly oriented parallel to the bilayer normal under conditions of zero voltage. Separated local field spectra of the ^{15}N -chemical shift and N-H dipolar splitting indicate that the N-H bond vectors for residues in the C- and N-terminal segments both have angles relative to B_0 of 25° , consistent with a linear α -helical configuration. Collision-gradient EPR experiments of site-directed spin-labeled analogs are consistent with the solid-state NMR results and indicate that the C-terminus lies outside the membrane in the aqueous phase. Based on these experiments several models for alamethicin gating can be eliminated. Models involving an insertion or conformational change in the peptide that lead to an enhanced peptide dipole-electric field interaction are consistent with the experimental data and will be presented.

1. Schwarz, G. and Robert, C.H. (1992) Biophys. Chem. 42, 291
2. Schwarz, G. and Arbuzova, A. (1995) BBA, in press
3. Arbuzova, A. and Schwarz, G. (1995) submitted for publication

Su-Pos285

A SLIGHT OUTER LEAFLET PERTURBATION PROMOTES PEG-INDUCED FUSION OF LIPID VESICLES (J. Lee* & B.R. Lentz) Dept. of Biochemistry and Biophysics, Univ. of North Carolina, Chapel Hill, NC 27599-7260.

Poly(ethylene glycol)-induced fusion of two different vesicle systems has been examined: dipalmitoylphosphatidylcholine (DPPC) large, unilamellar vesicles (LUV) and cardiolipin (CL):dioleoylphosphatidylcholine (DOPC) (1:10) LUV. A slight perturbation was established in DPPC LUV by hydrolyzing 0.8% of outer leaflet lipid with phospholipase A_2 to produce lyso-PC and palmitate that were then removed by bovine serum albumin. Ca^{2+} is purported to alter the shape of the CL molecule, so addition of 5mM Ca^{2+} to the external compartment of CL:DOPC LUV should create defects in outer leaflet packing of these vesicles. Contents mixing and leakage studied by ANTS/DPX assays showed that both vesicle systems fused only when the outer leaflet was perturbed as described. Two fluorescent probes (C_{12} -NBD-PC and TMA-DPH) were used to detect changes in outer leaflet molecular packing between non-fusing and fusing systems. The steady-state fluorescence intensity of C_{12} -NBD-PC added externally to either vesicle system was enhanced in fusing relative to non-fusing vesicles. Phase-resolved measurements of probe lifetime showed that this was mainly due to enhanced partitioning in the fusing systems of probe from a micellar into a membrane environment. C_{12} -NBD-PC showed only a slightly larger lifetime in fusing versus non-fusing membranes. Similarly, the lifetime of TMA-DPH was insensitive to whether this probe was incorporated into non-fusing or fusing vesicles. The failure of probe lifetimes to detect more polar membrane interiors suggests that the perturbations we produced took the form of local defects that were effectively filled by probe molecules. However, defects were apparently detected in terms of altered probe partitioning. The results suggest that creating packing defects in contacting bilayer leaflets is at least one means of promoting membrane fusion. Supported by USPHS grant GM32707.

Su-Pos287

TRANSLOCATION OF FLUORESCENT LIPOPHILIC DYES ACROSS LIPID BILAYERS. ((G.B. Melikyan, B.N. Deriy, F.S. Cohen)) Dept. Physiology, Rush Medical College, Chicago, IL 60612.

The lipophilic dyes octadecylrhodamine B (R18) and DiI-C18, widely used to monitor membrane fusion, are thought to remain in the monolayer leaflets in which they are placed. We report that contrary to this view both dyes translocate from one leaflet to the other in a voltage-dependent manner. Current transients that resulted from movement of the positively charged headgroups of R18 or DiI across voltage-clamped neutral planar bilayer membranes had time constants, τ , that decreased with increased voltage; $\tau(0$ mV) of the concentration-driven 'off' transients at the end of the voltage pulses were insensitive to the pulse amplitudes. Charge translocation was much slower than for hydrophobic ions such as tetraphenylborate: $\tau(0)$ was about 550 ms for R18 and 790 ms for DiI-C18 when 6 mol% of dye was in the membrane. DiI with shorter 12 carbon hydrocarbon chains (DiI-C12) translocated faster, $\tau(0) = 353$ ms. The total charge translocated was proportional to voltage in the low voltage range and saturated at high voltages. Charge movement was almost completely eliminated and the time constants for the residual current transients were dramatically increased when membranes were brought below their phase transition temperatures. At relatively high self-quenching concentrations (4-10%) of R18, translocation was associated with changes of fluorescence intensity, due to concentration-dependent quenching. Supported by NIH GM27367.

Su-Pos289

EFFECTS OF CYTOCHALASINS, SACCHARIDE POLYMERS, MOVEMENTS OF THE RECEPTOR OF TARGET CELLS ON SENDAI VIRUS-CELL FUSION. ((M. Wagner¹, T.D. Flanagan², and S.Ohki¹)) Department of Biophysical Sciences¹ and Microbiology², SUNY at Buffalo, Buffalo, NY 14214

Sendai virus-cell fusion has a strongly temperature-dependent characteristic; below 20°C, little fusion occurs while virus binds cells, and, above 20°C the fusion rate increases sharply with temperature. In order to determine which part of the membrane (viral envelope or target cell membrane) is responsible for such a temperature dependent phenomenon, virus-erythrocyte ghost fusion was measured at different temperatures under various conditions; the target cells treated with cytoskeleton affectors (cytochalasin B and D), the presence of various poly-saccharides, the use of lipid vesicles bearing the receptor (G_{d1a}) of the cell attachment protein of virus, etc. A fluorescence fusion assay, R_{18} , was used to determine the extent of fusion. It was found that the rate or extent of fusion varied depending on the conditions employed, however, the threshold temperature characteristic was little altered for all cases experimented. From this observation, it is deduced that the temperature-dependent characteristic of Sendai virus-target cell fusion is due to the nature of viral surface proteins.

Su-Pos286

TRANS-BILAYER LIPID REDISTRIBUTION ACCOMPANIES POLY(ETHYLENE GLYCOL)-INDUCED MEMBRANE FUSION Will Talbot, Lian-Tsing Zheng, and Barry R. Lentz; Dept. of Biochemistry & Biophysics; Univ. of North Carolina; Chapel Hill, NC 27599-7260.

Small, unilamellar vesicles (SUV) or large, unilamellar vesicles (LUV) containing a small amount of N-(4-nitrobenzo-2-oxa-1,3-diazole)-phosphatidylethanolamine (NBD-PE) have been made asymmetric in NBD-PE by reduction of outer leaflet probe with externally added sodium dithionite. Following removal of dithionite, transbilayer redistribution of NBD-PE could be quantitatively evaluated in terms of the observed loss of fluorescence intensity upon readition of dithionite. Vesicle rupture in the presence of PEG was measured both by loss of fluorescence associated with release of trapped Tb^{3+} complexed with dipicolinic acid (DPA) and by increase of fluorescence from 8-aminonaphthalene-1,3,6-trisulphonic acid (ANTS) released from vesicles in which it is complexed with a quenching agent. A Tb^{3+} /DPA assay was also used to monitor PEG-induced vesicle fusion. NBD-PE redistributed slowly (~2%/hr) in all SUV or LUV examined. NBD-PE redistribution was not accelerated by treatment of vesicles with PEG below concentrations that induced vesicle rupture or fusion. At or near PEG concentrations that induced vesicle rupture, NBD-PE redistribution was always observed. SUV prepared from hen egg yolk phosphatidylcholine (egg PC) or from dioleoylphosphatidylcholine (DOPC)/dilinolenoylphosphatidylcholine (diC_{18:3}PC) (85/15) mixtures were found to fuse without rupturing in certain ranges of PEG concentration. Under these conditions, the percent NBD-PE redistribution was proportional to the percent of one round of fusion, with a proportionality constant of roughly 0.2. It appears that inter-leaflet lipid redistribution accompanies whatever membrane structural changes are required for fusion but that lipid redistribution is not completed during the fusion process. Supported by USPHS grant GM32707.

Su-Pos288

CELLS HEMIFUSED BY GPI-LINKED INFLUENZA HEMAGGLUTININ CAN BE INDUCED TO FULLY FUSE. ((G.B. Melikyan, S.A. Brenner, D.C. Ok, J.M. White¹, F.S. Cohen)) Rush Medical College, Chicago, IL and U. of Virginia, Charlottesville, VA¹ (Sponsored by R.A. Levis).

Cells expressing the ectodomain of influenza virus-hemagglutinin linked to membranes via a lipid (GPI-HA) merge their outer leaflets with those of RBC membranes without transfer of aqueous contents, referred to as hemifusion. Hemifusion results in the formation of a single bilayer diaphragm composed solely of the inner leaflets of the two membranes. This suggests that the ectodomain of fully assembled HA induces hemifusion, whereas the transmembrane and, perhaps, cytoplasmic domains are required for the destabilization of the bilayer diaphragm. The normally stable diaphragm between hemifused GPI-HA cell-RBC pairs can be destabilized, either osmotically or chemically. Brief application of a hypotonic solution caused extensive lysis of RBCs loaded with 6-carboxyfluorescein, with transfer of the dye into 10% of the hemifused GPI-HA-expressing cells. Alternatively, the bilayer diaphragm was selectively destabilized, without extensive hemolysis, by the addition of cationic amphiphilic agents -- chlorpromazine, dibucaine, or trifluoperazine -- known to preferentially partition into the inner leaflets of cells and to cause hemolysis at mM concentrations. In contrast, anionic (e.g. trinitrophenol) or zwitterionic (lyssolecithin) compounds that incorporate into outer leaflets did not induce the transition from hemifusion to full fusion. Supported by NIH GM27367 and AI22470.

Su-Pos290

HIV DERIVED FUSION PEPTIDES: ORGANIZATION WITHIN MEMBRANES AND CAPACITY TO INHIBIT CELL-CELL FUSION ((¹Yossef Kliger, ¹Amir Aharoni, ¹Doron Rapaport, ²Philip Jones ²Robert Blumenthal and ¹Yecheil Shai)). ¹Department of Membrane Research and Biophysics, Weizmann Institute of Science, Rehovot, 76100 Israel, and ²Section on Membrane Structure and Function, Laboratory of Mathematical Biology, NCI, NIH, Bethesda MD, 20892 U.S.A. (Spon. by S.R. Caplan)

Peptides representing the 33 a.a. residues N-terminal of gp41 of HIV-1 (WT), and its V2E analogue, were synthesized, fluorescently labeled and spectroscopically and functionally characterized. Peptide-induced vesicle fusion was demonstrated by a lipid mixing assay, and electron microscopy. Only the WT peptide induced membrane fusion and bilayer perturbation of negatively-charged phospholipid vesicles. Circular dichroism spectroscopy in trifluoroethanol revealed similar α -helical contents in both peptides. Using fluorescently-labeled peptide analogues we found that; (i) both peptides bind strongly to phospholipid membranes ($K_D \sim 10^4 M^{-1}$), (ii) their N-termini are located within the hydrophobic core of the membrane, (iii) they self-associate and coassemble in the membrane, and (iv) they are susceptible to proteolytic digestion when bound to membranes, with a faster kinetic for the V2E analogue. Using fluorescence video imaging microscopy we found that both peptides (V2E > WT) could inhibit human cell-cell fusion. The results support a model where α -helical structure and self-association of peptides are necessary conditions for membrane fusion. The observed differences in the peptides' fusogenic abilities are hypothesized to result from differences in the peptides' degree of penetration into the membrane and induction of membrane destabilization. The data support HIV-cell fusion models where the fusion peptide play a crucial role in fusion induction by destabilizing the bilayer and by triggering the association of viral fusion protein molecules.

Su-Pos291

UNFOLDING PATHWAYS OF INFLUENZA HEMAGGLUTININ.
 ((David P. Remeta¹, Mathias Krumbiegel², Robert Blumenthal², and Ann Ginsburg¹)) ¹NHLBI and ²NCI, NIH, Bethesda, MD 20892

Hemagglutinin (HA) is the major surface membrane glycoprotein responsible for binding influenza virus to sialic-acid containing receptors in target cells. Fusogenic activity is triggered by a pH-dependent conformational change of HA in the acidic milieu of the endosomes. The conformational and thermal stability of HA (M_r 220,000) purified from influenza strain X31 has been investigated to characterize the pH and temperature-induced unfolding pathways. Comparison of near UV circular dichroism (CD) and intrinsic tryptophanyl residue fluorescence spectra reveals a significant loss of HA tertiary structure as the native conformation (pH 7.4) is exposed to fusogenic conditions (pH 4.8) at 37.0 °C. Distinct intermediate states are formed on the acid-induced unfolding pathway. The apparent disruption of tertiary structure coupled with a proton-induced increase in hydrophobicity and relatively invariant secondary structure are consistent with a model in which HA adopts a *molten globule* conformation in the fusogenic state. Elucidation of the thermal unfolding pathway by differential scanning calorimetry (DSC) suggests that changes in the number, size, and stability of thermodynamic domains as a function of pH may be attributed to the overall loss of tertiary structure. There is a significant decrease in the transition temperature (66.5 to 40.3 °C) and concomitant reduction in unfolding enthalpy (980 to 100 kcal/mol) as the conformational change occurs (pH 7.4 to 5.0). Despite the observed loss of tertiary structure, far UV CD spectra and thermal progress curves indicate that HA secondary structure is actually stabilized as the protein is exposed to fusogenic conditions. The proton-induced destabilization of tertiary structure (correlated with observed decreases in T_m and ΔH_{cal}) and apparent stabilization of secondary structure are novel features of hemagglutinin.

Su-Pos293

Influenza Virus-Liposome Lipid Mixing is Leaky and Largely Insensitive to the Material Properties of the Target Membrane

((Tong Shangguan^{1,3}, Dennis Alford^{1,2} and Joe Bentz¹)) ¹Department of Bioscience and Biotechnology, Drexel University, Philadelphia, PA 19104; ²Center for Blood Research Laboratory, Boston, MA 02115; ³The Liposome Company, Inc., Princeton, NJ 08540.

We have studied the kinetics of lipid mixing between influenza PR/8 virus and target liposomes as a function of various target membrane material properties. A pre-binding step was used to reach fusion-rate limiting conditions. To test the hypothesis that monolayer intrinsic curvature and void stabilization are important factors determining the rate of fusion, we studied the lipid mixing kinetics of dioleoylphosphatidylcholine/ganglioside liposomes both in the presence of exogenous lyso-oleoylphosphatidylcholine (LPC) and with endogenous LPC, dioleoylglycerol (DOG), arachidonic acid (AA), or hexadecane (HD). While exogenous LPC reversibly inhibited lipid mixing only at very high concentrations, 4 mol% endogenous LPC, DOG, AA and HD showed no significant effect. Using liposomes with various membrane rupture tension values, no correlation between target membrane rupture tension and rate of lipid mixing was revealed. Further investigations detected leakage of liposome contents during lipid mixing. For encapsulated molecules smaller than 450 MW, the kinetics of leakage is very similar to that of lipid mixing. Leakage was also detected for encapsulated molecules up to 10,000 MW, suggesting that HA mediated lipid mixing is a very leaky process. Since "non-leaky fusion" has been the foundation of all proposed influenza fusion models, this result indicates the need for a major revision in our modeling. Supported in part by research grant GM-31506 (JB).

Su-Pos295

PHOTOACTIVATED ENHANCEMENT OF LIPOSOME FUSION AND LEAKAGE: CRITICAL FUSION TEMPERATURE ADJUSTMENT.

((Christina R. Miller, Doyle E. Bennett, Daniel Y. Chang and David F. O'Brien))
 C.S. Marvel Laboratories, Department of Chemistry, University of Arizona, Tucson, Arizona 85721

Photoinduced activation of liposome fusion was investigated. Photopolymerization of large unilamellar liposomes (LUV) composed of dioleoylphosphatidylethanolamine (DOPE) and 1,2-bis[10-(2'-hexadecyloxy)decanoyl]-sn-glycero-3-phosphatidylcholine (bis-SorbPC) facilitated liposome-liposome fusion. Fusion was characterized by assays for lipid mixing, aqueous contents mixing, and aqueous contents leakage. Differing extents of photopolymerization were shown to change the temperature at which fusion between liposomes occurred i.e. the critical fusion temperature. The composition of the photosensitive donor liposomes, DOPE/bis-SorbPC, and the target liposomes, either unirradiated DOPE/bis-SorbPC or DOPE/DOPC, was varied to select suitable liposome systems for fusion at 37 °C. A 4:1 ratio DOPE/bis-SorbPC was usefully employed for photoactivated fusion in the physiological temperature range.

Su-Pos292

INDIVIDUAL INFLUENZA HEMAGGLUTININ-MEDIATED MEMBRANE FUSION EVENTS FROM FUSION PORE OPENING TO DILATION.

((R. Blumenthal¹, D.P. Sarkar¹, S. Durell¹, D.E. Howard² and S.J. Morris²))
¹NCI, NIH, Bethesda, MD and ²UMKC, Kansas City, MO

We monitored fusion of cells expressing influenza hemagglutinin (HA) with single erythrocytes (RBCs) labelled with both a fluorescent lipid (DiI) in the membrane and a fluorescent solute (calcein) in the aqueous space. Using a fluorescence video microscope which allows for simultaneous, real-time, video rate imaging of up to four fluorophores [Morris *et al.*, J. Microscopy Soc. America 1:59-66 (1995)], we studied the sequence of events involved in HA-induced cell-cell fusion. Initial fusion pore opening between an RBC and HA-expressing cell produced a change in RBC membrane potential ($\Delta\psi$) which was monitored by a decrease in DiI fluorescence. The change in $\Delta\psi$ was indicative of a flow of ions (ϕ_i), which had been measured previously by capacitance patch clamp techniques. This was followed by two distinct stages of fusion pore development: the flux of fluorescent lipid (ϕ_L) and the flux of a large aqueous fluorescent dye (ϕ_s). Single channel-style analysis allowed us to separate the kinetics of $\phi_i \rightarrow \phi_L$ from that of the $\phi_L \rightarrow \phi_s$ transitions. Both follow an S-shaped time course. If we assume that the $\phi_i \rightarrow \phi_L$ transition is controlled by several independent membrane-bound particles (e.g., HA trimers) each with a probability n of being in the correct position to allow lipid flux, the data are consistent with four such particles. We present a model for HA-mediated membrane fusion that is consistent with these data.

Su-Pos294

STRUCTURAL AND ELASTIC PROPERTIES OF DOPE/DOG MIXTURES.

((M.M.Kozlov, S.Leikin', N.Fuller', and R.P.Rand')) FB Physik, Frie Universität Berlin, Germany; ²CDT, NIH, Bethesda, MD 20892, U.S.A.; and ³Brock University, St. Catharines, ONT, Canada.

Diacylglycerol, a biological membrane second messenger, is a strong perturber of phospholipid planar bilayers. It converts multibilayers to the reverse hexagonal phase (H_{II}), composed of highly curved monolayers. With the aim of defining its structural and mechanical effects, we have used X-ray diffraction and osmotic stress of the H_{II} phase to measure structural dimensions, spontaneous curvature and bending moduli of dioleoylphosphatidylethanolamine (DOPE) monolayers doped with increasing amounts of dioleoylglycerol (DOG). By plotting structural parameters of the H_{II} phase with changing water content in a special coordinate system, we show that elastic deformation of the lipid monolayers can be described as bending around a neutral plain of constant area. The monolayer rigidity is sufficiently high so that the stretching at the neutral plane is negligibly small. This plane is positioned ≈ 7 Å behind the Luzzati lipid/water interface. As the mole fraction of DOG increases to 0.3, the neutral plane shifts ≈ 0.3 Å closer to the lipid/water interface; the radius of spontaneous curvature decreases from 29 Å to 19 Å; and the bending modulus, $k_b/kT=12.2$ (± 0.5), remains constant. The spontaneous curvature is linear with DOG mole fraction so that the monolayer can be treated as an ideal mixture of the two components with specific radii of spontaneous curvature 29 Å (DOPE) and 11 Å (DOG). Measures of molecular areas and volumes allow us to estimate the relative disposition of DOG molecules within the monolayer.

Su-Pos296

INNER MONOLAYER FUSION ASSAYS: CHARACTERIZATION OF BILAYER

TRANSLLOCATION OF HEADGROUP NBD PROBES ((Paul Meers*, Andrew Janoff and Shaikat Ali))The Liposome Company, 1 Research Way, Princeton, NJ 08540-6619 (Spon. P. Meers)

Lipid dilution fusion assays suffer from potential artifacts that result from exposure of the fluorescent probe on the outer monolayer of labeled vesicles. An inner monolayer labeled fusion assay was recently introduced to eliminate these problems (Meers *et al.*, 1992; Biochemistry 31, 6372). A key aspect of such assays is that fluorescent NBD-lipids on the inner monolayer of vesicles should not significantly redistribute to the outer monolayer before or during the fusion assay. Therefore, the effects of various environments and probe structures on the transbilayer movement have been studied. Decreasing translocation rates were observed for N-NBD-phosphatidylethanolamine(PE), N,N-dimethyl-N-NBD-PE and N-NBD-phosphatidylserine(PS), respectively. In phosphatidylcholine (PC) vesicles at 25 °C in buffer, the translocation half times were approximately 2 and 10 hours for the former two probes, respectively and almost no redistribution of the N-NBD-PS probe was seen even at 20 hours. These data suggest that the headgroup hydration may determine the relative rates. By contrast, the acyl chain structure of any given probe did not significantly affect transbilayer diffusion. The N-NBD-PS probe translocation rate was also not dependent on vesicle size. Therefore, long term fusion experiments with inner monolayer labeled vesicles should be viable with this probe under many conditions. The membrane environment of the probe also played an important role. For instance, N-NBD-PE translocated much more rapidly in PC membranes than in PS membranes. Translocation rates in primarily PE-containing positively charged membranes below the PE hexagonal II phase transition temperature were generally comparable to the corresponding PC-containing membranes, but were found to be greater above the hexagonal II phase transition temperature, despite no apparent actual formation of a hexagonal phase. Exposure of liposomes containing these probes to rat plasma accelerated translocation and induced leakiness to dithionite. The plasma induced translocation and leakage was due to a nondialyzable factor and was not inhibited by PEG-lipids.

Su-Pos297

DOUBLE WHOLE CELL RECORDINGS OF HA-MEDIATED FUSION BETWEEN HAB2 AND PLC CELLS. ((V.A.Frolov¹, A.Ya.Dunina-Barkovskaya², J.Zimmerberg³, & Yu.A.Chizmadzhev¹)) ¹Frumkin Electrochem. Inst., Russ. Acad. Sci., Moscow 117071, ²Belozersky Inst. of Physico-Chemical Biology, MSU, Moscow, 119899, ³LTPB, NICHD, NIH, Bethesda, MD 20892

NIH 3T3 HAB2 cells, which express influenza hemagglutinin (HA), fuse to human red blood cells (RBC). This system (HAB2/RBC) is used to study HA-induced fusion. Using fluorescent markers, we recently showed that NIH 3T3 HAB2 cells can fuse to cells other than RBC. Of several cell lines tested (PLC/PRF/5, BHK-21, MDCK, HeLa, Vero) as fusion partners for HAB2, only PLC (a human hepatocarcinoma cell line) and BHK cells fused with HAB2 cells. PLC cells were chosen for electrophysiological studies, as each cell in the PLC/HAB2 cell pair can be easily distinguished and are equally accessible for micromanipulation. We performed double whole-cell measurements of intercellular conductance in PLC/HAB2 cell pairs under conditions that activate HA (proteolytic cleavage of HA0) and that trigger fusion (low pH). When cell pairs were superfused with acid solution, the induction of intercellular conductance was observed in ~50% of 20 pairs of cells, starting ~1-2 min after the pH drop. First, intercellular conductance increased from 0 to hundreds of pS, then continued up to 1-5 nS. Flickering was observed. In several experiments, a voltage-dependent activation of the induced intercellular conductance was observed. This activation was detected only when the difference in holding potential of the two cells (applied for 20-50 ms) exceeded 50mV. This voltage-dependent activation may reflect the mechanical properties of the fusion pore, as according to theoretical calculations the inter-cell potential creates a substantial (several Din/sm) force at the walls of the pore.

Su-Pos299

PURIFICATION OF PERIPHERIN, A CANDIDATE FUSION PROTEIN IN PHOTORECEPTOR ROD CELLS. [[K. Boesze-Battaglia]] Dept. Molecular Biology UMDNJ-SOM, Stratford, NJ 08084

Retinal rod outer segments maintain their structural integrity through the formation of new disk membranes at the base and the shedding of older disks at the apical tip. Mutations in the carboxyl terminal region of peripherin disrupts this structural integrity. Peripherin is a 68kDa dimer, that forms exclusive protein domains at the rim of the disk. Given peripherin's location at this rim region; the region that must interact with the plasma membrane prior to a fusion event, it is proposed that this protein may play a role in membrane fusion events in this system. We report here the purification of peripherin using Concanavalin A affinity chromatography and chromatofocusing techniques. Peripherin chromatofocused with a pI of 4.8; isoelectric-focusing gels show a pI of 4.6-4.8. Light dependent phosphorylation using γ -³²P-ATP detected a ³²P labeled band with a pI of 4.0-4.5 using IEF and autoradiography. Upon western blot analysis, this band was immunoreactive with peripherin monoclonal antibody 2B6 (generously provided by R. Molday). Since peripherin can be isolated in a disk membrane lipid rich fraction from Con-A chromatography, the role peripherin may play in liposome-R₁₈ labeled plasma membrane fusion could be studied. R₁₈ lipid mixing fusion studies showed peripherin is able to enhance the initial rates of fusion between R₁₈ labeled plasma membrane and disk membrane liposomes. Supported by EY10420.

Su-Pos298

COOPERATIVE MODEL FOR BACULOVIRUS-INDUCED MEMBRANE FUSION KINETICS. ((I. Pionsky, J. Zimmerberg)) NICHD, NIH, Bethesda, MD 20892.

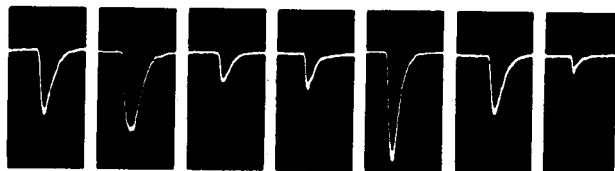
Time-resolved admittance measurement technique was used to study baculovirus-induced membrane fusion. A low pH triggering solution was delivered by second pipette located ~15 μ m from a cell pair. A delay time from the onset of the delivery pressure pulse to the appearance of a fusion pore was measured. The probability that a fusion pore has not appeared at time t (P) was defined as $P=1 - N(t)/N$, where N(t) is the number of pores that have not yet formed by time t and N is the total number of experiments. A Hodgkin-Huxley-like formalism was applied to fit P. We hypothesize that fusion is controlled by two kind of independent elements: "m" and "h". For fusion to occur, several (n) "m"-type and one "h" elements should enter a permissive state. Acid pH drives the reaction with first-order kinetics: $1 - p_m \leftrightarrow p_m$; $1 - p_h \rightarrow p_h$, where p_m , p_h are probabilities of "m", "h" to be in permissive state. The over-all non-permissive probability for fusion, P, is equal to $1 - p_m^n \times p_h$. The following fitting parameters were obtained (\pm SEM): $n=19.21 \pm 3.82$, $k_1=6.7 \pm 0.42$ s⁻¹, $k_2=0.03 \pm 0.0006$ s⁻¹, $k_3=1.78 \pm 0.0075$ s⁻¹, where k_1 , k_2 are forward and backward rate constants for "m", and k_3 is a rate constant for "h". Attempts to fit P to several non-cooperative branched or sequential reaction schemes failed. If cooperative element "m" corresponds to a fusion peptide, then 6-7 trimers of gp64 form a "fusion machine", providing a platform for ~19 peptides to come out from a protein's core to activate fusion. The "h" element of the proposed scheme could represent a preparatory modification of a membrane microenvironment or a movement of the whole complex to the right orientation for fusion. Although this model is pure hypothetical, it shows that this cooperative scheme has enough mathematical complexity to fit the experimental data and supports the idea that fusion occurs in the midst of a small number of gp64 trimers; consistent with independent measurements of initial pore conductance.

EXOCYTOSIS AND ENDOCYTOSIS

Su-Pos300

REAL-TIME DETECTION OF SINGLE EXOCYTOTIC EVENTS IN NON-NEURONAL CELLS. ((S.V. Popov)) Department of Physiology and Biophysics, University of Illinois at Chicago, Chicago, IL 60612

Fibroblasts were incubated in a culture medium containing 40 mM acetylcholine (ACh) for a period of 2 to 20 min. After washing the cells with fresh culture medium, a *Xenopus* myocyte was manipulated into contact with the fibroblast. Whole cell voltage clamp recordings from the myocyte revealed current events that resembled miniature endplate currents found at developing neuromuscular synapses. The use of myocytes in the detection of ACh secretion from transmitter-loaded fibroblasts provides the real-time assay for the exocytotic fusion of endosome-derived vesicles with the plasma membrane in non-neuronal cells.



Su-Pos301

THE KINETICS OF THE OPENING AND CLOSURE OF THE FUSION PORE IS MARKEDLY ALTERED IN MAST CELLS FROM RUBY-EYE MOUSE. ((A.F. Oberhauser* and J.M. Fernandez)) Mayo Clinic, Rochester, MN 55905; *Univ. of Chile and C.E.C.S., Santiago, Chile.

There is growing evidence suggesting that the exocytotic fusion machinery is the result of multiple gene products. It is, however, not yet clear how these proteins assemble to form a fusion pore. We have found a genetic mutation that dramatically affects the fusion pore function. Membrane capacitance measurements done on degranulating mast cells obtained from ruby-eye mice (*ru/ru*), revealed that the incidence of transient fusion events was increased by about 3-fold with respect to that measured in mast cells from wild type mice. The fraction of the total fusion events that are transient was 0.27 ± 0.06 (12 cells) in normal mast cells and 0.76 ± 0.04 (10 cells) in *ru/ru* mast cells. We also found that during the initial phase of the degranulation (the first 50 to 130 s), most of the fusion events showed little (<0.5pC) or no release of 5HT (monitored by amperometry), in contrast with the large amperometric spikes (about 1 pC) that were associated with the fusion events in later phases of the degranulation. It is unlikely that the *ru* mutation affects the mechanism of 5HT uptake into the granules, since after the incubation of *ru/ru* mast cells with 5 μ M 5HT, all fusion events were accompanied by large amperometric spikes. We suggest that the fusion events observed in the early phase of the degranulation of *ru/ru* mast cells represents the exocytosis of a pool of granules that have been depleted of 5HT due to several rounds of transient fusion events. Thus, the pigment mutant ruby-eye (*ru/ru*) may prove valuable in understanding the molecular basis of fusion pore opening and closure.

Su-Pos302

EXOCYTOSIS IN ADIPOCYTES IS ACTIVATED BY PURINERGIC RECEPTOR STIMULATION. ((P.A. Pappone & S.C. Lee)) Section of Neurobiology, Physiology & Behavior, Univ. of Calif., Davis CA 95616

Adipocytes secrete a number of biologically active substances, but the factors regulating their release are not known. We used patch voltage clamp membrane capacitance (C_m) and FM1-43 fluorescence measurements to determine cell membrane surface area during exposure to extracellular ATP and other P_{2U} agonists in cultured rat brown fat cells. μ M ATP activated 10-100% increases in C_m in perforated patch clamped cells and ~3-fold larger increases in FM1-43 fluorescence. Norepinephrine and insulin had little effect on surface area. Extracellular ATP could also activate Ca^{2+} -dependent K and Cl conductances and a Ca^{2+} -independent cation conductance, but conductance and C_m responses were not correlated. Normal C_m responses to extracellular ATP were present in whole-cell recordings when the pipet solution contained ATP. Exocytosis was not triggered by intracellular Ca^{2+} , since similar C_m responses could be elicited in nominally calcium-free extracellular solution with intracellular calcium buffered to 100 nM with 10 mM BAPTA. These findings suggest that P_{2U} purinergic receptors activate secretion in adipocytes through means other than increasing intracellular calcium levels.

Su-Pos304

HIGH SPEED ANALYSIS OF EXOCYTOSIS IN *PARAMECIUM*.

((Sergey Levin, Birgit H. Satir)) Department of Anatomy and Structural Biology, Albert Einstein College of Medicine, Bronx, NY 10464.

Exocytosis in the unicellular eukaryote *Paramecium* occurs very rapidly upon stimulation with the biological secretagogue lysozyme in a Ca^{2+} -dependent manner. Each cell contains several thousand dense core secretory vesicles docked in place under the cell membrane which can be either globally or locally induced to release. The release event is observed as an expansion of the secretory products from the 4 μ m docked vesicle to a 40 μ m spear-like protein structure outside the cell easily visible in the light microscope. In this study we have analyzed this event using high speed motion analysis. Axenic cultures of late log phase cells were harvested, washed twice in Mg^{2+} containing PIPES buffer and transferred to PIPES buffer containing 1mM KCl, 5mM $CaCl_2$, pH 7.2. In addition, the cells were exposed to $Ni(Ac)_2$ [100 μ M] to immobilize the cells. Immobilized cells were placed on a coverslip and secretagogue added onto the cells triggering exocytosis. A local region on a single cell was chosen for recording at 200 frames/sec. The event actually observed is the expansion of the secretory content itself after membrane fusion has occurred. The expansion of the secretory products occurs in about 15 to 20 msec. Three stages of the secretory product expansion can be distinguished. Membrane fusion itself must occur prior to product release in < 5 msec. The next intermediate stage (expansion to 20 μ m) occurs after additional 5 to 10 msec and full expansion is completed by 15-20 msec. Duration of exocytosis in *Paramecium* appears to be comparable to those reported for neurons.

Su-Pos306

RAPID EXOCYTOSIS IN SINGLE CHROMAFFIN CELLS RECORDED FROM ADRENAL SLICES ((T. Moser and E. Neher)), Max-Planck-Institute for Biophysical Chemistry, 37077 Göttingen, Germany

Studies on isolated, cultured chromaffin cells have revealed a weak coupling of hormone release to single action potentials and consequently a delayed secretory response (Zhou and Misler (1995) J Biol Chem 270: 3498-3505). These data indicate the absence of a strict co-localization of release sites and calcium channels in isolated chromaffin cells. As, unlike in primary culture, chromaffin cells in the intact tissue are polarized, we asked whether they might possess a spatially closer coupling of calcium entry and exocytosis. Therefore, we performed cell membrane capacitance measurements on chromaffin cells in thin slices (150/250 μ m) from murine adrenal glands. Interestingly, secretion could be triggered by short depolarizing voltage pulses of only 2 to 5 ms, by tail-current injections through calcium channels, and by simulated action potentials. During repetitive stimulation by short (5ms) depolarizing pulses the observed variance between trials indicated, that responses were composed of units as expected for large dense core granules. By applying depolarizing pulses (to +10mV) of different durations we identified a finite pool of release ready granules of about 18 vesicles (37 ± 7.2 fF, $n = 6$), which was released at a very high rate (243 ± 56 s $^{-1}$). A pool of similar size has been described in isolated rat chromaffin cells (Horrigan FT & Bookman RJ (1994) Neuron 13: 1119-1129). The release rate of this pool was, however, substantially slower (about 20 s $^{-1}$), indicating higher calcium concentrations ($[Ca^{2+}]$) seen by the secretory machinery of the release ready vesicles and thus closer coupling of calcium entry and exocytosis in chromaffin cells in slices. The results indicate that chromaffin cells in situ secrete fast enough to respond to single action potentials.

Su-Pos303

Plasma Membrane Tether Force Decreases During Secretion

Jianwu Dai, H. Ping Ting-Beall & Michael P. Sheetz, Department of Cell Biology and Mechanical Engineering and Materials Science, Duke University, Durham, NC 27710

During stimulated secretion, plasma membrane area increases and then endocytosis increases to retrieve the added membrane. This suggests that there is a membrane parameter that regulates cell secretion. We report here that membrane tubes or tethers drawn from rat basophilic leukemia (RBL) cells by a laser tweezers exert considerable retractile force (22.87 ± 2.96 pN) nearly independent of tether length. Upon stimulation of secretion by DNP-BSA or by loading Ca^{2+} with A23187, this retractile force drops to less than ~10-12 pN. The decrease in force occurs as rapidly as ~5 sec after addition of the antigen and recovers to the original level when secretion stops. Blocking secretion by Ca^{2+} chelation or monomeric ligand addition inhibits the drop in force but altering cytoskeletal actin organization by cytochalasin B treatment does not. After secretion stops tether force recovers; but blocking endocytosis by potassium loading or ATP depletion, blocks recovery of tether force. Decrease in tether force with secretion results primarily from decrease in a membrane tension and not decrease in membrane bending stiffness. The morphological changes of the cells under different conditions are also observed by scanning electron microscopy. The inverse correlation between a membrane tension and stimulation of endocytosis leads us to speculate that a high membrane tension may inhibit endocytosis thereby regulating plasma membrane area. This work was supported by grants from NIH, HFSP and MDA.

Su-Pos305

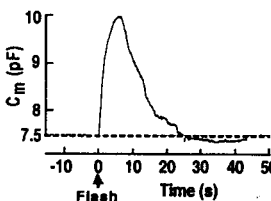
SIMULTANEOUS MEASUREMENTS OF CHANGES IN MEMBRANE RESISTANCE AND CAPACITANCE INDUCED BY BLACK WIDOW SPIDER VENOM (BWSV). ((D. Barnett and S. Misler)) The Jewish Hospital, Washington Univ. Med. Ctr., St. Louis, MO. 63110 and St. Louis Univ., Parks College, Cahokia, IL 62206

Membrane impedance measurements employing dual frequency excitation (DFE) have been used to estimate changes in membrane capacitance (C_m) under conditions where membrane resistance (R_m) is low or rapidly changing. Using our digital DFE approach with optimized parameter estimation (Biophys. J. 68:A116), we have examined the time courses of ΔC_m and ΔR_m produced, in patch-clamped rat adrenal chromaffin cells, by exposure to BWSV, a secretagogue whose actions include a large, sustained increase in membrane permeability of susceptible cells. At a physiological $[Ca]_o$ ($= 2$ mM and no Mg), where local puffs of BWSV cause massive quantal discharges, measured by amperometry, and visible cell swelling, noisy 3-5 fold decreases in R_m precede the onset of increases in C_m . Thereafter, C_m increases by 10-20% over the next minute. At very low $[Ca]_o$ (≤ 20 nM, and no Mg), where puff of BWSV fail to provoke amperometric events, similar decreases in R_m , developing in a more stepwise fashion, produce, at best, 10-fold smaller increases in C_m than those seen in 2 mM Ca. In contrast, processing the raw data using standard single frequency techniques (e.g. Lindau-Neher) results grossly underestimated and widely varying estimates of C_m . These results support (i) the usefulness of a carefully applied DFE approach for estimation of C_m and R_m in complex situations where both parameters are rapidly changing and (ii) the role of Ca entry via a BWSV-induced conductance as a key mechanism of its action. (Support: NIH DK37380)

Su-Pos307

Ca-TRIGGERED EXOCYTOSIS IN AN EPITHELIAL CELL LINE. ((J.R. Coorsen, H. Schmitt, & W. Almers)) M.P.I. Heidelberg, FRG. (Spon: P. Honerjäger)

We have studied Ca-triggered exocytosis by capacitance (C_m) measurements in Chinese Hamster Ovary (CHO) cells. Cells (initial $C_m = 11.9 \pm 0.9$ pF, $n = 13$) were loaded through the patch pipette with solutions of known free $[Ca]$. With $[Ca] = 4$ μ M, C_m increased by $25 \pm 7\%$ ($n=8$) in 2 min, mostly reaching a maximum in that time. With 0.1 μ M $[Ca]$, C_m did not change ($0.2 \pm 0.2\%$, $n=5$). When $[Ca]$ was raised to higher values (28 ± 4 μ M, $n=10$; fura-2/AM) by flash photolysis of Ca-DM-nitrophen (see Fig.), C_m rose by $23 \pm 5\%$ ($n=9$) within 40 s or earlier; photolysis of Mg-DM-nitrophen had no effect. The increase was similar to that at 4 μ M $[Ca]$, but it happened much faster. In 4 of 7 cells, C_m reached a peak in 11 ± 2 s and then declined to baseline with a half-time of 20 ± 4 s, suggesting complete membrane retrieval. Preliminary studies with NIH 3T3 fibroblasts gave similar results. Thus, CHO and 3T3 cells are capable of Ca-triggered exocytosis, as suggested for fibroblasts (Girod et al., J. Neurosci. 15, p. 2826, 1995).



Su-Pos308

SINGLE CHROMAFFIN GRANULES BENEATH THE PLASMA MEMBRANE VIEWED BY TIR FLUORESCENCE MICROSCOPY.

((J.A. Steyer and W. Almers)) Max-Planck-Institut für medizinische Forschung, 69120 Heidelberg, FRG. (Spon. by F. Tse)

An argon laser beam suffering total internal reflection (TIR) at a glass-water interface was used to illuminate (and excite fluorescence in) a 150 to 250 nm thick layer immediately adjacent to the glass slide (Axelrod et al., 1984; Annu Rev Biophys Bioeng 13: 247). Fluorescence was viewed with a 1.4 NA oil objective. We verified TIR by comparing epifluorescence and TIR views of a suspension of fluorescent 280 nm beads. Bovine chromaffin cells attached to glass were stained with acridine orange, a dye known to partition into their secretory (chromaffin) granules. Under epifluorescence, the entire cell glowed uniformly. TIR elicited fluorescence in a smaller area, presumably the "footprint" of the cell on the glass. TIR fluorescence was punctate. The fluorescent points probably represent single chromaffin granules docked beneath the plasma membrane. (a) Their number ($1.47 \pm 0.20/\mu\text{m}^2$) was similar to that of docked granules counted in electron micrographs ($1.39 \pm 0.07/\mu\text{m}^2$; Parsons et al., Neuron, in press). (b) They disappeared abruptly and in succession under conditions stimulating Ca-triggered exocytosis. After 6 min in 60 mM K and 5 mM Ca, only $51 \pm 6\%$ ($n=5$) of the points remained. In control experiments where Mg replaced Ca and 0.1 mM Cd blocked Ca channels, no points were lost ($103 \pm 16\%$ remaining). Thus, TIR allows space- and time-resolved observation of single exocytic events.

Su-Pos310

CAGED-CALCIUM, CAPACITANCE, AND EXOCYTOSIS ((R. Heidelberger and G. Matthews*)) MPI. f. biophys. Chemie, Göttingen, Germany and *SUNY@Stony Brook, Stony Brook, NY

Stimulation of exocytosis by flash-photolysis of caged-calcium has recently been suggested to produce non-secretory related capacitance changes (Oberhauser et al., (1995). *J. Physiol (Paris)* 89:71). We have examined this premise in goldfish retinal bipolar neurons, taking advantage of the ability to study either somata or synaptic terminals in isolation. Following flash-photolysis of DM-nitrophen caged-calcium, synaptic terminals show a rapid increase in membrane capacitance. In contrast, no capacitance increase was seen in isolated somata/dendrites that lacked synaptic terminals ($N=5$). To address whether global elevation of $[\text{Ca}]_i$ in terminals recruits the same pool of fusible membrane as that stimulated by voltage-gated Ca-current, capacitance responses driven by Ca-current were compared with those elicited by flash-photolysis. The control amplitudes of the capacitance response following either stimulus were nearly identical (flash: 161 ± 42 fF; pulse: 142 ± 39 fF; (mean \pm sem; $N=7$)). Depolarizations were then used to deplete the readily-releasable pool of synaptic vesicles and followed by a UV flash. When the flash occurred within 5 seconds of the pulse, minimal additional membrane was added (28 ± 10 fF; $N=6$), and the flash/pulse ratio of added capacitance was 0.10 ± 0.02 . When the flash occurred > 60 seconds after the pulse, the flash/pulse ratio was 1.01 ± 0.17 ($N=7$). These data indicate that both flash-photolysis of caged calcium and opening of calcium channels tap the same pool of fusible membrane. Furthermore, this membrane pool is specifically localized to synaptic terminals.

Su-Pos312

NEW INSIGHTS INTO PARASITE-HOST CELL INTERACTIONS, AS REVEALED BY SIMULTANEOUS ELECTRICAL AND OPTICAL MEASUREMENTS ((Suss-Toby Edith*, G.E. Ward*, and J. Zimmerberg*)) Laboratories of Theoretical and Physical Biology, "NICHED" and Parasitic Diseases, NIAID*, NIH, Bethesda MD 20892.

The formation of an intracellular vacuole during invasion is a critical step in infection for many pathogenic microorganisms. The membrane of this vacuole serves as a critical interface between the pathogen and the host cell cytoplasm. To address the longstanding question of whether the membrane which forms around an internalizing *Toxoplasma gondii* parasite (the parasitophorous vacuole membrane, or PVM) is derived from the host cell membrane or from lipids secreted by the parasite during invasion, we used time-resolved capacitance measurements and video microscopy to assay host cell surface area during invasion. We found no significant increase in surface area during parasite internalization and PVM formation, arguing strongly that the PVM consists primarily of invaginated host cell membrane. Pinching off of the PVM from the host cell membrane, which occurred on average 139s after the parasite appeared to be completely inside the host cell, was seen as a 0.219 ± 0.006 pF drop in capacitance, which corresponds well to the predicted surface area of the PVM ($\sim 30\mu\text{m}^2$). During pinching off, a fission pore forms; its conductance was determined over a range of 8nS to 100pS and exhibited semistable conductance levels. Often, the fission pore demonstrated a rapid relaxation from a semistable conductance to a larger conductance, followed by a second constriction and complete closure. Our correlated electrical and optical measurements also revealed a large transient current (spike) across the host cell membrane at the exact moment that it is first contacted by the apical end of the parasite. Every successful invasion (>100) was preceded by a spike. Work is currently in progress to understand the mechanism underlying the parasite induced spike formation and host cell invagination during invasion. Applying electrophysiology to further explore these findings will shed light on the membrane events associated with parasite invasion such as membrane fission and fission pore formation.

Su-Pos309

ACTIVATION OF PROTEIN KINASE C (PKC) ENHANCES SECRETION FROM CHROMAFFIN CELLS PRIMARILY BY INCREASING THE SIZE OF THE READILY-RELEASABLE POOL (RRP) OF SECRETORY GRANULES ((K. D. Gillis, R. Moessner and E. Neher)), Max-Planck-Institute for Biophysical Chemistry, 37077 Göttingen, Germany

Phorbol myristate acetate (PMA), an activator of protein kinase C (PKC), has previously been shown to increase catecholamine secretion from intact and permeabilized adrenal chromaffin cells, however, the mechanism of PKC enhancement is not well understood. We have used membrane capacitance measurements to assay exocytosis (ΔC_m) elicited by depolarization or elevation of Ca_i^{2+} via photolysis of caged compounds. Three different protocols were used for estimating the size of the RRP: 1) Increasing the duration of test depolarizations leads to a maximal ΔC_m ($=\text{RRP}$), 2) ΔC_m responses to a pair of depolarizing pulses exhibits depression, and 3) Elevation of Ca_i^{2+} via flash photolysis of DM-Nitrophen leads to an "exocytic burst" ($\Delta C_m = \text{RRP}$). Results using each of these protocols indicate that PMA increases the size of the RRP. The kinetics of the final Ca_i^{2+} -dependent step in secretion were inferred from the time course of the exocytic burst. In some cells, PMA lead to a small decrease in the delay for the start of the burst. In most cells, however, PMA primarily affected the amplitude and not the time course of the exocytic burst. Since Ca_i^{2+} was elevated to a level where the secretory rate is steeply dependent on Ca_i^{2+} (20-40 μM), similar burst kinetics suggest that the Ca_i^{2+} -sensitivity of the final step was not fundamentally altered. Thus PMA appears to primarily affect steps in secretion before the final release step.

Su-Pos311

COMPARISON OF CAPACITANCE AND AMPEROMETRIC MEASUREMENT OF SECRETION FOLLOWING FLASH PHOTOLYSIS OF CAGED-CALCIUM ((M. Haller, R.Chow*, R.Heidelberger, J. Klingauf, E.Neher)) MPI for biophys. Chemie and *MPI for exp. Medizin, 37077 Göttingen

The exocytotic response following flash photolysis of caged-calcium can be observed simultaneously by membrane capacitance measurement and amperometry. Recently, the onset of the amperometric events was reported to lag the onset of capacitance increase by 0.5 seconds in chromaffin cells (Oberhauser et al., (1995) *J Physiol (Paris)* 89:71-75). We monitored secretion from chromaffin cells with high-time resolution amperometry and capacitance techniques and used the photolabile Ca-chelator DM-nitrophen to rapidly elevate $[\text{Ca}^{2+}]_i$ to less than $\sim 50\mu\text{M}$. Under these conditions, we typically did not observe such long delays. For a more quantitative analysis, the amperometric current after a flash was compared to sweeps generated by a theoretical model. The model assumes instantaneous release of molecules from a reflective spherical surface with subsequent diffusion towards an absorbing disk. Model curves for release events occurring at a number of locations along the perimeter of the cell were created. In order to generate simulated traces that can be directly compared to experimental amperometric traces, release rates and the number of vesicles released were estimated from the corresponding capacitance traces. Single release events were assigned to locations along the perimeter of the cell by a random number generator with the appropriate probability distribution. This information was then used in combination with the model curves to create the simulated trace. For small increases in capacitance (< 80 fF), simulated and experimental amperometric traces were qualitatively similar with regard to the number of spikes observed. For larger increases in capacitance, the amperometric traces displayed a relatively small number of secretory spikes superimposed on a smooth pedestal which was not reproduced by the simulations. The comparison of experimental data and simulations suggests that for small rises in capacitance, membrane capacitance and amperometric measurements are in good agreement.

Su-Pos313

cAMP MAINTAINS A FAST RATE OF ENDOCYTOSIS IN RETINAL BIPOLAR PRESYNAPTIC TERMINALS. ((H. von Gersdorff & G. Matthews)) Dept. of Neurobiology, SUNY at Stony Brook, NY 11794-5230.

The rate of endocytosis after a bout of depolarization-activated exocytosis was studied by measuring the associated change in membrane capacitance in acutely isolated giant synaptic terminals of goldfish retinal bipolar neurons. Depolarization from -60 mV to 0 mV for 250 msec elicited a capacitance increase (exocytosis) of about 150 fF, followed by an exponential return back to basal capacitance (endocytosis). In control experiments, capacitance jumps elicited within the first 20 secs after whole-cell break-in recovered back to baseline with an average time constant of 0.98 ± 0.09 sec (mean \pm s.e.m.; $N=11$), while those elicited from 30 to 200 secs after break-in had an average time constant of 1.47 ± 0.12 sec ($N=10$). If cAMP (0.2 mM) was included in the patch pipette, the depolarization-activated capacitance increase was comparable to control, but the average time constant of recovery decreased to 0.45 ± 0.05 sec ($N=11$). This fast rate of endocytosis with cAMP was maintained for 200 sec after break-in, provided baseline $[\text{Ca}]_i$ was below 250 nM. Control and cAMP-containing terminals had identical depolarization-activated $[\text{Ca}]_i$ transients as monitored by fura-2 and comparable amplitude of calcium current. These preliminary results thus suggest that cAMP-dependent processes may be important in regulating the rate of endocytosis within synaptic terminals. (Supported by NIH grant EY03821 and NRSA Fellowship EY6506).

Su-Pos314

ELUCIDATION OF THE CLEARANCE MECHANISM FOR PERFLUOROCARBON EMULSION PARTICLES ((V. Obraztsov, D. Smith, and G. Neslund.)) Dept. of Biochem. & Cell Biology, Alliance Pharmaceutical Corp., San Diego, CA 92121.

Intravenous infusion of perfluorocarbon (PFC) emulsions, as oxygen carriers, have been observed to be cleared from the circulation within several days for both humans and swine and much longer for rabbits. Presumably, nonspecific binding of plasma proteins to the PFC emulsion is responsible for the natural removal of the particles by fixed macrophages residing in the liver and spleen. The purpose of this study was 2-fold: (1) to determine the relative affinity that purified plasma proteins have toward the PFC emulsions *in vitro*, and (2) to determine what human-, swine-, or rabbit-specific proteins bind to the PFC emulsions in plasma under *in vitro* and *in vivo* conditions. When added as single human protein *in vitro*, fibrinogen, followed by IgG, and then albumin, displayed the highest affinity for a PFC emulsion, all of which reached similar saturation levels on a molar basis. Albumin was able to compete with irreversible binding of IgG (but not fibrinogen) for the particle surface when added together *in vitro*. PFC emulsions exposed to plasma (blood circulation) for 2, 24, or 144 hours *in vitro* or *in vivo* were measured for nonspecific binding of protein to their surface with an optical biosensor analyzer and by western blotting. The PFC emulsions, after extensive washing, were able to retain adsorption of albumin, fibrinogen, α_2 -macroglobulin, complement 3b, and/or fibronectin, depending on the plasma source or animal species. This adsorption is a normal benign process since the PFC emulsions were not found to activate platelets, complement, or the contact activation system. For nearly all *in vitro* and *in vivo* studies, the PFC emulsions in the presence of plasma irreversibly bound albumin, but not IgG. In conclusion, certain plasma proteins can nonspecifically bind to PFC emulsions *in vitro* and *in vivo* which may help to explain the natural removal process of these particles from the blood pool.

Su-Pos316

CONTINUOUS MEASUREMENT OF CELL-FREE ENDOSOME FUSION BY A NOVEL FLUORESCENCE METHOD: EVIDENCE FOR REGULATION BY Ca-CALMODULIN PROTEIN KINASE. ((Neil Emans and A.S. Verkman.)) U.C.S.F., CA 94143-0521. (Intro. by S.B. Shohet)

A quantitative real time assay of cell-free endosomal vesicle fusion was developed and applied to study fusion mechanisms in endosomes from Baby Hamster Kidney (BHK-21) cells. The assay is based on an irreversible ~10-fold increase in BODIPY-avidin (B-av) fluorescence upon binding of biotinylated conjugates (Emans and Verkman, *Biophys. J.* 69:716-728). B-av and biotin-dextran were internalized for 10 min at 37 °C into separate populations of BHK-21 cells. Post nuclear supernatant fractions underwent ATP and temperature dependent fusion as measured in a sensitive custom-built microfluorimeter by the continuous increase in B-av fluorescence. Fusion processes were detected with 200 ms time resolution in sample volumes of 50 μ L containing endosomes derived from $\sim 4 \times 10^4$ cells. The fusion time course consisted of a distinct lag phase (5-700 s), followed by an approximately exponential rise ($t_{1/2}$ 20-30 min; fusion efficiency 15%); the lag phase was remarkably shortened by pre-incubation of endosomes at 22 °C or by increased endosome concentration, indicating a rate-limiting step involving endosome-endosome interaction. Fusion was inhibited by ATP depletion (85%), GTP γ S (84% at 50 μ M), N-ethylmaleimide pre-treatment (100% at 1 mM) and AIF $_3$ (48% at 40 μ M). Endosome fusion was inhibited by calmodulin (50% at 1040 U/ml); inhibition was reversed by 30-60 μ M W-13, a Ca-calmodulin kinase inhibitor. The results establish a sensitive real time fluorescence assay to quantify the kinetics and extent of endosome fusion in a cell-free system, and demonstrate regulation by calcium-calmodulin dependent protein kinase.

Su-Pos315

THE ROLE OF HELPER LIPIDS IN CATIONIC LIPOSOMES AS A VECTOR FOR GENE TRANSFER. ((Sek Wen Hui, Marek Langner*, Ya-Li Zhao, Edward Hurley and Patrick Ross.)) Biophysics Department, Roswell Park Cancer Institute, Buffalo, NY 14263. *Present Address: Department of Physics and Biophysics, Agriculture University, Wroclaw, Poland.

Unsaturated phosphatidylethanolamine (PE) as well as phosphatidylcholine (PC) are added as helper lipids to dioleoyl-trimethylammonium propane (DOTAP) to form cationic liposomes, which are used as vectors to carry the reporter β -galactosidase gene (pSV-GAL) to transfect CHO cells. PE-containing DNA:cationic liposome complexes aggregate immediately after adding to transfection medium. PC-containing complexes form granules on the cell surface only after added to the cells for an hour, and the process is inhibited by cytochalasin-B and low temperature. Confocal microscopy of cells treated with labelled lipids (rhodamine-PE) and DNA (by YOYO) shows internalized granules containing both DNA and lipids after an hour of exposure. Those granules remaining on cell surfaces are enriched in DNA, as a residue of cationic liposomes fusing with plasma membranes. More DOPC than DOPE is taken into endosomes, as indicated by fluorescence quenching and bilayer surface pH measurements. The transfection efficiency of CHO cells by PC-containing complexes is about 2.5 times that by PE-containing ones. Increasing the degree of unsaturation in PE also increases the transfection efficiency. We conclude that the formation of proper size granules on the cell surface is a crucial step in endocytosis-mediated transfection. Bilayer stability of the helper lipid is important for DNA escape from endosomes, but the influence is secondary to granule-triggered endocytosis. (Supported by GM30969 from NIH)

Su-Pos317

CALCULATED EFFECTS OF LOW PH ON DIPHTHERIA TOXIN: IMPLICATIONS FOR MEMBRANE TRANSLLOCATION ((A. Windemuth and B. Honig.)) Dept. of Biophysics, Columbia University, New York, NY 10032.

We study the mechanisms that trigger the translocation of the transmembrane (T) and catalytic (C) domains of diphtheria toxin into the endosomal membrane. We use a hybrid statistical mechanical/Tanford-Roxby approach to calculate protonation states of titrable residues and the pH dependent stability of the association of protein domains. Our calculations clearly show a reduced affinity at low pH between the transmembrane (T) and the receptor binding (R) domain of diphtheria toxin. This is consistent with the hypothesis of open monomer formation prior to cell membrane insertion as discussed by M. J. Bennett and D. Eisenberg. We discuss the implications of individual titrable residues and the properties of the surface exposed by R-T dissociation for the mechanism of membrane translocation.

LIPIDS

Su-Pos318

IMPEDANCE SPECTROSCOPIC ANALYSIS OF 1-PALMITOYL-2-OLEOYL PHOSPHATIDYLETHANOLAMINE AQUEOUS SUSPENSIONS. ((K.M. Anisur Rahman and J.M. Collins.)) Departments of Electrical Engineering and Physics, Marquette University, Milwaukee, WI 53201-1881.

Lipid molecules form liquid crystalline arrays in the presence of water in part due to the interaction of their polar head groups with water. These arrays will then exhibit relaxation phenomena due to the dipolar nature of their interactions. Impedance spectroscopy is a well established technique in materials science for studying dielectric relaxation phenomena and has the ability to discriminate between different kinds of polarization processes as well as between bulk and interfacial effects. We analyzed 1-palmitoyl-2-oleoyl phosphatidylethanolamine (POPE) saturated with water and saturated with 30 mM CaCl $_2$ at both 25°C and at 60°C. In general we observe more than one relaxation process occurring in the samples. We also observe an marked increase in dc conductivity as the sample temperature is increased and when CaCl $_2$ is present in solution. At elevated temperatures we observe a significant change in the complex impedance response of the samples which appears to be consistent with a phase transition. We discuss these results with reference to previous XRD and DSC measurements for POPE aqueous suspensions.

Su-Pos319

MIXED LANGMUIR MONOLAYERS OF LOCAL ANESTHETICS AND PHOSPHOLIPIDS.

((Ailton Cavalli¹, Galina Borissevitch¹, Marcel Tabak² and Osvaldo N. Oliveira Jr.¹)) ¹Instituto de Física de São Carlos USP, ²Instituto de Química de São Carlos USP, C.P. 780, 13560-970, São Carlos, SP, Brasil.

Local anesthetics have been investigated using various techniques aiming at an understanding of their interaction with biological membranes. Langmuir monolayers have the advantage of molecular control. In this work, we present results for two local anesthetics, namely dibucaine (DIB) and tetracaine (TTC), which form stable monolayers when mixed with dipalmitoyl phosphatidyl choline (DPPC) in chloroform solution. Ultrapure water (pH = 5.9) was used as the subphase. The two drugs caused the monolayer to expand, in particular in their liquid-expanded phase. In the condensed phase the area occupied by the DIB molecule is the same as that of DPPC, which is not true for TTC, where areas per molecule are larger than for pure lipid. There is no hysteresis in the surface pressure and surface potential isotherms, with no loss of material into the subphase. This illustrates the strong binding of these water soluble anesthetics to the lipids in highly organized model systems. The changes in the monolayer characteristics induced by these anesthetics are thought to reflect the possible molecular mechanism of their pharmacological action.

Support: CNPq, FAPESP, FINEP, CAPES

Su-Pos320

INTERACTION OF DIPYRIDAMOLE DERIVATIVES WITH LIPIDS IN HIGHLY ORGANIZED MODEL SYSTEMS

((Galina Borissevitch¹, Iouri E. Borissevitch², Marcel Tabak² and Osvaldo N. Oliveira Jr.¹)) ¹ - Instituto de Física de São Carlos-USP, ² - Instituto de Química de São Carlos-USP, C.P. 780, 13560-970, São Carlos, SP, Brasil.

The vasodilator and antitumor drug coactivator dipyridamole (DIP) and its derivatives (DIPD), varying by the nature and/or the position of the side substituents, can bind to detergent micelles and form stable Langmuir monolayers when mixed with phospholipids in chloroform solution. DIPD are present in the monolayer at all stages of its formation due to their high affinity to lipids notwithstanding their high water solubilities. The nature and the position of DIPD side substituents and charge state of DIPD and the lipid define their location in the monolayer. DIPD with lower hydrophobicity lie closer to the subphase-monomolayer interface. For each DIPD its non-protonated form locates farther from the interface than the protonated one, the location described by the sequence (from the hydrophobic part): DIP₂RA14>RA47>RA25. The same sequence was derived from our experiments on fluorescence quenching of DIPD associated with detergent micelles. From the other hand, the above mentioned factors define the depth of disturbances in the monolayer phase state, followed by the position of the point at the π -A isotherm, where the plateau describing the coexistence of the liquid and condensed phases, begins. It is described by the sequence: DIP₂RA14>RA25>RA47. The biological activity of DIPD determined as the inhibition of the phosphate or adenosine transport across the membranes of red blood cells, decreases according to the sequence: DIP₂RA14>RA47>RA25. So, deeper location of DIP and RA14 along with their stronger disturbing effect upon the lipid organized system as compared with more hydrophilic RA47 and RA25 could explain their higher biological activity.

Support: CNPq, FAPESP, FINEP and CAPES

Su-Pos322

CHOLESTEROL-INDUCED CHANGES IN THE INTERFACIAL MOLECULAR PACKING OF SPHINGOMYELINS AND GALACTOSYL CERAMIDES: NEW INSIGHTS PROVIDED BY COMPRESSIBILITY MODULI MEASUREMENTS

((J. M. Smaby, V. S. Kulkarni, M. Mømsen, H. L. Brockman, & R. E. Brown)) The Hormel Institute, University of Minnesota, Austin, MN 55912

Sphingomyelins (SMs) and galactosylceramides (GalCers) containing identical acyl chains were synthesized and their mixing behavior with cholesterol was investigated using Langmuir film balance techniques. The nature of cholesterol's interactions with the sphingolipid derivatives was determined by measuring both the cross-sectional area condensation of the sphingolipid and the elastic moduli of area compressibility (C_a^{-1}) of the mixed films. Of particular interest were surface pressures (30-35 mN/m) thought to mimic those encountered in membranes. We noted that the cholesterol-induced area condensations of SMs always exceeded those of GalCers when the sphingolipids were "chain-matched" and in similar phase states in the absence of cholesterol. Despite the smaller cholesterol-induced changes in cross-sectional molecular area observed with GalCers, these lipids packed at similar or slightly higher surface densities than the corresponding SMs. The nature of the increased sphingolipid packing density was assessed by comparing the C_a^{-1} values of the mixed-component films. The results showed that the cohesiveness of GalCer-cholesterol films exceeded that of SM-cholesterol films. Conclusions were based on investigation of GalCers and SMs with palmitoyl (16:0), stearoyl (18:0), oleoyl (18:1 ^{Δ^9}), nervonoyl (24:1 ^{Δ^{12}}), lignoceroyl (24:0), and linoleoyl (18:2 ^{$\Delta^9,12$}) acyl residues. [Supported by USPHS Grant GM-45928 and the Hormel Foundation].

Su-Pos324

PHOSPHATIDYLCHOLINES WITH SATURATED, ASYMMETRIC-LENGTH ACYL CHAINS: A LANGMUIR FILM BALANCE INVESTIGATION

((S. Ali, J. M. Smaby, H. L. Brockman, and R. E. Brown)) The Hormel Institute, Univ. of Minnesota, Austin MN 55912

Phosphatidylcholines (PCs) with stearyl (18:0) *sn*-1 chains and variable length, saturated *sn*-2 acyl chains were synthesized and investigated at the air/water interface using a Langmuir-type film balance. Surface pressure and dipole potential were monitored as a function of lipid molecular area under an argon atmosphere and over a buffered saline subphase at various constant temperatures between 10 and 30°C. In this temperature range, (18:0, 8:0) PC and (18:0, 10:0) PC displayed only liquid-expanded behavior. Similar results were obtained for (18:0, 12:0) PC at 15, 20, 24, and 30°C, but not at 10°C. Further increases in *sn*-2 chain length [e.g. (18:0, 14:0) PC and (18:0, 16:0) PC] resulted in films that displayed two-dimensional phase transitions of a liquid-expanded to liquid-condensed nature at many of the temperatures in the 10 to 30°C range. However, di-18:0 PC displayed only liquid-condensed behavior in the 10 to 30°C range. Accurate assessment of the transition behavior was aided by computation of the elastic moduli of area compressibility. Dipole potential measurements provided information about the general orientation of the PC molecules as well as a means to evaluate the contribution of the *sn*-2 chain's terminal methyl group to the overall molecular dipole moment. [Supported by USPHS Grant GM-45928 and the Hormel Foundation]

Su-Pos321

LYOTROPIC PHASES OF DIPHYTANOYL PHOSPHATIDYLCHOLINE ((T. Harroun*, K. He*, W. T. Heller*, S. J. Ludtke*, H. Huang*, C-H Hsieh*, W. Wu*)) *Rice University, Houston, TX 77251-1892; *Institute of Life Science, National Tsing Hua University, Hsinchu, Taiwan 30043

Diphytanoyl (3,7,11,15-tetramethylhexadecanoic) phosphatidylcholine is often used in membrane research, owing to its virtue of having long chains (16:0) but still in the liquid crystalline (L- α) phase in room temperature. No L- α to gel phase transition was detected by differential thermal analyses over the temperature range +120°C to -120°C (Lindsey et al., 1979). This was attributed to the presence of methyl groups at regular intervals along the acyl chain which causes the trans and one of the gauche rotamers to be energetically nearly equivalent, and moreover, the steric requirements of the methyl branches prevent efficient lateral packing of the acyl chains. However, the lipid (DPhPC) exhibits a rich phenomena of phase changes when it is dehydrated. Starting in the lamellar phase at full hydration, DPhPC first underwent a lamellar to lamellar phase transition at ~85-90%RH. The molecular configuration of the new lamellar phase is still unknown. Upon further dehydration, DPhPC changed into either a cubic phase or hexagonal phase depending on sample preparation. (2)H and (31)P NMR and X-ray diffraction studies are presented. The lamellar to cubic phase transition is found to occur at hydration state of approximately 10 water molecules per lipid as seen by the characteristic change of the respective (2)H and (31)P NMR spectra. Both the lamellar to hexagonal and lamellar to cubic phase transitions were detected by X-ray diffraction.

Su-Pos323

MODULATION OF BILAYER NANOTUBE ASSEMBLY IN HYDRATED GALACTOSYL CERAMIDES: EFFECTS OF ACYL MONOUNSATURATION

((V. S. Kulkarni, W. H. Anderson and R. E. Brown)) The Hormel Institute, University of Minnesota, Austin, MN 55912

Our recent freeze fracture electron micrographic studies of hydrated galactosylceramides (GalCer) revealed that acyl structure plays in key role in determining mesomorphic structure. When GalCer contained nervonoyl (24:1 ^{Δ^{12}}) acyl chains, small tubular bilayers, i.e. "nanotubes" resulted [Kulkarni, V. S., Anderson, W. H., & Brown, R. E. (1995) *Biophys. J.* 69(5): in press]. To investigate the role that *cis* double bond position and hydrocarbon chain length play in modulating bilayer "nanotube" formation in GalCers with monounsaturated acyl chains, we synthesized GalCer species having *N*-erucic (*N*-22:1 ^{Δ^{12}}), *N*-eicosenoic (*N*-20:1 ^{Δ^{11}}), or *N*-oleic (*N*-18:1 ^{Δ^9}) acyl chains. Freeze-etch electron micrographs of aqueous dispersions, quenched from the gel state, showed that 22:1-GalCer forms long, straight tubes of uniform diameter (25-30 nm); whereas, 20:1-GalCer formed long, helically-twisted tubes (diameter 30-40 nm). 18:1-GalCer showed a variety of mesomorphic structures including long straight tubes, ribbon-like structures, elongated sheet-like rolls, and occasional spherical vesicles. Differential scanning calorimetry showed that 22:1-GalCer and 20:1-GalCer had main exothermic transitions near 60°C which is comparable to that of 24:1-GalCer (T_m =59.3°C) but quite different than that of 18:1-GalCer (45.1°C). These observations suggest that the hydrophobic chain-chain interactions of GalCers profoundly influence the formation of tubular bilayer self-assemblies. [Support: USPHS grant GM-45928 and the Hormel Foundation]

Su-Pos325

PHOSPHATIDYLCHOLINUM COMPOUNDS: A NEW CLASS OF CATIONIC PHOSPHOLIPIDS WITH TRANSFECTION ACTIVITY AND UNUSUAL PHYSICAL PROPERTIES. ((G.W. Ashley, M.M. Shida, R. Qiu, M.K. Lahiri, P.C. Levisay, R.D. Jones, K.A. Baker & R.C. MacDonald)) Northwestern University, Evanston, IL 60208-3500

Phosphatidylcholines may be converted to cationic phospholipids (PC⁺) by alkylating the phosphate oxygen with trifluoromethylsulfonic acid esters. The ethyl derivative, O-ethylphosphatidylcholinium, is stable in chloroform for years, in water for weeks. DioleoylPC⁺ is susceptible to hydrolysis by some, but not all, common phospholipases. It forms liposomes which can be very large and unilamellar. SUVs are generated by sonication in seconds. PC⁺'s with a variety of saturated and unsaturated chains form complexes with DNA, some of which are highly effective transfecting agents. In addition to mediating DNA Transfection, several of these compounds are capable of delivering other molecules to cultured cells. DNA in cationic lipid complexes formed at a 1:1 charge ratio is sequestered from the aqueous phase, but is released by neutralizing about 10% of the cationic charge with anionic lipid. Cationic lipids are unusually surface active; ethyl DPPC+ suspensions generate a monolayer at their air interface more than 10X faster than do DPPC suspensions. The phase transition temperature of the former lipid is about 5 degrees lower than that of the latter and surprisingly insensitive to ionic strength. (Supported by NIH GM52329)

Su-Pos326

CHARACTERIZATION OF PHOSPHOLIPID CRYSTALS BY MAGIC ANGLE SPINNING (MAS) NMR (Wen Guo*, Michel Groesbeck*, Amir Salmon*, Steve O. Smith*, and James A. Hamilton*, Department of Biophysics*, Boston University School of Medicine, 80 E. Concord St. Boston MA 02118 and Department of Molecular Biophysics and Biochemistry*, Yale University, New Haven, CT 06511).

Phospholipids are very difficult to grow into well defined single crystals, and x-ray crystallographic data are thus extremely limited. The only single crystal that has been reported for the biologically important phospholipid, phosphatidylcholine (PC), is the dihydrated form of dimyristoylPC (DMPC). Although this structure is extensively cited as the model for the conformation of PC in liquid-crystalline bilayers, the interfacial conformation may be significantly affected by hydration. MASNMR can yield high resolution spectra of crystalline lipids and does not require single crystals to yield quantitative information about the crystal structure. To investigate the effects of hydration on the interfacial conformation of DMPC crystals, we prepared anhydrous and dihydrated crystalline DMPC, and fully hydrated DMPC. The anhydrous form has not been previously characterized, to our knowledge. The ^{13}C MASNMR spectra are highly resolved and unique for each crystal type, as are the differential calorimetric curves. The carbonyl spectral region shows two sets of signals for each C=O group for both anhydrous and dihydrate crystals and only one set for the fully hydrated sample. The presence of a second set of resonances for the two crystal forms signifies two nonequivalent molecules in the unit cell. To determine the conformation of the glycerol/carbonyl region, we are performing slow spinning MASNMR experiments to determine the CSA of individual signals and rotational resonance MASNMR experiments to measure the inter-chain distance between two ^{13}C -enriched sites: the C=O (sn1) and the $\text{CH}_2\text{C=O}$ (sn2). In the anhydrous crystal, the internuclei distance was estimated as 5.5 Å. Preliminary results suggest substantial conformation changes occur when the degree of hydration is changed.

Su-Pos328

THE L_α - L_β PHASE TRANSITION IN PHOSPHATIDYLCHOLINE LIPID BILAYERS: A DISORDER-ORDER TRANSITION IN TWO DIMENSIONS. ((V.A. Raghunathan¹ and J. Katsaras²)) ¹Raman Research Institute, Bangalore - 560 080, India and ²Atomic Energy of Canada Limited, Chalk River, Ontario, Canada, K0J 1J0.

The structure of the L_β phase exhibited by hydrated dipalmitoylphosphatidylcholine (DPPC) has recently been established from x-ray diffraction studies on oriented bilayers [J. Katsaras and V.A. Raghunathan, *Biochemistry* 34, 4684 (1995)]. In this study, we reanalyze the powder diffraction data reported in the literature on a number of hydrated lipids with phosphatidylcholine headgroups. As in DPPC, the L_β phase in all these systems is found to be characterized by two-dimensional ordering of the entire lipid molecule on a superlattice of the hydrocarbon chain lattice.

Su-Pos330

IMAGING BILAYER HETEROGENEITY WITH AFM IN SOLUTION. ((D.M. Czajkowsky, J. Mou and Z. Shao)) Department of Molecular Physiology & Biological Physics, University of Virginia, Box 449, Charlottesville, VA 22908. (Sponsored by NIH and NSF)

AFM has been demonstrated to be one of the most powerful methods in the study of bilayer structures in solution¹⁻³. With AFM, several new phenomena have been described, such as the Tris induced ripple phase in DPPC bilayers¹, alcohol induced interdigitated domains in saturated gel state PC bilayers² and the ripple phase in asymmetric bilayers with saturated and unsaturated phospholipids³. We now add to these observations with images of bilayers domains in asymmetric bilayers composed of anionic and zwitterionic phospholipids. In supported unilamellar bilayers with DPPC in the leaflet facing the substrate and mixtures of DOPC and POPS or of DOPC and SOPS in the other leaflet, domains of different thickness, ~1 nm, are clearly resolved by AFM in a buffer containing PBS and EDTA at room temperature. These images may be interpreted as thicker, PS rich and thinner, PC rich domains, where the difference in thickness results from the greater compressibility of DOPC compared with POPS. We also found that poly-L-lysine binds to the thicker PS domains. Since in the presence of EDTA at room temperature, these lipids are in the fluid state, this observation may be the first direct indication of fluid-fluid phase separation, which has been suggested based on other measurements⁴, but still under intensive discussion.

References: ¹Mou, J. et al., *Biochemistry* 33:4439(1994). ²Mou, J. et al., *Biochemistry* 33:9981(1994). ³Czajkowsky, D.M. et al., *Biochemistry* (in press). ⁴Huang, J. et al., *Biophys. J.* 64:413(1993).

Su-Pos327

MATERIAL PROPERTY CHARACTERISTICS FOR LIPID BILAYERS CONTAINING LYSOLIPID. ((Doncho V. Zhelev)) Department of Mechanical Engineering and Materials Science, Duke University, Durham, NC 27708-0300

The area expansion modulus and tensile strength of egg phosphatidylcholine (EPC) membranes are measured in the presence of monooleoylphosphatidylcholine (MOPC). The values of both membrane characteristics decrease as the molar concentration of MOPC increases. The measured apparent area expansion modulus decreases from 167 mN·m⁻¹ for pure EPC membrane to 49 mN·m⁻¹ for a membrane containing 50 mol % MOPC. This significant decrease of the apparent area expansion modulus is attributed to the change of membrane area due to the tension dependent exchange of MOPC between the bathing solution and the lipid membrane. The apparent area expansion modulus has three major components: one related to the intrinsic area expansion modulus of EPC and the other two related to the intrinsic modulus and to the exchange of MOPC, respectively. The last two components are the contribution of MOPC to the apparent area expansion modulus and are combined in an effective area expansion modulus of MOPC. The value of this effective modulus is on the order of 22 mN·m⁻¹. The dependence of the membrane's tensile strength on the presence of MOPC is similar that of the apparent area expansion modulus. The membrane strength decreases from 9.4 mN·m⁻¹ for a pure EPC membrane to 0.07 mN·m⁻¹ for a membrane containing 50 mol % MOPC. The measured tensile strength is used to calculate the line tension of membrane defects that are responsible for membrane failure. This line tension decreases ten times as the concentration of MOPC is increased from zero to 50 mol %. The results suggest that membrane failure, induced by the application of mechanical stress, occurs through the evolution of pre-existing defects rather than the formation of new ones.

This work is supported by grant 2R01 GM 40162 from NIH.

Su-Pos329

THE EFFECT OF PHLORETIN ON THE HYDRATION OF PHOSPHATIDYLCHOLINE BILAYERS. ((G.L. Jendrasiak, R. L. Smith)) East Carolina University School of Medicine, Greenville, N.C. and ((T. J. McIntosh)) Duke University Medical Center, Durham, N.C.

Seelig, *Biochemistry* 1991, 30, 3923 based on NMR has found that phloretin added to phosphatidylcholine bilayers greatly decreases the hydration of the bilayers. We have used gravimetric techniques to measure the water in egg phosphatidylcholine (EPC) as well as to (EPC) phloretin (PH) bilayers and have found that the presence of the phloretin significantly decreases the water adsorbed by EPC over the relative humidity range 0 to approximately 100%. For example at 95% relative humidity EPC adsorbs approximately 11 water molecules per phospholipid molecule whereas with phloretin added in a molar ratio of 3:2 EPC to phloretin, the adsorption per EPC molecule is approximately 8 water molecules. X-ray defraction experiments over the same range of relative humidities show that phloretin decreases both bilayer thickness and the thickness of the fluid space between adjacent bilayers. Calculations of the BET constants for EPC in the presence of PH indicate that 0.75 EPC molecules are affected by one PH molecule. The analog of PH 4'-hydroxyvalerophenone has a much smaller effect on the hydration of EPC. Our results are in agreement with those of Seelig but the effect of the presence of phloretin on the water binding is much less than that found by these other workers.

Su-Pos331

PHOSPHOLIPID EXCHANGE BETWEEN MIXED MICELLES OF PHOSPHOLIPID AND TRITON. ((M.J. Thomas, K. Pang, Q. Chen and M. Waite)) Department of Biochemistry, The Bowman Gray School of Medicine of Wake Forest University, Winston-Salem, NC 27157.

Studies of phospholipase action requires that we understand the enzyme's regulation by the substrate phospholipid (PL). If the enzyme is limited to PL on a single micelle, hydrolysis ceases upon exhaustion of that pool. However, if the PL exchange between micelles exceeds the catalytic rate all PL is available for hydrolysis. To study hepatic lipase we have employed the Triton X-100 mixed-micelle system under conditions of our studies are such that the number of micelles exceeded the number of enzyme molecules by 10⁴ and substrate availability may limit hydrolysis. Here we present our results on the exchange of 1,2-dioleoyl-sn-glycero-3-phosphocholine (DOPC) between micelles of purified 1-(1,1,3,3-tetramethylbutyl)phenoxy-4-nonaoyethylene (OPE-9). These studies have measured exchange using stopped-flow fluorescence and nmr steady-state techniques. Using the spin label 1-palmitoyl-2-(16-doxyl-stearoyl)phosphatidylcholine, nmr measurements gave an exchange rate of 23000 s⁻¹. These measurements were repeated using fluorescence quenching techniques that employed 1-palmitoyl-2-(12-[(7-nitro-2,1,3-benzoxadiaz-4-yl)amino]-dodecanoyl)-sn-glycero-3-phosphocholine as the reporter, but gave only a limiting exchange rate of > 600 s⁻¹. Recent work by Soltys and Roberts (*Biochemistry*, 1994) using fluorescence quenching techniques showed a average intermicellar exchange rate of 500 s⁻¹. Therefore the estimated PL exchange rate for DOPC in Triton micelles is about 4 times larger than the enzyme's catalytic rate (K ≈ 120) and may be as much as 150 times larger.

Su-Pos332

DETECTION OF CRYSTALLINE CHOLESTEROL IN HUMAN ATHEROSCLEROTIC TISSUE BY MAGIC ANGLE SPINNING (MAS) NMR ((James A. Hamilton*, Joel Morrisett*, Michael E. BeBakey**, Gerald M. Lawrie**, Wen Guo**)) Department of Biophysics*, Boston University School of Medicine, Boston MA 02118 and Departments of Medicine* and Surgery**, Baylor College of Medicine, Houston TX 77030.

Accumulation of crystalline unesterified cholesterol (CHOL) in tissue is an important pathological process in several diseases, most notably atherosclerosis. Detection of crystalline CHOL in excised tissues is generally achieved by light microscopy in combination with cryomicrotomy or histology. High resolution ^{13}C NMR spectra can be obtained for crystalline CHOL by the method of MASNMR with cross polarization transfer (CP). The anhydrous and the monohydrate crystal forms are readily distinguished in several spectral regions, including C-5, C-6, and C-18, which are also resolved from most other lipid resonances. Accordingly, we have used MASNMR to examine atherosclerotic plaques, which can contain crystalline CHOL in addition to phospholipids, triglycerides, and cholesterol esters. Human carotid artery segments were obtained by endarterectomy and cut into small segments for ^{13}C MASNMR analysis at 75 MHz. Without CP, spectra of plaques showed primarily cholesterol ester resonances. Since these resonances were present also when the sample was spun at 7° off the magic angle, the cholesterol esters were in a liquid state at 37°C . Signals for lamellar-incorporated CHOL were also detected in the MASNMR experiment. With CP, signals of the cholesterol ester were suppressed and those for CHOL greatly enhanced. Spectra showed mainly a solid CHOL phase and a lamellar phospholipid/CHOL phase. By varying the experimental conditions, signals for the more mobile lamellar phase were almost eliminated, giving a spectrum nearly identical to that of pure CHOL monohydrate. Plaques which showed crystalline CHOL contained, by chemical analysis, a >2 fold molar excess of CHOL with respect to phospholipid. Thus CHOL in a crystalline form can be detected by CP MASNMR in excised plaques with little interference from other lipids, which in some cases are chemically more abundant.

MEMBRANES - BILAYERS AND OTHER MODELS I

Su-Pos334

EPIFLUORESCENCE MICROSCOPY STUDIES OF MIXED LIPID LANGMUIR MONOLAYERS, ((Suzanne Amador, Kathryn Long, Nicholas Wilder*)) Physics Department, Haverford College, Haverford PA 19041.

Epifluorescence microscopy and Langmuir-film balance methods were used to examine monolayers of various lipid mixtures, with the aim of determining the effects of varying degree of chain saturation, detailed lipid composition, and in-plane dipole concentration on the monolayers' phase behavior. Systems studied included various mixtures of the saturated phospholipids dipalmitoylphosphatidylcholine (DPPC), dipalmitoylphosphatidylglycerol (DPPG); the unsaturated phospholipids dioleoylphosphatidylglycerol (DOPG), egg-PG, and plant-phosphatidylinisol (PI), and palmitic acid. Films with similar lipid compositions have been studied as models for pulmonary surfactant. Monolayer films were studied over the entire range of gas, liquid-expanded (LE), liquid-condensed (LC) and "solid" phases at fixed temperature. Variables studied included different ratios of DPPC to the phospholipids PG or PI with differing degrees of unsaturation, and the inclusion of different concentrations of PA for fixed phospholipid composition. Lipid composition influenced the overall shape of the isotherm, including changing the onset of the LE and LC phases and altering the shape of the two-phase LE/LC coexistence region, as well as altering the collapse pressure. Quantitative shape analyses were performed on LC domains to determine the effects of in-plane dipole concentration on domain shape.

Su-Pos336

THE INTERACTIONS OF ACYL CARNITINES ON MODEL MEMBRANES. ((Jet K. Ho, James A. Hamilton*)) Dept. of Biophysics, Boston University School of Medicine, 80 E. Concord Street, W-302, Boston, MA 02118. (Spon. by G.G. Shipley)

Esterification of fatty acids to the small polar molecule carnitines is a required step for the regulated flow of fatty acids into mitochondrial inner matrix. The unique properties and functions of acyl carnitines have generated much interest in their role in myocardial ischemia and recovery from hypoxia. We have studied the interactions of acyl carnitines with model membranes [egg phospholipid (PC) vesicles] by ^{13}C NMR spectroscopy. Using acyl carnitine with ^{13}C enrichment of carbonyl carbon of the acyl chain, NMR signals from acyl carnitines on the inner and outer leaflet of small unilamellar vesicles are detected by ^{13}C NMR spectroscopy in vesicles prepared by co-sonication of PC and acyl carnitine. Following addition of acyl carnitines to the outside of PC vesicles, only the signal for acyl carnitine bound to the outer leaflet is observed. The failure to observe the signal for acyl carnitines on the inner leaflet until after hours of equilibrium shows extremely slow spontaneous diffusion ("flip-flop") or lack thereof. This result is consistent with the zwitterionic nature of carnitine head group and the known requirement of transport proteins for movement of acyl carnitines through the mitochondria membrane. The partitioning of acyl carnitines (8-18 carbons) between water and PC vesicles was studied by monitoring the ^{13}C carbonyl chemical shift as a function of pH and concentration of vesicles. Significant partitioning into the water phase was detected for acyl carnitines with chain lengths of 12 carbons or less. The effect of acyl carnitines on the integrity of the bilayer was examined in vesicles with up to 25 mol% myristoyl carnitines; no gross disruption of the bilayers was observed. Thus, the pathological effects of acyl carnitines are unlikely to be caused by membrane disruption.

Su-Pos333

SPECTROSCOPIC MONITORING OF COPPER-INDUCED LIPID OXIDATION IN LIPOPROTEINS AND UNFRACTIONATED PLASMA ((Dov Lichtenberg, Edith Schnitzer, Ilya Pinchuk and Menahem Fainaru Tel Aviv University, Sackler Faculty of Medicine, Tel Aviv 69978, ISRAEL

Lipid oxidation plays a key role in lipid-related pathologies, including atherosclerosis. Much effort is therefore devoted to the evaluation of plasma lipid oxidizability. Most procedures are based on kinetic studies of the accumulation of conjugated dienes following copper addition to isolated lipoproteins. This procedure is very limited in two respects: 1. Determination of the accumulation of the main intermediates (hydroperoxides) and products (7-keto cholesterol, enals and dienals) requires separation of these products (by HPLC) at many time points. On the other hand, continuous spectroscopic measurements (usually done at 234 nm) yield only an estimate of the overall production of oxidation products. 2. The need for fractionation of lipoproteins (usually LDL) is likely to introduce ambiguities due to alteration of the system during fractionation. We have developed ways to overcome these limitations: 1. By studying the time dependence of the UV spectrum we have developed a method to study the time dependence of accumulation of hydroperoxides, enals, dienals and 7-keto cholesterol from continuous monitoring of the absorbance at four wavelengths. 2. By developing an optimized method, based on our data regarding LDL oxidation in the presence of albumin, which enables evaluation of the oxidizability of plasma lipids from continuous spectroscopic measurements of copper-induced oxidation in diluted unfractionated plasma-citrate. Possible utilization of our newly developed techniques will be discussed.

Su-Pos335

CHOLESTEROL INDUCES LIPID MICRODOMAIN FORMATION IN DOCOSAHEXAENOIC ACID-CONTAINING MIXED PHOSPHOLIPID MEMBRANES. ((W. Stillwell, A.C. Dumauld and L.J. Jenks*)) Department of Biology, Indiana University-Purdue University at Indianapolis, Indianapolis, IN 46202-5132.

Here we test the hypothesis that the omega-3 fatty acid docosahexaenoic acid (DHA) may induce lipid microdomain formation in cholesterol-rich membranes. As models of biological membranes, we employ lipid monolayers and bilayers made from mixtures of 18:0, 18:1 PC/18:0, 22:6 PC to which different amounts of cholesterol are incorporated. Phospholipid-cholesterol interactions are followed in bilayers by MC540 fluorescence and in monolayers by pressure-area isotherms using a Langmuir film balance. These experiments indicate that cholesterol interacts much more strongly with the oleic acid-containing PC than with the DHA-PC. Using differential scanning calorimetry and pressure-area measurements on the mixed phospholipid bilayers and monolayers we demonstrate cholesterol-induced lateral phase separation. Finally lipid microdomains are visualized in the mixed phospholipid monolayers by digital imaging microscopy as a function of lateral pressure using the fluorescent probe NBD-cholesterol. From these experiments we conclude that part of DHA's biological impact may be caused by its role in affecting membrane structure/function through lipid microdomain formation in cholesterol-rich membranes.

Su-Pos337

PHASE SEPARATION OF CHOLESTEROL MONOHYDRATE FROM LIPID BILAYERS CONTAINING PHOSPHATIDYL SERINE, PHOSPHATIDYL CHOLINE, AND CHOLESTEROL ((Jeff Buboltz, Juyang Huang, and Gerald W. Feigenson*)) Section of Biochemistry, Molecular and Cell Biology, Cornell University, Ithaca, NY 14853

In lipid bilayers containing phosphatidylserine (PS) and/or phosphatidylcholine (PC), at high mole fractions of cholesterol, pure cholesterol monohydrate crystals phase separate. The identity of the cholesterol monohydrate was established by means of x-ray diffraction and optical microscopic observation of the crystals. The mole fraction at which the crystals separate, i.e. the saturation of the lipid bilayer with cholesterol, can be determined by three different methods: (i) surface tension of the monolayer in equilibrium with the lipid bilayers or multilayers; (ii) aqueous Ca^{2+} concentration in equilibrium with the lipid multilayers and with $\text{Ca}(\text{PS})_2$; and (iii) filtration of lipid multilayer suspensions containing radiolabeled cholesterol and phospholipids. The critical mole fraction of cholesterol at which the cholesterol monohydrate crystals separate was determined for several different PS/PC ratios and for ionic strengths between 0.01 and 0.80.

Su-Pos338

TREATMENT OF ELECTROSTATIC INTERACTIONS IN MONTE CARLO SIMULATION OF COEXISTING PHASES OF PHOSPHATIDYL SERINE AND PHOSPHATIDYL CHOLINE MEMBRANES ((Juyang Huang and Gerald W. Feigenson)) Section of Biochemistry, Molecular and Cell Biology, Cornell University, Ithaca, NY 14853.

We developed several techniques to account for the electrostatic energy in simulation of coexisting phases of binary PS/PC lipid mixtures: (i) When phase separation occurs, different regions have different charged lipid concentration, membrane potential, and ion screening. We developed a new "mask-evaluation" method which continuously evaluates the local concentration of charged lipids and assigns corresponding values of electrostatic energy to that region. This "mask-evaluation" method is crucial for simulation in a 2-phase region. Without it, simulations would not show correct coexisting phases. We found the optimum mask size is about 13x13 lipids: large enough to avoid treating lipid clusters as different phases in 1-phase regions, but small enough to detect sensitively any new phase formation; (ii) It is important to include the free energy of the aqueous screening ions for the free energy calculation. These ions react to the distribution of charged lipids to minimize the total free energy (including both the membrane and the ionic double layer); (iii) We found an efficient way to relax a lipid mixture to equilibrium in a 2-phase region by allowing lipids to exchange positions over any distance. Which can be hundreds time faster than the traditional Kawasaki method.

Su-Pos340

WATER PERMEABILITY AND MECHANICAL PROPERTIES OF POLY-UNSATURATED LIPID MEMBRANES. ((K.C. Olbrich, W. Rawicz*, E.A. Evans*, and D. Needham)) Dept. of Mechanical Engineering and Materials Science, Duke University, Durham, NC 27708-0300. *Dept. of Physics and Pathology, UBC, Vancouver, BC, Canada V6T 2B5.

Important properties of lipid membranes include their mechanical strength and low permeability to various molecules. These properties directly impact two important biological functions of lipid membranes, providing mechanical cohesion and providing a barrier to the transport of water and other biomolecules. To determine the relationship between the degree of unsaturation of the lipid molecules (structure) and mechanical and transport properties of lipid bilayers, micropipet techniques were used to measure the area expansion modulus, failure tension and water permeability of individual giant lipid vesicles (~20-30 μ m diameter). The water permeability was determined by transferring individual vesicles into a slightly hyperosmotic solution and tracking the osmotic volume change of the vesicle as a function of time. The vesicles were made from various mixtures of stearoylcholinephosphatidylcholine (SOPC), containing one double bond per molecule (18:0/18:1c9), and diinolenoylphosphatidylcholine (DLNCP) lipids, containing six double bonds per molecule (18:3c9,12,15). The water permeability of the lipid membranes ranged from 2.0×10^{-3} cm/s for pure SOPC (1 double bond/molecule) to 4.0×10^{-3} cm/s for a 1:1 SOPC/DLNCP mixture (average of 3.5 double bonds/molecule). These results imply that the addition of double bonds near the bilayer interior disturbs the packing of the hydrocarbon chains and introduces additional free volume in the ordered hydrocarbon region near the headgroups. Additional free volume in this region increases water diffusivity and solubility and thus promotes water permeation. The area expansion modulus decreased from ~190 dyn/cm for pure SOPC to ~140 dyn/cm for the SOPC/DLNCP mixture. The packing impediment imposed by the additional double bonds increases the effective area per molecule, which acts to lower the area expansion modulus of the lipid bilayer. Supported by: NIH Grant GM40162-05 and MRC Grant MT7477

Su-Pos342

DIFFERENTIAL SCANNING CALORIMETRIC STUDY OF A SERIES OF CHOLESTEROL-CONTAINING DIELAIDOYL PHOSPHO- AND GLYCOLIPID BILAYERS. ((T.P.W. McMullen, B.C.-M. Wong, E.L. Tham, R.N.A.H. Lewis and R.N. McElhaney)) Department of Biochemistry, University of Alberta, Edmonton, Alberta, Canada, T6G-2H7.

Cholesterol, a major component of eukaryotic plasma membranes, interacts with many different phospho- and glycolipids in natural membranes. To determine how bilayers containing different lipids respond to cholesterol, we examined the thermotropic phase behavior of cholesterol-containing dielaidoylphosphatidylcholine (DEPC), -phosphatidylethanolamine (DEPE), -phosphatidylglycerol (DEPG), -phosphatidylserine (DEPS), -monoglucosyl diacylglycerol (DEMGD) and -diglucosyl diacylglycerol (DEGDG) bilayers. By standardizing the hydrocarbon chain length and structure of the host bilayers, we eliminate confounding effects due to hydrophobic mismatch. In all cases there is evidence for cholesterol-rich and cholesterol-poor domains at low cholesterol concentrations and cholesterol always progressively decreases the enthalpy and cooperativity of the gel to liquid-crystalline phase transition. However, the shifts in transition temperature and enthalpy vary for each lipid as a function of cholesterol concentration. With the non-bilayer-forming lipids DEPE and DEMGD, cholesterol progressively increases both the temperature and the enthalpy of the lamellar/ H_1 phase transition. Thus headgroup hydration and interfacial hydrogen bonding play an important role in mediating cholesterol-host bilayer interactions.

Supported by the Medical Research Council of Canada and by the Alberta Heritage Foundation for Medical Research.

Su-Pos339

MICRODOMAINS IN MEMBRANE ARCHITECTURE. ((C. W. Meuse and I. W. Levin)) Laboratory of Chemical Physics, NIDDK, NIH, Bethesda, MD 20892-0510.

Phospholipids with varying degrees of *sn*-2 chain unsaturation are important components of biological membranes. The packing motifs of mixed chain polyunsaturated lipids involve microdomains or clusters which maximize the van der Waals interactions between the saturated *sn*-1 chains. In order to corroborate the existence and function of these microdomains, we have coupled $\text{CF}_3(\text{CF}_2)_5(\text{CH}_2)_{10}\text{COOH}$ to 1-palmitoyl- d_{31} lysophosphatidylcholine ($\text{PF}_{13}\text{PC}-d_{31}$) because the helical nature of fluorocarbons mimics the helical nature of polyunsaturated chains. The thermotropic properties of multilamellar dispersions of the fluorinated and unsaturated lipids were compared using differential scanning calorimetry and Raman spectroscopy. Raman spectra were collected at various temperatures to characterize the inter and intrachain order/disorder characteristics of various parts of the lipid acyl chains as the systems undergo gel to liquid crystalline phase transitions. Similarities between the unsaturated and fluorinated lipids, such as broad phase transitions, indicate the formation of microdomains. The different phase transition temperatures indicated by Raman spectral parameters arising from different regions of the acyl chains also support the existence of microdomains. In contrast to fluorinated lipids, however, the unsaturated lipids display hysteresis between heating and cooling scans indicating different reasons for microdomain formation. In the fluorinated lipids, the fluorinated sections, which do not disorder at the lipid phase transition, simply undergo a phase separation process. For mixed, unsaturated lipid systems, the saturated *sn*-1 chain undergoes both a structural phase transition and a lateral phase separation process.

Su-Pos341

ASSOCIATION AND RELEASE OF PROSTAGLANDIN E-1 FROM LIPOSOMES. ((P. Ahl, D. Cabral-Lilly, S. Davidson, J.C. Franklin, F.P. Mauro, S. Minchey and A. Janoff)) The Liposome Company, Princeton, NJ

The interaction of PGE1 with bilayers was studied in several liposomal systems. CD measurements show that the wavelength of maximum absorbance of PGE1 in solution blue shifts approximately 8 nm with increasing solvent polarity. For liposomal PGE1, CD results show a red shift at pH 4.5. Results from DSC together with this data indicate that at low pH, PGE1 is located mainly within the lipid membrane, not in the aqueous phase. The amount of 3H-PGE1 initially associated with EPC, POPC or DSPC liposomes was determined using size exclusion filters and centrifugation. This amount was found to be dependent on pH of the buffer (pH 4.5 >> pH 7.2) and fluidity of the bilayer (EPC = POPC > DSPC), but independent of the lamellarity of the liposome. In all cases, addition of cholesterol reduced the amount of PGE1 associated with the liposome. The time-dependent release of PGE1 from the liposomes was determined by rapidly diluting the sample 100-fold into pH 7.2 buffer. Lipid saturation was a key factor influencing this release. Gel phase liposomes of DSPC showed a rapid initial release of PGE1 corresponding to the amount in the outer monolayer, followed by a very slow, almost negligible release of the remaining PGE1. A rapid initial release also occurred in fluid phase membranes, followed by a more gradual release of the remaining PGE1 over several hours. This release rate could be slowed by increasing the lamellarity of these liposomes, or adding cholesterol to decrease the fluidity of the membrane.

Su-Pos343

CALORIMETRIC AND SPECTROSCOPIC CHARACTERIZATION OF THE THERMOTROPIC PHASE BEHAVIOR OF N-SATURATED 1,2-DIACYL PHOSPHATIDYLGLYCEROLS. ((Y.-P. Zhang, R.N.A.H. Lewis and R.N. McElhaney)) Department of Biochemistry, University of Alberta, Edmonton, Alberta, Canada.

The thermotropic phase behavior of a homologous series of n-saturated 1,2-diacyl phosphatidyl-glycerols was studied by a combination of differential scanning calorimetry, Fourier-transform infrared spectroscopy and ^{31}P -NMR spectroscopy. When dispersed in aqueous media of low-ionic strength (@ 0.1 molar salt) and at near neutral pH, fully hydrated dispersions of these lipids exhibit fairly energetic and highly cooperative gel/liquid-crystalline phase transitions at temperatures comparable to those exhibited by the corresponding 1,2-diacyl phosphatidylcholines. Upon incubation at low temperatures, these lipids all form "subgel" phases at rates which decrease with increases in hydrocarbon chain length and are also dependent upon whether the chains contain an odd- or an even number of carbon atoms (odd-numbered < even-numbered). Each of these lipids initially forms a well ordered but moderately hydrated structure which upon further low-temperature incubation transforms to a more ordered structure which appears to be poorly hydrated structures and exhibits complex hydrogen-bonding patterns in the headgroup and interfacial regions of the lipid bilayer. Moreover, with increases in hydrocarbon chain length, the complexity of these patterns decrease and tend towards those commonly observed with fully hydrated phospholipid bilayers. These observations can be rationalized by considerations of the effects of hydrocarbon chain length on the balance between the hydrophobic and hydrophilic driving forces operating in these lipid bilayers.

Supported by the Medical Research Council of Canada and by the Alberta Heritage Foundation for Medical research.

Su-Pos344

DIRECT DETERMINATION OF THE MEMBRANE AFFINITIES OF INDIVIDUAL AMINO ACIDS IN A POLYPEPTIDE: A HOST-GUEST STUDY. (T. E. Thorgerisson, C. J. Russell, and Y.-K. Shin) Department of Chemistry and Lawrence Berkeley Laboratory, University of California, Berkeley, CA 94720.

For a detailed understanding of the topology and structure of membrane proteins it is necessary to know the membrane affinities of individual amino acids. To directly measure membrane affinities, fourteen uncharged amino acids were introduced individually at a guest site in a 25-residue peptide derived from the membrane-binding presequence of cytochrome C oxidase and the peptides were labeled with a nitroxide spin label. The free energies of transfer from the phospholipid bilayer to water ($\Delta\Delta G$ relative to glycine) were determined by examining the partitioning into bilayers using electron paramagnetic resonance. The $\Delta\Delta G_{\text{bilayer}}$ values are in agreement with hydrophobicities assessed from 1-octanol-water partitioning of N-acetyl-amino-acid amides [Fauchere & Pliska, *Eur. J. med. Chem.-Chim. Ther.* **18**, 369-375 (1983)]. The effects of temperature on the free energy of membrane insertion were also studied, revealing increased binding of the peptide to the bilayer with increasing temperature. These results quantitatively confirm the role of the hydrophobic effect in membrane-protein interactions.

Su-Pos346

PERMEATION OF OPIOID PEPTIDES ACROSS ANIONIC MODEL MEMBRANES (Marek Romanowski, Xiaoyun Zhu, Victor J. Hruby, and David F. O'Brien) University of Arizona, Department of Chemistry, Tucson, AZ 85721

One of the major obstacles in drug delivery is low permeability of cell membranes to various peptide-derived pharmacological agents. According to the model for passive transport across the membranes, the total flow of permeant molecules is related to the product of the water-membrane partition coefficient and the diffusion coefficient, and to the water-membrane interfacial barrier. We investigated the effect of a membrane charge on the permeability and interaction of analgesic peptide ligands with model membranes. A mixture of zwitterionic phospholipids with addition of cholesterol served as the model of biological membranes. The lipid membrane charge density was controlled by the addition of anionic 1-palmitoyl-2-oleoylphosphatidylserine. Two classes of highly potent analgesic peptides have been tested, c[D-Pen⁵, D-Pen⁶]enkephalin and biphallin, a quasi-dimeric analog of enkephalin. By applying the equilibrium dialysis method we found that the negatively charged lipids enhance partitioning or binding to the membrane. At the same time however the transmembrane flux of the peptide, as determined by the permeability assay, is diminished. We attribute this effect to the electrostatic adsorption of the peptide molecules at the polar membrane-water interface that prevents the peptide from entering the hydrocarbon membrane interior, effectively reducing the transmembrane flux. Because c[D-Pen⁵, D-Pen⁶]enkephalins are zwitterionic whereas biphallins are dicationic, these peptides may interact differently with negatively charged membranes. Indeed, we found that the addition of the anionic lipids to the membrane composition affects more strongly the interaction of dicationic biphallins than that of zwitterionic enkephalin analogues. The observed effects indicate that the negative charge naturally present in cell membranes may hamper the transport of some peptide drugs, especially cationic ones, across the cell membrane. Supported by NIDA Grant 06284.

Su-Pos348

PHOSPHATIDYLETHANOL AS A ¹³C NMR PROBE REPORTING PACKING CONSTRAINTS IN PHOSPHOLIPID MEMBRANES (A.V. Victorov, N. Janes, T. F. Taraschi and J. B. Hoek) Dept. of Pathol., Anat., and Cell Biol., Thomas Jefferson Univ. Med. College, Philadelphia, PA 19107

13-CH₂-ethyl labeled phosphatidylethanol (PEth) was used to probe the interleaflet packing density difference in small and large unilamellar phospholipid vesicles (SUVs and LUVs, respectively). The intrinsically tighter lipid packing in the inner leaflet of the SUVs resulted in the splitting of the CH₂-ethyl ¹³C-resonance into two distinct components originating from PEth molecules residing in the inner and outer leaflets. The splitting of the ¹³C NMR signal from the PEth headgroup appears to be unique among naturally occurring phospholipids. We present data suggesting that this splitting is due not only to differences in intrinsic curvature, but also to unequal electrostatic interactions and phospholipid hydration on the inner and outer surfaces of the SUV. The PEth resonance splitting was insensitive to pH changes over the range 4.2-9 and cannot be accounted for by differences in pK_a of PEth inside and outside the SUV. In ¹³C NMR spectra of LUVs, where packing constraints in both monolayers are approximately similar, only a single narrow symmetrical CH₂-ethyl signal was observed. We conclude that the unique splitting of the PEth ¹³C-resonance reported here can be used to characterize the lipid packing conditions in various membranes and to monitor the transbilayer distribution/movement of PEth.

Su-Pos345

SPECIFIC BINDING AND CONTENTS DELIVERY OF LIPOSOMES CONTAINING CD4 TO CELLS EXPRESSING THE HIV-1 ENV GLYCOPROTEIN. (C. Larsen, D. Alford, M. Stevenson and C. Nicolau) Center for Blood Research Labs, Harvard Medical School, 800 Huntington Ave., Boston, MA 02115.

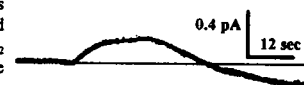
We produced liposomes with various lipid compositions containing a reconstituted purified recombinant form of CD4 (tmCD4, composed of the extracellular, transmembrane and truncated cytoplasmic domains). Recovery of liposome-associated tmCD4 was determined by a flow cytometry assay, ELISA and SDS-PAGE. Liposomes contained the equivalent of more than 30 tmCD4 epitopes per 1 μm^2 surface area. Specific binding of HIV-1 gp120 to CD4-liposomes was demonstrated using recombinant gp120 in a flotation binding assay. Flow cytometry was used to investigate the binding of liposomes (\pm tmCD4; containing a fluorescent marker) to cells at 4 °C and 37 °C. The cell lines tested were a parent B-cell line (BJAB) and a transfected BJAB line expressing the HIV-1 envelope fusion glycoprotein (gp120/41). CD4-liposomes bound specifically to the cell line expressing gp120/41. Fluorescence microscopy and inhibition of protein synthesis were used to detect specific contents delivery of CD4-liposomes containing either FITC-dextran or gelonin.

Su-Pos347

PHOSPHOLIPASE A2 ACTIVITY ON PLANAR LIPID BILAYERS GENERATES A SMALL, TRANSIENT CURRENT THAT IS VOLTAGE-INDEPENDENT ((Stephen N. Alix and Dixon J. Woodbury)) Department of Physiology, Wayne State University School of Medicine, Detroit, MI 48201.

Addition of bee venom phospholipase A2 (PLA₂) to the front solution of a bilayer consistently produced a voltage-independent current (see fig). The signal was transient (~1 min) and usually biphasic (upward current represents movement of positive charge towards the front solution). The signal is proportional to membrane size and is dependent on Ca²⁺ and lipid type. PLA₂ activity on large membranes (>100 pF) made of 70% palmitoyl-oleoyl-phosphatidylethanolamine (POPE) and 30% phosphatidylcholine (POPC) not only produced a current but also led to membrane rupture within 5 min. Addition of PLA₂ in the absence of Ca²⁺ or to membranes made of 100% diphtanoyl PC (non-substrate) produced no current and did not break the bilayer.

We hypothesize that the initial current is due to deprotonation of membrane-bound fatty acids (FA), a product of PLA₂ activity. The declining phase may be due to: product inhibition, FA flip-flop, and/or disassociation of FA into solution. A kinetic model predicted currents similar to those observed experimentally. The model is based on the known reaction of PLA₂ with lipids and on partitioning of enzyme and products between solution and membrane. These results illustrate an easy and extremely sensitive method to measure reaction rates, enzyme specificity and Ca²⁺ dependence of PLA₂ activity.



Su-Pos349

A RAMAN SPECTROSCOPIC STUDY OF MONOUNSATURATED PHOSPHATIDYLCHOLINES: EFFECT OF DOUBLE BOND POSITION ((L.H. Kidder, T.M. Heme*, C. Huang**, and I.W. Levin)) Laboratory of Chemical Physics, NIDDK, NIH, Bethesda, MD 20892. **Dept of Biochemistry, University of Virginia School of Medicine, Charlottesville, VA 22908.

Raman spectroscopic studies of multilamellar lipid dispersions of 1-palmitoyl-2-oleoylphosphatidylcholine [POPC], possessing a *cis*-double bond at the 9,10 position of the sn-2 acyl chain, have suggested the formation of microdomains or clusters. The presence of microclusters permits spatially localized bilayer structural changes to regulate membrane functions associated with the conformational reorganizations of integral membrane components. To elucidate further the propensity of POPC to form microdomains, and to probe the biological significance of the predominance of the sn-2 chain 9,10 positional isomer, we have investigated the Raman spectral behaviour of a series of bilayer dispersions in which the *cis*-double bond of POPC is repositioned along the sn-2 chain. In order to observe separately the spectroscopic behavior of both chains, the POPC derivatives were synthesized with a deuterated sn-1 chain. The sn-2 chain *cis*-double bond of the various species is located at position Δ^7 , Δ^8 , $\Delta^{9,10}$, $\Delta^{11,12}$, or $\Delta^{13,14}$ respectively. Raman spectral order/disorder parameters provide information pertaining to the inter- and intra-chain interactions as a function of temperature. The gel to liquid crystalline phase transition temperatures were determined to be: 4.7°C for Δ^7 , -11°C to +3°C for $\Delta^{9,10}$, 9.5°C for $\Delta^{11,12}$, and 11°C for $\Delta^{13,14}$. Observed biphasic temperature contours demonstrate the inequivalent phase transition behavior of the upper and lower portions of the sn-2 chains.

*present address NIST, Gaithersburg, MD 20899-0001

Su-Pos350

AFM OF THE RIPLE PHASE IN ASYMMETRIC LIPID BILAYERS. ((D.M. Czajkowsky and Z. Shao)) Department of Molecular Physiology & Biological Physics, University of Virginia, Box 449, Charlottesville, VA 22908. (Sponsored by NIH and NSF)

The ripple phase is the least understood of the phospholipid phases. Most of the explanations proposed so far involve the size of the headgroup¹, the degree of the acyl chain tilt² and the extent of the chain movement³, yet the possibility of forming a common ripple structure with leaflets of different composition has not been addressed before. With the AFM in solution, we have observed the ripple phase in bilayers with saturated phosphatidylcholine in one leaflet and anionic, unsaturated phospholipids in the other leaflet at room temperature for the first time⁴. The fact that none of these lipids alone would form the ripple phase under these conditions clearly illustrates the importance of interleaflet interactions. Moreover, we found that there are specific ions and particular lipid combinations that are required for the formation of this ripple phase. This suggests, respectively, that the ripple phase may not be entirely a property of the lipids alone, and that the apposition of particular lipids may have a significant role in the bilayer morphology, which may be part of the reason for the particular lipid asymmetry observed in all cellular membranes.

References: ¹Cevc, G., *Biochim. Biophys. Acta* 1062:59(1991). ²Lubensky, T.C. and MacKintosh, F.C., *Phys. Rev. Lett.* 71:1565(1993). ³Schneider, M.B. et al., *Biophys. J.* 43:157(1983). ⁴Czajkowsky, D.M. et al., *Biochemistry* (in press).

Su-Pos352

PROTEIN KINASE C ACTIVATION BY LIPID LATERAL HETEROGENEITY WITHIN PHOSPHATIDYLCHOLINE/PHOSPHATIDYLSELINE/DIACYLGLYCEROL VESICLES ((A.R.G. Dibble, A.K. Hinderliter, J.J. Sando and R.L. Biltonen)) Dept. of Pharmacology, University of Virginia, Charlottesville, VA 22908.

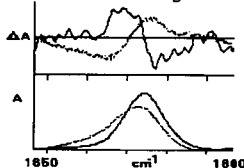
To test the hypothesis that the activation of protein kinase C (PKC) is strongly influenced by lateral heterogeneities of the components of the lipid bilayer, the thermotropic phase behavior of the ternary lipid mixture dimyristoylphosphatidylcholine (DMPC)/dimyristoylphosphatidylserine (DMPS)/dioleoylglycerol (DO) was compared with the ability of this system to activate the enzyme. Differential scanning calorimetry (DSC) and Fourier transform infrared spectroscopy were used to monitor the main (i.e., gel-to-liquid crystalline) phase transition as a function of mole fraction DO (x_{DO}) in DMPC/DO, DMPS/DO, and [DMPC/DMPS (1/1, mol/mol)]/DO unilamellar and multilamellar vesicles. In each case, when $0 < x_{DO} < \sim 0.3$, DO significantly broadened the transition and shifted it to lower temperatures; but when $x_{DO} > \sim 0.3$, the transition became highly cooperative, i.e., narrow, again. The coexistence of overlapping broad and narrow transitions was clearly evident in DSC thermograms of multilamellar vesicles from $x_{DO} \sim 0.1$ to $x_{DO} \sim 0.3$, with the more cooperative transition growing at the expense of the broader transition as x_{DO} increased. These results are consistent with the coexistence of DO-poor and DO-rich domains throughout the range $x_{DO} \sim 0.1$ to $x_{DO} \sim 0.3$. PKC activity was measured using [DMPC/DMPS (1/1, mol/mol)]/DO ternary mixtures as the lipid activator. Above the main phase transition of the lipids, PKC activity increased gradually with increasing x_{DO} from $x_{DO} \sim 0.1$ to $x_{DO} \sim 0.4$. Below the main phase transition, PKC was activated in a biphasic manner from $x_{DO} \sim 0.1$ to $x_{DO} \sim 0.3$. We infer from these results that the ability of these ternary mixtures to activate PKC positively correlates with, in the fluid state, the amount of DO-rich domains and, in the gel state, with the amount of interface between DO-poor and DO-rich phases. (Supported by NIH grants DK07320, DK07642, and GM31184.)

Su-Pos354

Evidence of DMPC Structure and Phase Transitions

(Ping Xie, David Zakim and Max Diem) Hunter College: City Univ of New York, and Medical College, Cornell Univ. NY, NY 10021 (Spon. by M. Diem)

We report the first vibrational CD (VCD) results to characterize the conformational changes of dimyristoylphosphatidylcholine (DMPC) in various chemical environments. Since the C-O-C bond flexible, it can determine the conformation of the hydrocarbon chain. The carbonyl groups of the ester linkage are accessible to observation via VCD, and present a sensitive probe to determine the conformation of DMPC. We find that the orientation of the carbonyls reflect conformational changes of the apolar chain of DMPC. The different absorption frequencies of the two carbonyl groups in DMPC allow us to distinguish between inter- or intramolecular dipolar coupling. In non-polar solvent, the carbonyl groups couple within one molecule and create a positive/negative pattern in the VCD spectrum that is temperature independent. In polar solvent, hydrogen bonding will cause a conformational change.



line) and in D₂O (dotted line) at 5°C (conc.: 40mg/ml).

In aqueous solution, the phase transition of DMPC can be monitored by the orientation change of carbonyls. This implies that the distance between the nonpolar chains is related with to the geometry of the two carbonyl groups.

Fig. 1 The absorption and VCD spectra of DMPC in HCl₃ (solid

Su-Pos351

RELATIONSHIP BETWEEN ACTIVATION OF PHOSPHOLIPASE A₂ AND THE LIPID-CHAIN-LENGTH DEPENDENCE OF BILAYER PHYSICAL PROPERTIES ((T. Hønger,¹ K. Jørgensen,¹ J.H. Ipsen,¹ P.L. Hansen,¹ O.G. Mouritsen,¹ A. Dibble,² and R.L. Biltonen²))

¹Department of Physical Chemistry, The Technical University of Denmark, DK-2800 Lyngby, Denmark, and ²Departments of Pharmacology & Biochemistry, University of Virginia, Charlottesville, VA 22908.

We have studied the temperature and lipid-chain-length dependence of the characteristic lag time, τ , for the onset of rapid Phospholipase A₂-catalyzed hydrolysis of initially one-component large uni-lamellar vesicles of zwitterionic phospholipids. For dimyristoylphosphatidylcholine (DMPC), dipalmitoylphosphatidylcholine (DPPC), and distearoylphosphatidylcholine (DSPC) the lag time is found to display a pronounced minimum at the respective gel-fluid phase transition temperature, T_m . This minimum is deeper and more broad the shorter the lipid chain is. For DPPC and DSPC, $\tau(T)$ furthermore exhibits a local maximum above T_m . Previously we have shown that a structural instability in the lipid bilayer towards high-curvature aggregates occurs concomitantly with the rapid increase in the rate of hydrolysis at time τ . The combined experimental results are discussed in relation to the well-known chain-length effects on bilayer lateral heterogeneity as well as in relation to effects that couple to the elastic properties of lipid membranes.

(Supported by grants from the Danish Research Council and NIH.)

Su-Pos353

ELECTRICAL MANIPULATION OF MOLECULES IN PLANAR SUPPORTED BILAYERS ((Jay T. Groves and Steven G. Boxer)) Chemistry Department, Stanford University, Stanford, CA 94305-5080.

Unilamellar phospholipid vesicles will spontaneously fuse with an appropriate hydrophilic surface to form an extended planar membrane. This structure is generally separated from the solid support by a 20 Å film of water which serves to preserve the fluid nature of the membrane. We are taking advantage of this mobility to develop new methods of electrically manipulating molecules in planar supported bilayers. We have employed electric fields to generate concentration gradients of charged components in confined regions of the supported membrane¹. The concentration profiles observed are well described by a simple model based on competition between diffusion and electric field-induced drift. Analysis of the drift velocity and steady state concentration profiles of fluorescently labeled probes enabled us to determine the in-plane diffusion coefficient of the probe molecules providing verification of the model. We have extended these electrical manipulations to a glycan-phosphatidyl inositol-linked form of the major histocompatibility complex. This membrane tethered protein was observed to move rapidly and could be isolated into highly concentrated corrals. Our current direction involves integration of electrodes into the solid support to generate more sophisticated field geometries and achieve higher degrees of control.

¹ J. T. Groves and S. G. Boxer, *Biophys. J.*, Nov. 1995

Su-Pos355

THE INTERACTION OF DETERGENTS WITH PHOSPHOLIPIDS: THE INTERMEDIATE REGION BETWEEN VESICLES AND MICELLES

((A. Walter, E. Makosky, J. Brinkman, J. Ridge, K. Barnes, K. Lokin. Biology Dept., St. Olaf College, Northfield, MN 55057.))

The vesicle-micelle transition is an essential step in dissolving, reconstituting and preparing two-dimensional crystals of membrane proteins. This intermediate region contains lamellar structures, co-existing lamellar and elongated micellar structures and a region of elongated micelles that decrease in size to spheroidal micelles. We have examined the vesicle-micelle transition with a variety of nonionic and ionic detergents with egg phosphatidylcholine (EPC) and bovine brain phosphatidylserine (PS) vesicles using a range of techniques: contents leakage to mark the loss of bilayer integrity, energy transfer probes on the lipids to follow lipid rearrangements, static light scattering and macroscopic and light microscopic observations. Uncharged systems (EPC+nonionic detergents) aggregated at intermediate levels of detergent to form large multilamellar structures. Dodecylmaltoside (DoDM) and dodecylsucrose (DoDS) induced two regions of tight aggregates: the one near the micellar boundary was visco-elastic reminiscent of similar structures formed by EPC and cholate (Walter, et al., *Biophys. J.* 66:A300, 1994). Aggregation was associated with structural changes that permit leakage and aggregation/leakage was a slow cooperative event lasting over minutes with octyl sucrose whereas the molecular rearrangements were complete within seconds. Net charge on the lipid or on the detergent inhibited the aggregation event: however, positively charged cetyltrimethylammonium and negatively charged PS formed aggregates at intermediate and large complexes at high detergent concentration. The formation of aggregates appeared to be pathway-dependent, i.e., occurred only (or more readily) in the vesicle-to-micelle direction. This is consistent with the concept that this transition is rarely an equilibrium process. Supported by NSF # MCB-9496272.

Su-Pos356

SURFACE PROPERTIES OF DPPC LIPOSOMES DEHYDRATED AND REHYDRATED IN TREHALOSE. (Lagomarsino, E., De La Lanza, S., Bernik, D.L. y Disalvo, E.A.) Laboratorio de Fisicoquímica de Membranas Lipídicas y Liposomas, Química General e Inorgánica, Facultad de Farmacia y Bioquímica, UBA.

In this work we present results indicating that the hydration of DPPC liposomes prepared in trehalose and dehydrated under vacuum show different surface properties in the gel state in comparison to the regular gel phase.

Fluorometric measurements performed on DPPC liposomes with merocyanine 540, dansyl phosphatidylethanolamine (DPE) and dansyl hexylamine (DA) show that the surface of liposomes dehydrated in trehalose are partially in the fluid state upon rehydration in water. However, the effect of the sugar seems to be located at the interface since no changes in the transition temperature are observed when this is measured with diphenylhexatriene. The electrophoretic mobility changes with the pH of the media in a different trend when liposomes prepared in water are compared to those dehydrated and rehydrated in trehalose.

With funds from Fundación Antorchas and UBACyT.

Su-Pos358

SIMULATION OF A FULLY HYDRATED DMPC BILAYER USING THE NYT BOUNDARY CONDITIONS ((S. W. Chiu, S. Subramaniam, and E. Jakobsson)) University of Illinois, National Center for Supercomputing Applications, Urbana, IL 61801

A fully hydrated (over 30 waters/lipid) fluid phase bilayer has been computed using the NYT boundary conditions. This method is similar to constant pressure with the exception that the components of the internal virial in the lateral direction are adjusted to account for the surface tension at the interface (in this case 23 dynes/cm) rather than the pressure in the experimental apparatus. In comparison to a previous simulation with this method but with only 23 waters/lipid (Chiu et al, 1995, Biophys. J 69:1230) the surface area per phospholipid is a bit larger (about 60 as compared to 57.3 square angstroms) and the dipole potential across the interfacial region is larger (about 200 as compared to 130 mv) than the previous simulation. Distinct "fingers" of water can be seen penetrating the interfacial region down to the tops of the hydrocarbon chains. The dipole potential is an exceptionally sensitive measure of the accuracy of the simulations, since its entire magnitude depends on a fine balance between the orientational polarization of the waters and of the polar regions of the phospholipids. Reducing the (group-based) cutoff of the electrostatic calculations to 15 angstroms from 20 angstroms causes the simulated dipole potential to have the wrong sign. Increasing the cutoff from 20 angstroms to 25 angstroms changes the magnitude slightly. We are experimenting on the effect of variations in patch size as well as electrostatic methodology on the accuracy of the simulations. (Supported by NSF and NCSA)

Su-Pos360

QUANTITATION OF CURVATURE STRESS IN MEMBRANES ((Y.C. Lee, T.F. Taraschi, and N. Janes)) Dept. of Pathology, Jefferson Medical College, Philadelphia, PA 19107

The membrane bilayer structure is maintained by a delicate balance of forces in the headgroup and acyl-chain regions. Mismatches in packing in either region induce a tendency toward membrane curvature which is offset by similar changes in the apposed leaflet; consequently, the curvature is not expressed (frustrated curvature stress), but is stored as potential energy with a latent ability to destabilize the bilayer structure.

Quantitation of the stress requires its expression. Our approach is to study the cooperative equilibrium between the planar bilayer (L_α) and the highly curved inverted hexagonal structure (H_{II}). Dilute lipids (solutes) are introduced into a phosphatidylethanolamine (PtdEtn) membrane matrix (solvent) and changes in the equilibrium midpoint temperature (T_{bh}) are interpreted using classical thermodynamics. Curvature stress in the H_{II} state is considered relaxed by changes in the cylinder radius. The solute distribution among structures is nearly equal, indicating that the entropy of mixing makes little contribution to the equilibrium balance. The enthalpic stress imparted by the solute upon the membrane is the dominant driving force modulating T_{bh} . Changes in T_{bh} are readily expressed in terms of the enthalpic stress imparted or relieved on the membrane. This allows for a systematic study of the headgroup-dependence of curvature stress, when acyl-homology is maintained. For example, the small hydroxyl-headgroup of a diacylglycerol is shown to increase the curvature stress and destabilize the bilayer structure of a PtdEtn membrane matrix by 15.1 J / mf%. By contrast, the large headgroup of phosphatidylcholine is shown to stabilize the bilayer structure and relieve stress by 9.3 J / mf%. USPHS AA00163, AA07186, AA07215.

Su-Pos357

SMALL ANGLE X-RAY SCATTERING FROM LIPID BILAYER IS WELL DESCRIBED BY MODIFIED CAILLÉ THEORY, BUT NOT BY PARACRYSTALLINE THEORY

((R. Zhang^{1,5}, S. T-Nagle², W. Sun¹, R. L. Headrick³, T. C. Irving⁴, R. M. Suter¹, and J. F. Nagle^{1,2})) ¹Physics Dept. & ²Biological Science Dept., Carnegie Mellon University, Pittsburgh, PA 15123; ³Cornell High Energy Synchrotron Source, Ithaca, NY 14853; ⁴MacCHESS, Division of Biochemistry, Molecular and Cell Biology, Ithaca, NY 14853; ⁵(current) Chemistry Dept., The Ohio State University, Columbus, OH 43210. (spon. by R. Zhang)

X-ray scattering data at high instrumental resolution are reported for multilamellar vesicles of L_α phase lipid bilayers of DPPC at 50 °C under varying osmotic pressure. The data are fitted to two theories that account for non-crystalline disorder, paracrystalline theory (PT) and modified Caillé theory (MCT). The modified Caillé theory provides good fits to the data, much better than the PT fits. The particularly important characteristic of MCT is the long power law tails in the scattering. PT fits (as well as ordinary integration with no attempt to account for the non-crystalline disorder) increasingly underestimate this scattering intensity as the order h increases, thereby underestimating the form factors used to obtain electron density profiles. Our MCT fits yield fluctuation corrected bilayer form factors, as well as fluctuation parameters which are directly related to interactions between bilayers.

Supported by NIH GM44976

Su-Pos359

AVIDIN-BIOTIN INTERACTIONS AT VESICLE SURFACES: ADSORPTION AND BINDING, CROSS BRIDGE FORMATION, AND LATERAL INTERACTIONS.

((D. A. Noppl and D. Needham)) Dept. Mechanical Engineering & Materials Science, Duke Univ., Durham, NC 27708-0300

Densely-packed domains of membrane proteins are important structures in cellular processes involving ligand-receptor binding, receptor-mediated adhesion and macromolecule aggregation. We have used the biotin-avidin interaction at lipid vesicle surfaces to mimic these processes, including the influence of a surface grafted polymer, polyethyleneglycol (PEG). Single vesicles were manipulated by micropipet in solutions of fluorescently-labeled avidin to measure the rate and amount of avidin binding to a biotinylated vesicle as a function of surface biotin concentration and surface-grafted PEG. The rate of avidin adsorption was found to be 4 times less with 2 mol% PEG⁷⁵⁰ than for the unmodified surface, and 10 mol% PEG completely inhibited binding of avidin to biotin for a two minute incubation. Using two micropipets, an avidin-coated vesicle was presented to a biotinylated vesicle. In this vesicle-vesicle adhesion test, the accumulation of avidin in the contact zone was observed, again by using fluorescent avidin. Also, by controlling the vesicle membrane tension, this adhesion test provided a direct measure of the spreading pressure of the biotin-avidin-biotin cross bridges confined in the contact zone. Assuming ideality, this spreading pressure gives the concentration of avidin cross bridges in the contact zone. The rate of cross bridge accumulation was dependent on the diffusion coefficient of the lipid-linked "receptors" and, once adherent, the membranes failed in tension before they could be peeled apart. PEG⁷⁵⁰ did not influence the mechanical equilibrium because it was not compressed in the contact zone, but it did perform an important function by eliminating all non-specific adhesion. This vesicle-vesicle adhesion experiment, with a lower limit of resolution of 0.01 dyn/cm, now provides a new and useful method with which to measure the spreading pressures and therefore colligative properties of a range of membrane-bound macromolecules.

Grants: North Carolina Biotechnology Center 9413 ARG-0018 and NIH GM 40162-06 Alabama 35294

Su-Pos361

EVIDENCE THAT NONBILAYER PHASE PROPENSITY IS IMPORTANT FOR BIOLOGICAL MEMBRANES. USE OF AMPHIPATHIC PEPTIDE ANALOGS WITH OPPOSITE EFFECTS. (I.V. Polozov[#], A.I. Polozova[#], V.K. Mishra[†], G.M. Anantharamaiah[†], J.P. Segrest[†], and R.M. Epand[†]) [#]Department of Biochemistry, McMaster University Health Sciences Centre, 1200 Main St. West, Hamilton, Ontario L8N 3Z5, Canada; [†]Departments of Medicine and Biochemistry and the Atherosclerosis Research Unit, University of Alabama Medical Center, Birmingham, Alabama 35294

Previously we have reported that apolipoprotein (class A) and lytic (class L) peptide analogs have a reciprocal effect on some properties of biological and model membranes. By analogy to the reciprocal effects of phospholipid shapes on membrane structure, it was proposed that the wedge shape of class A helixes stabilizes bilayers, while the inverted wedge shape of class L helixes destabilizes membranes. We examined the lipid requirements for the observation of a reciprocal effect between 18L (class L) and Ac-18A-NH₂ (class A) on the vesicle aqueous contents leakage, vesicle fusion, and peptide-membrane binding for a number of pure lipids and binary mixtures. We found that the reciprocal effect of these two peptides is restricted to zwitterionic membranes with a high propensity for nonbilayer phase formation (DOPE, Me-DOPE, DOPC:DOPE, DOPC:Me-DOPE). For both leakage and fusion, the decrease in the content of nonbilayer phase forming lipid results in less reciprocal effects. In zwitterionic membranes without nonbilayer forming lipids, as well as in membranes containing acidic lipids, class A peptides were destabilizing and peptide effects were essentially additive. As reciprocal effects are pronounced in biological membranes, we suggest that membrane nonbilayer phase propensity is a property of biological membranes.

Su-Pos362

MECHANISM OF MEMBRANE PERMEABILIZATION BY L-CLASS AMPHIPATHIC LYTIC PEPTIDES. ((I.V. Polozov^a, A.I. Polozova^a, V.K. Mishra¹, G.M. Anantharamiah¹, J.P. Segrest¹, and R.M. Eppard¹)) ^aDepartment of Biochemistry, McMaster University Health Sciences Centre, Hamilton, Ontario L8N 3Z5, Canada; ¹Departments of Medicine and Biochemistry and the Atherosclerosis Research Unit, University of Alabama Medical Center, Birmingham, Alabama 35294

Various naturally occurring lytic amphipathic peptides were found to share the same structural motif classified as L class amphipathic alpha helix (Segrest et al., Proteins, 8, 103, 1990). The 18L model peptide, features the consensus sequence averaged from the number of naturally occurring peptides. We found the mode of 18L peptide membrane permeabilization to be strongly dependent on lipid composition. In zwitterionic membranes (DOPC:DOPE) we found 18L peptide capable of simultaneous induction of both vesicle aqueous content leakage and vesicle fusion. Both vesicle fusion and aqueous contents leakage were observed in the range of bound peptide/lipid ratios 1:50 to 1:10 and on the time scale of hundreds of seconds. At the same peptide/lipid ratios at higher lipid concentration, more fusion and less leakage was observed than at lower lipid concentrations. Thus we suppose that vesicle leakage and fusion are alternative ways of releasing membrane strain imposed by peptide insertion. We conclude that 18L peptide destabilizes the membrane, leading to a transient formation of large defects in the membrane which result generally in contents leakage, but in the presence of bilayer-bilayer contact can lead to vesicle fusion. The size of the defects was estimated from the leakage of fluorescent dextrans and was found big enough for the passage of 20,000 M.W. molecules. In membranes containing acidic lipids (DOPC:DOPG, DOPG) 18L caused leakage but not fusion. While leakage was observed at approximately the same peptide/lipid ratios as for zwitterionic membranes the kinetics of leakage was different. The initial rate of leakage could be resolved only by using stopped-flow and essentially the process of leakage was going to completion within the first minute. We suppose that leakage in this case proceeds concomitantly with peptide insertion and/or translocation to the inner leaflet of bilayer. Linear dependence of the extent of leakage on peptide/lipid ratio indicates that leakage is not mediated by peptide association in the membrane.

Su-Pos364

TRANSMEMBRANE PERMEATION OF PHLORETIN MONITORED BY DIPOLE POTENTIAL AND MICROELECTRODE MEASUREMENTS ((E.E.Pohl, T.I.Rokitskaya^a, Y.N.Antonenko^a, P.Pohl)) Inst. Med. Physik und Biophysik, Martin-Luther-Universität, 06097 Halle, Germany; ^aA.N.Belozersky Institute of Physico-Chemical Biology, State University, Moscow 119899, Russia

The abilities of phloretin to modify the intrinsic dipole potential of bilayer lipid membranes and to diffuse across membranes were investigated. The transmembrane movement was found to be limited by the permeation through the membrane itself at basic values of pH and limited by the transport across the unstirred layer (USL) adjacent to the membrane at acidic pH values. Measurements of both the dipole potential difference between the two membrane layers and the proton concentration profile within the USL allowed to distinguish between USL-phenomena and adsorption related effects. The method of inner membrane field compensation and the microelectrode technique were used respectively. Their combination allowed to carry out phloretin permeability measurements within a wide concentration range. Both the dipole potential and the parameters of the USL were combined in a mathematical model. It describes the transmembrane movement where phloretin is treated like a weak acid. Arguments in favour of a stepwise diffusion through a bilayer involving different classes of binding sites were not found.

Su-Pos366

THE WATER PERMEABILITY OF MODEL MEMBRANES CONTAINING LIPIDS WITH FOUR ACYL CHAINS. ((G.L. Powell, E.K. Wright, M.A. Smith, T.D. Betts, and E.A. Kaisheva)) Biological Sciences, Clemson University, Clemson, SC 29634-1903.

Water permeability is a property of biological membranes, fundamental to osmolar regulation of cells. Water flux is strongly dependent on the lipid phase and lipid composition. The nature of the polar head group, acyl chain length and the degree of unsaturation all influence the water permeability of model membranes. Using dioleoylphosphatidylcholine as the bulk lipid, addition of a few percent of bovine cardiolipin decreased the permeability of these vesicles more than 50% (Jagannathan and Powell, Biophys. J. 66(1994) A382). The fatty acid composition of cardiolipin is unusual consisting of 87% linoleate. Another key property of cardiolipin is its ability to form an inverted hexagonal phase. Using the method of isotope effects on light scattering (Engelbert and Lawaczek (1985) Ber. Bunsenges Phys. Chem. 89, 754-759) and large unilamellar vesicles of defined radius, we have systematically examined the water permeability of phospholipids which can assume hexagonal phases: phosphatidylethanolamines, cardiolipin, and tetraoleoyl pyrophosphatidic acid (TOPPA). Dioleoylphosphatidylethanolamine (DOPE) in mixtures with dioleoylphosphatidylcholine (DOPC) shows almost constant water permeability up to 80% where the inverted hexagonal phase is expected to appear, the water permeability of dilinoleoyl PE between 0-40 mol percent increases about 50%, dilinoleoyl PE also increases the water permeability. TOPPA, with its small polar head group and four oleoyl chains, is only found in an inverted hexagonal phase (Powell and Hsu, 1995 - submitted). The water permeability between 0-10 mol% TOPPA mixed with DOPC decreased about 30%. The lipids with four acyl chains we have tested which can form inverted hexagonal phases seem able to reduce water permeability to a greater extent than phosphatidylethanolamines. The water permeability increased for phosphatidylethanolamines containing acyl chains with increasing numbers of double bonds. While not examined in this study, other effects such as hydration of the polar head group, may prove significant. (Partially supported by a grant from the Public Health Service, HL 38190).

Su-Pos363

LIPID MEMBRANES MAY DEVELOP A DYNAMIC SUPERSTRUCTURE IN THE FLUID STATE. ((B.Klößgen, W.Helfrich)) Fachbereich Physik, Freie Universität Berlin, Arnimallee 14, D-14195 Berlin, Germany.

For some years, we have worked to obtain a direct proof for the existence of anomalous surface structures in the lamellar state of fluid lipid membranes. These features were proposed in addition to the now well known undulations of fluid membranes. They can probably be attributed to Gaussian curvature of higher order, and they should be sensitive to membrane stress. According to a model that we proposed several years ago, a fluid membrane will develop a somehow ruffled surface at reduced tension, consisting of a disordered arrangement of saddles. These may cooperatively assemble into stable folds or ridges of the membranes. Cryo transmission electron microscopy was employed to get a direct proof of the suspected appearance by high resolution pictures. At first, we had to learn about artifacts induced by freezing in closed systems like lipid vesicles. Using a fast plunger device will not totally avoid the build-up of mechanical tension in the membranes. This stress can destroy tension sensitive structures and even result in membrane ruptures. However, it seems that vesicles with shapes of high surface area as compared to the included volume can avoid the production of mechanical stress by undergoing a fast shape transition. We therefore improved our preparation techniques towards the production of vesicle populations with an increased probability of non-spherical vesicles. To avoid effects of any phase separation (also upon cooling) we used only synthetic lipids of high purity and of a single component. In these samples we now reproducibly observed that fluid membranes prepared from one pure lipid component in distilled water may exhibit grainy or ruffled surfaces. This surface feature disappears at the edges of higher curvature where the membranes bend down into the interior of the thin water lamellas. It is also not present in small vesicles and in thin tubes, whereas it seems to develop as a dominant feature over the membrane regions of low curvature. When the graininess is not yet fully developed, both smooth and ruffled domains seem to coexist within one membrane. In addition to the extended superstructure, deep ridges appear in lipid vesicles as an effect of the postulated cooperative assembly of local saddles.

Su-Pos365

SYNTHESIS, MEMBRANE-BINDING, AND DIFFUSION OF SEMI-SYNTHETIC PROTEIN PROBES CONTAINING N-TERMINAL FATTY-ACIDS AND HYDROPHOBIC PEPTIDES. ((Chadler T. Pool, Thomas E. Thompson.)) University of Virginia, Department of Biochemistry, Charlottesville, VA 22908

In order to produce novel protein probes for examining membrane domain structure, we have modified bovine pancreatic trypsin inhibitor (BPTI) by specifically attaching fatty acids and hydrophobic peptides at the N-terminus, and specifically attaching a fluorophore as well as a small peptide at Lys-15. The N-terminus and Lys-15, the site of trypsin binding, are at opposite poles of BPTI. In order to protect Lys-15, Trypsin was bound to BPTI. This complex was then reacted with o-methylisourea resulting in the guanidination of the three unprotected lysines to homocitrulline. This reaction does not modify the N-terminal amine. The N-terminal amine was then reacted with several saturated fatty-acid esters or with the highly soluble heterobifunctional cross linker, sulfo-SMCC. The fatty-acid anhydrides were attached using a tetrahydrofuran, phosphate buffered solvent system, thus eliminating the need for detergents normally employed with such anhydrides. The Trypsin/BPTI complex was then dissociated using a Sephadex G-50 column and an acetic acid buffer. The resulting product consists of BPTI with three guanidinated lysines (referred to as G-BPTI), with a fatty-acid or sulphydryl-reactive crosslinker attached to the N-terminus, and Lys-15 free for linking to any amine-reactive reagent. Polyalanine peptides containing a C-terminal cysteine, and N-terminal leucine residues were cleaved in the presence of SDS and then immediately reacted with G-BPTI possessing the sulphydryl-reactive-crosslinker. All products were analyzed using electrospray or laser-desorption mass spectroscopy. In order to look at binding and diffusion of the protein probes, studies utilizing equilibrium dialysis and fluorescence recovery after photobleaching (FRAP) are currently under way. Several different lipid systems will be studied. (Supported by NIH Grant GM 14628)

Su-Pos367

CELL MEMBRANE REVERSIBLE "AGING" DETECTED BY LAURDAN GP IS ASSOCIATED WITH AN INCREASE IN CHOLESTEROL CONTENT. ((M. Levi¹, A.M. Giusti², C.J. Cruz³, P. Wilson⁴, S. Nguyen¹, E. Gratton², O. Saporita¹, T. Parasassi¹)) ¹Univ. of Texas Southwestern Medical Center, DVMC and Yavneh, Dallas, TX 75216, ²Istituto di Superiore di Sanita, Roma, Italy, ³UIUC, Dept. Physics and LFD, 1110 W. Green St., Urbana, IL 71801, ⁴Istituto di Medicina Sperimentale, CNR, Roma, Italy.

Laurdan (2-dimethylamino-6-lauroyl-naphthalene) GP (generalized polarization) has been measured in two human cell lines, promyelocytic HL60 cells and proerythroblastoid K562 cells, routinely subcultured twice per week in RPMI 1640 with 10% fetal calf serum. The GP measurements were performed on the asynchronously growing populations 24 and 96 hours after the medium renewal. The GP value increased linearly with time after the medium renewal. The increase in GP was reversible with the next medium renewal, i.e., the initial lower GP value was recovered after 24 hours from the passage in fresh medium. At 96 hours, there was a 30% increase in the GP in HL60 cells and a 20% increase in the GP in K562 cells. We tested the hypothesis that a major reason for the increase in GP is the aging induced change in membrane lipid composition. The results showed that from the first to the fifth day of asynchronous growth after the medium renewal, 1) the total cholesterol content increased from 78.7 to 110.3 nmol/mg protein in HL60 cells, and from 90.8 to 126.1 nmol/mg protein in K562 cells, and 2) the total cholesterol to total phospholipid mole ratio increased from 0.496 to 0.624 in HL60 cells, and from 0.643 to 0.834 in K562 cells. Interestingly, similar to the changes of the GP, the changes in cell membrane lipid composition were also completely reversible in 24 hours, when the cells were in a fresh culture medium. We conclude that the time-dependent linear increase in the GP of Laurdan in HL60 and K562 cells is associated with marked changes in cell cholesterol content. Although the molecular basis for such a lipid modification in cell membranes within a few days of subculture remains unknown, the reported findings may reflect on the time-dependent regulation of the biosynthesis and/or degradation of cell membrane cholesterol and phospholipids.

Su-Pos368

EFFECTS OF GADOLINIUM ON ELECTROSTATIC AND THERMODYNAMIC PROPERTIES OF LIPID MEMBRANES ((Yu.A. Ermakov, A.Z. Averbakh, V.I. Lobyshev and S.I. Sukharev*)) A.N.Frumkin Institute of Electrochemistry, Moscow 117071, Russia, *Laboratory of Molecular Biology, University of Wisconsin, Madison, WI 53706.

Trivalent cation Gd^{3+} is a non-specific blocker of several diverse types of mechanosensitive (MS) channels regardless of their ion selectivity, unitary conductance, or origin. Such a generalized effect exerted by submillimolar concentrations of Gd^{3+} may not be due to its direct action on MS channel proteins alone, but may be mediated by its binding to phospholipids thus modifying mechanical properties of the lipid bilayer where the channels are embedded. Isotherms of Gd^{3+} adsorption to planar lipid bilayers or liposomes were measured by intramembrane field compensation or electrophoretic techniques, respectively. Apparent binding constants for Gd^{3+} increased as the surface charge increased in the membranes formed from phosphatidylcholine and phosphatidylserine (PC/PS) mixed at different ratios. Comparison of data obtained by both techniques revealed a large change of dipole potential (150 mV) on the surface of phosphatidylserine membranes in the presence of micromolar Gd^{3+} , which may result from the reorientation of polar headgroups or water dipoles. Differential scanning calorimetry of liposomes made of DMPC, DMPS or their mixtures showed satellite peaks up-shifted as much as 12 degrees from the main peak indicating the formation of a new high-melting phase in the presence of Gd^{3+} . We hypothesize that Gd^{3+} initiates "frozen" lipid domains around MS channels which may restrain conformational transitions in such proteins. (Partially supported by INTAS grant No 93-3372)

TRANSMEMBRANE SIGNALING - MONOVALENT IONS

Su-Pos369

EFFECTS OF MEMBRANE SURFACE CHARGE ON Ba^{2+} BLOCK OF LARGE CONDUCTANCE Ca^{2+} -ACTIVATED K^{+} CHANNEL (J.B. Park, P.D. Ryu and E. Moczydlowski*) College of Veterinary Medicine, Seoul National University, Suwon 441-744, Korea, *Dept. of Pharmacology, Yale University, School of Medicine, 333 Cedar St., New Haven, CT 06510, USA.

Negative surface charges of bilayer membrane have been shown to increase conductance and open-state probability (P_o) of the large conductance Ca^{2+} -activated K^{+} (BK) channels (Moczydlowski et al., *J. Membr. Biol.* 83:273-282, 1985). In this study, we compared Ba^{2+} -induced changes in fast and slow gateings, conductance and P_o of BK channels incorporated into planar lipid bilayers composed of phosphatidylethanolamine (PE) and phosphatidylserine (PS) under symmetrical 0.1 M KCl and 0.2 mM internal Ca^{2+} . BK channel in PS membrane had longer mean open time (170 ± 38 ms, mean \pm sem, $n=12$) and shorter mean closed time (0.38 ± 0.012 ms) than those in PE membrane (30 ± 7.1 ms, $n=5$; 0.84 ± 0.29 ms). In addition, the slope conductance was larger by 43 % in PS membranes (360 ± 8.7 pS) than in PE membranes (251 ± 9.9 pS). Dwell time histograms of typical long closures induced by external Ba^{2+} at 20 mV were well fitted with two time constants of 0.12 and 4 sec. Both mean block times were not dependent on external Ba^{2+} (0.5-20 mM) and type of membrane lipid. Mean burst times were reduced as Ba^{2+} concentration increased, but the rates of reduction seen in PE and PS membranes were not different. Such trend was also observed from dwell-time analysis of the fast events within bursts. However, the conductance and P_o of BK channels in PS membranes were more effectively reduced by external Ba^{2+} than in PE membranes. Respective values of $K_d(0)$ for the conductance were 2.7 mM in PS and 22 mM in PE and K_d for the P_o , 5 mM in PS and 9.9 mM in PE membranes. Our data suggest that the effect of negative membrane surface charge on the Ba^{2+} block of BK channels is significant in reducing the conductance, but little significant in blocking BK channel gating under our experimental conditions. (supported by KSEF 941-0700-002-2).

Su-Pos371

Voltage-dependent blockade by external divalent cations mediates outward rectification of TOK1 channels in patches. ((K. A. Ketchum, W. J. Joiner, A. J. Sellers, L. K. Kaczmarek and S. A. N. Goldstein)) Departments of Pediatrics, Cellular and Molecular Physiology, Pharmacology and Genetics, Yale University, New Haven, CT. 06536.

TOK1 is the first cloned K^{+} channel with 2 P domains in one polypeptide. *Xenopus laevis* oocytes expressing TOK1 exhibit a unique channel phenotype: K^{+} ions flow outward at voltages above the K^{+} equilibrium potential (E_K). The TOK1 current-voltage relation (I-V) thus shifts with external K^{+} concentration (K_{ext}). The I-V relation of inward rectifier K^{+} channels results from block of outward currents by internal Mg^{2+} (or polyamines) at voltages above E_K (and so shifts with K_{ext} as well). We asked, therefore, if TOK1 rectification results from block of inward currents by external divalent cations. Single TOK1 channels in outside-out excised membrane patches have a conductance of roughly 35 pS and a "flickery" appearance (in mM, bath: 140 KCl, 0.3 $CaCl_2$, 1 $MgCl_2$, 10 HEPES, pH 7.1; pipet: 140 KCl, 1 $MgCl_2$, 5 EGTA, 10 HEPES, pH 7.1). Removing external divalents from the bath allows inward flux of K^{+} ions through TOK1 channels at hyperpolarized potentials that were previously electrically quiet. Outward currents at depolarized voltages also increase. This leads to a largely linear I-V relation from -90 to 90 mV, even with Mg^{2+} at the intracellular patch surface. Returning divalents to the bath eliminates inward currents and restores rectification. These results support the notion that voltage-dependent blockade mediates rectification of TOK1 channels. That the TOK1 I-V relation in whole cells shifts with E_K is consistent with this idea as well. The data do not support the idea that ion channels endogenous to oocytes mediate TOK1 currents. Some TOK1 attributes, such as its single channel conductance and "flicker", are reminiscent of YKCl1, a channel recorded in yeast plasma membrane by Gustin et al. in 1986.

Su-Pos370

MULTIPLE C-TERMINAL DOMAINS CONTRIBUTE TO Ca^{2+} -BINDING AND ACTIVATION OF HSLO Ca^{2+} -ACTIVATED K^{+} CHANNELS. ((Jeffrey D. Krause¹, Christine D. Foster² and Peter H. Reinhart¹)) ¹Dept. of Neurobiology, Duke University Medical Center, Durham NC 27710, and ²Dept. of Pharmacology, Glaxo-Wellcome, Research Triangle Park, NC, 27709.

Ca^{2+} -activated K^{+} (K_{Ca}) channels are present in virtually all cells and are structurally intriguing as they combine a voltage sensor and a Ca^{2+} sensor. In this study we used the shortest human K_{Ca} channel isoform (hbr1) containing no alternate exons at any of four identified RNA splice sites. We probed protein domains potentially contributing to Ca^{2+} -activation of hbr1 using a combination of site-directed mutagenesis and functional analysis by patch clamping *Xenopus* oocytes. Three types of mutations were made: charge-neutralizing, hydrogen bond-donor to hydrogen-bond acceptor, and hydrophobic to hydrophilic changes. In Mg^{2+} -free solutions 10 μM Ca^{2+} half-maximally activates hbr1, and the half-maximal activation voltage is left-shifted 22 mV per 10-fold increase in Ca^{2+} . Mutations in three distinct regions of the protein reduce the activating potency of Ca^{2+} by two to three orders of magnitude. Within the S9-S10 linker neutralization of a single aspartate residue lowers the Ca^{2+} -sensitivity of hbr1 approximately 100-fold, and neutralization of two acidic residues reduces the Ca^{2+} potency 200-fold. The additive nature of these mutations is consistent with the notion that these aspartate residues may interact electrostatically with Ca^{2+} . Neutralization of a single aspartate residue within the S6-S7 linker results in a channel with 1000-fold lower Ca^{2+} -sensitivity than wild-type hbr1. Mutations within a third region (S4-S5 linker) also reduce the Ca^{2+} sensitivity 100-fold. None of these mutations altered the steepness of the voltage dependence, nor the slope of the Ca^{2+} dependence (20-24 mV/10-fold change in Ca^{2+}). These results indicate that domains hundreds of amino acids apart contribute to the Ca^{2+} -binding and activation domains in K_{Ca} channels. Supported by NIH grant # NS31253 to PHR.

Su-Pos372

A THIRD CRYPTIC P-DOMAIN IN TOK1 IS NOT REQUIRED FOR ION CHANNEL FUNCTION.

((K.A. Ketchum and S.A.N. Goldstein)) Departments of Pediatrics and Cellular and Molecular Physiology, Boyer Center for Molecular Medicine, Yale University School of Medicine, New Haven, Connecticut 06536-0812.

The outwardly-rectifying K^{+} channel TOK1, cloned from *Saccharomyces cerevisiae*, has a unique primary structure with 2 P-domains bounded by hydrophobic segments on one polypeptide (*Nature*, 1995, 376:690-5). A third cryptic P-like sequence, not bounded by hydrophobic residues, is found at the TOK1 N-terminus. To test whether this latter P-like region contributes to ion channel function, the first 17 TOK1 amino acids were deleted (TOK1 Δ 17). Channel function was assessed by two-electrode voltage clamp of wild-type and TOK1 Δ 17 constructs expressed in *Xenopus* oocytes. Unlike voltage-gated K^{+} channels, which are activated by depolarization over a fixed voltage range to pass outward currents, the voltage at which TOK1-induced currents are first observed changes in response to external K^{+} ion concentration. The voltages at which conductance increases noticeably are -94 \pm 4 mV in 2 mM KCl, -46 \pm 6 mV in 20 mM KCl and -2 \pm 4 mV in 100 mM KCl, close to the K^{+} equilibrium potential predicted for each solution by the Nernst equation. These changes in activation potential are also apparent in normalized conductance/voltage plots, indicating that shifts cannot be attributed to driving force-induced changes in TOK1 current magnitude. Whole-cell TOK1 currents are selective for K^{+} over both Na^{+} and Cl^{-} and thus are insensitive to substitution of chloride by aspartate or sodium by N-methylglucamine. TOK1 Δ 17 channels are expressed and function in a fashion largely indistinguishable from wild-type. Moreover, patch recordings show that single channel conductance is not significantly altered by deletion. These observations indicate that the N-terminal P-like region is not necessary for K^{+} channel function.

Su-Pos373

UNUSUAL EFFECT OF APAMIN ON HOLDING CURRENT IN GUINEA PIG TAENIA COLI CELLS. (Povstyan A.V., Rekalov V.V. & Shuba M.F.) Bogomoletz Institute of Physiology, Bogomoletz Str. 4, Kiev-24, 252601 GSP, Ukraine.

The effect of apamin - a bee venom neurotoxin, widely known as blocker of small conductance Ca^{2+} -activated K^+ channels (SK) - has been studied on the holding current in single smooth muscle cells from guinea pig taenia coli using "whole-cell patch" voltage clamp method. Addition of apamin ($5 \cdot 10^{-6}$ M) to bath solution led to the deflection of holding current into inward direction and increased membrane conductance. The current-voltage curves of ionic currents have been obtained at the potentials between -110 and -60 mV and were linear before and after action of apamin. Currents responses to a voltage ramp were fitting as straight lines and intersected by the extrapolation close to the sodium equilibrium potential. Substitution of sodium ions (Na^+) in bath solution by choline ions (Ch^+) prevented the effect of apamin, but after substitution of Ch^+ by Na^+ in the presence of apamin, this effect appeared; and substitution of Na^+ by Ch^+ in the presence of apamin removed this effect. The obtained results indicate, that depolarization of the cell, caused by apamin could be explained by the activation of sodium conductance of membrane, but not inhibition of SK conductance.

Su-Pos375

INACTIVATION AND EXTERNAL POTASSIUM SENSITIVITY IN HERG POTASSIUM CHANNELS. (J. Wang, M.C. Trudeau and G.A. Robertson) Dept. of Physiology, Univ. of Wisconsin Medical School, Madison, WI 53706.

HERG is a human voltage-gated K^+ channel with the pronounced inward rectification properties and pharmacological specificity characteristic of cardiac I_{Kr} (Trudeau et al., Science 269:92, 1995; Sanguinetti et al., Cell 81: 299, 1995). The I-V relationship of HERG expressed in frog oocytes exhibits negative slope conductance at positive voltages and the channels have a pronounced inward rectification that significantly reduces outward current at all activating voltages, suggesting an inactivation mechanism with a rate that is faster than the rate of channel activation. To determine whether the inward rectification is caused by a pore-blocking mechanism, we measured the rate of fast inactivation at different $[K_o]$. We evoked outward transient currents at positive potentials subsequent to a two-step prepulse designed to sequentially activate, inactivate and remove inactivation from the open channels. The rate of inactivation was reduced at elevated $[K_o]$, suggesting an interaction in the pore between an internal blocking particle and external K^+ . This reduction in the rate of inactivation was accompanied at higher $[K_o]$ by the emergence of a transient peak of outward current evoked by depolarizing voltage steps above 20 mV from a holding potential of -80 mV. Steady-state current amplitudes also increased. Thus the slowing of inactivation kinetics is apparently responsible for the emergence of the early, transient component of outward current in our experiments and may account for the paradoxical increase in outward currents observed in I_{Kr} and HERG channels when external K^+ is elevated. Supported by NHLBI and American Heart Association of Wisconsin.

Su-Pos377

ROLE OF TYROSINE PHOSPHORYLATION IN POTASSIUM CHANNEL ACTIVATION FUNCTIONAL ASSOCIATION WITH PROLACTIN RECEPTOR AND JAK-2 TYROSINE KINASE. (N. Prevarskaya, R. Skryma, P. Vacher and Bernard Dufy) Laboratory of Neurophysiology, University of Bordeaux II, CNRS URA 1200, Bordeaux.

Chinese hamster ovary (CHO) cells stably transfected with the long form of the prolactin (PRL) receptor (PRL-R) cDNA were used for PRL-R signal transduction studies. Patch-clamp technique in whole-cell and cell-free configurations was employed. Exposure of transfected CHO cells to 5 nM PRL led to increase of Ca^{2+} and voltage-dependent K^+ channel (KCa) activity. The effect was direct as it was observed also in excised patch experiments. Protein tyrosine kinase (PTK) inhibitors (genistein, lavendustin A, and herbimycin A) decreased in a concentration and time dependent manner the amplitude of the KCa current in whole-cell experiments and the open probability of KCa channels in cell-free experiments. The subsequent application of PRL was ineffective. The protein tyrosine phosphatase (PTP) inhibitor orthovanadate (1mM) stimulated KCa channel activity in excised patches, indicating that receptors can be modulated in opposite directions by PTK and PTP. Moreover, in whole-cell experiments as well as in excised patch recordings, anti-JAK2 tyrosine kinase antibody decreased the KCa conductance and the open probability of the KCa channels. Subsequent application of PRL was no longer able to stimulate KCa conductance. Immunoblotting studies using the same anti-JAK2 antibody revealed the constitutive association of JAK2 kinase with PRL-R.

We conclude that: (1) KCa channels are regulated through tyrosine phosphorylation/dephosphorylation; (2) JAK2 tyrosine kinase constitutively associated with PRL-R is implicated in PRL stimulation of KCa channels.

Su-Pos374

SUBSTANCE P MODULATION OF K^+ AND Ca^{2+} CURRENTS IN GUINEA-PIG STELLATE GANGLION NEURONS. (R. Gilbert, J. Ryan, M. Horackova, F. Smith, M.E.M. Kelly) Depart. Pharmacology, Physiology and Anatomy, Dalhousie Univ., Halifax, Nova Scotia, B3H 4H7. (Spon. by S.E. Howlett).

We used whole-cell patch-clamp recording to study the effects of Substance P (SP) on membrane potential and ionic conductances in dissociated and cultured adult stellate ganglion neurons (SGNs). Substance P (500 nM) decreased the action potential (AP) after-hyperpolarization (AHP) amplitude and duration by $59 \pm 20\%$ and $40 \pm 27\%$, respectively ($n=5$). In the presence of SP neurons fired repetitive APs in response to depolarizing current injection. Voltage-clamp measurement of ionic currents in SGNs revealed that SP inhibited outward K^+ current ($37 \pm 6\%$, $n=14$) in all cells tested. In the presence of $20 \mu M$ Cd^{2+} SP had no significant effect on outward K^+ current suggesting that SP inhibits a Ca^{2+} -activated K^+ current. The actions of SP were blocked by the NK₁ antagonist CGP-94823 ($1 \mu M$) and attenuated by inclusion of GDP β S in the pipette, but were unaffected by preincubation of the cells with pertussis toxin. SP inhibition did not appear to require protein kinase (PK) activation, since neither the PKC inhibitor GF109203X or bath application of forskolin or dibromocAMP/IBMX reduced this effect. In voltage-clamp, SP produced PTX-insensitive inhibition of voltage-dependent Ca^{2+} current ($42 \pm 18\%$, $n=7$). Thus, SP may modulate neuronal excitability in mammalian SGNs via a PTX-insensitive G protein coupled pathway, which produces inhibition of Ca^{2+} current and subsequent inhibition of Ca^{2+} -activated K^+ current. (Supported by the MRC Canada).

Su-Pos376

A POTASSIUM SK K_{Ca} CHANNEL IN THE ENDOPLASMIC RETICULUM CONTROLS THE FREE $[Ca^{2+}]_{ER}$. (T. Nguyen, and P. Verdugo.) Center. for Bioengineering, University of Washington WD-12, Seattle WA 98195.

Calcium stored in the Endoplasmic Reticulum (ER) have a critical role in signal transduction. Sequestered Ca is thought to be in two fractions inside the ER: a bound fraction (Ca-B) with a K_d of 25-250 μM , in equilibrium with a free Ca^{2+} fraction. The concentration of free Ca^{2+} in the ER cisterna ($[Ca^{2+}]_{ER}$) is thought to remain constant at high μM levels. However, there is evidence suggesting that the association of Ca to the Ca-binding glycoproteins of the ER might not be fixed but regulated (Ikemoto 1992). The studies described here were designed to investigate the dynamics of $[Ca^{2+}]_{ER}$ in respiratory ciliated cells in primary tissue culture, using the fluorescent Ca-probes Rhod2-AM, Mag-Indo1-AM, and Orange5N-AM. Results show that in non-stimulated ciliated cells, $[Ca^{2+}]_{ER}$ remains at about 20 μM , increasing drastically to levels $> 60 \mu M$ following purinergic stimulation with 100 μM ATP. This quick increase in $[Ca^{2+}]_{ER}$ is followed by an increase in the cytosolic $[Ca^{2+}]_C$, and a corresponding increase in ciliary beat frequency. These data further indicate that the Ca-B \leftrightarrow $[Ca^{2+}]_{ER}$ exchange can not be described as a simple mass equilibrium with a fix K_d . Experiments in permeabilized models show that: (i) IP₃ (3 μM) can mimic the increase of $[Ca^{2+}]_{ER}$ produced by ATP in intact cells; (ii) this increase in $[Ca^{2+}]_{ER}$ can be readily blocked by apamin (100 nM); (iii) the entry of K^+ into the ER cisterna by this SK type K_{Ca} channel is necessary and sufficient for the increase of $[Ca^{2+}]_{ER}$; and (iv) that the K_{Ca} channel of the ER turns on at a $[Ca^{2+}]_C$ of about 200 nM. When the ER membrane was short-circuited to K^+ and H^+ ions by the ionophore nigericin (10 μM), the K-induced Ca unbinding inside the ER was found to be a non-linear pH-dependent process of high cooperativity, which does not follow a simple ion exchange stoichiometry. These results are the first evidence that: (i) there is an SK K_{Ca} in the ER of ciliated cells; (ii) that Ca-gated inflow of K^+ into the ER results in a non-linear increase of $[Ca^{2+}]_{ER}$, which precedes the release of Ca^{2+} to the cytosol. These observations provide new evidence on how $[Ca^{2+}]_C$ can control $[Ca^{2+}]_{ER}$ release in ciliated cells and perhaps in other cells as well. Supported by UW-RRF

Su-Pos378

EXTRACELLULAR NUCLEOTIDES ACTIVATE NON-SELECTIVE CATION AND K^+ CONDUCTANCES IN RAT OSTEOCLASTS. (A.F. Weidema, J. Barbera, S.J. Dixon, S.M. Sims) Dept. Physiology and Div. Oral Biology, University of Western Ontario, London, Ontario, Canada.

Nucleotides are important signalling molecules that mediate a variety of biological responses. Extracellular ATP elevates intracellular free Ca^{2+} concentration ($[Ca^{2+}]_i$) in osteoclasts, but its effects on ion channels remain to be determined. Membrane currents were recorded from freshly isolated osteoclasts of neonatal rats using the perforated patch configuration. ATP was applied to cells by pressure ejection from a micropipette (1-100 μM). At a holding potential of -60 mV, ATP activated an initial inward current that peaked rapidly, declined and was followed by an outward current. The initial current showed inward rectification and reversed close to +10 mV (K^+ currents blocked with CsCl in the pipette). Reduction of extracellular Na^+ from 130 mM to 10 mM shifted the reversal potential ≈ 30 mV negative, consistent with ATP activating a non-selective cation current (P_{Na} -receptor). The second phase of current was outward at all potentials positive to E_K and in some cells showed oscillations. The outward current was blocked with CsCl in the patch pipette and reversibly inhibited by extracellular quinine (100 μM). These results are consistent with ATP evoking Ca^{2+} -dependent K^+ -current, possibly via a P_{2U} -receptor. We investigated the role of $[Ca^{2+}]_i$ in activation of K^+ -current using simultaneous Fura-2 fluorescence and patch clamp techniques. ATP-mediated elevation of $[Ca^{2+}]_i$ was accompanied by activation of K^+ -current. These results indicate the presence of at least two nucleotide receptors (P_{2X} , P_{2U}) in rat osteoclasts. Extracellular ATP may lead to osteoclast activation and bone resorption in areas of trauma and inflammation. SUPPORTED BY THE ARTHRITIS SOCIETY.

Su-Pos379

INTERACTION OF DETERGENTS WITH POTASSIUM CHANNELS. ((Gerhild Höllerer and Stefan H. Heinemann)) Max-Planck-Gesellschaft z.F.d.W., AG Molekulare & zelluläre Biophysik, D-07747 Jena, Germany.

The effects of detergents were investigated on cloned potassium channels, expressed in *Xenopus* oocytes. Application of Triton X-100 to the bath solution resulted in a dose-dependent reduction of the peak current through the delayed rectifier channel Kv2.1 and a fast, time and voltage dependent, current decline (time constant = 50 ms at 100 μ M). Effects of Triton could be observed at concentrations as low as 1 μ M. While the reduction of peak current was readily reversible upon wash, the induced inactivation was only removed very slowly. No competition of the apparent channel inactivation with extracellular TEA was observed. Moreover, tail current kinetics was accelerated after application of Triton. Both findings are inconsistent with an open-channel block mechanism. The hydrophilic part of Triton alone (PEG) did not affect the channel when applied at a concentration of 100 μ M. In order to elucidate the molecular basis for the Triton-induced inactivation, we studied its effects on mutants of *Shaker*BD6-46 channels (T449V, A, K and A463V) which show various degrees of C-type inactivation. The absolute effect of Triton strongly depended on the speed of C-type inactivation as 100 μ M increased the rate of inactivation in all mutants by about the same factor (10-20). These results suggest that Triton binds to the channel or the lipid phase such that the energy barrier between the resting channel and the C-type inactivated conformation is lowered by an amount approximately constant for the investigated channel mutants.

Su-Pos381

PRESENCE OF Zn^{2+} -SENSITIVE Na^+ CURRENTS IN RAT BRAIN SEPTUM. ((H.A. Hartmann¹, L.V. Colom², M.L. Sutherland², and J.L. Noebels²)) Departments of Molecular Physiology and Biophysics¹ and Neurology², Baylor College of Medicine, Houston, TX 77005.

Na^+ currents underlie cell electrical excitability. Zn^{2+} -sensitivity is a property of the Na^+ currents expressed from the cardiac tissue isoform; classical brain Na^+ channels are Zn^{2+} -resistant. Recently, Zn^{2+} -sensitive Na^+ currents have been described in neurons from the rat medial entorhinal cortex (White *et al.*, *Neuron*: 11, 1037-47, 1993). To locate the expression of mRNA of the cardiac isoform in the rat brain, we used *in situ* hybridization. Two antisense oligonucleotide probes (P_1 and P_2) were designed to the rat heart Na^+ channel cDNA nucleotides 1914 to 1958 for P_1 , and 6301 to 6350 for P_2 . The 45-mer for P_1 corresponded to amino acids 638 to 652 of the intracellular linker between repeats I and II, and the 50-mer for P_2 corresponded to a 3'-untranslated region. The 3' end-labelled oligos with [³⁵S]dATP were hybridized to rat brain slices at 42°C overnight, washed at 55°C and exposed for 30 days. Two sets of control probes were used: antisense probes were hybridized in the presence of 50-fold excess of the appropriate unlabelled oligo, and sense probes were also designed and used. Both P_1 and P_2 gave an identical, highly specific localization, labeling the septal area in juvenile and adult brains. Whole-cell patch recordings from enzymatically-isolated rat septal neurons demonstrated the presence of a Zn^{2+} -sensitive Na^+ current. In 25% of the neurons tested, 50% of the Na^+ current was reduced by 100 μ M Zn^{2+} . These results suggest the presence of a heart-like Na^+ channel in the septal region of the mammalian brain. Septal neurons regulate excitability of the hippocampus, a brain region involved in memory and learning. Thus, Zn^{2+} -sensitive Na^+ current may have a role in modulating these septo-hippocampal functions.

Su-Pos383

CHARACTERIZATION OF TWO STEADY-STATE CONDUCTANCES MEDIATED BY THE ELECTROGENIC HUMAN DOPAMINE TRANSPORTER. ((M.S. Sonders¹, M.P. Kavanaugh, and S.G. Amara²)) HHMI¹ and Vollum Institute, Portland, OR 97201. (Spon. by N.V. Marrion)

The human dopamine transporter (hDAT) is a member of the family of neurotransmitter transporters which are dependent on external Na^+ and Cl^- ions for substrate translocation. Expression in *Xenopus* oocytes of hDAT cDNA cloned from human midbrain confers the ability to accumulate [³H]DA with comparable kinetics and ionic and pharmacologic sensitivities to neural DA transport. Utilizing two-electrode voltage clamp methods, we have found that hDAT is electrogenic since it gives rise to steady-state inward currents correlated with [³H]DA translocation and since the DA transport velocity and transport-associated currents display similar exponential dependence on membrane potential (e-fold per 87 mV). Correlation of [³H]DA uptake velocity with net charge movement in voltage-clamped oocytes yields a charge-to-DA flux ratio of approximately 4⁺ at potentials -120 to -30 mV. This value is larger than the value of 2⁺ generally predicted from uptake studies with DAT.

In addition to the transport-associated current, hDAT expression confers on oocytes a tonic cation leak conductance which is inhibited by substrates and non-substrate uptake blockers (e.g. cocaine) alike. In contrast to the transport-associated currents, the leak conductance is dependent on neither Na^+ nor Cl^- ions. Ion-substitution experiments were used to calculate the relative permeabilities of cations for the leak conductance from shifts in the reversal potential, yielding an order of $H^+ \gg Li^+ > Na^+ \approx K^+$.

Grants 5T32DA07262 and DA07595 supported this work.

Su-Pos380

ADENINE NUCLEOTIDES REGULATE A VOLTAGE-DEPENDENT AND GLUCOSE-SENSITIVE POTASSIUM CHANNEL IN NEUROSECRETORY CELLS. ((C.G. Onetti, J.J. Lara and E. Garcia)) CUIB, Universidad de Colima. Apdo. Postal 199, 28000 Colima, México. (Spon. by J. Muñiz)

In X organ neurons of crayfish, glucose decreases a K^+ current. The electrophysiological properties of the channels mediating this current is unknown at present. Glucose-sensitive channels were studied in excised inside-out patches. They were selective to K^+ ions, and the unitary conductance was 112 pS in symmetrical K^+ . An inward rectification was observed when intracellular K^+ was reduced. Using a quasi-physiological K^+ gradient, a non-linear $I-V$ relation were found showing an outward rectification and a slope conductance of 51 pS. The open-state probability (P_o) increases with membrane depolarization. The channel was activated from a threshold of about -60 mV and the activation midpoint was -2 mV. P_o increases as a result of an enhancement of the mean open time and a shortening of the longer period of closures. P_o decreases noticeably at 50 μ M of internal ATP, and single-channel activity was totally abolished at 1 mM of ATP. The half-blocking concentration of ATP was 174 μ M. AMP-PNP produced a decrease of open-state probability. The channel activity was also inhibited by glibenclamide (10 μ M). Internal application of ADP activates this channel suggesting that it has two separated sites for the regulation by adenine nucleotides. An optimal range of internal free Ca^{2+} ions (0.1 to 10 μ M) is required for the activation of this channel. These results suggest that although the glucose-sensitive K^+ channel of XO neurons shares properties with K_{ATP} channels in other tissues, it seems to be a different subtype of K_{ATP} channel. Glucose-sensitive potassium channel contributes to macroscopic outward current by at least 29%. Therefore, this channel might be important in the regulation of spontaneous discharge pattern of crayfish neurosecretory cells.

Su-Pos382

TIME COURSE OF SODIUM CURRENT DECAY DIFFERS IN SOMA VERSUS GROWTH CONE OF N1E-115 NEUROBLASTOMA CELLS. ((J. Zhang, R.M. Davidson¹ and L.M. Loew²)) Neuroscience Program, Department of Periodontology¹ and Physiology², University of Connecticut Health Center, Farmington, CT 06030.

Cell-attached patch-clamp recordings were obtained from soma and growth cone membranes of differentiated N1E-115 neuroblastoma cells (1-4 days). Sodium currents evoked by a step depolarization pulse from a holding potential of -80mV (relative to the resting potential of the cells) were averaged over 64 to 200 trials and the declining phase of the averaged current was fitted with a single exponential to obtain the time constant of decay (τ_d). For both soma ($n=10$) and growth cone patches ($n=8$), τ_d was voltage dependent; there was a decrease in τ_d as the step depolarization (-30 to 40 mV) became more positive. Furthermore, at voltages ranging from -20 to 0 mV, mean τ_d values obtained from growth cone patches were about one-half of those obtained from the soma. At voltages of -20, -10, and 0 mV, the growth cone τ_d was 0.87 ± 0.13 ms, 0.76 ± 0.08 ms, and 0.53 ± 0.05 ms, respectively, whereas the soma τ_d was 2.10 ± 0.32 ms, 1.54 ± 0.31 ms, and 1.03 ± 0.15 ms (Mean \pm S.E.M., $P < 0.05$). A kinetic analysis of single sodium channel current revealed that the distribution of open dwell times from both soma and growth cone was best-fitted by a single exponential, with a time constant (τ_o) less than 1 ms. However, in contrast to τ_d , the τ_o values obtained from soma and growth cone did not differ significantly nor display voltage-dependence (consistent with the finding of Aldrich *et al.*, *Nature* 306:436-441, 1983). These findings suggested that inactivation rates were similar, and the differences in τ_d between soma and growth cone resulted from differences in activation rates. Furthermore, the similar τ_o values in soma and growth cone together with similar single channel conductance (around 17pS in the present study) indicate that the sodium channels in this cell line represent a homogeneous molecular population. Assuming that N1E-115 neuroblastoma cells utilize the same voltage-dependent mechanism to activate the soma and growth cone sodium channels, the faster activation of growth cone sodium channels might be explained by the higher electric field in the growth cone membrane (Bedlack, Jr. *et al.*, *Neuron* 13, 1187-1193, 1994). The intramembrane electric field could act as an offset to the transmembrane voltage, effectively setting a growth cone channel at a depolarized position relative to the same type of channel in the soma.

Su-Pos384

LOCALIZATION OF THE QUINACRINE NONCOMPETITIVE INHIBITOR BINDING SITE ON THE OPEN-CHANNEL CONFORMATION OF THE TORPEDO ACETYLCHOLINE RECEPTOR. ((D.A. Johnson and S. Aryes)) Division of Biomedical Sciences, University of California, Riverside, Riverside, CA 92521

Voltage-dependent inhibitors (VDIs) of the nicotinic acetylcholine receptor (nAChR) are widely thought to act sterically by entering and "plugging" the open channel of the nAChR. However, quinacrine, a fluorescent VDI, has been recently shown to bind to the nAChR at a site near the lipid membrane domain when the nAChR is in a closed desensitized configuration, suggesting that, at least, one VDI might act allosterically outside the channel (Valenzuela *et al.*, *J. Biol. Chem.*, 267, 8238, 1992). To show that quinacrine also binds outside the open channel, we used a short-range lipophilic quencher to assess the proximity of the nAChR-bound quinacrine to the lipid membrane domain. Specifically, we assessed the ability of 5-doxyloleate (5-SA) to affect quinacrine emission following the rapid mixing of an agonist with the nAChR. 5-SA (80 μ M) reduced the amplitude of the rapid agonist-induced change in quinacrine emission by ~40%, indicating that the quinacrine was binding to a site near the lipid membrane domain and, therefore, presumably at a distance from the channel lumen. Control experiments established that 5-SA had no effect on either the ability of the receptor to undergo agonist-induced conformational changes or the magnitude of the emission from the dansyl-C₆-choline as it binds to the agonists binding sites. (Supported by NSF grant 9215105)

Su-Pos385

INCOMPLETE CLOSURE AND OUTWARD RECTIFICATION OF CLC-0 CHLORIDE CHANNEL INDUCED BY SINGLE POINT MUTATIONS. ((Uwe Ludewig, Michael Pusch, and Thomas J. Jentsch)) ZMNH, Hamburg University, 20246 Hamburg, Germany

The chloride channel from *Torpedo* electric organ, CLC-0, is controlled by two distinct voltage-dependent gates. The voltage-dependence of the "fast" activation gate is tightly linked to chloride permeation. A lysine residue in the channel protein (K519) had been identified being important for fast voltage-dependent gating. K519 is located after domain 12, within a stretch of amino acids that is conserved among CLC-0, -1, -2 and -K chloride channels. Here we systematically investigate the effect of neighbouring mutations on the gating and permeation of CLC-0. While most conservative substitutions had only slight effects on fast gating or permeation, more drastic mutations changed kinetics and voltage-dependence of fast gating and pore properties such as ion selectivity and rectification. In addition, several mutations accelerate slow gating. In some mutants, including K519E, the minimal macroscopic open probability of fast gating saturates at negative voltages at a nonzero value. By non-stationary noise analysis we show that K519E mutant channels fully deactivate at these voltages, but deactivated channels have a residual conductance, a "leaky closed state". This is in contrast to wild type CLC-0 channels, where fast gates shut the channel completely. The mutant channels can be closed by the slow gate. Our results establish the involvement of amino acids carboxy-terminal to domain 12 in permeation, fast and slow gating and are compatible with the previous finding that the predominant amount of gating charge for fast gating is conferred by the permeating ion itself.

Su-Pos387

BAND 3 REGULATES MEMBRANE RIGIDITY BY TWO DISTINCT MECHANISMS ((J.A.Chasis, D.W.Knowles, J.A.Gimm G.Lee, S.McGee, D.Anstee, N.Mohandas)) University of California, Lawrence Berkeley National Laboratory, Berkeley, CA. *South Western Regional Transfusion Center, Bristol, UK.

Interactions between ligands and their cell surface receptors are the initial event in a host of signaling processes which are the fundamental currency of life. Many of these processes initiate a transmembrane signal which involves the cytoskeletal structure. Because of the wealth of knowledge of the components of the red cell membrane we are using it as a model system to study the molecular mechanisms in these types of signal transductions. Binding of a monoclonal antibody BRAC18, to the 3rd extracellular loop of Band 3, induced a dose-dependent rigidification of the membrane, measured by ektacytometry, and a lateral immobilization of its receptor, measured by FRAP and fluorescence-imaged microdeformation. Membrane rigidification was not induced by binding of BRAC18 Fab but was present after binding of a second IgG, to the membrane bound Fab fragment implying that a bivalent ligand was crucial for ligand-induced membrane rigidification. Both FRAP and microdeformation experiments showed that BRAC18 immobilized Band 3 indicating an increased interaction between Band 3 and the cytoskeleton. This mechanism of membrane rigidification is clearly different from that observed after ligand binding to the other major erythrocyte membrane protein, Glycophorin A (GPA). Ligand binding to GPA rigidifies the membrane not through clustering of Band 3 but through a transmembrane signaling process which involves a cooperative interaction between GPA and Band 3. We conclude that Band 3 can regulate membrane material properties by two distinct mechanisms, one involving the clustering of Band 3 and resultant reorganization of the skeletal network and the other through increased interaction between the cytoplasmic domain of Band 3 and the cytoskeletal network.

NMR/EPR

Su-Pos388

MULTIDIMENSIONAL NMR STUDIES OF THE STRUCTURE OF HUMAN INTESTINAL FATTY ACID BINDING PROTEIN (I-FABP). ((Fengli Zhang*, Christian Lucke*, Leslie J. Baier**, James C. Sacchettini*, and James A. Hamilton*)) *Department of Biophysics, Boston University School of Medicine, Boston, MA 02118; **Phoenix Epidemiology and Clinical Research Branch, NIDDK, NIH, Phoenix, AZ 85016; *Department of Biochemistry, Albert Einstein College of Medicine, New York, NY 10461

Human intestinal enterocytes secrete a small (131 amino acid) protein, I-FABP, that binds fatty acids with high specificity. This soluble, cytosolic protein may be involved in intracellular trafficking of fatty acids. Recently an allele (A54 to T54) was found in Pima Indians with insulin resistance and increased fatty acid oxidation. The 3D solution structures of human I-FABPs are being studied by multidimensional nuclear magnetic resonance spectroscopy. The I-FABPs were expressed and purified from *E. Coli.* with and without ¹⁵N-enriched media. The sequential assignments were completed by using two dimensional homonuclear spectra (COSY, TOCSY, and NOESY), heteronuclear spectra (HSQC, HMQC-TOCSY, and HMQC-NOESY), and three dimensional spectra (NOESY-HMQC and TOCSY-HMQC). The tertiary structure of each protein is being calculated by a distance geometry program DIANA and energy minimization program XPLOR based on NOE constraints obtained from NOESY, 2D HMQC-NOESY, and 3D NOESY-HMQC spectra. A comparison of the structures of the normal and the T54 allele of I-FABP will yield new insights into the mechanism of binding of fatty acids and the role of I-FABP in transport and metabolism of intracellular fatty acids.

Su-Pos386

INCREASED CYTOSKELETAL INTERACTION OF GLYCOPHORIN A AND BAND 3 INDUCED BY GLYCOPHORIN A RECEPTOR LIGANDS. ((D.W.Knowles, J.A.Gimm, L.Tilley*, N.Mohandas, J.A.Chasis)) University of California, Lawrence Berkeley National Laboratory, Berkeley, CA. *Biochemistry Dept., La Trobe University, Bundoora, Vic.

One key mechanism of signal transduction across cell membranes involves ligand-induced conformational changes in membrane receptor proteins resulting in increased association of the receptor with the cytoskeleton. Using the red cell as a model system we have previously shown that binding of monoclonal antibody ligands to the exoplasmic domain of glycophorin A (GPA) rigidified the membrane by inducing a cooperative interaction between GPA and band 3. To characterize the molecular mechanism of this form of transmembrane signaling we used the technique of fluorescence imaged microdeformation to quantitate the induced density gradient in the spectrin/actin based cytoskeleton in the deformed state. The subsequent redistribution of other membrane components shows the ability of the component to move down the density gradient and is a measure of its association with the cytoskeleton. In the non-liganded state both GPA and band 3 partially redistribute following microdeformation with band 3 showing a steeper density gradient than GPA but not as steep a gradient as cytoskeletal-actin indicating that Band 3 is more associated with the cytoskeleton than GPA. Binding monoclonal R10 at saturation to GPA, *in situ*, resulted in a dramatic increase in the slope of the density gradient of both GPA and band 3. In each case the density gradient became cytoskeletal-actin like, implying that ligand binding induces complete association of these two proteins with the cytoskeleton. To test the role of the GPA cytoplasmic domain in inducing these cytoskeletal linkages, we utilized MVV red cells which contain a mutant GPA with a truncated cytoplasmic domain. Binding R10 to MVV cells did not induce any change in the gradient of either band 3 or GPA. These data imply that R10 binding in normal red cells initiates a cooperative interaction between the cytoplasmic domains of GPA and band 3. This interaction increases the association of each protein with the cytoskeleton. The lateral immobilization of both membrane receptors is responsible for increased membrane rigidity. Thus, ligand-induced alterations in red cell membrane properties appears to be an excellent model to study the role of cooperative action of the cytoplasmic domains of two different proteins in signal transduction.

Su-Pos389

¹³C NMR DYNAMICS STUDIES OF PALMITIC ACID IN RAT INTESTINAL FATTY ACID BINDING PROTEIN. ((L. Zhu, M. D. Kemple, E. Kurian†, and F. G. Prendergast†)) Dept. of Physics, Indiana University-Purdue University Indianapolis, Indianapolis, IN 46202, and †Dept. of Biochem. and Mol. Biol., Mayo Foundation, Rochester, MN 55905.

Recombinant rat intestinal fatty acid binding protein (I-FABP) is a 15.4 kDa protein which tightly binds a number of long chain fatty acids with a stoichiometry of 1:1. The dynamics of palmitic acid, isotopically enriched with ¹³C at either the second position or at the terminal methyl, were investigated by ¹³C NMR relaxation measurements (T₁, T₂ and the steady-state NOE) when bound to I-FABP at pH 5.5 and 23 °C. For comparison, the dynamics of this fatty acid were also examined in methanol and in 40 mM MPPC (1-palmitoyl-2-hydroxyl-sn-glycero-phosphocholine) micelles. The data were analyzed using the model-free approach of Lipari and Szabo. Overall rotational correlation times were < 1 ns, 6 ns, and 9 ns in methanol, I-FABP, and the MPPC micelles, respectively. Order parameters were largest in I-FABP and smallest in methanol. Also as expected, the methyl carbon was much more mobile than the carbon at position two. The dynamics are consistent with the headgroup of the fatty acid being anchored when the fatty acid is bound to I-FABP. Supported in part by NSF Grant DMB-9105885 (MDK) and PHS Grant GM34847(FGP).

Su-Pos390

STRUCTURAL STUDIES BY NMR OF THE N-TERMINAL DOMAINS OF THE CHAPERONE PROTEIN DnaJ. ((K. Huang, J. M. Flanagan and J. H. Prestegard)) Yale University, New Haven, CT 06511, Brookhaven National Lab, Upton, NY 11973. (Spon. by J. H. Prestegard)

The ATPase stimulatory activity of DnaJ, which is central to the mechanism of the DnaK-DnaJ chaperone machine, resides in the N-terminus of DnaJ, which includes a "J-domain" (1-78) and a glycine phenylalanine rich "G/F" domain (79-104). The solution structures of an ^{15}N labeled DnaJ(1-78) fragment and the solution structures of an ^{15}N and ^{13}C doubly labeled DnaJ(1-104) fragment show that the presence of the "G/F" domain affects the helix packing of the "J-domain" even though the "G/F" domain itself is not well structured. This is consistent with the fact that the "J-domain" alone doesn't have a good ATPase stimulatory activity. To further understand the structural features of DnaJ required for ATPase stimulation, we prepared an ^{15}N ^{13}C doubly labeled DnaJ(1-78) fragment. ^{13}C assignments were obtained with an HNCACB experiment and an HCCH-TOCSY experiment. Furthermore, stereo specific assignments of nonequivalent β methylene protons and χ angles for both DnaJ(1-78) and DnaJ(1-104) were determined from information from $^3\text{J}(\text{H}\alpha\text{-H}\beta)$, $^3\text{J}(\text{N-H}\beta)$, $^3\text{J}(\text{N-}^{13}\text{CO})$ and $^3\text{J}(\text{C-}^{13}\text{CO})$ coupling constants. Solution structures of both DnaJ(1-78) and DnaJ(1-104) are being refined and the resulting structures will be presented together with mutagenetic studies in an attempt to reveal the structural basis of the ATPase stimulatory activity of DnaJ.

Su-Pos392

MEASURING PROTEIN SELF-ASSOCIATION USING PULSED-FIELD-GRADIENT NMR SPECTROSCOPY ((A.J. Dingley, J.P. Mackay, and G.F. King)) Department of Biochemistry, The University of Sydney, Sydney NSW 2006, Australia

It has recently been demonstrated that pulsed-field-gradient (PFG) NMR spectroscopy provides a facile alternative to conventional techniques such as analytical ultracentrifugation and quasi-elastic light scattering for measuring the self-association of biological macromolecules such as proteins^{1,2}. Under most circumstances, the technique can be used to reliably estimate the molecular weight of the diffusing species³. While these initial studies both employed single-quantum ^1H coherence to measure the translational diffusion coefficients of the diffusing species, it is well known that multiple-quantum coherences are generally more sensitive to the gradient pulses³. This provides a significant advantage when studying large macromolecular complexes as the duration allowed for diffusion between the gradient pulses can be shortened in order to minimize magnetization losses due to transverse relaxation. We will compare PFG NMR studies of two model proteins, one which is monomeric and the other which self-associates extensively, using both ^1H single-quantum coherence and various heteronuclear multiple-quantum coherences. We will show that PFG NMR experiments employing heteronuclear multiple-quantum coherence are suitable for studying large macromolecular complexes and that they have the added advantage of allowing the elimination of signals from unlabelled solvents and solutes.

- Altieri, A.S. *et al.* (1995) *J. Am. Chem. Soc.* **117**, 7566-7567.
- Dingley, A.J. *et al.* (1995) *J. Biomol. NMR* **6**, in press.
- Kay, L. & Prestegard, J.H. (1986) *J. Magn. Reson.* **67**, 103-113.

Su-Pos394

A COMPLETE METHOD FOR DETERMINING PROTEIN STRUCTURE FROM SOLID-STATE NMR ORIENTATIONAL DATA. ((R.R. Ketchum^{1,2}, M. Brennen^{1,2}, W. Hu^{1,3}, K.-C. Lee^{1,3}, S. Huo¹, J. Quine⁴, B. Roux⁵, and T.A. Cross^{1,2,3})) ¹National High Magnetic Field Laboratory, ²Institute of Molecular Biophysics, ³Department of Chemistry, ⁴Department of Mathematics, Florida State University, Tallahassee, FL 32306-4005, ⁵Department of Chemistry, University of Montreal, Montreal, Quebec, Canada H3C3J7.

The completion of an ongoing project in our lab to determine the global structure of a protein in the solid state has been achieved. We present here a complete outline of the method.

Orientational constraints derived from ^{15}N and ^{13}C chemical shifts, ^{15}N - ^1H and ^{15}N - ^{13}C dipolar splittings, and $\text{C-}^2\text{H}$ quadrupolar splittings are used to determine a complete initial structure. This method generates stable coordinates and reduces structural ambiguities inherent in the solid state NMR data. Refinement by simulated annealing exhaustively searches conformational space of the molecule consistent with the experimental data.

The method is implemented in a suite of programs and applied to gramicidin A, a peptide for which there exists an abundance of experimental data. The method produces 65,536 initial structures that all have the same structural motif and vary only in the orientation of the peptide plane normals to the channel axis. This ensemble is generated combinatorially from two different peptide plane orientations. Refinement of this ensemble produces a single final structure.

Su-Pos391

^1H NMR STUDIES COMPARING THE STEREOSELECTIVITY OF SIALIDASES FROM THE CHINESE HAMSTER OVARY CELLS AND *SALMONELLA TYPHIMURIUM* LT2. ((Y.-H. Kao, L. Lerner, and T. G. Warner)) Genentech, Inc., South San Francisco, CA 94080

Sialidases are a family of glycohydrolytic enzymes that release sialic acid residues from glycoproteins and glycolipids. The sialidases from viral and bacterial sources have been well studied and the X-ray structures of several sialidases have been determined. Although there is only a moderate degree of sequence homology (~35%) among these enzymes, the overall fold and the active site geometry are remarkably similar. ^1H NMR studies have shown that these enzymes cleave a variety of sialyl conjugate substrates by releasing the alpha anomer of sialic acid as product. Thus, the enzyme hydrolysis proceeds with an overall retention of configuration at the anomeric center (C-2) of the sialic acid molecule, presumably as a result of a double displacement type reaction. The correlation between the stereoselectivity of substrate hydrolysis and the structural organization of the catalytic domain of bacterial and viral sialidases and other glycohydrolases is remarkable. In contrast to the bacterial and viral enzymes, mammalian sialidases have not been well characterized. There are no significant amino acid sequence identities between the mammalian and microbial sialidases. It would be of great interest to determine if the mammalian enzymes share a similar topology and catalytic mechanism with their microbial counterparts. However, the three dimensional structures of mammalian sialidases are not yet available. In this poster, one-dimensional ^1H NMR spectroscopy was employed to compare the reaction mechanisms in the hydrolysis of 4-MU-Neu5Ac catalyzed by sialidases from *Salmonella typhimurium* LT2 and from Chinese hamster ovary (CHO) cells. The data suggest that stereoselectivity of the CHO sialidase is similar to that of microbial sialidases.

Su-Pos393

AUTOMATED PROBABILISTIC METHOD FOR ASSIGNING BACKBONE RESONANCES OF (^{13}C , ^{15}N)- LABELED PROTEINS. ((J. A. Lukin^o, A. P. Gove¹, S. N. Talukdar¹, and C. Ho^o)) ^oDepartment of Biological Sciences and ¹Robotics Institute, Carnegie Mellon University, Pittsburgh, PA 15213.

We have developed a computer algorithm for assigning backbone and $^{13}\text{C}/\beta$ resonances of a protein of known primary sequence. Input to the algorithm consists of cross-peaks from ten heteronuclear 3D-NMR experiments: HNCA, HN(CA)CO, HN(CA)HA, HNCACB, HCACO, HCA(CO)N, HNCO, HN(CO)CA, HN(CO)HA, and CBCA(CO)NH. Data from these experiments performed on the 226-residue glutamine-binding protein (GlnBP) are analyzed statistically using Bayes' theorem to yield objective probability scoring functions for matching chemical shifts. Such scoring is used in the initial stage of the algorithm to combine cross-peaks from the first five experiments to form intra-residue segments of chemical shifts $\{N_i, H_i^N, C\alpha_i, C\beta_i, C_i'\}$ while the latter five are combined into inter-residue segments $\{C\alpha_i, C\beta_i, C_i', N_{i+1}, H_{i+1}^N\}$. Given a tentative assignment, the second stage of the procedure calculates probability scores based on the likelihood of matching the chemical shifts of each segment with: (i) overlapping segments; and (ii) chemical shift distributions of the underlying amino-acid type (and secondary structure, if known). This joint probability is maximized by rearranging segments using an optimized simulated annealing program. The automated assignment method is tested using cross-peaks simulated from previously-assigned proteins. By applying the procedure to the observed cross-peaks of GlnBP, we are progressing toward the complete backbone resonance assignment of this 25 kDa protein. ^oSupported by NIH NRSA fellowship # 1F32GM17034-01.

Su-Pos395

COMPUTER GENERATION OF ALIGNED SPECTRA FROM AXIALLY ASYMMETRIC NMR POWDER SPECTRA. ((M. Alan McCabe and Stephen R. Wassall)) Department of Physics, Indiana University-Purdue University Indianapolis, Indianapolis, IN 46202-3273.

In studies of membranes the extent of acyl chain motion in phospholipid molecules can be monitored by the quadrupolar interaction from ^2H (deuterium) NMR (nuclear magnetic resonance). The Hamiltonian for this interaction is orientation dependent according to

$$\mathcal{H} \propto [(3 \cos^2\theta - 1) + \eta \sin^2\theta \cos 2\phi]$$

where θ is the polar angle between the external magnetic field and a symmetry axis of the molecule, ϕ is the azimuthal angle and η is the asymmetry parameter. Samples typically consist of a superposition of domains at all orientations which yields powder pattern spectra. The construction of profiles of order along a perdeuterated lipid acyl chain is facilitated by the depaking technique which calculates a spectrum as if all the domains from this random distribution of orientations are aligned at a single orientation¹. This method has previously been applied only to the case of fast axial rotation or $\eta = 0$. Here we extend the technique via a new algorithm to more complicated systems with slow axial rotation and nonzero asymmetry parameters. Examples of applicable systems include aligned (θ fixed) phospholipids in the gel phase, peptides incorporated into gel phase membranes, and large proteins in liquid crystalline membranes.

- M. A. McCabe and S. R. Wassall, Fast Fourier Transform Depaking, *J. Mag. Reson., Ser. B*, **106**, 80-82 (1995).

Su-Pos396

PROGRESS IN THE STRUCTURE DETERMINATION OF BACTERIAL MERCURY TRANSPORT PROTEINS MERP AND MERT USING NMR SPECTROSCOPY. ((R.A. Steele, D.M. Brabazon, G. Veglia, S. Ghandi, and S.J. Opella)) Department of Chemistry, University of Pennsylvania, Philadelphia, PA. 19104. (Spon. by R. Steele)

Bacteria containing plasmids that encode the proteins of the mercury detoxification system survive in the presence of chemicals containing Hg(II), which are toxic to nearly all living things. The structures of merP (periplasm), a 72 residue water soluble globular protein that binds Hg(II), and merT (transport), a 116 residue hydrophobic membrane protein responsible for transferring the Hg(II) from merP to the cell cytoplasm are being determined by NMR spectroscopy. The three-dimensional structure of merP, which is a 72 residue water soluble protein with a metal binding site, as determined by multidimensional solution NMR methods using uniformly ^{15}N and dual $^{13}\text{C}/^{15}\text{N}$ labeled samples will be presented. MerT has also been expressed and isotopically labeled; progress in determining its structure through an approach that utilizes a combination of solution NMR experiments on micelle samples and solid-state NMR experiments on oriented and unoriented bilayer samples will be described.

Su-Pos398

NMR STRUCTURAL STUDIES OF CHANNEL FORMING PEPTIDES IN MEMBRANE ENVIRONMENTS. ((Jennifer J. Gesell¹, Ana P. Valente¹, Mauricio Montal² and Stanley Opella¹)) ¹Department of Chemistry, University of Pennsylvania, Philadelphia, PA 19104 and ²Department of Biology, University of California, San Diego, La Jolla, CA 92093. (Spon. by J. Gesell)

Some of the best characterized channel forming proteins are ionotropic neurotransmitter receptors. Conventional structural studies of these receptors in native membrane environments are severely limited by protein size, complexity, and difficulty in crystallization. A promising approach to their analysis is to synthesize or biologically express peptide sequences corresponding to functional segments of the proteins and study them using both solid state and solution NMR spectroscopy. Three dimensional heteronuclear solution NMR experiments are being used to determine the structure of the peptides in detergent micelles. The structures of the peptides embedded in lipid bilayers are being determined by solid state NMR experiments in oriented samples. Recent results in membrane environments of the predicted channel lining segments (membrane spanning segment 2) of a variety of receptors will be presented.

Su-Pos400

SOLID STATE ^{13}C AND ^{15}N NMR INVESTIGATIONS OF COLLAGEN

((K. V. Lakshmi, D. K. Lee, A. M. Clark & R. J. Wittebort)) Department of Chemistry, University of Louisville, Louisville, KY 40292

Mechanical properties of collagen fibers are thought to result from a cross-linked assembly of ordered, supercoiled helical molecules but the interactions that stabilize the secondary structure of collagen are less understood. Precise characterization of molecular order is an essential prerequisite for understanding the structure and function of fibrous proteins. In the present study, ^{13}C and ^{15}N solid state NMR methods are utilized to investigate uniaxially aligned collagen fibers to determine the orientation of individual peptide planes relative to the fiber axis. In solids, anisotropic (*i.e.* orientation dependent) interactions such as magnetic shielding of the nucleus are a source of structural information. Because of the anisotropy of these interactions, the NMR frequency depends on the molecular orientation relative to the magnetic field. Consequently, signals which shift in a characteristic way are observed on rotating suitably oriented samples while randomly ordered (powder) samples exhibit broad resonances which determine the principal components of the coupling tensor. For oriented fiber systems, narrow spectra were obtained when the axis of orientation was aligned with the applied magnetic field and, in turn, the molecular orientation of tensors has been determined. Heteronuclear dipolar couplings (such as ^{15}N - ^2H couplings) that yield internuclear distances have also been determined in these oriented systems. In parallel, MAS spectra of collagen and related peptides have been studied and these allow for comparative conformational determination.

Su-Pos397

MEMBRANE PROTEIN STRUCTURE AND TOPOLOGY BY NMR SPECTROSCOPY. (F.M. Marassi, F.C.L. Almeida, A. Ramamoorthy, Y. Kim, M. Zasloff, S.L. Schendel, W.A. Cramer and S.J. Opella) Univ. of Pennsylvania, Philadelphia, PA. Magainin Pharmaceuticals, Plymouth Meeting, PA. Purdue Univ., West Lafayette, IN (Spon. by S.J. Opella)

The structural properties of four membrane proteins are compared. Magainin II (23 residues), fd coat protein (50 residues), Vpu from HIV-1 (81 residues) and colicin (190 residues) are being investigated by a combination of solid-state and solution NMR spectroscopy. Detergent micelles and the lipid bilayers provide appropriate membrane model systems. The high resolution structure of the fd filamentous bacteriophage major coat protein was obtained using multidimensional solution NMR spectroscopy in SDS micelles and compared directly to that deduced from solid-state NMR measurements in bilayers. The protein has two α -helices, one spanning the hydrophobic core of the micelle and the other lying on its surface. The solid state NMR studies on this and the other proteins were carried out on ^{15}N -labeled samples in phospholipid bilayers oriented between glass plates, in a flat coil probe. The ^{15}N amide chemical shift tensor enables trans-membrane and in-plane orientation of helices to be distinguished. Using this approach, the TM and in-plane segment of the fd coat protein were identified, in agreement with the results from the solution NMR. The larger colicin and Vpu proteins have TM (ca. 20 % for colicin) and in-plane segments, consistent with the umbrella model for colicin channel insertion. The 190 residue colicin channel domain is the largest membrane protein examined with this approach. Magainin was studied using three-dimensional solid state NMR experiments, that correlate ^{15}N chemical shift, ^1H chemical shift and ^{15}N - ^1H dipolar coupling. These measurements demonstrate the feasibility of complete protein structure determination in a membrane by solid state NMR.

Su-Pos399

NMR STRUCTURAL STUDIES OF SHORT PEPTIDES DISPLAYED ON THE COAT PROTEIN OF FD FILAMENTOUS BACTERIOPHAGE. ((R. Jelinek, M. Monette, H. Gratkowski and S.J. Opella)) Department of Chemistry, University of Pennsylvania, Philadelphia, PA 19104. ((T. D. Terry, P. Malik, J. Greenwood, A.E. Willis and R.N. Perham)) Department of Biochemistry, University of Cambridge, Tennis Court road, Cambridge, CB2 1QW, England. (Spon. by M. Montal)

Peptides and protein segments play major roles in immunological and biochemical processes. Thus, structure determination of short peptides is highly important for elucidating immune mechanisms, and for developing vaccines. In this work, we demonstrate the application of NMR spectroscopy to determine the structures of immunogenic peptides expressed on the surface of fd filamentous bacteriophage. Specifically, multi-dimensional solution NMR has been applied to the epitope-containing coat proteins of fd filamentous phage, solubilized in water with detergent micelles. Solid state NMR experiments, on the other hand, take advantage of the spontaneous orientation of the phages in the magnetic field of the NMR spectrometer to extract spectroscopic and geometrical parameters used in structure calculations. The techniques are demonstrated for peptide epitopes which have been identified as the primary recognition sequences for HIV-1, malaria, and foot-and-mouth-disease viruses.

Su-Pos401

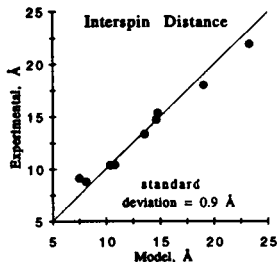
DETERMINING SOLUTION STRUCTURE OF *C. ELEGANS* SPLICED LEADER RNA USING SEGMENTAL LABELING AND NMR. ((Jing Xu and D. M. Crothers)) Department of Molecular Biophysics and Biochemistry, Yale University, School of Medicine, New Haven, CT 06520. (Spon. by D. M. Crothers)

Spliced leader RNAs are a class of RNAs that donate the common 5' mini-exon to the 3' splice site of a separate precursor mRNA transcript in a process called trans-splicing, which happens in nematode, trypanosome and other lower eukaryotes. The structure of the 22 nucleotide long mini-exon and the first 38 nucleotide segment from the *C. elegans* spliced leader RNA 1 are studied by NMR. The possibility of forming two different secondary structures complicated the task of secondary structure determination by 2D H_2O -NOESY because of the significant imino degeneracy in these two structures. Such ambiguity was resolved using a segmental labeling method developed in this lab, by which only a portion of the RNA is isotopically labeled. The unusual stability of the mini-exon molecule suggested special interaction within the loop region. However, the assignment of the spectra turned out to be difficult because of insufficient sequential NOE connectivity and severe chemical shift overlap. Segmental labeling and the recently developed through-bond sequential assignment are being employed to overcome the problem.

Su-Pos402

AN EPR SPECTROSCOPIC RULER FROM 8 TO 25 Å. (M.D. Rabenstein and Y.-K. Shin) Department of Chemistry, and Division of Structural Biology, University of California, Berkeley, CA 94720

An electron paramagnetic resonance (EPR) "spectroscopic ruler" was developed using 9 α -helical polypeptides each modified with two nitroxide spin labels. In order to calculate their spatial separation, the EPR line broadening due to electron-electron dipolar interactions in the frozen state was determined. This was achieved by a novel deconvolution method using spectra of both singly and doubly labeled molecules. The Fourier transform of the spectrum of the doubly labeled molecule is divided by the Fourier transform of the monoradical spectrum. Back-transformation yields the dipolar broadening function, from which the distance is calculated. This method was used to determine the separation of two spin labels from 8 to 25 Å. Results agreed well with a simple α -helical model with a standard deviation of 0.9 Å. This technique is applicable to complex systems such as membrane receptors and channels that are difficult to access with high resolution NMR or X-ray crystallography, and is expected to be particularly useful for systems for which optical methods are hampered by the presence of light interfering membranes or chromophores.



Su-Pos404

Q-BAND ENDOR STRUCTURAL INFORMATION ON THE COPPER LIGANDING ENVIRONMENT OF COPPER-CONTAINING NITRITE REDUCTASE. ((Andrei Veselov*, Anita Toffanin†, James P. Shapleigh†, and Charles P. Scholes*)) *Dept. of Chemistry, SUNY at Albany, Albany, NY 12222 and †Dept. of Microbiology, Cornell University, Ithaca, NY 14853.

Nitrite reductase catalyzes the reduction of nitrite (NO_2^-) to nitric oxide (NO). The enzyme contains two types of copper, a Type 2 copper where nitrite reduction occurs and a Type 1 blue-green copper that has an electron transfer function. The enzyme studied is from a denitrifying variant of *R. sphaeroides*, and it was overexpressed in a heterologous *E. coli* system. The ENDOR technique probes for covalent spin density and distance-dependent dipolar couplings whose details exceed the resolving power of protein X-ray crystallography. The magnetic fields used for Q-band (34 GHz) ENDOR, as opposed to X-band (9 GHz) ENDOR, removed spectral overlap of nitrogen and protons. The findings are: 1) Exchangeable proton couplings at the Type-2 center, whereby such protons were estimated at 3–4 Å distance from copper and were found perturbed but not eliminated by nitrite binding. 2) High resolution of histidine nitrogen hyperfine and quadrupole detail (no longer overlapped by protons at Q-band), where this coupling is perturbed by nitrite binding. 3) Evidence for hyperfine coupling of order 1 MHz to ^{15}N -nitrite. 4) Evidence for large hyperfine couplings of order 20 MHz to cysteine protons of the Type 1 blue-green center, to be compared with cysteine proton couplings of other blue copper centers. Supported by NIH Grant GM 35103.

Su-Pos406

NON-TRANSFERRIN IRON(III) BINDING SITES ON THE INTERIOR SURFACE OF ENDOSOMES. ((J.A. Watkins, J.J. Lorio, R.J. Donohoe*, S.L. Mecklenberg*, C.-Y. Li, E.J. Besser, D.M. Rimmer, and J.Glass*)) Center for Excellence in Cancer, Research, Treatment, and Education, LSU Med. Ctr., 1501 Kings Hwy., Shreveport, LA 71130-3935 and *Chemical Science and Technology Division, CST-4, Los Alamos National Laboratory, Los Alamos, NM 87544.

The events between dissociation of Fe(III) from transferrin (Tf) followed by reduction and translocation of Fe(III) across the membrane of rabbit reticulocyte endosomes have been poorly understood. Manipulating the preparation and taking advantage of the reductant dependence allows investigation of the Fe(III) binding equilibria and EPR spectra of the endosomes. Endosomes containing ^{59}Fe -Tf bound and unbound with ^{59}Fe , were permeabilized with 0.025% CHAPS and diluted to 0.025% CHAPS in order to minimally disrupt the putative native complexes. The affinity of Tf for Fe at pH 7, is 10^6 – 10^7 M^{-1} at pH 7.0 with a Hill constant (α) of 0.3, under these detergent buffer and ionic strength conditions. In vesicles at pH 6.0, the affinity is decreased to 10^4 – 10^5 M^{-1} and negative cooperativity is maintained ($\alpha=0.09$). Three non-Tf Fe(III) binding sites (S_1 – S_3) are detected with $K_1=10^6 \text{ M}^{-1}$ that have positive cooperativity ($\alpha=1.6$) indicating cooperative Fe(III) transfer from Tf to the S_1 sites. EPR spectra (8–77 K) of Tf were obtained for endosomes with most iron associated as Fe-Tf for which the characteristic Tf spectrum is obtained with some loss of Fe from the N-lobe. Copper and possible iron-sulfur groups were also detected. Endosomes with Fe partially dissociated (>40%) from Tf, gave spectra with a Tf g-value of 4.1 ± 0.1 and no fine structure. These results support models where the Fe binding sites of Tf are perturbed and multiple iron acceptor sites are involved in the routes of transit for Fe out of the endosome. Paramagnetic signals of the acceptor sites were not detected.

Su-Pos403

INTERACTION OF SPIN LABELED T4 LYSOZYME WITH α -CRYSTALLIN ((Y.-L. Zhang, H. Mchaourab, Q.-L. Huang, J. Horwitz, W. Hubbell)) Jules Stein Eye Institute and the Department of Chemistry & Biochemistry, University of California, Los Angeles, CA 90095-7008 (spon. by J.C. Voss)

Alpha crystallin is apparently important for maintaining long-term transparency of the eye lens. In this study, the chaperon-like properties of this protein were investigated using spin-labeled mutants of T4 lysozyme as protein ligands. Five mutants of T4 were prepared, each containing either a single nitroxide side chain at a destabilizing site or a nitroxide side chain in combination with a destabilizing mutation elsewhere in the molecule. Although the mutants have reduced thermal stability compared to the wild type, they have native-like structure at 37° as indicated by their enzymatic activity, EPR spectra and far/near UV CD spectra. Remarkably, these stable, folded proteins spontaneously associate with α -crystallin at 25–37° to form a complex as evidenced both by EPR spectroscopy and gel filtration. Nitroxide side chains at various positions in the T4 sequence are all strongly immobilized in the complex, although some are located at mobile surface sites in the folded protein. This suggests extensive contact between α -crystallin and the bound T4 along much of its length. The above results demonstrate that a single point mutation in a protein that results in 3–5 kcal/mol destabilization is sufficient to trigger binding to the small heat shock protein α -crystallin. The mechanism could involve association of T4 with α -crystallin followed by unfolding, or direct binding of unfolded T4 (equilibrium) with α -crystallin. Results of time-resolved EPR studies designed to distinguish these mechanisms will be presented.

Su-Pos405

ASSIGNMENT OF TYPE 2 BINDING SITES IN CYTOCHROME C OXIDASE. ((H. Yuan, W. E. Antholine, and P. M. H. Kroneck,†)) Biophysics Research Institute, Medical College of Wisconsin, Milwaukee, WI, USA, and †Facultät für Biologie, Universität Konstanz, Germany

Cytochrome c oxidase (COX) from bovine heart contains the EPR-detectable mixed-valent [$\text{Cu}_2(\text{L}1.5)\dots\text{Cu}_2(\text{L}1.5)$], $S=1/2$ center¹ and the EPR non-detectable Cu_2 site. The addition of four equivalents of Cu^{2+} to COX did not aggregate the enzyme or affect its activity. ESR parameters for these sites are $g_1=2.22$ and $A_1=195 \text{ G}$ (see Fig). Nitrogen superhyperfine structure was observed in the g region. These parameters are very close to that for Cu^{2+} , which is bound to the 2 β -histidine of the β chain N-terminus in tetramer hemoglobin.² By analogy, tentative assignments of these binding sites are proposed to be at the N-terminus of subunits of COX, for example subunit IV where the sequence is A-H-G-S.... Nitrogen donor atoms from the α -amino group of the amino terminal residue, the imidazole group of histidine, and the peptide nitrogens comprise the binding site. To our knowledge, a type 2 signal with these parameters has only been found at the N-terminus for which histidine is either the 2nd or 3rd residue. At the N-terminus the flexibility of the protein chain is not yet hindered by α -helix or β -sheet constraints. (Supported by NIH grant RR01008).

1. Antholine *et al.* *Eur. J. Biochem.* 209:875–81, 1992.
2. Antholine *et al.* *J. Inorg. Biochem.* 25:95–108, 1985.

Su-Pos407

UV PHOTOLYSIS OF TRYPTOPHAN IN COD PARVALBUMIN. ((P. J. Angiolillo, Lin Li, W. W. Wright and J. M. Vanderkooi)) Johnson Research Foundation, Dept. Biochem. & Biophys., School of Medicine, Univ. of Penn. Philadelphia PA 19104

Cod Parvalbumin (Type III) contains a single buried tryptophan whose triplet yield is decreased by a factor of ≈ 3 in the calcium depleted protein. This decrease in yield is concomitant with a $\approx 20 \text{ nm}$ hypsochromic shift of the fluorescence and a slight bathochromic shift and broadening of the phosphorescence, signaling a conformational change. Low temperature EPR was studied as a function of Ca^{2+} and temperature. Under photolysis in the range (250–400 nm) both forms ($\pm \text{Ca}^{2+}$) demonstrated free radical production at g values of 2.004 and the formation of a photoexcited triplet state. The EPR spectrum at 4 K of parvalbumin with Ca^{2+} showed the evolution of hydrogen atom generation ($a(\text{H})=50.9 \text{ mT}$) in addition to unresolved hyperfine transitions centered about g2. The Ca^{2+} -free form did not show hydrogen atom generation nor did it demonstrate any hyperfine structure with UV photolysis of times exceeding 60 min. Temperature study of the EPR signals (post photolysis) showed that the hydrogen atoms generated in Ca^{2+} parvalbumin disappeared by 35 K along with temperature-dependent changes in the hyperfine structure in the g2 region. The Ca^{2+} -free parvalbumin demonstrated essentially temperature independent changes in the free-radical resonance up to 100 K along with no evidence of hyperfine structure. We postulate environment dependent photochemical processes that may be useful in probing the protein structure surrounding a chromophore (tryptophan) (Supported by PO1 GM48140).

Su-Pos408

SIMULATION OF NMR NOESY AND HOESY SPECTRA OF FLEXIBLE PEPTIDES IN SOLUTION ((H. Déméné and I. Sugár))
Department of Biomathematical Sciences, Mount Sinai School of Medicine,
one Gustave L. Levy Place, New York, NY 10029-6574.

In the process of elucidating the structure of peptides and small proteins based on NMR data, back simulation of homonuclear NOESY spectra helps us to check and refine the predicted model structures. However, up to date, NOESY 2D simulations have assumed that the molecules are rigid and adopt a single conformation in solution. This can be certainly considered to some extent valid for big proteins, but is much less certain for polypeptides.

In order to take into account the flexibility and the dynamics of such molecules, we have developed a program called FLEX, which generates 2D NOESY spectra for molecules which are assumed to adopt different non-rigid conformations in solution. The Model-Free approach of Lipari and Szabo was used to mimic the dynamical properties of each conformation. The exchange between the different conformations was modelled using an exchange matrix, so that FLEX is able to deal with multiple conformations either in slow exchange or in fast exchange at the NMR scale.

The results of the simulations of 2D homonuclear NOESY experiments will be presented here, as well as the simulation of heteronuclear relaxation experiments which are thought to provide also valuable information on the dynamical motions of the molecule. Emphasis will be put on the information that can be gained not only from the NOE data, but also from the lineshapes and the absence of NOEs. Supported by Rhone Poulenc Rohrer (France).

Su-Pos410

SIMULATIONS OF RADIO FREQUENCY FIELDS IN CARDIAC MRI.
((R.W. Singerman, T.J. Denison, R.S. Balaban, H. Wen)). Laboratory of Cardiac Energetics,
National Institutes of Health, Bethesda, MD 20892.

The human body attenuates and distorts the radio frequency fields employed in cardiac MRI. In particular, the conductivities and dielectrics of muscle and fat lead to rf absorption and rf resonances, both of which lead to image distortion and degradation. In order to quantify the above effects, we have performed electrodynamic simulations of radio frequency fields from a surface coil above a symmetric three-dimensional model of the human chest. Simulations give good agreement with the rf field behavior as measured in the chest in a 4 Tesla (171 MHz) imaging system. Simulations for 3.0 Tesla (126MHz) and 1.5 Tesla (63 MHz) have also been performed. At 1.5 Tesla, we observe attenuation of the rf field in the human heart, but little field distortion in the heart as compared to the unloaded coil. At 4 Tesla, we observe strong distortion, due to dielectric resonances, as well as attenuation. Values for rf field attenuation are shown below. The results of these studies should be useful for both improving image reconstruction and ultimately choosing the optimal magnetic field for cardiac imaging.

Table: Circularly polarized component of RF field (in gauss) in cardiac MRI as a function of Larmor frequency and position in the body. The loaded coil refers to a coil above a human chest. The unloaded coil values refer to the field of a coil in free space. All coils are driven with a 141 Amp current at the given frequency.

	Unloaded 63 MHz	Loaded 63 MHz	Unloaded 126 MHz	Loaded 126 MHz	Unloaded 171 MHz	Loaded 171 MHz
Center of Coil	10.5	8.0	10.8	5.3	11.5	3.8
Top of Heart	8.0	6.2	8.5	4.8	9.0	4.0
Middle of Heart	4.0	3.0	4.5	2.2	5.0	2.0
Back of Heart	2.0	1.2	2.0	0.6	2.5	0.6

PEPTIDES

Su-Pos411

CHARACTERIZATION OF CALMODULIN-BINDING PEPTIDES USING PHAGE-DISPLAY RANDOM PEPTIDE LIBRARIES. ((W.J.Stevenson¹, J.D.Brennan¹, I.D. Clark², A.G.Szabo³, N.B.Adey³, H.L.Hanson³ and B.K.Kay^{3,4}))
¹Dept. of Chemistry and Biochemistry, University of Windsor, Windsor, Ontario, Canada, N9B 3P4, ²Institute for Biological Sciences, NRC of Canada, Ottawa, Ontario, Canada, K1A 0R6, ³Dept. of Biology and ⁴Curriculum in Genetics & Molecular Biology, University of North Carolina, Chapel Hill, NC 27599-3280, USA

Calmodulin (Cam) binds calcium and modulates the activity of a large number of cellular proteins by binding to short domains (ie., ~20 amino acids) with target proteins. Homologous peptides in which different amino acids were substituted in selected locations were synthesized and their binding to Cam was examined. In this way the residues which modify the binding characteristics could be understood. Each of the peptides contained at least one tryptophan residue. The steady state and time resolved fluorescence of this residue were used to characterize the local structure of the bound peptide. As well the steady state fluorescence provided a convenient method to determine the binding affinities. The data showed that small changes in peptide sequence affected the structure of the bound peptide and its location in the Cam complex. The binding and structures of these peptides were compared with the MLCK peptide (1) and Dedman's peptide (2).

¹Dedman, J.R. et al. (1993) *The Journal of Biological Chemistry* 268: 23025-23030.

²O'Neill, K.T., DeGrado, W.F., (1990) *Trends in Biochemical Sciences* 15: 59-64.

Su-Pos409

3D GATED EPR IMAGING OF THE BEATING HEART. ((Periannan Kuppusamy, Michael Chzhan, Penghai Wang and Jay L. Zweier)) Division of Cardiology and the EPR Center, Department of Medicine, Johns Hopkins Medical Institutions, Baltimore, MD 21224. (Spon. by J. L. Zweier)

In vivo or *ex vivo* electron paramagnetic resonance imaging, EPRI, has been established as a powerful technique for determining the spatial distribution of free radicals and other paramagnetic species in living organs and tissues. While instrumentation capable of performing EPR imaging of free radicals in whole tissues, and isolated organs has been previously developed, it was not possible to image rapidly moving organs such as the beating heart. We have, therefore, developed EPR instrumentation capable of performing gated-spectroscopic and imaging measurements on isolated beating rat hearts at L-band. A synchronized pulsing and timing system was developed enabling gated acquisitions of up to 256 images per cycle, with rates of up to 16 Hz. The temporal and spatial accuracy of this instrumentation was verified using a specially designed beating heart-shaped phantom with acoustically driven sinusoidal motion at a cycle rate of 5 Hz. Gated EPR imaging was also performed on a series of isolated rat hearts perfused with nitroxide spin labels. These hearts were paced at a rate of 6 Hz with either 16 or 32 gated images were per cardiac contractile cycle. The images enabled visualization of the time dependent alterations in the free radical distribution and anatomical structure of the heart which occurs during the cardiac cycle.

Su-Pos412

ELECTROSTATIC EFFECTS ON TRYPTOPHAN FLUORESCENCE IN DIPEPTIDES (M.J. Weller, A.G.Szabo) Dept. of Chemistry and Biochemistry, University of Windsor, Windsor, Ontario, Canada, N9B 3P4

Time resolved fluorescence has been extensively used in studies of proteins to provide information about their structure, function and dynamics. The multiexponential decay of a single tryptophan in proteins has been shown to originate from side chain rotamers, each having a different excited state lifetime. The decay associated spectra of each of these components have been shown to have different spectral maxima in a number of proteins. A possible rationalization of this effect is that each rotamer experiences a different electric field within the protein. In order to examine this hypothesis, the fluorescence decay behaviour of a number of dipeptides which have different net charges were studied. Chen and Knutson¹ have previously reported the effects of the local dipoles and electrostatic charge on the decay times of Trp in dipeptides. The current study furthers the investigation by correlating the electrostatic charge with the decay associated spectra.

¹Chen, R. F. et al., (1991) *Biochemistry* 30: 5184-5195.

Su-Pos413

SIDE CHAIN EFFECTS ON UV π - π^* CIRCULAR DICHROIC SPECTRA OF CATION COMPLEXES OF CYCLO(Pro-Gly)₃
 ((Tamara Baumgartner and Kathryn Thomasson)) Chemistry Department, Box 9024, University of North Dakota, Grand Forks, ND 58202-9024.

Cyclo(Pro-Gly)₃ is a synthetic cyclic peptide capable of binding and transporting cations across natural and synthetic membranes. Cyclo(Pro-Gly)₃ adopts structures that depend on the solvent and cation species bound. The peptide's UV circular dichroic (CD) spectrum is sensitive to the different conformations. Internal coordinates published from crystallographic (Kartha et al. *Proc. Natl. Acad. Sci. USA*, 79, 4519-4522, 1982) and NMR (Madison et al. *J. Am. Chem. Soc.*, 96, 6725-6734, 1974) data for the Mg²⁺ and Ca²⁺ complexes were energy minimized using DISCOVER cvff. The resulting Cartesian coordinates were used to predict the π - π^* CD spectra applying the dipole interaction model. Because the dipole interaction model is sensitive to side chain structure, the conformation of the proline side chain was thoroughly searched using torsion constraints. CD predictions for structures with the proline side chain having χ^2 positive most resembled the experimental spectrum for the magnesium complex. Similar CD predictions were observed for one of the calcium complex backbones. Thus, there may be preferential ring puckering in the cation complexes of cyclo(Pro-Gly)₃.

Su-Pos415

CONFORMATIONAL MEMORIES AND THE EXPLORATION OF BIOLOGICALLY RELEVANT PEPTIDE CONFORMATIONS: AN ILLUSTRATION FOR THE GONADOTROPIN-RELEASING HORMONE. ((F. Guarnieri and H. Weinstein)) Department of Physiology and Biophysics, Mount Sinai School of Medicine, New York, NY 10029. (Spon. by W.A. Brodsky)

A recently developed technique of Conformational Memories [F. Guarnieri and S.R. Wilson, *J. Comp. Chem.*, 16:648,1995] is illustrated with the study of the decapeptide gonadotropin-releasing hormone (GnRH) and the mutant peptide Lys8-GnRH. The conformational space of the peptides is explored fully with multiple Monte Carlo Simulated Annealing (MC/SA) random walks using the Amber* force field and the Generalized Born / Surface Area (GB/SA) continuum solvation model of water as implemented in the MacroModel molecular modeling package. The collective histories of all the random walks are transformed into mean field dihedral distribution functions called "Conformational Memories" (35 for GnRH, one for each torsion angle). Conformational families of the peptides at 309K are obtained from these results with a biased sampling technique which explores only the areas found to be populated in the Conformational Memories. A large family of GnRH structures that comprises over 85% of the population is identified by clustering conformations according to a pairwise root mean square deviation criterion. Members of this family of conformations share a distinctive *beta*-type turn in the backbone that involves residues 5-8. This conformation is shown to correspond to the preferred geometry of a structurally constrained analog of GnRH that binds to the GnRH receptor with high affinity. In contrast, GnRH analogs such as Lys8-GnRH have their major conformational family exhibiting an extended backbone, and belong to the group of low affinity ligands. The results suggest a correlation between high affinity at the GnRH receptor and the ability of the peptides to adopt a conformation that exhibits the characteristic *beta*-type bend. Thus, the method of Conformational Memories is shown to provide a powerful and reliable tool for the computational exploration of structure-function relations of flexible peptides. Supported by NIH grants DK46943, K05 DA00060, and ST32DA07135.

Su-Pos417

PROBING THE ACCESSIBILITY OF FUNCTIONAL GROUPS IN THE NEUROPEPTIDES, LEU-ENKEPHALIN AND MORPHICEPTIN USING PARAMAGNETIC GDDOTA⁻¹

((Christine Wiemer, Frank Rinaldi, Joseph Kohles, Joseph Moryl and Matthew Petersheim)). Dept. of Chemistry, Seton Hall University, South Orange, New Jersey, 07079-2694.

¹H NMR relaxation experiments using the paramagnetic agent, gadolinium (III) 1,4,7,10-tetraazacyclododecane-1,4,7,10-tetracarboxylate (GdDOTA⁻¹) were completed to measure the apparent accessibilities of the hydrogens of the δ -opioid, leu-enkephalin (Tyr-Gly-Gly-Phe-Leu) and the μ -opioid, morphiceptin (Tyr-Pro-Phe-Pro-NH₂), which, due to the slow interchange of the cis and trans amide linkages to the proline residues, give rise to four isomeric forms present in solution: cis-Pro/cis-Pro, cis-Pro/trans-Pro, trans-Pro/cis-Pro, and trans-Pro/trans-Pro. The GdDOTA⁻¹ induced relaxation is pseudocontact in nature since the octadentate DOTA⁻¹ forms an inert chelate that prohibits coordination of the Gd(III) by the peptides. Relaxation induced by the GdDOTA⁻¹ varies steeply with steric accessibility and was found experimentally to be influenced by electrostatic attraction to the N-terminal ammonium on both peptides and repulsion by the leu-enkephalin anionic C-terminus. Molecular modeling was employed to generate energy minimized structures from numerous conformational grid searches to probe the steric accessibility of the hydrogens of the peptides in various conformations and subsequently, to compare them with the experimental values previously obtained. NMR scalar coupling constants and results from the grid searches suggest two predominant conformers for the cis-Pro/trans-Pro, morphiceptin isomer. Molecular dynamics simulations of the two main conformers in a periodic box of water molecules were also completed to investigate fluctuations in the hydrogen accessibilities of the predominant isomers. This approach is both simple and versatile in the characterization of peptide topochemistry in solution.

Su-Pos414

PHOTOACOUSTIC DETECTION OF PHOTOINDUCED VOLUME CHANGES IN AQUEOUS SOLUTIONS OF TRYPTOPHAN AND TRYPTOPHAN CONTAINING DIPEPTIDES

((L. Brancaloni; C.Viappiani)) INFN - Dipartimento di Fisica, Università di Parma, viale delle scienze, 43100 Parma, Italy

Time-resolved photoacoustics has been used to investigate the volume changes induced in aqueous solution by photoexcitation of tryptophan and tryptophan containing dipeptides. Three heat decays have been detected; a fast one, characterized by a subnanosecond lifetime, an intermediate transient living some tens of nanoseconds and a microsecond-lived state. The transients are accompanied by volume changes of non thermal origin, likely originating from solute-solvent rearrangement. The data have been analyzed with a model in which we included the photoionization, the production of the cation radical, the subsequent deprotonation of the radical to free radical and the formation and decay of the triplet state. We tentatively assign the nanosecond transient to an intramolecular deexcitation mechanism other than the decay of a second triplet state, previously postulated in the literature. We believe that the mechanisms leading to the detectable volume changes are photoionization, deprotonation of the cation radical, formation (or decay) of the triplet state and formation (or decay) of the intermediate transient.

Su-Pos416

STRUCTURE AND CONFORMATION OF SEQUENTIALLY RELATED PEPTIDES: CRYSTAL STRUCTURE OF L-PHENYLALANYL GLYCYLGLYCINE (FGG). Seth Hoffman and T. Srikrishnan, Center for Crystallographic Research and Department of Biophysics, Roswell Park Cancer Institute, Buffalo N.Y. 14263.

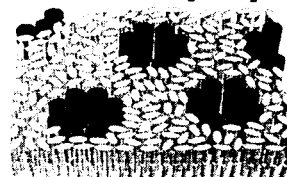
A systematic structural investigation of sequentially related peptides is of great importance for the elucidation of the structure-function relationship of peptides and in deducing the possible conformations of polypeptides. Although GGG has an extended antiparallel β -structure, crystal structures of other tripeptides of the sequence GGX and XGG show a wider range of conformations ranging from the extended, many kinds of folded conformations to a few helical conformations. In this line of investigation, the crystal structure of FGG was undertaken in our laboratory. Crystals of FGG (C₁₃H₁₇N₃O₄), grown by slow evaporation from an aqueous ethanol solution, are orthorhombic, space group P2₁2₁2₁, with the following cell dimensions: a = 5.459 (5), b = 15.299 (6), c = 16.047 (6) Å, V = 1340.2 Å³, D_c = 1.38 g/c.c., D = 1.384 g/c.c. and Z = 4. Complete three dimensional data was collected on a CAD 4 diffractometer (2643 reflections, 2305 >3 σ). The structure was solved by the application of direct methods and refined to a final R factor of 0.031. The molecule exists as a zwitterion in the crystal. The peptide units are *trans planar* ($\omega_1 = -178.6^\circ$ and $\omega_2 = 175.6^\circ$). The peptide backbone is *folded* with the torsion angles of $\psi_1 = -116.7^\circ$, $\omega = -178.6^\circ$, $\phi_2 = 88.8^\circ$, $\psi = 29.4^\circ$, $\omega = 175.6^\circ$, $\phi = -135.6^\circ$ and $\psi = -8.2^\circ$. For the phenylalanine side chain, $\chi_1 = 123.4^\circ$ and $\chi_2 = -56.3^\circ$. The molecules are linked together intermolecularly in an infinite sequence by head to tail hydrogen bonds, as is typical of charged peptides.

Work supported by the New York State Department of Health.

Su-Pos418

PEPTIDE PORES IN MEMBRANES DIRECTLY DETECTED BY NEUTRON IN-PLANE SCATTERING. ((Ke He, S.J. Ludtke, W.T. Heller, T. Harroun, H.W. Huang and D.L. Worcester)) Rice University, Houston, TX 77251-1892 and University of Missouri, Columbia, MO 65211.

Antimicrobial peptides isolated from the host defense system of animals have been shown to exert their activity directly on the lipid bilayer of cell membranes, but the molecular mechanism are not clear, due to the difficulty of discerning the high-order structures formed by the peptides in membranes. Previously we have shown that these peptides insert into the membrane when their concentrations exceed a lipid-dependent critical value. With neutron in-plane scattering we now show that inserted alamethicin creates aqueous pores. Neutron data were collected for alamethicin in DLPC, deuterated DLPC and DPhPC with D₂O or H₂O. Alamethicin appears to form pores in the barrel-stave fashion. The form factors for different deuteration conditions were calculated with the same pore configuration; multiplied by a simulated structure factor, they reproduced the data for all cases.



Su-Pos419

CIRCULAR DICHROISM AND NMR ANALYSIS OF A COMPACT PEPTIDE (99-140) FROM STAPHYLOCOCCAL NUCLEASE IN BOTH AQUEOUS AND 40% 2,2,2-TRIFLUOROETHANOL SOLUTIONS. ((Mark W. Maciejewski and Micheal H. Zehfus)) Department of Biochemistry and Division of Medicinal Chemistry, The Ohio State University, Columbus, Ohio 43210.

Structural domains are regions of proteins that fold spontaneously, even when removed from the intact protein. Several studies have linked the presence of structural domains with physically compact regions in proteins. An algorithm to locate domains based on compactness has been developed and used to analyze several proteins (M.H. Zehfus, *Prot. Eng.* 7: 335-340, 1994). When applied to staphylococcal nuclease, several compact units were located with the largest corresponding to residues 99-141. If this peptide is a structural domain, it should retain native-like structure when cleaved from the intact protein.

To see if this is true a peptide corresponding to residues 99-141 was obtained by chemical cleavage of a staphylococcal nuclease 141 residue mutant and tested structurally by CD and NMR. In aqueous solution, CD spectra show a largely random conformation that can be stabilized by the addition of 2,2,2-trifluoroethanol (TFE). Complete ¹H and ¹⁵N NMR assignments were obtained in both aqueous and TFE solutions. In aqueous conditions the chemical shift index (CSI) and NOE data show that residues 126-136 are helical, consistent with the native structure. However, the data for a second helix (99-107) was ambiguous. NOE data also showed the presence of three turn conformations at residues 107, 114-120, 137-138, and long range interactions between residues 106-138, and 101-124, all consistent with the native conformation. NMR structural data in TFE will also be presented. This structure is expected to be more native-like, since its CD spectrum displays a higher helical content.

Su-Pos421

PERMEABILIZATION OF NEUTRAL AND NEGATIVELY CHARGED LIPID BILAYERS BY A CATIONIC AMPHIPATHIC MODEL PEPTIDE AND ANALOGUES OF REDUCED HELICITY AND DECREASED HYDROPHOBICITY ((M. Dathe, T. Wieprecht, M. Beyermann, M. Bilenert)) Research Institute of Molecular Pharmacology, Alfred-Kowalke-Str. 4, 10315 Berlin, Germany

The importance of helicity and hydrophobicity of a cationic, potentially amphipathic model peptide for binding to model membranes and their permeabilization has been studied in CD spectroscopic investigations and dye release experiments from lipid vesicles. Double D-substitution of adjacent amino acid residues results in a position-dependent reduction of the helical content of the peptide while modification of the hydrophobicity was without influence on the helicity as probed by CD spectroscopy in aqueous TFE solutions. Changes in helicity and hydrophobicity had only slight influence on the peptide binding to highly negatively charged vesicles and the permeabilization of the bilayer at submicromolar peptide concentration. However, the membrane disturbing effect of the helical peptide was drastically enhanced with reduction of the negative surface charge of the lipid bilayer. On the other hand, the lytic effect was reduced by decreasing the hydrophobicity of the peptide. The results led to the conclusion, that hydrophobic interactions do not become effective in the peptide interaction with negatively charged vesicles. The peptides are anchored at the vesicle surface and, as a consequence, permeabilize the bilayer possibly by the formation of lipid clusters. Reduced surface charge of the vesicles and high peptide hydrophobicity lead to a promotion of hydrophobic peptide-lipid interactions, thus disturbing the inner apolar region of the bilayer and causing enhanced membrane permeability.

Su-Pos423

SOLID STATE NMR OF MELITTIN. ((S.R. Wassall¹, J. Hanna², F.G. Prendergast³, F. Separovic⁴ and R. Smith⁵)) ¹Department of Physics, IUPUI, Indianapolis, IN 46202; ²CSIRO Division of Coal and Energy Technology, North Ryde, NSW 2113, Australia; ³Department of Biochemistry and Molecular Biology, Mayo Foundation, Rochester, MN 55905; ⁴CRC for Molecular Engineering and Technology, CSIRO DFST, North Ryde, NSW 2113, Australia; ⁵Department of Biochemistry, University of Queensland, Brisbane, Qld 4072, Australia.

Melittin is a 26 residue peptide. Its structure within a phospholipid membrane has been proposed on the basis of solid state NMR data obtained using selectively ¹³C enriched analogues (1). Ten analogues with ¹³C at the peptide carbonyl were incorporated into phospholipid membranes aligned between glass plates. Reduced chemical shift anisotropies (CSA) that are consistent with a transmembrane α -helix possessing a bend close to the proline (Pro14) were measured in the liquid crystalline phase of the lipid.

Magic angle spinning (MAS) methods are being employed to determine how closely the structure of membrane incorporated melittin resembles the crystalline form. Specifically, interatomic distances in analogues ¹³C labelled at pairs of sites are being measured in polycrystalline and membrane samples by rotational resonance (RR). The labels have been introduced to define the N-terminal helix and the region of the bend between the N- and C- terminal helices produced by the proline. (Supported in part by NSF INT-9316922.)

1. Smith, R., Separovic, F., Milne, T.J., Whittaker, A., Bennett, F.M., Cornell, B.A. and Makriyannis, A. (1994) *J. Mol. Biol.* 241, 456.

Su-Pos420

INTERACTIONS OF AMPHIPATHIC PEPTIDES WITH PHOSPHOLIPID VESICLES ((Steven M. Bishop, Lucille Smith-Wright, Tahir Jamil, Paul S. Russo and Mary D. Barkley)) Departments of Chemistry and Biochemistry, Louisiana State University, Baton Rouge, LA 70803. (Spon. by K. Morden)

The two amphiphilic peptides, (KLAKKLA)₃ and (KLGGKLG)₃, show antimicrobial activity, whereas only the alanine containing peptide is cytotoxic towards eukaryotes. We have attempted to understand this selectivity by modeling the outer surfaces of eukaryotes and prokaryotes with differently charged phospholipid bilayers and studying vesicle-peptide interactions. Association isotherms obtained with peptides labeled with the fluorophore NBD, show that the fraction of (KLAKKLA)₃ bound to neutral DOPC vesicles reaches a maximum of 60% at a lipid to peptide ratio of 1000:1 whereas (KLGGKLG)₃ was poorly bound. Both were strongly bound to negatively charged vesicles. The isotherm profiles suggest peptide aggregation within the membrane except for (KLGGKLG)₃ on DOPC vesicles where the peptide appears monomeric. In both membrane environments, the secondary structure of both peptides in the bound form is close to 100% helical. The effect of each peptide on vesicle integrity was studied using a calcein leakage assay, in which (KLAKKLA)₃ was 2-3 times as effective at inducing leakage as (KLGGKLG)₃ to DOPC vesicles. Surprisingly, both peptides were 100x less effective towards negatively charged vesicles, even though they are more strongly bound. Vesicle size and integrity were also monitored using dynamic light scattering and fluorescence photobleach recovery techniques. We observed an increase in vesicle size with increasing peptide concentration which was more pronounced for the negatively charged vesicles. These results are discussed in relation to peptide activity, modeling eukaryotic and bacterial cell surfaces with neutral and negatively charged vesicles respectively.

Su-Pos422

DETERMINATION OF THE HELICAL REGION IN THE AMPHIPHILIC PEPTIDE MAGAININ-2-AMIDE USING A DOUBLE D-AMINO ACID REPLACEMENT SET. ((T. Wieprecht, M. Dathe, E. Krause, M. Beyermann, M. Bilenert)) Forschungsinstitut für molekulare Pharmakologie, A.-Kowalke-Str. 4, 10315 Berlin, Germany

The antibiotic peptide Magainin-2-amide (M2a) has been shown to act directly by enhancing the permeability of membranes. The positive net charge and the possibility of the peptide to adopt an amphiphilic α -helix are believed to be the main structural features for the membrane activity. However, different results exist about the amount of helicity and the location of the helical regions of M2a in TFE/water and bound to lipid bilayer systems. In this work we used a systematic double D-amino acid replacement set, which has recently been shown to be a useful tool for the location of helical regions in amphiphilic peptides, to determine the secondary structure of M2a in 50% TFE, in SDS micelles and bound to POPG-, POPC/POPG(3:1)- and POPC-small unilamellar vesicles by CD-spectroscopy. In TFE M2a is characterized by a weak helix over the entire peptide chain. Bound to SDS micelles, POPG-, POPC/POPG(3:1)- and POPC-vesicles M2a adopts a weak α -helix from the N-terminus up to amino acid position 8 and a stable helix between the positions 9 and 21 as indicated by different changes in helicity of the double-D analogs. Comparable structural properties of the peptide bound to POPG-, POPC/POPG- and POPC-vesicles show, that the secondary structure is independent of the content of negatively charged phospholipids. Consequently, electrostatic interactions do not influence the secondary structure of the lipid bound peptide. Furthermore, SDS micelles have been shown to be qualified to mimic M2a-lipid interactions, whereas TFE is an improper model system.

Su-Pos424

A COMPARATIVE STUDY OF MAGAININ, MELITTIN, AND CECROPIN P1 BY ORIENTED CIRCULAR DICHROISM. ((H.W. Huang, W.T. Heller, S. J. Ludtke, K. He, and T. Harroun)) Rice University, Houston, TX 77251-1892.

The magainins, melittin and cecropin P1 are all positively charged, helical peptides which are soluble in water, where they adopt a random coil conformation. The magainins are host defense peptides from the skin of frogs and cecropin P1 is a host defense peptide from the intestinal tract of pigs. Melittin is the active component of bee venom. All of these peptides adopt a helical conformation when associated with lipid bilayers. We employ oriented circular dichroism on various lipid systems containing these peptides to study how the peptide interacts with various lipid systems. Our lipid systems are aligned multiple bilayers intercalated with water layers. We can vary the relative humidity of the system continuously from approximately 75% to 100%, thereby changing the thickness of the water layer. Using this technique, we have been able to study the behavior of the above peptides in various lipid systems as they respond to changes in hydration. Both magainin and melittin are observed to insert to varying degrees into charged, uncharged, and mixed head group lipid bilayers. Cecropin P1 inserts to some extent into charged and mixed head group lipid bilayers. Unlike the other two peptides, cecropin P1 has been observed to dissociate from the head group region of uncharged head group lipid bilayers and enter the water layer, where it adopts a random coil conformation.

Su-Pos425

LIPID DEPENDENCE OF MEMBRANE THINNING CAUSED BY MAGAININ, MELITTIN AND ALAMETHICIN. ((S.J. Ludtke, K. He, T. Harroun, W.T. Heller, and H.W. Huang)) Rice University, Houston, TX 77251-1892.

The magainins are 23-residue (nonhemolytic) antibiotic peptides discovered in the skin of *xenopus laevis*. Melittin is a 26 residue (hemolytic) toxin from bee-venom. Alamethicin is a 20 residue (hemolytic) antibiotic peptide. All 3 peptides form alpha-helices when interacting with lipid bilayers. The orientation of these helices has a strong concentration and lipid dependence as shown by oriented circular dichroism. We have shown previously that for peptide concentrations below 1:50, alamethicin in DPhPC and magainin in (3:1) POPC/S cause the membrane to become thinner roughly in proportion to the added peptide. Further experiments have shown that this thinning effect does not occur in all lipids. Magainin in DMPC does not appear to cause any measurable thinning of the membrane. However, both magainin and melittin cause thinning in POPC membranes (without the presence of charged headgroups like PS or PG). This implies that the interaction with these peptides is not strictly a function of headgroup charge. Complete results for magainin and melittin in similar lipid systems will be presented.

Su-Pos426

THE EFFECT OF THE SIZE OF THE LIPID HEAD GROUP ON ALAMETHICIN-LIPID BILAYER INTERACTIONS. ((W.T. Heller, K. He, S.J. Ludtke, T. Harroun, and H.W. Huang)) Rice University, Houston, TX 77251-1892.

Current models of lipid peptide interactions indicate that peptides, such as the alpha-helical alamethicin, associate with lipid bilayers by adsorbing in the head group region of the bilayer. If the lipid to peptide ratio is high enough, the peptide will insert into the lipid bilayer parallel to the bilayer normal. The impetus for insertion is the energy cost of expanding the area of the bilayer's head group region to make room for the adsorbed peptides, thereby thinning the chain region, versus the free energy of peptides inserting into the bilayer. Using different ratios of diphytanoyl phosphatidylcholine and diphytanoyl phosphatidylethanolamine, we control the average size of the head group in an effort to determine if the size of the head group has an effect on the insertion of the peptide alamethicin into the lipid bilayers. We use oriented circular dichroism to determine the orientation of the peptide. We observe that as the average size of the head group decreases, the extent of insertion of the alamethicin decreases.

G-PROTEINS**Su-Pos427**

EFFECT OF G_{α} PROTEIN ANTISENSE OLIGONUCLEOTIDES ON β -ADRENERGIC MEDIATED STIMULATION OF CONTRACTION RATE IN NEONATAL RAT VENTRICULAR MYOCYTES. ((J.P. Egaminio, H.M. Colecraft, S-S. Sheu)) University of Rochester School of Medicine and Dentistry, Rochester, NY 14642.

G_{α} protein plays a crucial role in β -adrenergic modulation of cardiac excitation and contraction. In this study, antisense technology was employed to manipulate G_{α} gene expression in single cultured neonatal rat ventricular myocytes and the functional implications of these manipulations on the spontaneous contraction rate induced by β -adrenergic stimulation were assessed. Fluorescein-tagged, 20-mer phosphorothioated oligonucleotides targeted against G_{α} protein mRNA were followed within cells using fluorescence microscopy. Treatment of cells with oligonucleotide alone resulted in negligible uptake. Uptake was dramatically enhanced, however, when oligonucleotide was applied in the presence of the cationic liposomal preparation, transfectam. Initially, roughly 90% of the cells displayed intense nuclear and diffuse cytoplasmic fluorescence. By 80 hrs after treatment, only 10% of treated cells displayed this same degree of fluorescence. Functional assessment of G_{α} gene expression inhibition was carried out by measuring the effect of the β -adrenergic agonist, isoproterenol on the rate of spontaneous contractions in control and antisense treated cells. In control cells, 100 nM isoproterenol increased the rate of spontaneous contractions by 26 ± 4 beats per minute (bpm) as compared to 6 ± 2 bpm in cells with nuclear localization of anti G_{α} . Selectivity of the anti G_{α} treatment was demonstrated as cells treated with antisense to the m_1 muscarinic receptor (mAChR) responded to 100 nM isoproterenol with a 28 ± 5 bpm increase. Specificity of the treatment was established in that the anti G_{α} treatment did not affect the ability of 1 μ M carbachol or 100 nM forskolin to, respectively, decrease and increase the rate of spontaneous contractions. These results demonstrate the feasibility of use of antisense technology for the elucidation and manipulation of signal transduction pathways in primary cultured heart cells.

Su-Pos428

THE INTERACTION BETWEEN P21RAC AND ITS GDI PROTEIN ((Richard.W. Stockley, Miriam Hirschberg and Martin R. Webb)) National Institute for Medical Research, The Ridgeway, Mill Hill, London, NW7 1AA, U.K.

p21rac is a small GTP binding protein in the ras superfamily, related to rho. It has fairly well defined roles in organization of the cytoskeleton and in the superoxide response of neutrophils to bacteria. Like all the ras superfamily, it is presumed to act as a molecular switch and is active in the GTP form. The nucleotide state is controlled by a variety of GAPs accelerating GTP hydrolysis and by exchange factor protein exchanging GTP for GDP. In addition, members of the rho family form tight complexes with a GDI (guanine nucleotide dissociation inhibitor) protein. On its own, post-translationally modified p21rac is membrane bound due to the lipid at the C-terminus. Bound to GDI, it forms a highly soluble cytoplasmic complex.

We are using *E. coli*-expressed p21rac to study the basic biochemistry, as this form contains no lipid, and p21rac from a baculovirus expression system to examine the interactions with GDI. A range of kinetic and spectroscopic techniques, including the use of 2'(3')-O-(N-methylanthraniloyl)-GTP (mantGTP), are being used to investigate the mechanism of GTP hydrolysis, the interaction with GDI and associated conformation changes. We will also present a 1.35 Å resolution x-ray structure of p21rac complexed with the non-hydrolyzable analogue of GTP, GMPPNP, and its comparison with the structure of p21ras.

Supported by MRC, U.K.

Su-Pos429

MECHANISM OF THE INTERACTION OF P21RHO.GTP WITH RHO-GAP: COMPARISON WITH THE RAS-GAP MECHANISM. ((S.B.Ludbrook and J.F. Eccleston)). National Institute for Medical Research, Mill Hill, London NW7 1AA. UK.

The mechanism of rho-GAP activated GTPase of p21rho has been investigated by the use of the fluorescent analogue of GTP, 2'(3')-O-(N-methylanthraniloyl)GTP, (mantGTP), and stopped-flow spectrofluorimetry. In the absence of rho-GAP, the stoichiometric p21rho.mantGTP complex hydrolyses to the mantGDP complex with a rate constant of $5 \times 10^{-5} \text{ s}^{-1}$ (50mM Tris-HCl, pH7.5, 50mM NaCl, 2mM MgCl_2 , 1mM DTT, 25°C). On mixing p21rho.mantGTP with excess rho-GAP, a biphasic fluorescence signal from the mant fluorophore was obtained; first an exponential decrease in fluorescence followed by an exponential increase in fluorescence (20°C). The first process was linearly dependent on [rho-GAP] giving a second-order rate constant of $3 \times 10^6 \text{ M}^{-1} \text{ s}^{-1}$. The second process was hyperbolically dependent on [rho-GAP] with a limiting rate constant of 2 s^{-1} . Repeating the experiment with p21rho.mantGMPPNP, only an exponential decrease in fluorescence occurred, the observed rate constant being linearly dependent on [rho-GAP]. The results suggest that with p21rho.mantGTP the initial phase represents the binding of rho-GAP and the second phase represents the hydrolysis step. Therefore Rho-GAP causes activation of mantGTP hydrolysis by $>4 \times 10^4$ fold. Although there is no sequence homology between rho-GAP and ras-GAP, they display similar mechanisms and levels of GTPase activation.

Su-Pos430

COMPETITION BETWEEN Li^+ AND Mg^{2+} FOR THE METAL BINDING DOMAIN IN G PROTEINS ((Louis Amari, Chandra Srinivasan, and Duarte Mota de Freitas)) Department of Chemistry, Loyola University of Chicago, Chicago, IL 60626.

Although lithium carbonate has been used in the treatment of bipolar illness for a number of years, the molecular mechanism of lithium action still remains unknown. One hypothesis is that Li^+ competes with Mg^{2+} for Mg^{2+} -binding sites in biomolecules, in particular guanine nucleotide binding proteins (G proteins). Two types of G proteins, G_i and G_o , have been shown to stimulate and inhibit adenylate cyclase, and Li^+ has been shown to be an inhibitor of these two G proteins. It is conceivable then that the common site of lithium action could be at the Mg^{2+} binding sites on G_i and G_o , causing a decrease in the stimulation and inhibition of the signal transduction pathway. We have conducted fluorescence measurements for two different preparations of G proteins (Transducin extracted from bovine eye retinas, and recombinant G_{α}). The implications of our fluorescence data for the mechanism of Li^+ action will be discussed.

Su-Pos431

SOLID STATE NMR STUDIES OF THE ARGININE RESIDUES IN THE PHOTOCYCLE OF BACTERIORHODOPSIN ((A.T. Petkova, J.G. Hu, M. Bizounok, R.G. Griffin, and J. Herzfeld)) Dept. of Chemistry, Brandeis University, Waltham, MA 02254, Dept. of Chemistry and Francis Bitter Magnet Laboratory, Massachusetts Institute of Technology, Cambridge, MA 02139.

^{15}N CP/MAS studies of the photocycle of $[\eta_{1,2}\text{-}^{15}\text{N}_2]\text{Arg-bR}$ in 0.1 M NaCl at pH=10 revealed the presence of 'wing' peaks in the spectra of intermediates prepared by illumination at temperatures between -15° and -90°C . The two peaks appear downfield and upfield from the broad Arg resonance, and are separated by approximately 24 ppm. We have found a strong dependence of the 'wing' peak size on the trapping temperature. Solid-state NMR studies of light-adapted $[\epsilon\text{-}^{15}\text{N}]\text{Lys-bR}$ show that mixtures of photointermediates bR₅₆₈, N, M, and L in different proportions are trapped in this temperature range. It appears that the 'wing' peaks are associated with the M-state of bR, although the N-state may have a very small contribution as well. The peak intensities indicate a change in 2 of the 14 labeled nitrogen atoms. Selective inversion of the downfield 'wing' peak by rotor-synchronized CP/DANTE and subsequent spin diffusion resulted in a reduction of the size of both 'wing' peaks, similar to the change observed in $[\eta_{1,2}\text{-}^{15}\text{N}]\text{Arg.HCl.H}_2\text{O}$ when studied under the same experimental conditions. Thus the two 'wing' peaks represent nitrogen atoms from a single arginine residue in bR. This indicates that one arginine residue experiences relatively asymmetric interactions in the M intermediate. A possible candidate is Arg82 which is considered to be part of the Schiff base counterion complex, and is probably involved in an extensive H-bonding system. A study of arginine-containing crystalline model compounds is under way to further interpret the $\eta_{1,2}\text{-}^{15}\text{N}$ chemical shifts, especially with regard to the protonation state of the guanidyl group.

Su-Pos433

MECHANISM OF PHOSPHOLIPASE C β_2 ACTIVATION BY THE $\beta\gamma$ SUBUNITS OF G PROTEINS ((L. Runnels, J. Jenco, A. Morris and S. Scarlata)) Depts. of Physiol. & Biophysics and Pharm., S.U.N.Y Stony Brook, Stony Brook, NY 11794 (Spon. NIH GM53132)

To determine whether the $\beta\gamma$ subunits of G proteins activate phospholipase C β_2 (PLC β_2) by increasing its affinity to membrane surfaces or whether activation occurs by interactions between the membrane-bound species, we conducted a series of fluorescence experiments using purified proteins. We first assessed whether membrane association causes large scale conformational changes in PLC β_2 in the absence of G proteins. No changes were apparent by fluorescence quenching and energy transfer studies. Interestingly, G $\beta\gamma$ subunits show a detectable conformational change upon membrane association. Monitoring the binding of PLC β_2 to membranes with varying amounts of bound G $\beta\gamma$ subunits indicate that the presence of G protein does not alter PLC β_2 membrane affinity. Thus, G $\beta\gamma$ subunits do not activate PLC by recruiting the protein to membrane surface. Our data support a model whereby PLC β_2 is membrane-bound and diffuses along the surface until it encounters G protein. Monitoring the emission changes of fluorescent-labeled G $\beta\gamma$ show that PLC β_2 and G $\beta\gamma$ subunits on membrane surfaces interact with affinities in the micromolar range. The implication of these findings will be discussed.

RETINAL PROTEINS

Su-Pos434

RESTORING THE PHOTOCYCLE AND PROTON PUMPING IN THE MUTANT R82A OF BACTERIORHODOPSIN BY GUANIDINIUM HYDROCHLORIDE OR A SECOND MUTATION ON THE CYTOPLASMIC SURFACE.

((U. Alexiev¹, M. P. Krebs², R. Mollaaghababa², H.G. Khorana² and M.P. Heyn¹)). ¹Biophysics Group, Dept. of Physics, Freie Universität Berlin, D-14195 Berlin, Germany. ²Dept. of Biology, Massachusetts Inst. of Technology, Cambridge, MA 02139, USA.

In the bacteriorhodopsin mutant R82A an accelerated deprotonation of the Schiff base and a reversed proton release and uptake were observed (1,2). By adding guanidinium hydrochloride (GuHCl) or by introducing a second mutation on the cytoplasmic surface at helix G (G231C) a photocycle similar to wild type was obtained. However, the normal H⁺-stoichiometry and sequence of H⁺-release and uptake were observed only in the double mutant R82A/G231C, whereas GuHCl in R82A led to a reduced (10-15%) wild type proton signal. The proton concentration changes were measured with pyranine and with surface bound fluorescein in position 72 or 231. The time constant for proton release in R82A/G231C was 75.5 μs (on the surface), the same as for wild type. The pK_a's of the purple-blue transition (wild type: ≈ 2.6 ; R82A: ≈ 6.7 ; R82A/GuHCl: ≈ 5.5 ; R82A/G231C: ≈ 1) were analyzed and will be discussed in terms of the model proposed by Balashov et al.(2), which assumes a coupling of the protonation states of Asp85 and another group. Our results suggest, that the function of bR is not necessarily coupled to the existence of the arginine residue in position 82.

(1) Otto et al. (1990) PNAS 87, 1018-1022

(2) Balashov et al. (1993) Biochemistry 32, 10331-10343

Su-Pos432

SOLID STATE NMR STUDY OF THE L-INTERMEDIATE IN BACTERIORHODOPSIN ((J.G. Hu, B.Q. Sun, R.G. Griffin and J. Herzfeld)) Dept. of Chemistry, Brandeis University, Waltham, MA 02254 and Dept. of Chemistry and Francis Bitter Magnet Laboratory, Massachusetts Institute of Technology, Cambridge, MA 02139. (Sponsored by J.G. Hu)

The L₅₅₀ intermediate of bacteriorhodopsin (bR) has drawn much attention with respect to the mechanism of light-driven proton transport because it releases the Schiff base (SB) proton in the L \rightarrow M transition. Different conformations have been suggested for the retinal chromophore in the L intermediate and these correspond to different orientations of the SB proton in the transport pathway. To date, solid state NMR techniques have been proven powerful probes of other states of bR. In order to extend such studies to the L intermediate, we focused on the Schiff base (SB) nitrogen by monitoring the ^{15}N chemical shift in $[\epsilon\text{-}^{15}\text{N}]\text{Lys-bR}$ under conditions that stabilize the L intermediate. Upon illumination at low temperatures (as low as -130°C) with light of $>610\text{ nm}$, a new SB signal is detected in the ^{15}N NMR spectrum which disappears upon thermal relaxation at -80°C . The signal is in the range for a protonated SB but about 18 ppm downfield from bR₅₆₈ and 12 ppm downfield from bR₅₅₅. Comparison with the ^{15}N chemical shifts of model compounds, particularly 6-s-*trans*-13-*cis* protonated Schiff bases (pSB) of retinal, suggests that the H-bonding of the SB with its counterion is significantly stronger in L intermediate than in bR₅₅₅ (which in turn is stronger than in bR₅₆₈). The dissimilarity of the ^{15}N chemical shifts of bR₅₅₅ and L₅₅₀ occurs in spite of the similarity of their visible spectra. Comparison with the model compounds shows that bR₅₅₅ has a normal relationship between these two parameters and L is anomalous. This may be an indication of the proposed distortion of the polyene system in L.

Su-Pos435

PROTON TRANSPORT BY THE BACTERIORHODOPSIN MUTANT D85N INITIATED IN THE UNPROTONATED SCHIFF BASE STATE. ((S. Dickopf, U. Alexiev, M.P. Krebs*, H. Otto, R. Mollaaghababa*, H.G. Khorana* and M.P. Heyn)). Biophysics Group, Dept. of Physics, Freie Universität Berlin, D-14195 Berlin, Germany. *Depts. of Biology and Chemistry, MIT, Cambridge, MA 02139, USA.

At alkaline pH the bacteriorhodopsin mutant D85N has a λ_{max} of 405 nm and a deprotonated Schiff base. This state resembles the M-intermediate of the wild-type photocycle. Using time-resolved methods we show that this yellow form of D85N, which has an initially unprotonated Schiff base and which lacks the proton acceptor D85, transports protons in the same direction as wild-type when excited by 400 nm flashes. Photoexcitation leads in several ms to the formation of a redshifted (630 nm) intermediate with protonated Schiff base which decays in tens of seconds to the initial state (400 nm). Experiments with pH-indicator dyes show that at pH 7, 8 and 9 proton uptake occurs in about 5 to 10 ms and precedes the slow release (seconds). Photovoltage measurements reveal that the direction of proton movement is from the cytoplasmic to the extracellular side with major components on the ms- and second time-scales. The slowest electrical component could be observed in the presence of azide which accelerates the return of the blue intermediate to the initial yellow state. Transport thus occurs in two steps. In the first step (ms) the Schiff base is protonated by proton uptake from the cytoplasmic side, thereby forming the blue state. From the pH dependence of the amplitudes of the electrical and photocycle signals we conclude that this reaction proceeds as in wild-type, i.e. via the internal proton donor D96. In the second step (seconds) the Schiff base deprotonates releasing the proton to the extracellular side.

Su-Pos436

IN BACTERIORHODOPSIN L93A THE THERMAL REISOMERISATION IN THE ALL-TRANS-PHOTOCYCLE IS THE RATE LIMITING STEP ((U. Schweiger, J. Tittor and D. Oesterhelt)) Max-Planck-Institut für Biochemie, D-82152 Martinsried/ Germany.

In bacteriorhodopsin isomerisation of the C13-C14 double bond takes place during photoisomerisation and thermal isomerisation in the photocycles starting from all-trans and 13-cis-retinal as well as during light-dark-adaptation. Leucin 93 is in Van-der-Waals contact to the methyl group at C13 of retinal. Characteristic for the mutant L93A is the slow recovery of the initial state after photoexcitation of the all-trans form (factor 500 compared to wild type¹). The rate limiting step is the decay of a red shifted intermediate (12 nm compared to the initial state) following the M-intermediate. It differs from the O-intermediate known from the wild type in three properties: Firstly, the activation energy of its reaction to the initial state is 19 kJ/mol higher than in wild-type bacteriorhodopsin (see also ²). Secondly, its decay is accompanied by a 13-cis to all-trans isomerisation. And thirdly, its photochemistry involving a red and a blue shifted intermediate is different from the photochemical behaviour of the wild-type O-intermediate. By the absorption of a second photon, the slow thermal reisomerisation is bypassed. This pathway is responsible for the proton transport activity (25 % of the wild type) much higher than expected on the basis of a one photon cycle (0.2 %). The two photon driven transport cycle is also evident from the action spectrum of the proton transport activity.

¹ Subramaniam, S.; Greenhalgh, D.A.; Rath, P.; Rothschild, K.J. and Khorana H.G.; PNAS (1991), 88, 6873-6877.

² Delaney, J.K.; Schweiger, U. and Subramaniam, S. PNAS (1995), 92.

Su-Pos438

A HELIX TILT IN THE N-INTERMEDIATE OF THE BACTERIORHODOPSIN PHOTOCYCLE ((Janet Vonck)) Life Sciences Division, Lawrence Berkeley National Laboratory, University of California, Berkeley, CA 94720.

Much recent evidence suggests that a significant conformational change takes place upon formation of the N intermediate in the photocycle of the proton pump bacteriorhodopsin. To visualize these changes, difference maps were calculated from electron diffraction patterns of the bR ground state and the N intermediate of the mutant Phe219→Leu. Glucose-embedded samples of this mutant protein were first shown by Fourier transform infrared spectroscopy to have a long-lived N intermediate when illuminated at -3°C. Two independent 3-D difference maps were calculated from specimens tilted 25° and 45°, respectively. Both maps show essentially the same features, apart from the expected better vertical resolution in the higher tilt map. The largest conformational changes between bR and N are located in the half of the protein closest to the cytoplasmic surface, and they can be interpreted as an increased ordering on the G helix and an outward tilt of part of the F helix. This latter movement is likely to open a water accessible channel from the cytoplasm to Asp96 and the Schiff base, which makes Schiff base reprotonation from Asp96 possible and thus provides directionality to the proton pump. Supported by NIH grant GM51487.

Su-Pos440

CHARGE MOVEMENTS IN THE 13-CIS PHOTOCYCLES OF THE BACTERIORHODOPSIN MUTANTS ARG82LYS AND ARG82GLN. ((S. Misra, S. Balashov, T.G. Ebrey, Y. Feng*, R.K. Crouch* and D.R. Menick*)) Center for Biophysics and Computational Biology, Univ. of Illinois at Urbana-Champaign, Urbana, IL 61801; *Medical Univ. of S. Carolina, Charleston, SC 29425.

We have examined light-induced currents in gel samples of the Arg82Lys and Arg82Gln bacteriorhodopsin mutants in the pH 2-9 and 6-9 ranges respectively. In the Arg82Lys mutant, our results suggest that two phases of the photocurrent, with lifetimes of 30 and 300 μ s, are due to the photocycle of the 13-cis form rather than the all-trans form of the pigment. We investigated the pH dependence of these phases, the D₂O effect on the lifetimes of these phases, and their correspondence to absorbance changes at 660 nm. The presence of a D₂O effect suggests that the charge motion producing these current phases is proton or protonated amino acid movement within the molecule. The current amplitudes depend on the protonation states of at least two residues, one of which is Asp85 while the other may be Lys82. In Arg82Gln, a 10 μ s photocurrent is seen which also depends on the protonation state of Asp85 and shows similarity to the 30 μ s photocurrent of Arg82Lys. We attempt to explain these currents in terms of a model for interacting residues within the retinal binding pocket of bacteriorhodopsin.

Su-Pos437

INVOLVEMENT OF TYR-185 IN THE BACTERIORHODOPSIN M→N TRANSITION ((Gary J. Ludlam, Cheryl F.C. Ludlam, Sanjay Sonar, Matthew Coleman, Judith Herzfeld², Uttam L. Rajbhandary³ and Kenneth J. Rothschild)) Physics Department and Molecular Biophysics Laboratory, Boston University, Boston, MA 02215; ²Department of Chemistry, Brandeis University, Waltham, MA 02254 and ³Department of Biology, Massachusetts Institute of Technology, Cambridge, MA 02139

Attenuated total reflection-FTIR difference spectroscopy has been combined with site-directed isotope labeling (SDIL) to investigate protein conformational changes which occur in the M→N transition of the bacteriorhodopsin (bR) photocycle. It has previously been shown that this step involves a secondary structural change (R→T) of membrane α -helices of the protein along with a proton transfer from Asp-96 to the retinylidene Schiff base. In this work, we find that the Tyr-185 side chain undergoes a structural perturbation during this transition. Uniform isotope labeling of tyrosines with L-[ring-²H₄] and L-[ring-4-¹³C]Tyr was used to assign an intense negative band appearing at 1515 cm⁻¹ in the M→N difference spectrum to a tyrosine ring mode. SDIL shows that of the 11 tyrosines in bR, only Tyr-185 gives rise to this band. Polarized ATR-FTIR was used to characterize possible changes in the orientation of tyrosine during this transition. This work establishes that one of the largest changes during the R→T conformational switch is a perturbation of the Tyr-185 side chain, consistent with evidence that the Pro-185/Tyr-185 peptide bond is active and may function as a hinge, allowing bending of the F-helix in bR.

Su-Pos439

EVIDENCE FOR AN ICE-LIKE PROTON TRANSFER IN THE PROTON RELEASE PATHWAY AND LIQUID PHASE TYPE IN THE PROTON UPTAKE PATHWAY OF BACTERIORHODOPSIN. ((Johannes le Coutre and Klaus Gerwert)) Lehrstuhl für Biophysik Ruhr-Universität Bochum, D-44780 Bochum, Germany (Spon. by M. Engelhard)

Experimental evidence for the protontransfer via a hydrogen-bonded network in bacteriorhodopsin between the catalytic proton-donor asp 96 and the acceptor Schiff's base is given by FTIR studies (1). In order to characterise the complete proton-pathway in this light-driven proton-pump the kinetic isotopic effects due to ¹H/²H exchange were determined for the intramolecular protonuptake- and proton release-reactions. In a liquid phase H bonded network the rate limiting step is the restauration of the bonding (or Bjerrum) defect whereas in ice it is the restauration of the ionic defect. This different kinetic isotopic effects after ¹H/²H exchange. The results show a mechanism which is similar to ice in the proton release pathway and similar to water in the uptake pathway. The network on the release pathway seems to be stabilised by arg 82.

(1) le Coutre, J., Tittor, J., Oesterhelt, D., & Gerwert, K. (1995): *Proc. Natl. Acad. Sci. USA*, 92: 4962-4966.

Su-Pos441

ARGININE-82 CONTROLS THE pK_a OF THE PROTON RELEASE GROUP OF BACTERIORHODOPSIN ((R. Govindjee, S. Misra, S. P. Balashov, T. G. Ebrey, J.-X. Ma*, R. K. Crouch*, and D. R. Menick*)) Center for Biophysics and Dept. of Cell and Struct. Biology, UIUC, Urbana, IL 61801, and * Medical Univ. of S. Carolina, Charleston, SC 29425.

In the R82A and R82Q mutants of bR, at neutral pH, proton release is drastically delayed and occurs after the proton uptake. It was suggested that Arg-82 is associated with the proton release process, being a proton release group itself, or affecting the functioning of this group. In this study we have shown that upon an increase in pH from 7 to 8 (in 1 M NaCl and 25% glycerol) the time constant of proton release (measured with umbelliferone) decreases from 45 ms to ~2.5 ms in R82Q pigment. The transient H⁺ signal becomes similar to that in the wild type (release precedes the uptake) except that it has a smaller amplitude. We interpret this observation as follows: Arg-82 is not a proton release group itself but controls the pK_a of this group (as well as the pK_a of Asp-85). Upon substitution of Arg-82 with a neutral residue, the pK_a of this group in M intermediate shifts from 4.8 in the WT (Cao et al., 1993) to higher pHs (7.3 in 1 M salt) in R82Q, making this group almost nonfunctional at pH 7. Analysis of light-induced photocurrents in R82Q revealed a 1 ms component which appears at high pH with pK_a 8.2 (in 150 mM salt) which we tentatively ascribe to the proton release group. pH dependence of proton release was also studied for the R82K mutant. The pK_a of the proton release group is increased in this mutant but to a lesser extent as compared to R82Q. This work was supported by DOE Grant 95ER20171 to R.C. and NIH Grant GM52023 to T.G.E.

Su-Pos442

SPECIFIC LIPID REQUIREMENTS FOR NORMAL FUNCTION OF BACTERIORHODOPSIN (BR) PHOTOCYCLE. ((S. Dracheva, A. Mukhopadhyay, S. Bose, and R. W. Hendler)) Laboratory of Cell Biology, NHLBI, NIH, Bethesda, MD. 20892. (Spon. by M.R. Bunow).

Our laboratory has implicated purple membrane (PM) lipids as controlling factors for the normal function of the BR photocycle on the following basis. Mild Triton treatment removes the M_2 to 0 decay pathway seen in native membranes and also the control of the mol ratio of M_2 and M_3 intermediates by the intensity of actinic light, without destroying the trimer structure of BR (Mukhopadhyay et al., *Biochemistry*, 1994). During the Triton treatment, ~25% of the squalenes and lipopolysaccharide sulfate, and 7% of the phospholipids are physically removed from PM (Dracheva et al., submitted). All of the functions lost by Triton treatment are regained by incubating the treated PM with isolated PM lipids in high salt (Mukhopadhyay et al., this session). We are conducting studies with isolated PM lipids and combinations of these to define the specific lipid requirements for native BR function. Preliminary results point to an essentiality of PM phospholipid (PL) for the complete restoration of normal activity obtained with squalene addition. Non-native PL (egg asolectin) can restore some native function, but less efficiently than native PL. Squalene restorative activity is enhanced by native PL but not by asolectin PL. Complete fractionation of all PM lipids is underway to allow testing of all isolated components.

Su-Pos444

NATIVE PURPLE MEMBRANE (PM) LIPIDS CONTROL BOTH NORMAL AND COOPERATIVE/HETEROGENEOUS BEHAVIOR OF THE BACTERIORHODOPSIN (BR) PHOTOCYCLE. ((A. Mukhopadhyay, S. Dracheva, S. Bose, and R. W. Hendler)) Laboratory of Cell Biology, NHLBI, NIH, Bethesda, MD. 20892.

Native BR photocycle behavior, at pH's near neutrality, exhibits two M intermediates, with τ 's of ~2 ms (M_2) and ~6 ms (M_3). M_2 decays directly to the 0 intermediate, whereas M_3 bypasses 0 en route to BR. The mol fraction, $M_2/(M_2+M_3)$, decreases with increasing energy of actinic light. We previously found that brief exposure to dilute Triton drastically changes all of the above behavior without disturbing the normal BR-trimer configuration (Mukhopadhyay et al., *Biochemistry*, 1994). More recently we found that ~1/4 of the squalenes and lipopolysaccharide sulfate, but less than a tenth of the phospholipids are removed from PM by the treatment (Dracheva et al., *Biochemistry*, submitted). We now establish a group of measurable parameters that quantify the detergent-induced loss of normal photocycle behavior, specifically: 1.) The ability of actinic light to change mol fraction of M_2 ; 2.) Loss of the species M_2 , which is characterized both by its τ and its decay to 0; 3.) Decrease in amount of BR that can turn over; 4.) Greater than 10-fold increase in turnover time of M. 5.) Shift of position of A_{max} for BR from ~571 to ~561 nm. All of these parameters of normal BR turnover, lost by treatment with Triton can be recovered by adding back normal PM lipids in the presence of > 2M NaCl.

Su-Pos446

MOLECULAR MECHANISM OF PROTEIN-RETINAL COUPLING IN BACTERIORHODOPSIN. ((John K. Delaney, Ulrike Schweiger[†] and Sriram Subramaniam.)) Dept. of Biological Chemistry, Johns Hopkins University School of Medicine, Baltimore, MD 21205 and [†]Dept. of Biochemistry, Max-Planck Institute for Biochemistry, Martinsried, Germany.

Bacteriorhodopsin is a membrane protein that functions as a light-driven proton pump. Each cycle of proton transport is initiated by the light-induced isomerization of retinal from the all-*trans* to 13-*cis* configuration, and completed by the protein-driven re-isomerization of retinal to the all-*trans* configuration. Previous studies have shown that replacement of Leu 93, a residue in close proximity to the 13-methyl group of retinal, by Ala, resulted in a 250-fold increase in the time required to complete each photocycle. Here, we show that the kinetic defect in the photocycle of the Leu 93 → Ala mutant occurs at a stage after the completion of proton transport, and can be overcome in the presence of strong background illumination. Time-resolved retinal extraction experiments demonstrate the continued presence of a 13-*cis* intermediate in the photocycle of the Leu 93 → Ala mutant well after the completion of proton release and uptake. These results indicate that retinal re-isomerization is kinetically the rate-limiting step in the photocycle of this mutant, and that the slow thermal re-isomerization can be bypassed by the absorption of a second photon. The effects observed for the Leu 93 → Ala mutant are not observed upon replacement of any other residue in van der Waals contact with retinal, or upon replacement of Leu 93 by Val. We conclude that the contact between Leu 93 and the C-13-methyl group of retinal plays a key role in controlling the rate of protein conformational changes associated with retinal re-isomerization and return of the protein to the initial state.

Su-Pos443

MONITORING SYSTEM FOR ENERGY TRANSDUCTION BY BACTERIORHODOPSIN (BR) LIPOSOMES. ((R. W. Hendler^a, A. Mukhopadhyay^a, P. D. Smith^b, and H. Cascio^b)) ^aLaboratory of Cell Biology, NHLBI, NIH, ^bBEIP, NCRR, NIH, Bethesda, MD. 20892.

BR liposomes present a model system for converting an input energy (i.e. photons) into an electrochemical gradient for protons ($\Delta\mu_{H^+}$) through the action of a proton pump. The system is useful both for the study of its own energy-transducing mechanisms and as a vehicle for studying the effects of $\Delta\mu_{H^+}$ on other co-incorporated proteins, such as the F_1F_0 ATPase. However, the strong actinic light used to power the system, causes major problems in the measurements of parameters of energy transduction. These problems have been identified and solved. Problems: 1.) Scattered actinic light interferes with the measurement of internal pH by pyranine fluorescence (f1). 2.) Pyranine is partially photosensitive. 3.) The usual f1 probes for inside-negative $\Delta\psi$, Oxanols V and VI are extremely photosensitive. 4.) A SCN⁻-sensitive electrode for internal negative $\Delta\psi$ shows a transient light-dependent artifact. We will demonstrate how these problems can be managed, using both electronic and software devices. The computer-controlled system we describe provides the following information: initial (1st s) rate of H⁺-pumping, maximum level of H⁺-pumped, magnitudes of $\Delta\psi$ and ΔpH , and rate of H⁺-leakage under a $\Delta\psi$. The system has been used to study the effects of ionophores, internal buffer strengths, BR concentration, and other factors on the energy-transduction process. Some representative data will be presented.

Su-Pos445

PROTEIN AND LIPID STRUCTURAL CHARACTERISTICS ASSOCIATED WITH THE RECOVERY OF NORMAL BACTERIORHODOPSIN PHOTOCYCLE BEHAVIOR IN TRITON-TREATED PURPLE MEMBRANE ((S.M. Barnett, S. Dracheva, R.W. Hendler, and I.W. Levin)) ^aLaboratory of Chemical Physics, NIDDK, ^bLaboratory of Cell Biology, NHLBI, NIH, Bethesda, Maryland, 20892-0510.

Brief exposure of purple membrane (PM) to dilute Triton (0.1% Triton, 2 min) affects many aspects of the bacteriorhodopsin (BR) photocycle without destroying the trimer structure. Native bacteriorhodopsin photocycle behavior is recovered upon reconstitution with purple membrane lipids in high saline media (> 2M NaCl), but is only partially recovered, or not recovered at all, in lower NaCl concentrations (Mukhopadhyay et al., this session). Studies were performed on purple membrane after exposure to Triton and after lipid reconstitution at different NaCl concentrations to identify the infrared spectroscopic markers (and by extension, the structural aspects) in purple membrane which are associated with the recovery of normal bacteriorhodopsin function. Triton-induced protein conformational changes involving the α -helical and β -turn amide I modes are correlated with the degree of photocycle recovery. Normal bacteriorhodopsin photocycle behavior is also reflected by the relative intensity of the amide II mode at ~1545 cm⁻¹ (relative to the amide I mode at ~1660 cm⁻¹) and the nature of lipid association with the purple membrane bilayer. Bacteriorhodopsin and rhodopsin bleaching studies indicate that in retinal-binding proteins the loss of amide II intensity (relative to the amide I marker) arises from a perturbation of protein conformation. Results will be presented involving reconstitution with lipids extracted from native purple membrane (representing reconstitution with lipid classes) and selective reconstitution with specific lipid classes.

Su-Pos447

GUANIDINIUM RESTORES THE PURPLE CHROMOPHORE OF BACTERIORHODOPSIN IN THE R82Q MUTANT. ((R. Renthal and Y. J. Chung)) U. of Texas at San Antonio, San Antonio, TX 78249

Replacement of Arg at position 82 in bR by Gln or Ala has been shown to slow the rate of proton release and raise the pK of Asp 85. These results indicated that R82 is involved both in the proton release reaction and in stabilizing the purple chromophore. We now find that guanidinium chloride added from the aqueous medium dramatically lowers the pK of D85 in the R82Q mutant (obtained from J. Lanyi and R. Needleman). The absorbance change at 640 nm (blue to purple transition) at pH 5.8 follows a simple binding curve, with an apparent dissociation constant of 0.05 M. The chloride counter ion is not involved in the observed spectral changes, since NaCl up to 0.2 M has no observable effect on the R82Q chromophore at pH 5.8. Furthermore, guanidinium chloride does not affect the chromophore of the double mutant R82Q/D85N. Thus, guanidinium appears to bind to a specific site near D85, restoring the purple chromophore. In previous studies, we found evidence for two positions of the R82 side chain, one near D85 and one closer to the extracellular surface. Covalent coupling of a quaternary ammonium group to E74 interferes with the extracellular position of R82. We now find that modification of E74 has no effect on the pK of D85 in the R82Q mutant, and it does not block the access of guanidinium to its binding site near D85. (Supported by NIH GM08194)

Su-Pos448

WATER AND LIGHT ARE CRUCIAL COMPONENTS IN THE BINDING OF RETINAL TO BACTERIO-OPSIN. ((I. Rouso[†], I. Brodsky[‡], A. Lewis[†] and M. Sheves[†])) [†]The Department of Organic Chemistry, Weizmann Institute of Science Rehovot 76100 Israel and the [‡]Department of Applied Physics, Hebrew University of Jerusalem, Jerusalem 91904 Israel.

One of the most important questions in the field of membrane proteins is concerned with the role of water in the structure-function relationships that exist in proteins. We have used the binding reaction of the retinal chromophore to bacterio-opsin in order to decipher the role played by water in this protein structure. When the retinal is in the 9-cis configuration association with the apo protein bacteriorhodopsin occurs but actual binding of the retinal in the binding site, characterized by formation of the protonated Schiff base is prevented until light alters the retinal configuration. Dehydrated films, containing 9-cis retinal/bacterio-opsin complex, were studied in environments of controlled humidity in order to test the controlling role of water in the structural alterations that occur when all-trans retinal is formed with light and the protonated Schiff base is finally generated. The results obtained demonstrate that the amount of absorbed water molecules in the protein has a crucial role in controlling the protein conformation that lead to protein-ligand binding reaction. In addition, the light has a critical role in this complexation reaction, by regulating the amount of water that is absorbed by the 9-cis retinal/bacterio-opsin complex. This action of light is in addition to its accepted role of transforming 9-cis to all-trans retinal. Furthermore, this light control of protein conformation expresses itself in many ways. For example FTIR studies have indicated that certain residues in the bacterio-opsin, which undergoes light induced structural changes during the complexation reaction, also alter their exposure to proton/deuterium exchange.

Su-Pos450

ELECTROSPRAY MASS SPECTROMETRY: A METHOD FOR THE CHARACTERISATION OF GENETICALLY AND CHEMICALLY MODIFIED BACTERIORHODOPSINS. ((P. Hufnagel, U. Schweiger, C. Eckerskorn and D. Oesterhelt)) Max-Planck-Institut für Biochemie, D-82152 Martinsried, Germany.

The molecular mass determination of the integral membrane protein bacteriorhodopsin (BR) by electrospray mass spectrometry required the development of a method for denaturation of the protein into a monodisperse solution. This consists of precipitation of the protein and dissolution of the precipitate in an acidic organic solvent. BR samples analysed under these conditions showed a molecular mass of 26784.0 ± 0.6 Da which was identical within the error limits with the theoretical mass (26783.6 Da) of the polypeptide chain.

The method is quick and accurate enough for the discrimination of point mutants in the protein if the mutation is accompanied by a mass change of more than one dalton. Thus, most amino acid exchanges (exceptions are, for example, the isomers L/I and the pairs D/N and E/Q) can be detected by mass spectrometry. The method was successfully applied to several mutants of bacteriorhodopsin to control and confirm the intended mutations.

The point mutated bacteriorhodopsin D36C has been covalently modified in several ways and the accompanying mass changes monitored by mass spectrometry. This method has allowed the characterisation of the products of the chemical reaction. For example, the reaction with a maleimide leading to a thiolated succinimide was followed by hydrolysis to the corresponding succinamide as detected by a mass increase of 18 Da.

Su-Pos449

QUANTUM CHEMISTRY AND MOLECULAR DYNAMICS STUDY OF BACTERIORHODOPSIN ((Ilya Logunov and Klaus Schulten, Beckman Institute and Department of Chemistry and Physics, University of Illinois at Urbana-Champaign, Urbana, IL 61801))

Electronic excitations and conformational potential surfaces of retinal in vacuo and in bacteriorhodopsin have been determined by means of the *ab initio* CASSCF method. The calculations account for the protein environment by explicitly including all protein partial atomic charges into the electronic Hamiltonian. The calculations were applied to an ensemble of bacteriorhodopsins generated by molecular dynamics simulations using a CHARMM force field with special parameters for retinal torsions. From this approach resulted a spectrum of bacteriorhodopsin with a maximum at 520nm, a width of 120nm for the native pigment and a spectrum shifted by 50nm for the D85N mutant. Calculations were also carried out to describe the potential surface governing the dark adaptation of an ensemble of bacteriorhodopsins. The resulting rate of dark adaptation at room temperature ($k \sim 10^{-5} \text{ s}^{-1}$) and its 1000-fold enhancement through Asp-85 protonation are in agreement with observation (Balashov et al, Biochemistry, 32:10331,1993). The excited state potential surface governing the photoreaction of bacteriorhodopsin was determined for a protonated retinal Schiff base analogue containing four double bonds. The calculations confirm that rotation around the 13-14 bond is the predominant photoisomerization pathway.

Su-Pos451

A PROTEINLESS PHOTODRIVEN PROTON PUMP ACROSS LIPID BILAYERS ((K. Sun and D. Mauzerall)) The Rockefeller University, New York, NY 10021.

Biological ion and proton transmembrane pumps use proteins for their activities. We have recently made a proteinless hydrophobic ion pump with an efficiency (ions pumped/charges photoformed) of 30%. It is driven electrostatically by photoinduced charge transfer across a single lipid water interface (Sun and Mauzerall, submitted to BJ). We now report a similar system which pumps protons across a lipid bilayer. When CCCP (or FCCP) is added to the system of a planar lipid bilayer containing magnesium-porphyrin with an aqueous electron acceptor, the usual positive photo voltage and current seen on illuminating the membrane are gradually replaced by a negative voltage and current as the pH is reduced from 10 to 6. The negative current is stable for >10 s on continuous illumination. The positive current is the electron flow from the excited porphyrin to the acceptor and can only be made continuous by adding a donor to the trans side. The negative current is proven to be the proton current by observation of a kinetic isotope effect on replacing H₂O with D₂O: the amplitude increases three fold. This may be caused by the pK shift of the deuterated hydrophobic acid to a higher value. The photoformed P⁺ causes dissociation of a proton from neutral CCCP and the photogenerated fields drive the proton across the acceptor interface, thus initiating proton pumping across the membrane. Evidence for the mechanism will be presented. This simple system could be a progenitor of biological photodriven proton pumps. Supported by NIH GM 25693.

SELF-ORGANIZATION - BIOPHYSICAL METHODS

Su-Pos452

TOPOLOGY OF GEL PHASE DOMAINS AND MIXING PROPERTIES IN PHASE-SEPARATED TWO-COMPONENT PHOSPHATIDYLCHOLINE BILAYERS ((V. SCHRAM, H. N. LIN and T. E. THOMPSON)) Department of Biochemistry, University of Virginia, Charlottesville, VA, 22908.

To better understand the influence of the lipid mixing properties upon the lateral organization in a two-phase two-component phosphatidylcholine bilayer, the FRAP studies of DMPC/DPPC and DMPC/DSPC by Vaz and coworkers (Biophys. J., 1990, 58: 273-275 and Biophys. J., 1989, 56: 869-876) has been extended to lipid systems of greater non-ideality, 1-stearoyl-2-capryl-phosphatidylcholine / 1,2 dipalmitoyl-phosphatidylcholine (C18C10PC/DPPC) and 1-stearoyl-2-capryl-phosphatidylcholine / 1,2-distearoyl-phosphatidylcholine (C18C10PC/DSPC). The phase diagram of C18C10PC/DPPC, determined by differential scanning calorimetry, displays a limiting case of an eutectic, with the eutectic point too close to pure C18C10PC to be detected. Comparison of the FRAP data (diffusion coefficient and mobile fraction) over the four lipid mixtures for each system shows that when the non-ideality of the mixture increases (in the order DMPC/DPPC → DMPC/DSPC → C18C10PC/DPPC → C18C10PC/DSPC), the gel phase becomes more efficient in restricting long-range translational diffusion. This result suggests that in a phase-separated bilayer, the gel phase tends to organize in small and/or dendritic domains when the lipids mix well together, and in large and/or centrosymmetric domains in highly immiscible lipid mixtures. Monte Carlo simulations of spot FRAP experiments, in which the mixing properties are rationalized as a probability of aggregation of the gel phase lipid molecules during the lateral phase separation, have been used to analyze quantitatively these data in terms of both size and fractality of the gel phase domains. This work was supported by NIH grants GM-14629 and GM-23573.

Su-Pos453

PERCOLATION AND LATERAL COMPARTMENTALIZATION IN A TWO - PHASE TWO - COMPONENT PHOSPHATIDYLCHOLINE BILAYERS: A FLUORESCENCE QUENCHING STUDY. ((B. Píková¹, D. Marsh² and T.E. Thompson¹)) ¹University of Virginia, Charlottesville, VA 22908, USA ²Max-Planck Institut für Biophysikalische Chemie, Göttingen, Germany.

Fluorescence quenching of a lipid-linked fluorophore by a lipid-linked spin label quencher has been studied experimentally in two-component, two-phase lipid bilayers to examine the effect of phase connection and disconnection on quenching. Both fluorophore and quencher prefer the fluid phase. At the percolation threshold, the point at which the fluid phase becomes subdivided into many small disconnected domains, the quenching drops abruptly. This decrease in quenching is a function of the fraction of the fluid phase and is due to the heterogeneous distribution of fluorophores and quenchers over the fluid phase domains. We have carried out computer simulations of this system using a triangular lattice divided into closed compartments of variable size and reactant average occupancy. The simulations demonstrate that the degree of quenching is reduced in the disconnected system and the reduction is correlated with the size of the disconnected domains. The combination of experimental data with simulations leads to the conclusion that the increase in the fluid fraction with increasing temperature is caused by an increase in size of existing domains not by an increase of the number of fluid domains. This is in an agreement with a previous ESR study of spin-spin coupling in the same two-component two-phase bilayer system (Sankaram et al 1992, Biophys. J., 63:340-349). This work was supported by NIH grants GM-14629 and GM-23573.

Su-Pos454

INFRARED DETECTION OF MICROPHASE SEPARATION IN BINARY MIXTURES OF PHOSPHOLIPID BILAYERS IN THE GEL STATE. ((R.G. Snyder, W. Yan, R. Wang, H.L. Strauss, G.L. Liang and R. Mendelsohn*)) Department of Chemistry, University of California, Berkeley, CA 94720-1460; *Department of Chemistry, Newark College of Arts and Science, Rutgers University, Newark NJ, 07102

Microaggregation in lipid bilayers of gel-state binary mixtures of phospholipids have been measured over temperatures ranging from -19°C to just below the main transition. The measurements were made using an isotope infrared method in which domain size (1-100 lipids) is determined from the splitting (or width) of the methylene scissors bands (or band) associated with the acyl chains. The method requires that the chains of one component be deuterated. Demixing was studied in fully-hydrated mixtures of the type $d_{18}^n X/d_{18}^n Y$ at a molar concentration ratio of 4:1, where typically: $n=18$, $n'=20, 22$, or 24 ; and $X,Y=PC, PE$, or PA . The degree of aggregation was determined with reference to the random mixtures $d_{18}^n X/d_{18}^n Y$. We report here primarily on demixing in mixtures having components with like head-groups, but different chain lengths ($d_{18}^{18} PC/d_{18}^{20} PC$, $n'=20, 22, 24$) and mixtures with unlike head-groups, but nearly equal chain lengths ($d_{18}^{18} X/d_{18}^{20} Y$).

Su-Pos456

APPLICATION OF ELECTROPORATION FOR TRANSDERMAL DRUG DELIVERY. ((S.A. Gallo and S.W. Hui)) Department of Biophysics, Roswell Park Cancer Institute, Buffalo, NY 14263.

Electrical pulses were applied to permeate the stratum corneum of pig skin, in an effort to optimize conditions for transdermal drug delivery by electroporation. Trains of electrical pulses were applied to pig skin for a given duration, and the effects on the resistance of the skin were monitored. Initially the skin resistance falls during pulse application, but recovers immediately after the pulse. However, the skin resistance does not reversibly recover after the application of a given number of pulses. The resistance drop and its reversibility are dependent on the voltage and the total exposure time of the skin to the electric field.

Methylene blue, a charged water soluble dye, was used to monitor the permeability of the skin as a result of the electrical pulses. Penetration depth and intensity were also found to have a dependence on the voltage and exposure time. It was concluded that the electrical pulse is responsible for permeating the stratum corneum and enhances the penetration of the dye molecules.

Su-Pos458

PRODAN AND LAURDAN PARTITION BETWEEN THE LIPID PHASES AND WATER. ((Tiziana Parasassi, Ewa Krasnowska, Egidio Iorio, and Enrico Gratton*)) Istituto di Medicina Sperimentale, CNR, Roma, Italy and *Laboratory for Fluorescence Dynamics, Department of Physics, University of Illinois at Urbana-Champaign, Urbana, IL 61801, Urbana IL.

The spectroscopic features of PRODAN and LAURDAN (6-propionyl- and 6-lauroyl-2-dimethylaminonaphthalene, respectively) in phospholipid vesicles of different phase state have been compared. PRODAN shows a higher partitioning in the liquid-crystalline with respect to the gel phase. Instead, LAURDAN does not display a preferential partitioning between the phases and it is virtually non-fluorescent in the aqueous environments. PRODAN in water can be easily identified by the red emission band, particularly evident in gel phase vesicles. To separate the probe response arising from the lipid environment, a new method based on the measurement at three wavelengths has been developed for the determination of the generalized polarization (GP). The method effectively subtracts the contribution of PRODAN fluorescence arising from water. The three-wavelengths-GP can also be used to calculate PRODAN partition coefficient between lipids and the aqueous phase and between the gel and the liquid-crystalline phase of phospholipids. The presence of cholesterol in the bilayer strongly affects all PRODAN spectral features. In particular, the probe partitioning between the bilayer and water is dramatically changed. In gel phase phospholipids, the presence of cholesterol causes almost complete incorporation of the PRODAN into the membrane. [Research sponsored by CNR and *NIH grant RR03155.]

Su-Pos455

LIPID DOMAINS IN BIOLOGICAL MEMBRANES: SIZE DETERMINATION THROUGH THE ANALYSIS OF FRAP DATA. ((A. Lopez, L. Salomé, V. Schram and J.F. Tocanne)) Labo. Pharmac. Toxicol. Fondament. CNRS, 118 Route de Narbonne, F-31062 Toulouse Cedex, France.

The idea that biological membranes are not homogeneous systems with a regular distribution of their lipid and protein components, but are composed of microdomains becomes widely accepted. However, the structure, composition and size of these domains are still poorly understood. This is due to the fact that there is not a unique definition of these domains and that their description depends dramatically upon the approach used for their detection. Through computational modelization of Fluorescence Recovery After Photobleaching (FRAP) experiments, which considers the importance of proteins as obstacles to lipid diffusion, we have recently shown that above the percolation threshold, obstacles can form closed diffusion domains, the size of which can be determined by analyzing the changes in lipid lateral diffusion rate D and mobile fraction M which result from changes in the radius R of the illuminated area. For membranes of the confined type, these simulations predict that D and M should respectively increase and decrease upon increasing R . When applied to the D and M versus R FRAP data obtained by Edidin et al. for the plasma membrane of human fibroblasts and K78-2 hepatoma cells, this model consistently leads to the conclusion that both membranes would be of the confined type, with closed lipid domains of about 0.48 μm and 0.25 μm in size respectively. This approach sheds a new light on the potential of FRAP experiments, when coupled with theoretical analysis of the data, in investigating membrane lateral heterogeneities.

Su-Pos457

EFFECT OF CURVATURE STRESS ON CATIONIC LIPOSOME-INDUCED ERYTHROCYTE FUSION. ((Lin-Hong Li* and Sek-Wen Hui)). Biophysics Department, Roswell Park Cancer Institute, Buffalo, NY 14263. *on leave from Biomedical Engineering Department, Hunan Medical University, Changsha, China.

Dioleoyl-trimethylammonium propane (DOTAP) and phosphatidylethanolamine (PE) containing acyl chains of varying degree of unsaturation were used to form cationic liposomes, which were used to induce fusion between rabbit erythrocytes. Fusion was measured by phase and fluorescence microscopy, using dye diffusion as well as energy transfer assays. Fusion yields (FY) between cells, and between cell and vesicle, increases with curvature stress in cationic liposomes containing PE with increasing degree of acyl unsaturation, in the order of lysoPE < POPE < DOPE < DLinPE. Replacing the last 3 PEs with lysoPE lowers FY. Liposome-induced hemolysis follows the same order. Electrostatic shielding of cell surface charges by electrolytes in cell suspensions reduces FY and hemolysis. We conclude that cationic liposome-induced cell-cell fusion is mediated by these liposomes acting as a fusion bridge between cells. (Supported by GM30969 from NIH)

Su-Pos459

DIFFUSION IN MEMBRANES STUDIED BY FLUORESCENCE OXYGEN QUENCHING. ((Enrico Gratton*, Egidio Iorio, Anna Maria Giusti and Tiziana Parasassi)) Istituto di Medicina Sperimentale, CNR, Roma, Italy and *Laboratory for Fluorescence Dynamics, Department of Physics, University of Illinois at Urbana-Champaign, Urbana, IL 61801, Urbana IL.

The diffusion of molecular oxygen in membrane has been measured by fluorescence oxygen quenching, using probes of different lifetimes. Probes with longer lifetime should probe a large environment. Molecular oxygen is highly soluble in the hydrophobic interior of the bilayer and its diffusion is strongly dependent on the phase states of lipids. In general, in the liquid-crystalline phase oxygen diffusion is much faster. The apparent Stern-Volmer constant in the two phospholipid phases depends both on the lifetime of the fluorescent probe and on its size, i.e., on the perturbation introduced by the probe in the bilayer. For 2-dimethylamino-6-lauroyl-naphthalene (LAURDAN) the apparent Stern-Volmer constant differs by a factor of about 50 between the two phases, while for pyrene-butyric acid we can only observe a difference of a factor of about 2. Moreover, using long lifetime probes we observed that the fluorescence decay becomes multi-exponential as the oxygen concentration is increased. A static fluorescence component is difficult to imagine for molecular oxygen, and the effect on the lifetime seems to imply a dynamic process. This observation points out that the simple Stern-Volmer equation cannot be used to obtain the quenching rate in the membrane. We also studied the effect of different cholesterol concentrations on the apparent Stern-Volmer constant. In agreement with the non-monotonic modification of the bilayer properties as a function of cholesterol concentration reported by other experiments, we also observed that the apparent oxygen quenching rate is a non-monotonic function of the cholesterol concentration. [Research sponsored by CNR and *NIH grant RR03155.]

Su-Pos460

HIGH SENSITIVITY MEASUREMENT OF THERMAL CONDUCTIVITY AND SPECIFIC HEAT IN PHASE TRANSITIONS BY A TEMPERATURE EXCITATION/RELAXATION METHOD. ((A. Jin¹, C.P. Mudd² and N.L. Gershfeld)) ¹DCRT, ²NCRR, and NIAMS, NIH, Bethesda, MD 20892.

We have recently reported the development of a calorimeter with high sensitivity for specific heat measurements (Mudd et al, J. Biochem. Biophys. Methods 26,179, 1993). That instrument has now been modified to measure simultaneously the thermal conductivity, λ and specific heat, C_p of fluids with sensitivities of $3 \times 10^{-5} \text{ W m}^{-1} \text{ deg}^{-1}$ and $2 \times 10^{-5} \text{ cal g}^{-1} \text{ deg}^{-1}$, respectively. The limits of these sensitivities are defined primarily by the electronic noise and baseline stability of the calorimeter. Sample loading errors are the same magnitude as the electronic noise. Its operating principle is based on a temperature excitation/relaxation method in which both λ and C_p are evaluated from the temperature response curve. We have re-examined the region of the main transition temperature, T_m , for dispersions of DMPC (1 w %); both λ and C_p are proportional to $(T_m - T)^{-a}$, with $a > 1$ indicating that the main transition is first order. T_m is 23.79°C for our sample (>99.5 mole %). Anomalous high C_p values are observed for $T > T_m$ until 29°C, the critical temperature T^* for the formation of the unilamellar state (Gershfeld et al, Biophys. J. 65,1174, 1993). Thus, the transformation at T_m for DMPC appears to exhibit characteristics of two processes: a first-order melting of the aliphatic chains at T_m superimposed on a second process that is completed at T^* with the formation of unilamellar vesicles. We anticipate that this instrument will provide precise thermodynamic information on higher order phase transitions.

Su-Pos462

LINDANE SUPPRESSES THE LIPID-BILAYER PERMEABILITY IN THE MAIN TRANSITION REGION

M. Sabra, K. Jørgensen, and O. G. Mouritsen
Department of Physical Chemistry, The Technical University of Denmark,
DK-2800 Lyngby, Denmark

The effects of a small molecule, the insecticide lindane (γ -1,2,3,4,5,6-hexachlorocyclohexane), on unilamellar DMPC bilayers in the phase transition region have been studied by means of differential scanning calorimetry and fluorescence spectroscopy. The calorimetric data show that increasing concentrations of lindane broaden the transition and lower the transition temperature, without changing the transition enthalpy significantly. Lindane therefore enhances the thermal fluctuations of the bilayer. Fluorescence spectroscopy was used to measure the passive permeability of unilamellar DMPC bilayers to Co^{2+} ions. The data show that lindane seals the bilayer for Co^{2+} penetration and that this effect increases with increasing lindane concentration. The depression of the permeability in the transition region is discussed in terms of the molecular structure of lindane and its capacity to seal the bilayer membrane and at the same time enhance the thermal fluctuations.

Su-Pos464

LIGHT INDUCED RELAXATION, CONFORMATIONAL AVERAGING AND RELAXATION IN PHOTODISSOCIATED COHbA. ((J. Huang, J. Wang, M. Yang, I. Khan and J.M. Friedman)) Department of Physiology & Biophysics, Albert Einstein College of Medicine, Bronx, NY 10461

A computer controlled rastering assembly for cryogenic samples has allowed us to pursue nanosecond time resolved near IR transient absorption studies on the COHbA photoproduct over a wide range of temperatures (100-300K). The intensity, peak position and line shape of the iron displacement sensitive charge transfer band at ~760nm (Band III) are followed as a function of time and illumination time for photodissociated COHbA in a 75% glycerol:water solvent. The kinetics of ligand recombination are also monitored for the same sample. The geminate rebinding kinetics show a substantial increase in overall rate and quantum yield in going from 300 to 200 K with progressive slowing at lower temperatures. Evidence of kinetic hole burning (KHB) is apparent at early times up to temperatures approaching 300K. the termination of KHB pattern at early times as a function of temperature indicates that the acceleration of the geminate process upon decreasing the temperature from 300 to 200 K is related at least in part to a slow down in the rate of conformational averaging. At temperatures well below the glass transition at ~200 K dramatic light induced relaxation (see Nienhaus et al., Biochemistry 1994, 33,13413) is observed. Prolonged illumination of the sample at 100 K progressively generates a Band III photoproduct spectrum at 10ns that consists of two distinct peaks. The redder peak centered near the original position of the initial photoproduct spectrum (~763 nm), progressively and substantially narrows on the blue edge. Normal red edge KHB is also observed. As the blue edge of the initial peak disappears a new peak appears centered near the relaxed deoxy T state position (~750 nm). The line shape changes in both peaks indicate a mapping among the conformational substates of the relaxed and unrelaxed populations. The results raise the possibility that the blue edge population consists of trapped transition state structures.

Su-Pos461

SMALL-ANGLE NEUTRON SCATTERING STUDIES OF LIPID BILAYER STRUCTURE, SOFTNESS, AND THE EFFECTS OF CHOLESTEROL

J. Lemmich,¹ K. Mortensen,² J. H. Ipsen,¹ T. Hønger,¹ R. Bauer,³ and O. G. Mouritsen,¹

¹Department of Physical Chemistry, The Technical University of Denmark,
²Risø National Laboratory, Denmark, and ³Department of Physics, Royal Veterinary and Agricultural University of Denmark

The temperature dependence of the small-angle neutron scattering from fully hydrated multilamellar DMPC, DPPC, and DSPC lipid bilayers near the main phase transition is analyzed by means of a simple geometric model which yields both the lamellar repeat distance, the hydrophobic thickness of the bilayer, the interlamellar aqueous spacing, as well as the molecular cross-sectional area. The results for the different lipids are interpreted in terms of anomalous swelling behavior, thermal renormalization of bending rigidity, and critical unbinding transitions of interacting membranes. The effect of small amounts of cholesterol ($\lesssim 3\%$) in DMPC bilayers is a softening of the bending rigidity whereas larger cholesterol contents lead to the well-known bilayer stiffening.

Su-Pos463

DETECTION OF DYNAMIC LIPID-BILAYER HETEROGENEITY BY TWO-PROBE FLUORESCENCE ENERGY TRANSFER SPECTROSCOPY

S. Pedersen, K. Jørgensen, T. R. Bækmark, and O. G. Mouritsen
¹Department of Physical Chemistry, The Technical University of Denmark,
DK-2800 Lyngby, Denmark

The energy transfer between two fluorescent lipid probes, NBD-PE (donor) and N-Rh-PE (acceptor), incorporated into DPPC unilamellar and multilamellar lipid bilayers is studied as a function of temperature in the region of the main phase transition. The two probes have different relative solubilities in the gel and fluid lipid-bilayer phases. A distinct maximum in the fluorescence intensity of the donor is observed in the phase transition region indicating that the two probes are demixing and increasing their average separation. For the multilamellar system the pronounced maximum in the donor fluorescence intensity is associated with a corresponding minimum in the acceptor intensity. The observation is interpreted in terms of dynamic lateral heterogeneity that persists in the transition region due to strong density fluctuations. The interpretation of the experimental observations is supported by a detailed theoretical calculation using computer simulation on a microscopic model that takes full account of diffusion of the two probes and the lipid fluctuations characteristic of the main phase transition.

Su-Pos465

BIOPHYSICS OF THE CENTRAL CAVITY: CONFORMATIONAL AND FUNCTIONAL CONSEQUENCES OF EFFECTOR BINDING TO HbPRESBYTERIAN AND HbA.

(E.S. Peterson, J. Wang, D.S. Gottfried, S. Huang, S. Acharya and J.M. Friedman)) Department of Physiology & Biophysics, Albert Einstein College of Medicine, Bronx, NY

In the presence of chloride, HbPresbyterian (Asn β 108Lys) has markedly reduced oxygen affinity compared to HbA. This feature has made HbPresbyterian (HbP) a focus of attention in synthetic schemes to develop a Hb-based oxygen carrier. Very little is known about the molecular origins of its reduced oxygen affinity. HbP has an added positive charge (per $\alpha\beta$ dimer) in the middle region of the central cavity where chlofibrate type effectors bind. In many respects this protein also provides an opportunity to study how the solvent-accessible central cavity can be exploited to alter Hb reactivity. To these ends we have begun a systematic comparative biophysical study of HbA and HbP. In this presentation we discuss the interaction of the liganded ferrous forms of these protein with two classes of central cavity effectors: those specific to the DPG binding site and those that bind in the region near the α end of the central cavity (e.g. L35, a potent chlofibrate type allosteric effector). UV and visible Resonance Raman spectroscopy are used to probe the α 1 β 2 interface and the iron-proximal histidine linkage respectively. Geminate recombination and the slower solvent-derived recombination are used to examine ligand reactivity and the fraction of R and T state populations. Time-correlated single photon counting fluorescence lifetime studies are used to study the binding of HPT, a fluorescent analogue of DPG, to both proteins. Both COHbA and COHbP show similar conformational and functional responses to the effectors. Some distinct differences can be explained by postulating that the added positive charge in HbP creates a higher affinity effector binding site that can accommodate not only the chlofibrate type effectors, but the DPG type effectors as well. The results also indicate the possibility of long-range communication with the central cavity.

Su-Pos466

A HIERARCHY OF RELAXATION PHENOMENA OBSERVED IN HEMOGLOBIN EMBEDDED IN A ROOM TEMPERATURE TREHALOSE GLASS. ((M. Yang, J. Wang, A. Sheikh, D.S. Gottfried, E.S. Peterson and J.M. Friedman)) Department of Physiology and Biophysics, Albert Einstein College of Medicine, Bronx, NY 10461

Upon photodissociation COHb exhibits a wide range of nonequilibrium relaxation phenomena starting within some fraction of a picosecond and extending out to tens of microseconds. In addition equilibrium fluctuations result in conformational averaging. All of these dynamics can have an impact on ligand rebinding. In an effort to better understand the relationship between conformational dynamics and ligand binding reactivity, we have embedded COHbA in a room temperature trehalose sugar glass [Hagen et al., *Science* 269,959 (1995)] in order to decouple solvent dependent and solvent independent dynamics as well as reducing the amplitude for large scale conformational fluctuations. Ligand rebinding kinetics are followed as a function of temperature (60-300K) and compared to those observed in water-glycerol solvents (50-95% glycerol:water). Time resolved resonance Raman is used to determine the effect of the trehalose glass on the fast relaxation of the heme iron-histidine unit. Time correlated single photon counting fluorescence lifetime measurements are used to probe the overall dynamics of the globin as reflected in the distribution of lifetimes for the tryptophan residues in HbA. The results show that the trehalose glass does not impede the initial fast relaxation of the iron-histidine unit but does dramatically impede conformational averaging and completely eliminates ligand escape at all temperatures examined. The fluorescence studies show that when COHbA is embedded in the room temperature trehalose glass, the picosecond Trp lifetimes are nearly unchanged, but there is a complete absence of the nanosecond fluorescence decay (observed in aqueous solutions), which is replaced by a decay of 600-800 ps and an amplitude of approximately 1%. We ascribe this change in the fluorescence decay to a significant decrease in the coupled structural dynamics of the A (Trp's $\alpha 14, \beta 15$) and E helices that normally allow transient opening of the distal heme pocket.

Su-Pos468

SPATIAL DYNAMICS AND PATTERN FORMATION DURING CLOT GROWTH *IN VITRO*. ((F.I. Ataullakhanov, G.T. Guria, V.I. Sarbash, R.I. Volkova and V. Zamitcina)) National Research Center for Hematology, Moscow, Russia, 125167.

We studied the spatial and temporal characteristics of a growing clot *in vitro* by simultaneous monitoring of the production of thrombin and polymerized fibrin. Following contact with an activating surface thrombin concentration near the surface grows exponentially and propagates from the activating surface in a form of a thrombin wave. The amplitude and speed of the thrombin wave remain constant up until the wave stops abruptly at some distance from the activating point. Fibrin polymerization mimics the thrombin propagation after a small delay. The developed clot becomes surrounded by an "inactivation zone", in which coagulation is strongly suppressed. When coagulation threshold is decreased, the "stratified structures" can be formed, in which solid layers alternate with liquid blood.

We interpret the observed regimes of clot growth in terms of the hypothesis that blood is a new type of active medium. When coagulation is initiated two active waves propagate from a point of activation. Interaction of these autowaves determines the dynamics and size of a clot.

We constructed and analyzed the phenomenological and kinetic models of clot formation and thrombin production according to the reactions of the intrinsic coagulation pathway. The models agree well with the experimental data.

Su-Pos467

CRYSTAL STRUCTURE OF THE C-TERMINAL DOMAIN OF GELATINASE A. ((A. M. Libson¹, A. G. Gittis¹, I. E. Collier², B. L. Marmer², G. I. Goldberg², E. E. Lattman¹)) ¹Johns Hopkins School of Medicine, Baltimore MD 21205. ²Washington University School of Medicine, St. Louis MO 63110.

Gelatinase A is one of a family of extracellular matrix metalloproteases (MMP) which play a role in normal physiological processes such as cell morphogenesis and tissue repair. Overexpression of gelatinase A has been shown to promote tumor invasion and metastasis in certain malignant cells. Understanding the mechanism of spatial and temporal regulation of gelatinase A is critical in describing and controlling these processes. Regulation of gelatinase A has been shown to be mediated by its hemopexin-like C-terminal domain. Here, we report the crystallization and completed X-ray crystal structure of the hemopexin-like C-terminal of gelatinase A (gA-Ctd) determined at 2.15 Å. The gA-Ctd structure is one of the first reported examples of a four-bladed β -propeller protein comprised of four homologous, anti-parallel β -sheet domains which are symmetrically arrayed about a central pseudo four-fold axis. The four-fold axis forms a large channel-like opening in gA-Ctd in which a metal ion, Ca^{2+} , and a Na^+ and Cl^- ion pair are bound. The Ca^{2+} ion is coordinated exclusively by main chain carbonyl oxygens and water molecules representing a novel metal binding motif in proteins. Also, a Zn^{2+} metal ion is found coordinated by two symmetry related gA-Ctd molecules. With this structure, we have modeled a complete active gelatinase molecule which includes the catalytic and the fibronectin-like domains. Given the homology among MMPs, the overall fold of other MMP hemopexin domains is expected to be similar to that of gA-Ctd. The high degree of internal symmetry found in gA-Ctd suggests that it may have evolved from a gene duplication event.

CHEMOSENSORY TRANSDUCTION AND CHEMOTAXIS

Su-Pos469

AN APPROACH TO A SPATIAL DISTRIBUTION OF OLFACTORY RECEPTOR NEURONS WITH IDENTIFIED TUNING SPECIFICITIES. ((J. Hirono, T. Sato and M. Takebayashi)) Life Electronics Research Center, Electrotechnical Lab., Amagasaki, 661 Japan.

In odor responses to n-aliphatic odorants with a straight chain of 3-9 carbons, the relationship between spatial distances and odorant tuning specificities were examined in mouse olfactory receptor neurons (ORNs). The ORNs were isolated on a Cell-Tak coated cover glass by the tissue-printing method which was expected to reserve their relative spatial distance in intact tissue within about 200 μm . Odor responses were recorded optically by measuring intracellular calcium increases with fura-2. Tuning specificities were dependent on both the carbon chain length and the functional group (carboxyl and hydroxyl). In most ORNs, the sensitivity was maximal at a single carbon chain length, therefore, the value of similarity for their tuning specificities could be evaluated from the difference between the lengths. We found that ORNs responsive to n-aliphatic odorants tended to be distributed within close proximity to each other according to the increase in the similarity of the tuning specificities and there was a correlation between the spatial distance and the value of similarity. On the other hand, many ORNs did not respond to n-aliphatic odorants in the neighborhood of ORNs sensitive to subsets of the odorants. Our results also indicated that ORNs with quite different tuning specificities were distributed in the neighborhood.

Su-Pos470

SEPARATION OF WHITE BLOOD CELLS FROM RED BLOOD CELLS IN A MICROFABRICATED LATTICE ((R.H. Austin and Shirley S. Chan)), Dept. of Physics, Princeton University, Princeton, NJ 08544

Leukocytes (WBCs) are relatively rare in a healthy person: approximately 1 out of every thousand cells in the blood are WBCs, the rest are predominantly the un-nucleated erythrocytes (RBCs). Chemotactic control of WBC invasion of small openings (one micron or less) is a critical element in understanding, and perhaps someday controlling, the invasive and lethal transformation of WBCs in leukemia. Quantitative study and understanding of the physical phenomena involved in chemotaxis requires the ability to both capture from blood the relatively rare WBCs and then to challenge them with a precise array of variable sized openings in the presence of a known chemical gradient. We have recently been able to show that a suitably chosen opening in microlithographically constructed array structures can with 100% efficiency sort rare white blood cells from red blood cells and hold them for optical observation under a transparent glass lid. We have developed sensitive fluorescence and dark-field techniques to observe the signal transduction and motile response to both hydrodynamic shear fields and chemotactic patterns. Videos of this work will be shown.